Development of a mouse model of cochlear implantation

Nina Mistry

Ear Institute

University College London

A thesis submitted for the award of

MD(Res)

Declaration

I, Nina Mistry, confirm that the work presented in this thesis is my own. Where information has been derived from other sources, I confirm that this has been indicated in the thesis.

Acknowledgements

I would firstly like to express sincere thanks to my supervisors: Professor Shakeel Saeed for his support and direction throughout the project, and Professor Andy Forge for all his help, expertise and guidance along the way. I feel very privileged to have had you both as my mentors and appreciate your time and patience throughout. I am also indebted to Dr Ruth Taylor, without whose help, dedication and support, this work would not have been possible. Thank you for having the patience to answer my constant queries and questions and for keeping me going until the end. Thank you also to Mr John Oates whose guidance and infectious enthusiasm for all things otology-related, opened the door to this research opportunity.

Many thanks to Dr Lisa Nolan, not only for her constant intellectual support and help in the lab, but also for her friendship. Thanks also to Graham Nevill for his help and expertise. To my lab partner and friend, Kiran, thank you for sharing this journey and making it easier. Thanks also to all those who offered their knowledge, support and friendship throughout my time in the lab: Anwen, Naila, Miriam, Shreena and Peter. It was a pleasure to have got to know you all.

I would also like to thank the institutions that provided funding towards this research: the Royal College of Surgeons, Midland Institute of Otology, Otorhinolaryngological Research Society and the Royal Society of Medicine.

I am very grateful for the continuing support and dedication of my parents. All the achievements in my career to date, including this thesis, have only been possible due to the opportunities they have given me.

Lastly, I am extremely appreciative and indebted to my husband, Keith, and children, Nia and Rohan, who have provided a constant source of encouragement, optimism and support throughout this period. Without their help and reassurance this MD(Res) would not have been possible.

Abstract

Introduction: Despite the ongoing developments in cochlear implantation (CI) surgery and improvements in hearing preservation, the benefits gained have been overshadowed by the fact that a proportion of patients have lost part or all of their residual hearing in the implanted ear. The underlying cause of this loss remains unclear and prompts questions regarding the biological effects of CI on cochlear structure and function. Animal models are the only means of assessing the effects of CI at a cellular and molecular level. The range of naturally occurring and genetically-modified mice which mimic human deafness provide excellent opportunities for auditory research. To date, there are very few studies of CI in mice. The main aims were to develop a reproducible and viable technique of mouse CI and assess the response of the mouse cochlea to implantation.

Methods: CI via the round window was performed in C57BL/6J mice. Two age groups were chosen to examine the effects of implantation in the early and later stages of hearing loss, and to examine for any implantation-accelerated hearing loss. The contralateral cochlea acted as a control. Auditory brainstem response (ABR) audiometry prior to and at time-points following CI was undertaken. Following sacrifice, cochleae were harvested and prepared for histological examination.

Results: ABR analysis showed greater threshold shifts in the implanted ear compared to the control ear post-implantation, but substantial preservation of hearing, especially at the low frequencies. Cone beam computed tomography and light microscopy confirmed correct placement of the electrode array within the scala tympani. Histological analysis showed an inflammatory response and encapsulation of the implant in tissue with features suggesting the presence of fibrosis.

Conclusion: The results demonstrate that mouse CI via the round window is feasible and provides a means for exploring the interface between the biological and technological aspects of CI.

Table of Contents

List of Figures

List of Tables

List of Abbreviations

ABR	Auditory brainstem response
ARHL	Age-related hearing loss
BDNF	Brain-derived neurotrophic factor
CBCT	Cone beam computed tomography
CI	Cochlear implantation
CX/Cx	Connexin
DAPI	4',6-diamidino-2-phenylindole
EAS	Electroacoustic stimulation
EDTA	Ethylenediaminetetraacetic acid
FITC	Fluorescein isothiocyanate
IHC	Inner hair cell
IL-β1	Interleukin beta 1
K^+	Potassium ion
mV	Millivolt
NSHL	Non-syndromic hearing loss
NT-3	Neurotrophin 3
OHC	Outer hair cell
PBS	Phosphate buffered solution
ROS	Reactive oxygen species
SEM	Standard error of the mean
SGC	Spiral ganglion cell
SHL	Syndromic hearing loss
SNHL	Sensorineural hearing loss
TEM	Transmission electron microscopy
TGF- β1	Transforming growth factor beta 1
TNF-α	Tumour necrosis factor alpha
TRITC	Tetramethylrhodamine isothiocyanate
WHO	World Health Organization

CHAPTER 1: INTRODUCTION

Worldwide, there are approximately 360 million people who suffer disabling hearing loss, the majority being sensorineural in nature. Within the UK around 10 million people are affected by hearing loss with around 800,000 suffering with a severe or profound loss. As life expectancy is set to rise, the World Health Organisation (WHO) predicts that by 2030 there will be an estimated 14.5 million people in the UK with hearing loss, making it one of the top ten disease burdens ahead of conditions such as diabetes. Hearing loss is a major public health issue with significant personal and social consequences. Difficulties with speech interpretation may result in communication problems and delayed language acquisition. Social isolation and exclusion may also arise in older patients suffering with hearing loss (Action on Hearing Loss 2012; World Health Organization 2012)

Cochlear implants have revolutionised the treatment of profound hearing loss, however, their full potential is yet to be realised. At present, cochlear implantation (CI) is limited to selected patient groups and the effects of CI on residual cochlear structure and function remains to be fully addressed. This thesis is aimed at developing a novel mouse model of CI to aid investigation into the effects of implantation. This chapter provides a general description of the human auditory system before providing a background on cochlear implants and what is known to date regarding their biological effects on the inner ear. The use of animal models in CI studies is also discussed together with the advantages of using mice as a model for auditory research.

1.1 Anatomy and physiology of the human auditory apparatus

1.1.1 The external and middle ear

The auricle (or pinna) and external auditory canal constitute the external part of the ear and act to collect sound and aid transmission to the tympanic membrane. The structure and form of the external ear also allows the sound to be enhanced by acting as a resonator (Gates and Mills 2005; Wright and Valentine 2008). The middle ear comprises the tympanic cavity, Eustachian tube and the system of mastoid air cells. The tympanic cavity containing the ossicular chain and intratympanic portion of the facial nerve is housed within the temporal bone and is bounded laterally by the tympanic membrane and medially by the osseous labyrinth.

Sound travels via the external auditory canal to the tympanic membrane, a three-layered sheet-like structure whose displacement in response to sound allows energy to be transmitted to the semi-rigid ossicular chain. This consists of three bones; the malleus, incus and stapes. The most laterally placed ossicle, the malleus, is attached in part to the tympanic membrane and articulates at its head to the body of the incus. The incus in turn articulates with the head of the third and final ossicle, the stapes, via its lenticular process. The stirrup-shaped stapes has two crura which extend from the head to connect independently to the footplate, which in turn attaches to the oval window, coupling sound (acoustic) energy from the middle ear to the inner ear (Wright and Valentine 2008). The anatomy of the ear is demonstrated in Figure 1.1.

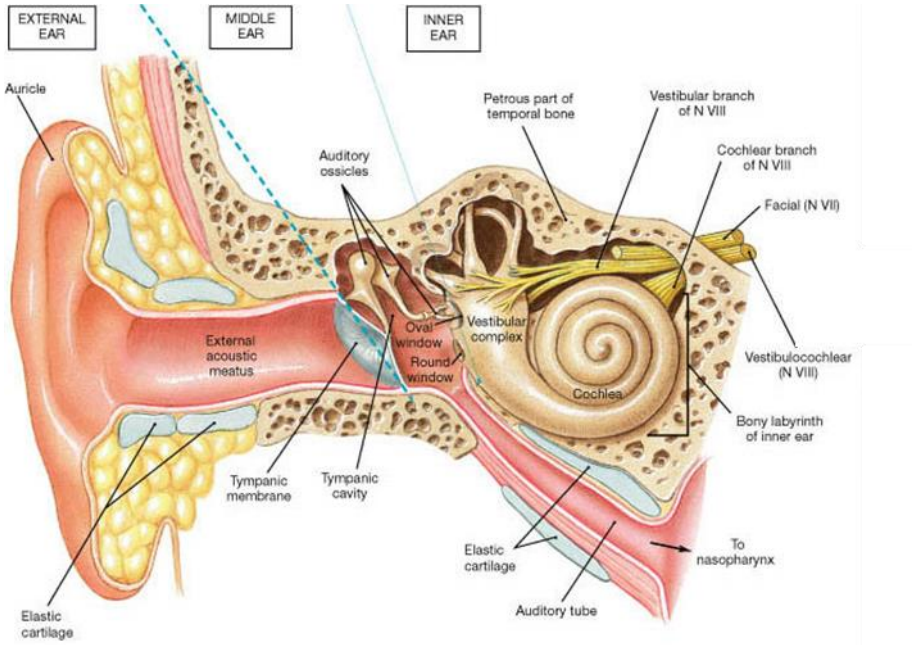

Figure 1.1 Normal anatomy of the human external, middle and inner ear
(Reproduced from http://droualb.faculty.mjc.edu/)

1.1.2 The inner ear

The inner ear consists of the cochlea, vestibule and semicircular canals. It is contained within the bony labyrinth or otic capsule which itself is embedded within the petrous portion of the temporal bone. The human cochlea has basic characteristics common to all mammals. It is essentially a spiral tubular structure lined with membranes which separate it into various fluid-filled compartments which converge at the vestibule (Furness and Hackney 2008). It is generally accepted that the human cochlea has two and three-fourth turns (Hardy M 1938) but studies have shown anatomical variations with up to three turns being present in some (Biedron et al., 2009).

The base of cochlea contains the round and oval windows. The former is membrane bound whereas the latter is covered by the footplate of the stapes. It is at the cochlea's base where high frequency sounds are detected, whereas the more apical portion is sensitive to low frequency sounds. The stapes overlying the oval window is the point at which the sound waves cause pressure changes within the cochlear fluids and allow transmission of sound to the inner

ear. Situated more inferior and posterior to the oval window, the round window vibrates in the opposite phase to those vibrations entering at the oval window, allowing release of the pressure induced secondary to sound stimulation. This dissipates energy within the otherwise incompressible internal cochlear fluids, preventing rupture of the delicate membranes (Furness and Hackney 2008) (Figure 1.2).

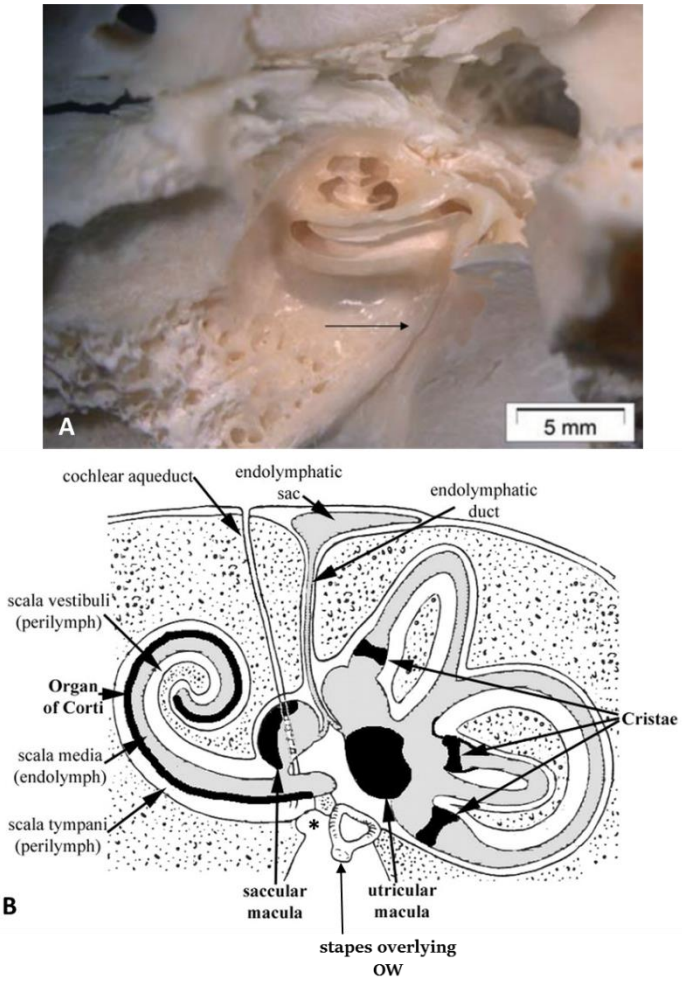

Figure 1.2 Human cochlea

A. Microdissection of human cochlea (left) contained within the bony labyrinth or otic capsule, which appears yellow in the image. (Taken from Rask-Andersen 2012)

B. Diagram of temporal bone cross-section showing inner ear. The membranous and bony canals of the cochlea and vestibule are shown. The stapes is shown overlying the oval window. Situated more posterior and inferior, the round window is marked by an * (Taken and adapted from Forge and Wright 2002).

1.1.2.1 Structure of the cochlea

The cone shaped modiolus acts as the central bony axis of the cochlea, occupying the initial two turns of the cochlea spiral. Projecting from the modiolus, the bilamellar osseous spiral

lamina also follows the cochlea turns and divides the bony canal into scala vestibuli above and the scala tympani below. At its medial border on the upper plate, the endosteum of the spiral lamina becomes thickened to form the spiral limbus, which projects into the cochlear duct. The area between the vestibular lip (superiorly) and the tympanic lip (inferiorly) of the spiral limbus is defined as the inner spiral sulcus. The spiral limbus is covered by interdental cells which when followed laterally lie in continuity with the cells lining the inner spiral sulcus and which medially (towards the modiolus) are continuous with epithelial cells forming part of Reissner's membrane. Secretions from the interdental cells form the tectorial membrane which projects from the vestibular lip to cover the central portion of the organ of Corti (Figure 1.3) (Krstic 1991).

The scala tympani and scala vestibuli, together with the scala media, compose the three main fluid-containing compartments within the cochlear duct. The scala vestibuli and the scala tympani converge at the helicotrema located at the cochlear apex. The scala media is an extension of the membranous labyrinth and is triangular in cross-section, bounded inferiorly by the basilar membrane and superiorly by Reissner's membrane. The latter membrane runs from the spiral limbus at the modiolus to the lateral bony cochlea wall and consists of a two-cell layer separated by a basement membrane. The basilar membrane extends from the osseous spiral lamina to the spiral ligament, a thickened area of endosteum on the inner aspect of the of the lateral cochlea wall. It is on top of the basilar membrane that the organ of Corti is positioned. The spiral ligament makes up part of the lateral cochlear wall together with the stria vascularis. Both of these latter structures play an important role in the maintenance of cochlear homeostasis (discussed below) (Figure 1.3) (Furness and Hackney 2008; Krstic 1991).

The scala media contains endolymph, a potassium (K^+)-rich fluid (approximately 140mM) which is low in sodium ions and varies in composition to most extracellular fluids. Within the cochlea the endolymph has a high positive electrical potential (approximately +80mV) called the endocochlear potential. This compartment is isolated both in an electrical and chemical manner from both the scala tympani and scala vestibuli which contain perilymph, a fluid high

in sodium and low in potassium ions. Maintenance of the endocochlear potential is essential to auditory function and relies on the effective separation of the two fluids at the level of the junctions between the epithelial cells surrounding the endolymphatic spaces (Forge and Wright 2002).

1.1.2.2 The Organ of Corti

The organ of Corti comprises a mosaic of supporting and sensory cells and is the key sensory component of the cochlea. Its surface is covered in part by the two sensory cells of the cochlea; the inner and outer hair cells (IHCs and OHCs). In the adult human cochlea, approximately 3000 IHCs are arranged as a single row and around 9000-10000 OHCs are organised in 3 or 4 rows along a length of about 35mm (Forge and Wright 2002; Wright 1983). The supporting cells are attached to the basilar membrane whereas the hair cells are located in the more luminal layer of the epithelium. The tunnel of Corti can be found running between the inner and outer hair cell rows and is bounded on its inner and outer aspects by inner and outer pillar cell rows respectively (Figure 1.3).

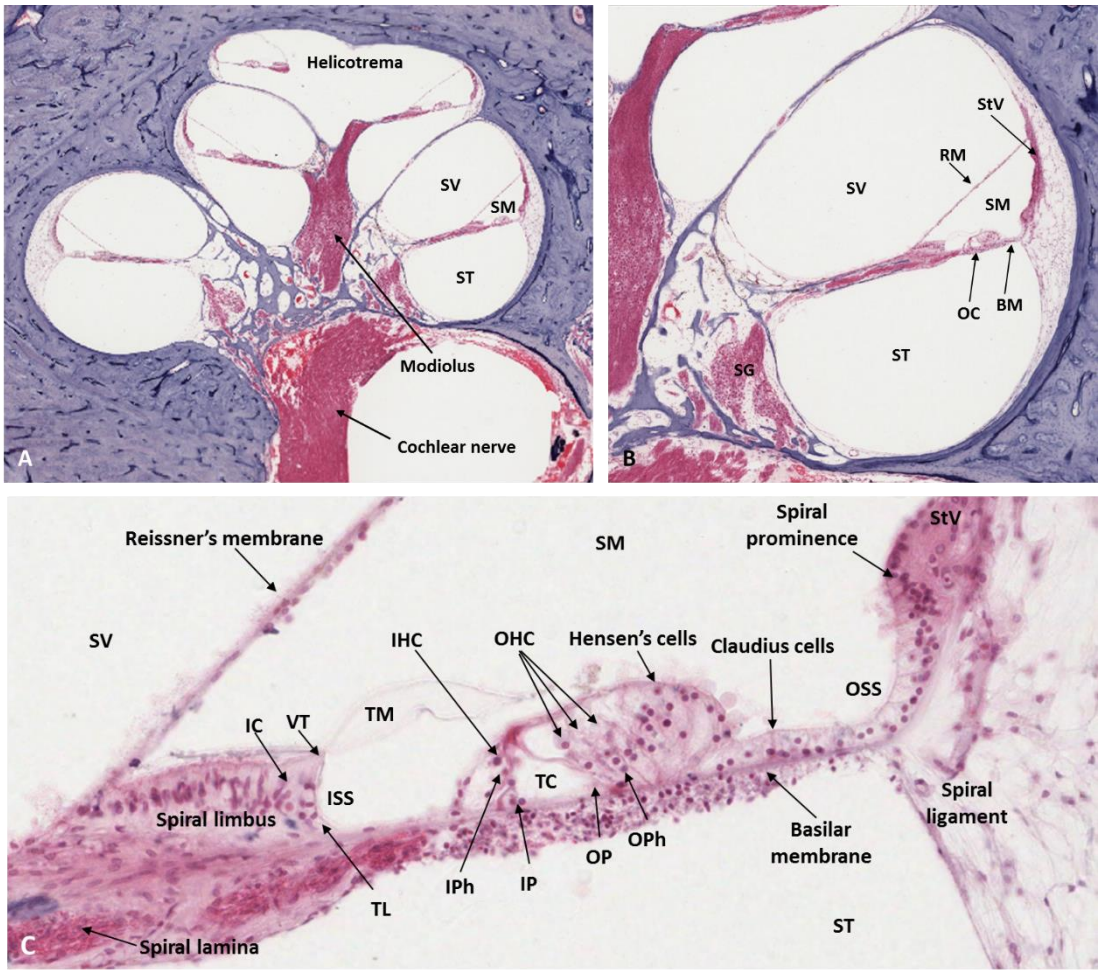

Figure 1.3 Histologic sections of human cochlea

A. Mid-modiolar histologic section showing normal human cochlea. The central spiral of the modiolus is seen together with the three fluid-filled compartments of the cochlea: scala vestibuli (SV), scala media (SM) and scala tympani (ST). The helicotrema represents the area where the scala tympani and scala vestibuli converge.

B. A higher magnification of the histologic section in B, shows the organ of Corti (OC) positioned upon the basilar membrane (BM). Reissner's membrane can be seen forming the roof of the SM. The spiral ganglion is located within the modiolus and contains the cell bodies of bipolar neurons relaying auditory information from the organ of Corti to the auditory (cochlear) nerve.

C. A higher magnification of histologic sections A and B, shows the organ of Corti in more detail. The sensory cells: inner hair cell (IHC) and outer hair cells (OHC) can be seen, together with their supporting cells including specialised Deiter's or phalangeal cells (inner and outer, IPh and OPh), inner pillar (IP) and outer pillar cells (OP), Hensen's and Claudius cells. The tunnel of Corti is also shown. The osseous spiral lamina and spiral limbus are shown, the latter with its vestibular lip (VL) and tympanic lip (TL) delineating the inner spiral sulcus (ISS). The outer spiral sulcus (OSS) is a groove between the spiral ligament and the organ of Corti. The interdental cells (IC) of the spiral limbus are also noted with the tectorial membrane (TM). The spiral prominence, stria vascularis (StV) and spiral ligament are also highlighted.

(Histologic sections taken and adapted from human temporal bone library at otopathologynetwork.org)

1.1.2.3 Hair cells

Outer hair cells of the organ of Corti are cylindrical in shape with a basally located nucleus. The sensory aspect of the OHCs lies at its apical portion, where the stereocilia are located. Here the arrangement of the stereocilia gives rise to the 'W' or 'V'-shaped characteristic appearance. The IHCs are located closest to the inner sulcus and modiolus, with their apical surface covered in stereocilia which project up towards the overlying tectorial membrane and endolymph of the scala media. The OHC stereocilia make contact with the overlying tectorial membrane, whilst those of the IHCs do not (Furness and Hackney 2008). The IHCs act to convey auditory information to the brain by transforming sound-induced motion of the basilar membrane into electrical signals which are conveyed via auditory nerve afferents. OHCs in contrast, are mechanical effector cells which act as the cochlear amplifier, enhancing the auditory stimulus by way of electromechanical feedback. They are responsible for increasing the frequency selectivity and amplitude of the basilar membrane vibration to low-level sounds (Ashmore and Kolston 1994; Fettiplace and Hackney 2006). The amplification of vibrations by OHCs occurs as a result of molecular motors which induce mechanical changes of the OHC in response to alterations in membrane potential. This motor protein is known as prestin and is found exclusively within the lateral plasma membrane of OHCs (Zheng et al., 2000).

1.1.2.4 Hair bundle

The sensory hair bundle is made up of stereocilia which increase in height progressively away from the modiolus. The kinocilium is a single distinct axonemal cilium which stands behind the row of the tallest stereocilia and is present during development of the hair bundle but degenerates thereafter as the cochlea matures and is not present in adulthood. The tip of each stereocilia is the point at which contact is made with the next. The apical portion of the OHC bundle is in contact with the overlying tectorial membrane. In the case of inner hair cells, however, contact with the overlying tectorial membrane is not made, rather the stereocilia are displaced by friction against the endolymphatic fluid (Robles and Ruggero 2001). Polarity of the hair bundle is defined by the position of the kinocilium and the longest row of hair cells.

Depolarisation of the hair cells occurs with a deflection of the stereocilia in the direction of the kinocilium, opening ion channels and allowing an influx of K^+ ions. Movement in the opposite direction causes a hyperpolarisation as channels are closed (Forge and Wright 2002)

1.1.2.5 Supporting cells

The supporting cells of the organ of Corti provide important architectural structure and support to the hair cells and epithelium. By intervening between neighbouring hair cells, the supporting cells prevent contact between adjacent hair cells. These cells also act to separate the hair cells from the basilar membrane by resting on the extracellular matrix that underlies the sensory epithelium (Forge and Wright 2002). The IHCs are enclosed completely by the inner phalangeal cells on the strial side and border cells on the modiolar side. Junctional complexes found at the apex of the cells connect them to the IHCs and to surrounding supporting cells. Both types of cells are thought to play a protective role by expressing transporters which remove glutamate (the primary neurotransmitter found at the base of hair cells) following its release, thereby preventing glutamate-induced nerve cell damage which can occur following an auditory insult (Furness and Hackney 2008). At the bases of the OHCs are the specialised Deiter's cells which project their thin phalangeal processes to intervene between the hair cells. It is the repetitive triangular configuration of the OHCs and their supporting Deiter's cells beneath the reticular lamina which gives them strong mechanical support. Further support at the outer edge of the organ of Corti is provided by both Hensen's and Claudius' cells (Figure 1.3) (Krstic 1991).

1.1.2.6 Ion transporting epithelia of the inner ear and maintenance of the endocochlear potential

As mentioned earlier, effective sensory transduction in the human inner ear is dependent upon maintenance of the endocochlear potential and tight regulation of K^+ ions. The latter is partly achieved through coupling and direct communication between all supporting cells via large

numbers of gap junctions. These function to remove intercellular K^+ ions from within the sensory epithelium as they pass from hair cells, thereby maintaining a low K^+ ion concentration around the base of the hair cell to create an environment conducive for stimulation and transduction (Forge and Wright 2002). Although this extensive communication exists between the supporting cells of the organ of Corti, no gap junctions have been identified between supporting cells and hair cells, providing functional isolation of the former (Forge et al., 2013; Jagger and Forge 2006; Santos-Sacchi and Dallos 1983; Taylor et al., 2012). Gap junctions play a vital role in fluid homeostasis and intracellular signalling within the inner ear (Kikuchi et al., 2000b). Two gap junction networks work together to mediate the circulation of K^+ between the perilymph and endolymph. The 'epithelial gap junction network' is composed of epithelial cells from the basilar membrane, supporting cells and outer sulcus cells. The 'connective tissue gap junction network' is formed by the intermediate and basal cells of the stria vascularis and the fibrocytes of the spiral ligament (Kikuchi et al., 2000a). The latter allows direct cell-to-cell communication between the basal and intermediate cells and also with spiral ligament fibrocytes. The interaction between cells in each network via the numerous gap junctions mean that the recycling of K^+ ions between the endolymph, hair cells, perilymph and spiral ligament can occur to effectively maintain the endocochlear potential (Forge and Wright 2002).

Stria vascularis

As the key secretory epithelia, the stria vascularis is a vital component within the cochlea responsible for the production and maintenance of the K^+-rich endolymph. It contains a complex network of capillaries and drains via venules found on the scala tympani side. Compartmentalisation of the stria vascularis exists with three distinct cell layers: basal, intermediate and marginal cells (Figure 1.4). Separation from Reissner's membrane and the spiral prominence occurs via the placement of spindle-shaped border cells (Ciuman 2009). The basal cells are elongated and placed in close apposition with gap junctions providing communication between adjacent cells. They act to separate the stria from the underlying connective tissue forming a border along the spiral ligament (Cable and Steel 1991).

Intermediate cells are derived from the neural crest and contain melanin pigment. Studies in mice have shown that these cells are not only essential for normal strial development, but that they are also vital in the production of the endocochlear potential (Steel et al., 1987).

The marginal cells are also actively involved in K^+ transport. Infoldings occurring at the basolateral aspect of the cells increase surface area for ion exchange and this together with the presence of condensed mitochondria and high levels of Na^+/K^+-ATPase, mean the cells are specially adapted for active transport of K^+. Although the marginal cells are in contact with the other cells in the stria through their processes, they are a functionally distinct unit lacking gap junctions both between each other and also between themselves and the intermediate and basal cells. Tight junctions do however exist between marginal cells and the line of cells providing a barrier against the endolymph on the apical side of the stria vascularis (Ciuman 2009; Forge and Wright 2002).

Spiral ligament

Cells of the spiral ligament are also thought to be important in the maintenance of cochlear homeostasis. Of the five different types of fibrocytes present within the spiral ligament, types II, IV and V have a role in drawing K^+ from the perilymph. This acts to generate an intracellular diffusion gradient to promote the movement of K^+ ions through gap junctions to strial basal cells and other fibrocytes. Type II fibrocytes are also active in pumping K^+ between the break that exists between the epithelial and connective tissue gap junction networks, thereby directing the flow of ions (Spicer and Schulte 1996).

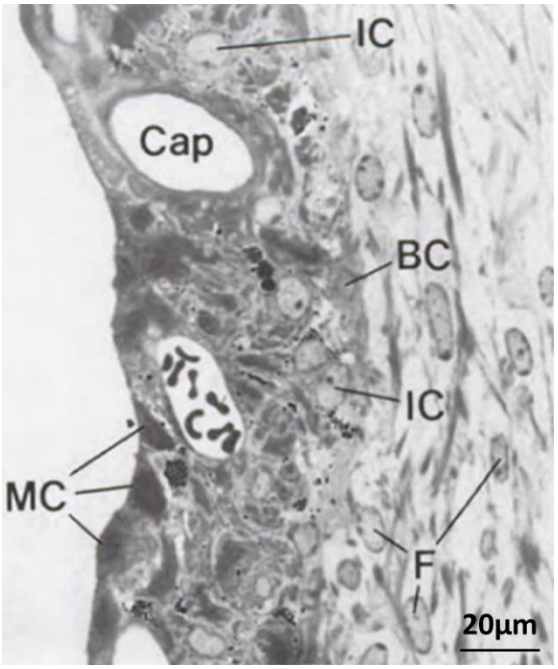

Figure 1.4 Stria vascularis

The basal cells (BC), intermediate cells (IC) and marginal cells (MC) cells and capillaries (C) are clearly seen. Adjacent fibroblasts of the spiral lamina are also labelled.

(Taken from Human Microscopic Anatomy, R.V. Krstic)

1.1.2.7 Cochlear tonotopicity

The basilar membrane is coupled to the overlying tectorial membrane via the hair cell stereocilia. As a result, oscillations of the basilar membrane give rise to movement of the hair bundles. Variations in compliance and stiffness along the basilar membrane mean that this movement is non-uniform; at the apex the membrane is wider and more compliant whereas towards the basal end, it is narrower and stiffer (Rask-Andersen et al., 2012; Robles and Ruggero 2001). In assessing the vibrational response of the basilar membrane to sound, von Békésy described the propagation of the wave travelling along the basilar membrane, increasing in amplitude and reaching a maximum before decaying. He related maximal displacement of the basilar membrane to a function of stimulus frequency. He described low frequency waves peaking at the cochlear apex and high-frequency stimuli causing maximal displacement of the basilar membrane at the basal end of the cochlea (von Bekesy 1956). This results in hair cells at the apical end of the cochlea being stimulated by low-frequency sounds and those in the basal cochlea being stimulated by higher frequencies, giving rise to a spatial or tonotopic representation of sound frequency along the length of the cochlea. This

concept of tonotopicity is maintained at every level within the auditory pathway all the way up to and including the auditory cortex (Figure 1.5) (Mann and Kelley 2011).

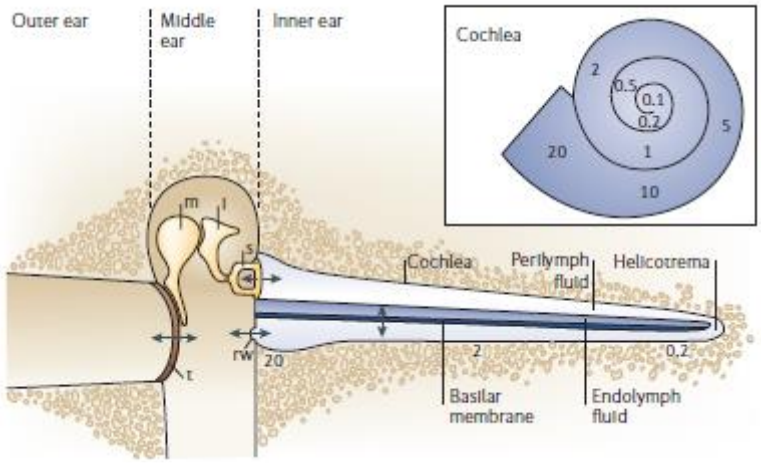

Figure 1.5 Pathway of sound conduction together with a tonotopic frequency map of the cochlea (inset in box). Vibrations of the tympanic membrane (t) in response to sound waves are transmitted by the ossicular chain (malleus (m), incus (i) and stapes (s) to create pressure waves within the cochlear fluids. These waves stimulate movement of the basilar membrane and stereocilia of the hair cells, where mechanical stimuli are converted to electrochemical stimuli. The cochlea is shown uncoiled in the main image and coiled in the inset image. Both are labelled with sound frequencies from 0.1 to 20kHz according the region of the cochlea that frequency stimulates. (Image taken from Fettiplace and Hackney, 2006).

1.1.2.8 Innervation of the organ of Corti

Innervation of IHCs occurs exclusively by afferent nerves. These neurons contribute to more than 90% of the neurons present within the spiral lamina and reflect the major role played by the IHCs in transmitting auditory information to the brain. The remaining 5-10% of afferent innervation arises from the OHCs. Conversely, efferent innervation to the organ of Corti mainly consists of medial olivocochlear efferents connecting with bases of OHCs, innervating both the ipsilateral and contralateral cochlea. Lateral olivocochlear efferents arising in the lateral superior olive, terminate on the peripheral processes of Type I SGCs below the IHCs of the ipsilateral cochlea. These arrangements reflect the primary roles of the hair cells: the IHCs as receptors and more of a modulatory role for the OHCs (Forge and Wright 2002; Raphael and Altschuler 2003).

Spiral ganglion cells (SGCs) are a key component of the neuronal pathway. The extensive afferent fibres arising from these cells combine to form the auditory nerve which in turn, transfers auditory data to the cochlear nucleus within the brainstem. The cell bodies of the SGCs are located within the modiolus and correspond to the course of the organ of Corti. Two types of SGC neurons exist; Type I which are large bipolar neurons which make up the majority (90-95%) and innervate the IHCs, and Type II, smaller and pseudounipolar neurons which innervate the OHCs (Raphael and Altschuler 2003)

As movement of the IHC stereocilia is activated, ion channels are opened allowing influx of K^+ and calcium ions. The resulting transduction current opens voltage-gated calcium channels in the basal and lateral wall of the IHC, which in turn drive calcium activated K^+ channels to open. These steps give rise to the release of the neurotransmitter glutamate at the base of the hair cell. Ribbon synapses exist between IHCs and the peripheral processes of Type I neurons. Presynaptic vesicles containing glutamate cover the ribbon within the active zone and ensure a continuous supply of vesicles are readily available for exocytosis at the plasma membrane (Trussell 2002). Each ribbon is capable of multivesicular release which is thought to enable sustained transmission in the presence of an ongoing sound stimulus (Glowatzki and Fuchs 2002). Whilst Type I neurons have a single peripheral process which makes contact with only one IHC, IHCs receive connections from multiple peripheral processes. As the neurotransmitter released from the hair cell makes contact with postsynaptic afferent boutons of the Type I neurons, an action potential is generated and transmitted to the brain via the auditory nerve (Raphael and Altschuler 2003; Trussell 2002).

Type II neurones innervate the OHCs and represent 5-10% of the population. OHCs differ from IHCs in that there are a lack of synaptic ribbons at the presynaptic terminal and far fewer neurotransmitter-containing vesicles present. When stimulated, OHCs do release neurotransmitter in response to transduction currents at the basal ends of the cells, however, there is a relatively poor synaptic transfer compared to IHCs. There is limited data on the role of Type II neurons compared to Type I neurons, however, studies have shown that they are

likely to operate as cochlear afferents and may act to provide integrated feedback from the cochlear amplifier (Jagger and Housely 2003; Weisz et al., 2009).

The central nerve processes from the SGCs enter the mid-modiolus at the cochlear apex and spiral down with the successive addition of more processes to the nerve bundle until it grows to its maximum diameter and exits at the internal acoustic meatus. Within the auditory nerve, the central portion carries low frequency fibres and the periphery contains fibres conveying high frequency information. This tonotopicity is maintained throughout the rest of the ascending auditory pathway up to the auditory cortex and includes the cochlear nuclear complex, superior olivary complex, inferior colliculus and medial geniculate nucleus (Saenz and Langers 2014).

1.2 Classification of hearing loss

Hearing loss can be classified by type (conductive, sensorineural,mixed or non-organic), severity, onset (pre- or postlingual) and cause (congenital or acquired) (Kochhar et al., 2007). Conductive hearing loss typically arises due to pathology affecting the external ear and or the middle ear. Examples of the former include wax occlusion, canal stenosis and atresias. In terms of the latter, middle ear disease giving rise to conductive hearing deficits can be temporary and fluctuating e.g. otitis media with effusion, or progressive e.g. otosclerosis. Audiological consequences are represented by the presence of an air-bone-gap and varying degrees of loss which can be amenable to surgical intervention often with promising results. Sensorineural hearing loss (SNHL) results from abnormalities of the cochlea, cochlear nerve or auditory pathway. Conditions may be hereditary or acquired and give rise to varying degrees of hearing deficits. A combination of both conductive and SNHL components give rise to a mixed type of loss. Problems occurring at the higher levels such as the vestibulocochlear nerve, brainstem and cerebral cortex can lead to central auditory dysfunction (Kochhar et al., 2007; Wright and Valentine 2008).

There are various classifications of hearing loss based on severity, with formal quantitative definitions grading hearing impairment on audiological criteria, with slight variations between organizations. The WHO classifies hearing loss into five categories (Table 1) (World Health Organization 2013). Disabling hearing impairment is classed as grade 2 or more with unaided hearing threshold levels for the better ear of 41 dB or more. The hearing threshold is defined as the lowest level sound that can be heard more than 50% of the time. A limitation of the WHO classification, however, is that it is based on the better hearing ear. Definitions of hearing impairment according to the British Society of Audiology (BSA) (British Society of Audiology 1988) are shown in Table 2 and are based on the average pure tone thresholds at 0.25, 0.5, 1, 2 and 4 kHz.

Table 1.1 WHO grades of hearing impairment (World Health Organization 2013)

Grade of impairment	Corresponding audiometric ISO value	Performance	Recommendations
0 - No impairment	25 dB or better (better ear)	No or very slight hearing problems. Able to hear whispers.	
1 - Slight impairment	26-40 dB (better ear)	Able to hear and repeat words spoken in normal voice at 1 metre.	Counselling. Hearing aids may be needed.
2 - Moderate impairment	41-60 dB (better ear)	Able to hear and repeat words spoken in raised voice at 1 metre.	Hearing aids usually recommended.
3 - Severe impairment	61-80 dB (better ear)	Able to hear some words when shouted into better ear.	Hearing aids needed. If no hearing aids available, lip-reading and signing should be taught.
4 - Profound impairment including deafness	81 dB or greater (better ear)	Unable to hear and understand even a shouted voice.	Hearing aids may help understanding words. Additional rehabilitation needed. Lip-reading and sometimes signing essential.

The audiometric ISO values are averages of values at 500, 1000, 2000, 4000 Hz.

Table 1.2 British Society of Audiology definitions of hearing loss (British Society of Audiology 1988)

Descriptor of hearing loss	Hearing level
Mild	20 - 40 dB
Moderate	41 - 70 dB
Severe	71 - 95 dB
Profound	Greater than 95 dB

1.3 Aetiology of hearing loss

There are a variety of genetic and environmental causes leading to hearing impairment. Acquired hearing loss can be caused by a range of environmental factors including ageing, ototoxic drugs, acoustic trauma and infections (Dror and Avraham 2009; Gibbin 2008; Kochhar et al., 2007). Prenatally, viral infections due the 'TORCH' organisms (**t**oxoplasmosis, **o**ther infections, **r**ubella, **c**ytomegalovirus and **h**erpes) together with drug exposure in utero and erythroblastosis fetalis can give rise to acquired SNHL. Postnatally, bacterial meningitis due to *Neisseria meningitides* is the most common cause of acquired SNHL in childhood. Other infectious causes include *Streptococcus pneumoniae, Haemophilus influenzae* and cytomegalovirus (Gibbin 2008; Kochhar et al., 2007). Hearing loss attributed to genetic factors is caused by mutations in various genes or regulatory elements which form part of the development of the structure and function of the ear. The interplay between environmental and genetic factors is also observed as triggers in the former can induce or contribute to hearing loss in an individual with an underlying genetic-susceptibility (Dror and Avraham 2009). Examples include PCDH15 and MYH14 as potential susceptibility genes in noise-induced hearing loss (Konings et al., 2009) and a mitochondrial mutation in the 12S ribosomal RNA gene predisposing to aminoglycoside ototoxicity (Fischel-Ghodsian 2005).

1.3.1 Genetic causes

The inheritance mode of mutations leading to genetic hearing loss can be autosomal dominant (DFNA), autosomal recessive (DFNB), mitochondrial or X-linked (DFN). Characteristically prelingual, autosomal recessive conditions account for between 77-93% of all cases of genetic hearing loss. Conversely, autosomal dominant causes account for 10-20%, with mitochondrial and X-linked disorders making up the remainder of cases (Duman and Tekin 2012). Inherited hearing impairment can be categorised as syndromic hearing loss (SHL) which is associated with other clinical features as well as hearing loss and non-syndromic hearing loss (NSHL), an inherited SNHL in the absence of additional clinical features.

A systematic review of the aetiology of bilateral SNHL in children revealed NSHL to account for 29.2% of cases, with a much smaller percentage 3.2% attributed to SHL (Morzaria et al., 2004). Although the majority of genetic hearing loss is sensorineural in nature, there are a few cases which lead to CHL (Dror and Avraham 2009). For example, mutations in the POU3F4 gene, located on the X chromosome, causes *DFN3* deafness which is characterised by stapes fixation and a middle ear conductive loss. Other inherited CHLs include Treacher Collins syndrome, Goldenhar syndrome and Osteogenesis imperfecta. (U.S.National Library of Medicine 2006).

A variety of genes for SHL have been discovered since the identification of the first gene, *USH2A* (for Usher syndrome) which was mapped in 1990. These include those for Stickler syndrome, Alport syndrome, Treacher-Collins syndrome, Waardenburg syndrome and Branchio-Oto-Renal syndrome (see table 3) (Dror and Avraham 2009; Hereditary Hearing Loss Homepage 2013; Kochhar et al., 2007). With regards to NSHL, the first recessive locus to be mapped in 1994 was the *DFNB1* which was later found to be associated with the *GJB2* or connexin 26 (CX26) gene (Dror and Avraham 2009). Mutations in the genes that encode connexins are the most common cause of NSHL loss, with up to 50% of reported cases due to mutations on CX26, the predominant connexin of the cochlea. Connexin 30 (CX30) is another major cause and is encoded by the gene *GJB6.* Connexins form part of intracellular gap junction channels and therefore play a vital role in cell-cell communication and electrolyte

transportation (Dror and Avraham 2009; Vivero et al., 2010). Associations of other mutations in CX26 or CX30 with various skin conditions in conjunction with hearing loss have also been noted, including keratitis-ichthyosis-deafness syndrome, Vohwinkel syndrome, palmoplantar keratoderma and Bart-Pumphrey syndrome (Xu and Nicholson 2013). Other autosomal recessive and autosomal dominant genes associated with NSHL are shown in Table 1.4 (Bitner-Glindzicz 2008).

Table 1.3 Genes associated with SHL (Hereditary Hearing Loss Homepage 2013; Kochhar et al., 2007)

Syndrome	Chromosomal locus	Gene symbol
Autosomal dominant		
Branchio-oto-renal (BOR)		
BOR1	8q13.3	EYA1
BOR2	1q31	Unknown
BOS3	14q	SIX1
Waardenburg		
WS1	2q35	MITF
WS2	3p14.1-p12.3	SNAI2
WS3 (Klein-Waardenburg syndrome)	2q35	PAX3
WS4 (Shah-Waardenburg or Waardenburg-Hirschsprung)	13q22 20q13.2-q13.3 22q13	EDNRB EDN3 SOX10
Stickler	12q13.11-13.2	COL2A1
STL1	6p1.3	COL11A2
STL2	1p21	COL11A
STL3	6q13	COL9A1
STL4		
Neurofibromatosis	22q12	NF2
NF2		
Treacher-Collins	5q32-q33.1	TCOF1
TCOF1		
Autosomal recessive		
Pendred	7q21-34	SLC26A4/PDS
Usher		
USH1A	14q32	Unknown
USHIB	11q13.5	MYO7A
USH1C	11p15.1	USH1C
USH1D	10q22.1	CDH23
USH1E	21q21	Unknown
USH1F	10Q21-22	PCDH15
USH1G	17Q24-25	SANS
USH2A	1q41	USH2A
USH2B	3p23-24.2	Unknown
USH2C	5q14.3-q21.3	VLGR1
USH3	3q21-q25	USH3A
Jervell and Lange-Nielsen		
JLNS1	11p15.5	KCNQ1
JLNS2	21q22.1-q22.2	KCNE1
X-linked		
Alport	Xq22 2q36-2q37 2q36-2q37	COL4A5 COL4A3 COL4A4

Table 1.4 Genes associated with NSHL. Autosomal recessive (below left) and autosomal dominant (below right) genes associated with NSHL (Taken from Bitner-Glindzicz 2008).

Locus	Gene	Protein
No locus assigned	*PRES*	Prestin
DFNB1	*GJB2(Cx26)*	Connexin26
DFNB1	*GJB6(Cx30)*	Connexin30
DFNB2	*MYO7A*	Myosin7A
DFNB3	*MYO15*	Myosin15
DFNB4	*SLC26A4*	Pendrin
DFNB6	*TMIE*	Transmembrane inner ear expressed gene
DFNB7/11	*TMC1*	Transmembrane cochlear expressed gene1
DFNB8/10	*TMPRSS3*	Transmembrane protease, serine 3
DFNB9	*OTOF*	Otoferlin
DFNB12	*CDH23*	Cadherin23
DFNB16	*STRC*	Stereocilin
DFNB18	*USH1C*	Harmonin
DFNB21	*TECTA*	Tectorin
DFNB22	*OTOA*	Otoancorin
DFNB23	*PCDH15*	Protocadherin15
DFNB28	*TRIOBP*	Trio and F-actin binding protein
DFNB29	*CLDN14*	Claudin14
DFNB30	*MYO3A*	Myosin3A
DFNB31	*WHRN*	Whirlin
DFNB36	*ESPN*	Espin
DFNB37	*MYO6*	Myosin6
DFNB67	*TMHS*	Tetraspan membrane protein of hair cell

Locus	Gene	Protein
No locus assigned	*CRYM*	Cyratallin, Mu
DFNA1	*DIAPH1*	Diaphanous
DFNA2	*GJB3(Cx31)*	Connexin31
DFNA2	*KCNQ4*	Voltage-gated potassium channel
DFNA3	*GJB2(Cx26)*	Connexin26
DFNA3	*GJB6(Cx30)*	Connexin30
DFNA4	*MYH14*	Myosin heavy chain 14
DFNA5	*DFNA5*	DFNA5
DFNA6/14	*WFS1*	Wolframin
DFNA8/12	*TECTA*	Tectorin
DFNA9	*COCH*	Cochlin
DFNA10	*EYA4*	Eyes absent 4
DFNA11	*MYO7A*	Myosin7A
DFNA13	*COL11A2*	Collagen11alpha2
DFNA15	*POU4F3*	Pou4 factor3
DFNA17	*MYH9*	Myosin heavy chain 9
DFNA20/26	*ACTG1*	Actin, gamma-1
DFNA22	*MYO6*	Myosin6
DFNA28	*TFCP2L3*	Transcription factor CP2-like3
DFNA36	*TMC1*	Transmembrane cochlear expressed gene 1
DFNA48	*MYO1A*	Myosin1A

1.3.2 Age-related hearing loss

Presbycusis can be defined as hearing loss due to the ageing process. Age-related hearing loss (ARHL) is a term used to encompass the cumulative effects of insults over a lifetime which may give rise to hearing impairment, including the effects of noise, genetic susceptibility, ototoxic agents, ageing and other systemic pathological processes. Although some authors choose to differentiate between the terms, presbycusis and ARHL are often used synonymously; this is especially because it is difficult to segregate ageing effects from the many other likely variables involved. ARHL is the main cause of acquired hearing loss worldwide and the most common sensory disability in the elderly. Cognitive, behavioural and emotional problems are recognised adverse effects associated with this type of untreated hearing loss, which may lead to depression, loss of self-esteem and social isolation (Gates and Mills 2005; Sprinzl and Riechelmann 2010).

For some elderly patients acceptance of the impairment as an inevitable consequence of the ageing process, together with reluctance, embarrassment and concerns regarding cost, means that they do not seek help. Conversely, other individuals experience denial in recognition and acceptance, attributing the difficulty to mumbling speakers (Gates and Mills 2005). The causes of ARHL can be classified according to anatomical and physiological alterations within the ear. With regards to the outer ear, changes including excess cerumen production and poor epithelial migration, often giving rise to wax impaction may have an effect on increasing the air-bone gap. However, these effects are minimal as are those associated with the ageing middle ear which include tympanic membrane alterations (thinning, stiffening and loss of vascularity) and arthritic changes within the ossicular joints.

The cochlea, however, is significantly affected by the ageing process (Chisolm et al., 2003; Gates and Mills 2005). Schuknecht originally described four categories of presbycusis based on histopathologic findings which were correlated with audiometric results. Sensory presbycusis was so-called due to primary hair cell loss within the organ of Corti. This was associated with the classic audiometric findings of high-frequency SNHL. The second type was neural presbycusis which occurred as a result of spiral ganglion neuron loss. Pure-tone

thresholds were found to be stable on testing, however, there was a progressive loss of word discrimination. Metabolic presbycusis presented following atrophy of the stria vascularis, a key component in maintaining the endocochlear potential. Pure tone audiometry showed a flat or descending result, however, word discrimination was maintained. The fourth and final type was described as cochlear conductive presbycusis, in the absence of a histological correlate, this was associated with a downward-sloping audiogram, with loss mainly in the higher frequencies (Schuknecht 1955; Schuknecht 1964). As research has progressed it has become clear that the underlying pathological processes occurring in the inner ear secondary to ageing cannot be simplified to the concept of these four predominant pathologic types. Rather it has emerged that ARHL occurs as a result of the complex interplay between risk factors (ageing, environment, co-morbidity and genetic predisposition) and intricate mechanistic pathways (Figure 1.6). The inner and outer hair cells as well as the SGCs, stria vascularis and spiral ligament represent potential sites for age-related damage. As it is highly metabolically active, the stria vascularis has been noted to be particularly sensitive to insults such as oxidative stress secondary to noise exposure, cell loss due to ageing and genetic aberrations. These factors together with microvascular disease, can compromise function and lead to hearing loss (Ohlemiller 2009). In a similar manner, multifactorial injury to the hair cells and cochlear nerve may be observed. Over time, the accumulation of damage from noise, oxidative insults, ototoxic drugs and ageing together with poor mechanisms of repair mean that hair cells are particularly vulnerable (Yamasoba et al., 2013).

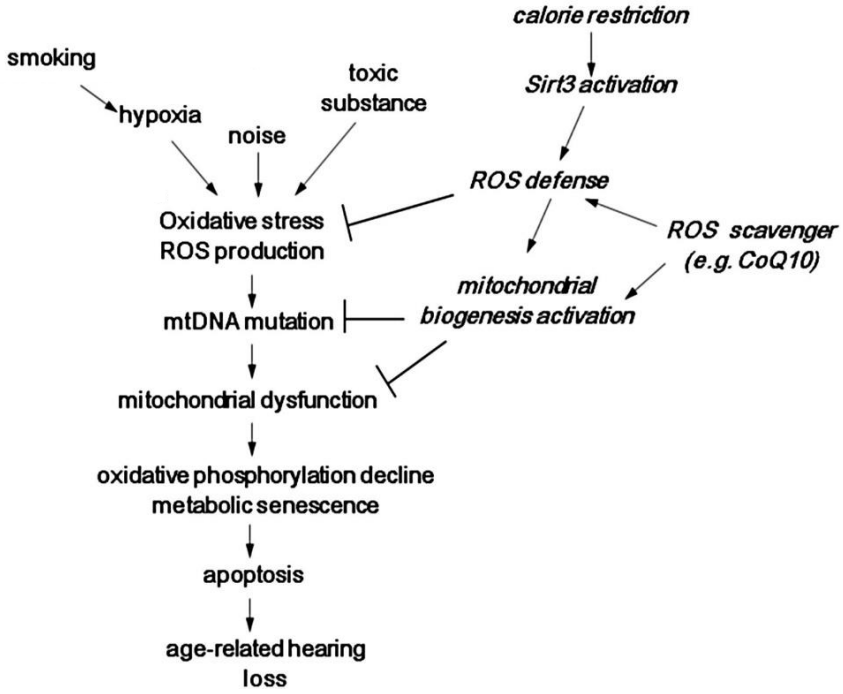

Figure 1.6 Conceptual model of the development of ARHL

(Adapted from Yamasoba et al., 2013)

1.4 Treatment of hearing loss: Cochlear implants

The treatment of hearing loss is dependent on the underlying cause, type and severity of the hearing impairment. Management can range from various types of amplification to more sophisticated middle ear, cochlear and brainstem implants. In patients with profound SNHL, cochlear implants are the most appropriate intervention strategy.

Cochlear implants are the most successful sensory prosthetic device developed to date, as shown by their capacity to restore some hearing to those with profound SNHL. With numbers continuing to rise, it is estimated that approximately 324,200 individuals have been implanted worldwide (National Institute on Deafness and Other Communication Disorders 2016). As discussed, normal cochlea function entails the conversion of acoustic energy via the hair cells of the Organ of Corti to electrical impulses which subsequently activate the neurones and SGCs of the auditory nerve. Information is then passed via the brainstem and auditory portion of the midbrain to the auditory cortex. Although SNHL may arise due to disorders at any point within this pathway, the majority are accounted for by damage to the sensory hair cells (Cosetti and Waltzman 2011). The fragility of these sensory components makes them particularly prone to a wide variety of insults including infections, ageing, drugs, noise and genetic defects. OHC losses cause degradation in frequency resolution and elevation of hearing thresholds, whereas destruction of the IHCs leads to a more profound hearing loss (Wilson and Dorman 2008b).

The function of the cochlear implant is, therefore, to bridge the gap left as a consequence of the missing hair cells. Consisting of a linear array of platinum electrodes, the prosthesis is inserted into the cochlea via the round window or through a cochleostomy, an opening into the cochlea generally sited anterior and inferior to the round window. The site of insertion is usually sealed with muscle tissue to prevent perilymph leakage. The electrode array is connected to a transducer mounted externally converting sounds into electrical signals. These signals act to stimulate remaining cochlear neural elements (spiral ganglion neurons) and provide the implant recipient with a useful representation of environmental sounds that assist the understanding of speech (Wilson and Dorman 2009).

1.4.1 Design and function of the cochlear implant

1.4.1.1 Components of cochlear implant systems

The key components within the cochlear implant system are illustrated below (Figure 1.7) with details regarding functionality given in Table 1.5. The raw signal detected by the external components comprising of the microphone and speech processor, is modified and refined prior to delivery to the implanted array. Various speech processing strategies are employed by the different implant manufacturers with the aim of converting the raw signal into one which highlights and retains features needed for speech recognition. The concept that speech consists of a variety of bands or formants of spectral energy forms the basis of many of the earlier speech processing strategies used in CI. These act to analyse the signal and identify the major spectral peaks in each frame before transmitting the information to the internal coil via inductive coupling through the skin.

Current devices use one or a combination of processing strategies which in broad terms aim to mimic the organ of Corti's tonotopic organisation. Information regarding consonants is conveyed across both low and high frequencies, whereas mainly lower frequencies correspond to vowels which are involved in the intonation, rhythm and the stress of speech. However, relaying an acoustic signal's temporal fine structure is often limited and therefore impacts on the CI users' perception of speech in noise (Fu et al., 1998; Schafer and Thibodeau 2004; Wolfe et al., 2009), perception of tonal language (Han et al., 2007; Xu et al., 2004) and their appreciation of music (Alexander et al., 2011; Gfeller et al., 1998).

In order for effective function of the implant, the individual components should work together as one system. A weakness within one component can cause a reduction in performance of the system as a whole. The auditory pathways within the brainstem and auditory cortex which act to convey the electrical information are also key components of the system. Variations in functional reliability and capabilities of this biological system can, therefore, explain the diversity of outcomes exhibited between implanted patients (Wilson and Dorman 2008a).

Figure 1.7 Components of a cochlear implant system

(A) Schematic of implant system in place

1. Microphone

2. Coil

3. Intracochlear electrode array

(B) Individual components of system

(Images from Cochlear® Ltd at www.cochlear.com)

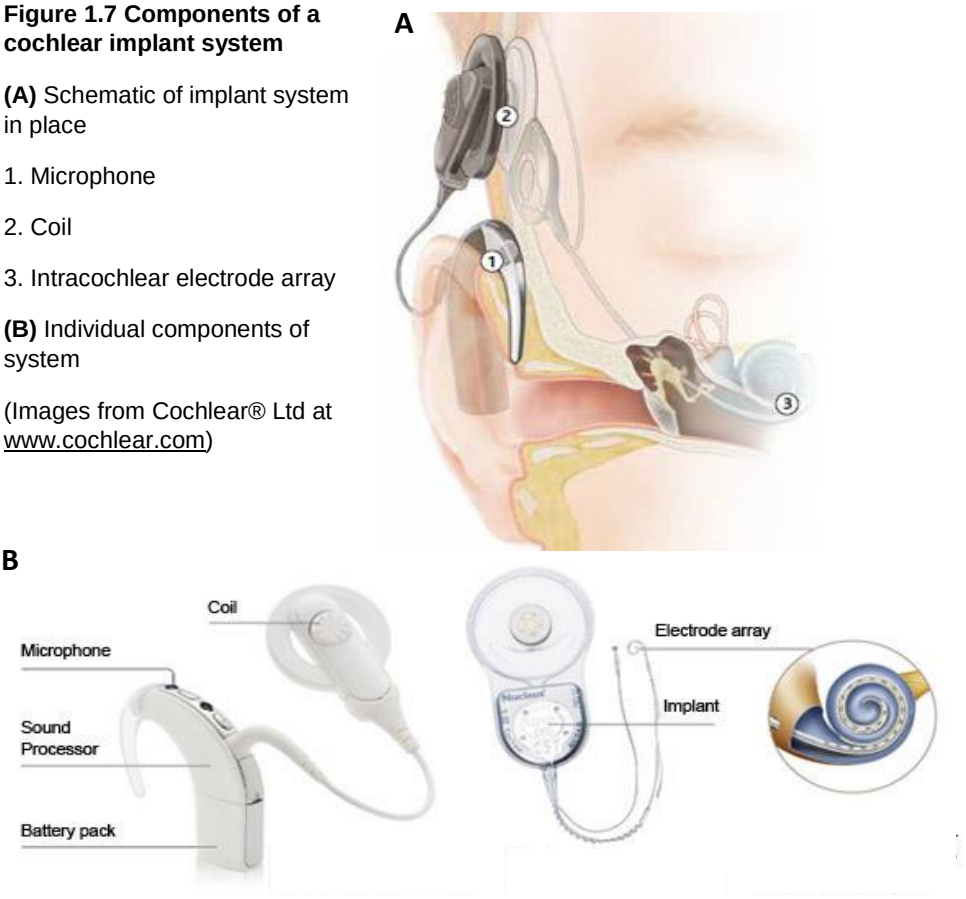

Table 1.5 Components of cochlear implant

Component	Function
Microphone	Environmental sound sensor
Speech processor	Transforms output from microphone into a set of stimuli for implanted electrode array
Transcutaneous link	Transmission of power and stimulus information across the skin
External transmitter coil	Produces radiofrequency signal
Receiver/stimulator	1) decodes information received from the external transmitter 2) uses the decoded information to generate stimuli
Multi-wire cable	Connects the outputs from the receiver/stimulator to the individual electrodes
Electrode array	Inserted into the scala tympani of the cochlea to provide electrical stimulation to neural components

1.4.1.2 Electrical stimulation of the auditory nerve

Both the afferent and efferent pathways between the peripheral and central auditory systems become disconnected as a result of the lack of hair cells in the deafened cochlea. In the absence of normal stimulation, without the presence of both sensory and supporting cells, peripheral cochlear nerve fibres which extend from the organ of Corti to cell bodies within the spiral ganglion, undergo retrograde degeneration. Whilst the underlying mechanism for this is controversial the overall result is the moderate to complete loss of peripheral processes within the cochlea (Shepherd and Javel 1997). The ultimate effect on SGCs, however, is variable as temporal bone studies have shown that they can often survive these insults and remain in large numbers (Hinojosa and Marion 1983). Survival of these neuronal cell bodies is important in CI as they are thought to be the presumed site of excitation, although should more peripheral processes be present, stimulation at these sites may also occur. The majority of CI systems in use at present require insertion into the scala tympani of the cochlea, with access gained either via the round window or a cochleostomy. Electrical currents pass along the array to electrodes lying within the scala tympani to produce stimulation of the remaining neural portions. The anatomical arrangement of the scala tympani lumen, which narrows from base to apex, together with the natural spiral curvature of the cochlea mean that insertion depths further than 30mm is precluded. The presence of partial cochlear ossification may also cause obstruction and limit insertion depth. Typical insertion depths vary from 18-26mm (Wilson and Dorman 2008a).

Cochlear implants are multichannel devices which are designed to allow stimulation of isolated neuronal subpopulations by each electrode contact when placed within the cochlea. The theory is that specific regional stimulation generates a different sound percept as the spatial arrangement of electrodes utilises the tonotopic arrangement of the cochlea. Low frequency tones are generated towards the electrodes placed more apically, whereas higher tones are generated by electrodes within the basal portion. Temporal coding of the auditory signal occurs based on the electrical stimulation of contacts over time. The number of nerve cells stimulated as a result of the current intensity stimulating a single contact determines loudness perception (Lenarz et al., 2013; O'Leary et al., 2009).

Current implant systems utilise a monopolar arrangement in which stimuli are presented to single electrodes within the array with reference to an electrode positioned in a more distant location, most commonly beneath the temporalis muscle or in some cases adjacent to the receiver/stimulator case. This wide spacing between the active and receiver electrode means that the current is spread over a wider neuronal range. A greater number of neurons are stimulated as a result and in turn this means that monopolar systems can achieve higher levels of loudness using comparatively lower levels of current and therefore, less battery power. The alternative is a bipolar system in which the electrodes are placed more closely as pairs with stimuli passing between them, hence stimulating a much more focused population of neurons. The monopolar system also has the advantage that differences in thresholds between electrodes within the array are much lower compared to the bipolar setup which in turn corresponds to increased ease and simplicity of speech processor fitting in patients (Wilson and Dorman 2008b; Wilson and Dorman 2009).

One challenge within the system is the non-specific stimulation of neurons adjacent to the target neuronal population which occurs as a result of current dispersal not only between electrodes, but also via the perilymph in a longitudinal manner along the cochlea. This means that although there can be between 12 and 22 electrode contacts within an implant, only around 8 distinct perceptual channels are available and functioning (Dorman et al., 1998; Friesen et al., 2001). This number is adequate for speech comprehension in quiet but not in the presence of background noise, where it is thought that up to 20 perceptual channels may be needed to hear well (Dorman et al., 1998). For users to appreciate music more than 30 channels which can also function on a specific spectral and temporal scale are required (Kong et al., 2004; Xu and Pfingst 2003). There are a variety of factors that can influence an implant's ability to stimulate a more discrete neuronal population. One is the proximity of the electrode to the target neurons. When the distance between the electrode and the nerve is increased, the current required to activate the target is increased which in turn leads to the greater perilymphatic spread and decay of the electrical signal. This can be overcome in part by increasing the space between electrodes, however, this also increases the distance over which the current will need to be transmitted, requiring more power. By bringing the neuronal

targets into closer apposition with the electrode, a smaller current can be used with less spread and reduced power requirements (Snyder et al., 2008; Wilson and Dorman 2008a; Wilson and Dorman 2009). One way in which this is achieved is through the use of perimodiolar electrodes. On insertion these implants curve to lay in closer apposition to the SGCs within the modiolus with electrodes positioned on the medial aspect of the electrode array. Although these implants have been shown to maintain tonotopicity, reduce thresholds, improve dynamic range and the specificity of neural excitation, these changes have not consistently translated to improvements in speech recognition or music appreciation (Shibata et al., 2011). Another important factor which can influence spatial specificity of the electrodes is the state of the implanted cochlea in terms of the presence of fibrosis, ossification and nerve survival. Improving spatial resolution at the electrode-neural interface may be approached in a variety of ways ranging from advancements in electrode design to improving the state of the implanted cochlear through soft-surgical techniques to studies exploring neuronal fibre regeneration. Such areas remain the focus of much ongoing research in the field and are necessary for gains in perceptual performance to occur.

1.4.2 Challenges in CI

1.4.2.1 Expansion of candidacy

Traditionally, candidates for cochlear implants have fallen into two main groups: infants and young children with congenital bilateral profound hearing loss; and postlingually deafened children and adults. The well-documented success in these groups has raised the profile of CI in the last 20 years. However, although the overall gains in these groups have been significant, there is still scope for improvement with regards to enhancing their understanding of speech in noise and appreciation of music. In order to address this and broaden the potential of CI, there have been continuing changes and improvements in technology and surgical technique. Such advances have also led to an expansion of candidacy to include groups who previously

would not have been considered such as children under the age of one, prelingually deafened adolescents and adults, patients with auditory neuropathy spectrum disorder, multiple disabilities or those with abnormal cochlear pathology such as deficient cochlear nerves (Cosetti and Waltzman 2011). Both children and adults have also reaped the benefits of bilateral CI which has shown positive results with regards to speech performance and sound localization (Bond et al., 2009). It has also led to patients with ARHL (Eshraghi et al., 2009; Lundin et al., 2013; Migirov et al., 2010; Noble et al., 2009; Rafferty et al., 2013; Sprinzl and Riechelmann 2010) and others with low-frequency residual hearing being implanted (Balkany et al., 2006; Boggess et al., 1989; Clark et al., 1995a; Gantz and Turner 2003; Hodges et al., 1997; James et al., 2005; Kiefer et al., 2004; Shiomi et al., 1999; Skarzynski et al., 2002)

1.4.2.2 CI in the elderly

Despite the increasing prevalence of ARHL with the expanding ageing population, CI in older patients has been met with hesitation. This is due to concerns regarding fitness for surgery, age-related degenerative changes in the auditory system and rehabilitative potential post-CI. However, research now suggests that age should not be used as the sole reason for rejecting an older patient for CI. The perception that advanced age is the key risk factor for general anaesthesia is outdated and several studies have shown that in fact it is well-tolerated and without significant morbidity and mortality (Alice et al., 2013; Coelho et al., 2009; Lundin et al., 2013). However, this is with the caveat that a thorough pre-operative evaluation is performed with relevant co-morbidities used as a predictor of perioperative complications rather than age alone (Carlson et al., 2010; Coelho et al., 2009). An intact auditory pathway, from functioning SGCs to cortex, is also required for successful CI and has been a further concern regarding CI in the elderly. A decline in general cognitive function and neural plasticity together with degenerative changes in the auditory system, both centrally and peripherally, means that there are multiple points at which the pathway may be adversely influenced by ageing, therefore affecting outcomes following CI (Cosetti and Waltzman 2011). Despite this a number of studies have shown improvements in speech perception after CI, with additional benefits in terms of

self-confidence and improved quality of life (Alice et al., 2013; Carlson et al., 2010; Eshraghi et al., 2009; Lundin et al., 2013; Migirov et al., 2010; Rafferty et al., 2013)

1.4.2.3 CI in patients with residual hearing

With regards to those patients with low-frequency residual hearing, implantation has involved use of electroacoustic stimulation (EAS) which comprises an electrode array for electrical stimulation of the higher frequencies, with conventional amplification to stimulate the low-frequencies. Many of the early studies into the use of EAS showed promising results following implantation including improvements in the patient's understanding of speech in noise and appreciation of music (Fraysse et al., 2006; Gantz et al., 2005; Gantz and Turner 2004; Gfeller et al., 2006; James et al., 2006; Lenarz et al., 2006). In many of these studies, however, hearing preservation outcomes varied as did the duration of follow-up.

A systematic review of EAS undertaken by Talbot and Hartley in 2008 included 253 EAS candidates from 23 trials where shorter electrodes were used. The results demonstrated some preservation of hearing in 87% of patients, with improvements in pitch perception. However, 24% of patients had a significant increase in their acoustic hearing loss and 13% lost all remaining residual acoustic hearing. The authors concluded that although the use of EAS shows great potential, the loss of residual hearing cannot be ignored, with ongoing larger clinical trials recommended (Talbot and Hartley 2008). Since the review, several authors have taken EAS forward with modifications in electrode design and surgical technique as discussed below.

A multicentre trial conducted in 2009 by Gantz and colleagues included 87 patients who were implanted with the 10mm Iowa/Nucleus Hybrid Implant (Hybid S, Cochlear™) consisting of 6 electrodes at its distal end. In an attempt to be minimally invasive and allow the best chance of preserving residual hearing, the electrode design was shorter (10mm), with a reduced diameter and was designed to sit within the scala tympani of the descending basal turn only, having been introduced via a cochleostomy. Initial results at one month post-CI showed that

residual low-frequency hearing was maintained in 98% of subjects and that some degree of hearing preservation was maintained between 3 and 24 months post-implantation in 91% of subjects. The majority of these patients found the use of EAS improved speech understanding compared to preoperatively when using bilateral hearing aids alone. However, 2 patients experienced complete hearing loss within the first month following implantation and a further 6 subjects in the subsequent follow-up period of 3 to 36 months. Overall, 91% of patients maintained some degree of hearing preservation. However, of those patients, 30% experienced threshold changes of more than 30dB (Gantz et al., 2009).

The Hybrid-L electrode (Cochlear™) is another shorter electrode (16mm) designed to be less traumatic but with a full complement of 22 electrodes, made to occupy 270° of the basal turn. In the case of the Hybrid S, if complete loss of residual hearing occurs, the patient may find the 6 active electrodes too few to gain appreciable hearing improvements and would therefore need to undergo removal and re-implantation with a longer electrode. With its 22 electrodes, the Hybrid-L has the advantage that should residual hearing be lost; the electrode can be used in the traditional manner without the need for replacement. Lenarz et al. (2009) reported preliminary findings of the Hybrid-L in a group of 32 patients, 24 of whom had substantial residual hearing at implantation. Use of EAS showed significant improvements in auditory performance in the implanted ear when compared to preoperative levels when using acoustic stimulation only. Their results showed that there were no cases of complete hearing loss and that residual hearing was preserved within 30dB and 15 dB in 96% and 68% of patients respectively. For the 16 patients for whom data at 12 months was available, 94% had maintained residual hearing within 30dB of the initial thresholds and 69% within 15dB (Lenarz et al., 2009). Other studies of EAS have also shown positive results in terms of hearing preservation, speech understanding and spatial awareness (Lorens et al., 2008; Skarzynski and Lorens 2010).

Despite the ongoing developments and improvements in EAS, the benefits gained have been overshadowed by the fact that a proportion of patients have lost a substantial part or all of their residual hearing in the implanted ear. This is significant since one of the major preconditions

of the device is hearing preservation. Although residual hearing appears to be preserved initially in many patients, progression of hearing loss can then occur at a faster rate than would be anticipated due to the natural process of their disease. The underlying cause of this loss remains unclear and prompts questions regarding the biological effects of CI on cochlear structure and function (Mowry et al., 2012; Santa Maria et al., 2013). Possible reasons for the loss have been proposed such as an immune reaction in response to the electrode and the impact of the combination of both acoustic and electrical stimulation at the hair cell causing loss of the afferent spiral ganglion neuron synapse (Mowry et al., 2012). In the early days of EAS it was anticipated that animal models would form the crucial basis for investigating many key questions such as the effects of electrical stimulation on the still functioning cochlea and preservation of hearing. However, as the initial clinical trials revealed such positive outcomes, the result has been for the basic science and clinical studies to progress alongside each other rather than in series (von Ilberg et al., 2011). The true long-term effects of EAS are yet to be ascertained. These concerns need to be addressed before EAS can be further extended in a wide-reaching manner to individuals with greater residual acoustic hearing such as children and elderly patients with ARHL.

1.4.2.4 Biological effects of CI

Intracochlear damage as a result of CI can be immediate or delayed. Immediate damage can occur at the site of insertion, along the electrodes trajectory and secondary to the disruption of the cochlear fluids. Delayed damage involves the host response to CI and the loss of function of intracochlear structures (Li et al., 2007). The extent of the traumatic damage and consequent potential death of remaining hair cells and neurons that is caused by the implant procedure is important due to the growing interest of CI in patients with residual hearing. Like many biomedically-active implantable devices, cochlear implants have the potential to provoke an acute inflammatory reaction initially. This then progresses to the chronic phase in response to the sustained presence of the electrode, ultimately resulting in the formation of a fibrous capsule around the implant (Richard et al., 2012). While a fibrotic reaction is most likely helpful

with respect to tissue repair at the site of insertion itself, increasing evidence suggests encapsulation of the implant significantly reduces electrical signal transmission between implantable devices and their target neurons. This may reduce the utility of the device by increasing power consumption, and increasing the spread of the electrical field generated by electrode stimulation (Fayad et al., 2009). The consequent reduction in the efficacy of signal coding, increases implant size, reduces battery life and in many patients the devices need to be replaced. It is not known whether the fibrotic reaction results from the surgical trauma at the site of the cochleostomy, from the muscle tissue used in sealing the incision, or from immune responses to the implanted foreign body within the cochlea, or a combination of any or all these factors.

1.4.2.5 Temporal bone studies of CI trauma

Evaluation of cochlear trauma and the effects of electrode insertion has generated ongoing interest from researchers. One of the first published studies documented mechanical damage from electrode insertion largely within the region of the spiral ligament (Shepherd et al., 1985). Since then there have been numerous studies. Investigation of the biological effects of CI in humans has mainly been restricted to cadaveric studies of temporal bones which have provided useful information (Cervera-Paz and Linthicum, Jr. 2005; Fayad et al., 2009; Kawano et al., 1998; Linthicum, Jr. et al., 1991; Marsh et al., 1992; Nadol, Jr. 1997; Nadol, Jr. et al., 2001; Somdas et al., 2007). Nadol et al. (2001) analysed the cochleae from 8 patients who had undergone CI with multichannel devices via cochleostomy. Duration of CI ranged from 1 to 8 years with patients aged between 54 to 84 years. Insertion-related trauma to the soft tissue of the lateral wall, predominantly of the ascending basal turn, was universal. Coinciding within the region of this trauma, neo-osteogenesis was also noted in 6 of the patients for whom there was no evidence of labyrinthitis ossificans pre-implantation. In 4 of the patients, the contralateral non-implanted temporal bone was available for comparison when assessing SGC numbers. The majority revealed no significant difference in terms of the SGC count. A negative correlation between SGC numbers and performance assessed during life using

single-syllable word recognition was also noted (Nadol, Jr. et al., 2001). These findings have been echoed by other authors (Fayad and Linthicum, Jr. 2006; Nadol, Jr. et al., 1994; Somdas et al., 2007). More recently, Seyyedi and Nadol (2014) analysed 28 temporal bones for an inflammatory response in patients implanted with multichannel devices. Their results revealed the presence of foreign body giant cell infiltration together with a granulomatous reaction in 27 of the 28 temporal bones. Significantly greater numbers of giant cells and lymphocytes were noted at the site of cochleostomy in comparison to the middle and tip portions of the electrode (Seyyedi and Nadol, Jr. 2014). All of the aforementioned studies were from temporal bones of patients who had undergone CI during life, however, cadaveric implants, where implants are performed on temporal bones after death, have also been used by researchers to provide valuable data on implantation trauma (Gstoettner et al., 1997; Shepherd et al., 1985; Welling et al., 1993).

1.4.2.6 CI trauma at a cellular and molecular level

Even in the absence of any macroscopic trauma, tissue trauma at a molecular level may still occur leading to hair cell damage and death (Eshraghi and Van De Water 2006). These mechanisms may be initiated via inflammatory and oxidative reactions. The presence of cytokines such as tumour necrosis factor alpha (TNF-α) is well-documented following injury in the cochlea and can initiate both intrinsic and extrinsic apoptotic programmed cell death pathways leading to hair cell death. The presence of reactive oxygen species following trauma can also activate apoptosis. The sustained presence of inflammation is associated with growth factors such as transforming growth factor-β1 (TGF- β1) which contribute to fibrous scar deposition through a fibroproliferative response (Bas et al., 2012a).

1.4.2.7 Surgical approach: round window vs cochleostomy

In order to ameliorate the effects of electrode insertion and minimise trauma, one focus has been to modify and optimise surgical techniques. Array insertion can be performed via the

round window or via a cochleostomy to access the scala tympani of the basal turn. Most surgeons have their own preference regarding their approach and as yet there is no consensus as to which is superior (Mangus et al., 2012). The round window provides direct access to the scala tympani and would appear to be the obvious choice, with several temporal bone studies demonstrating the potential for minimising collateral damage (Adunka et al., 2004; Briggs et al., 2006; Richard et al., 2012; Roland et al., 2007). Other advantages include avoiding noise exposure from the 130dB generated from drilling the cochleostomy (Pau et al., 2007) and a reduction in post-operative vertigo (Todt et al., 2008). However, negotiating the hook region on entering the round window is technically challenging, with the possibility of causing inadvertent damage to important structures which run in an anterior direction from the posterior round window margin such as the spiral ligament, basilar membrane, osseous spiral lamina and scala media. The alternative approach of the cochleostomy involves drilling a hole into the promontory to gain access to the scala tympani. Placement is usually anterior and superior to the round window membrane. This approach has the advantage that the hook region of the basal turn does not have to be negotiated (Mangus et al., 2012). Another method known as the extended round window approach, positions the cochleostomy at the anterior aspect of the round window. A recent meta-analysis of hearing preservation surgery for CI included 24 studies and revealed superior results with the cochleostomy approach compared to round window insertions. The former, however, included true cochleostomy approaches as well as extended round window insertions as the authors were unable to distinguish between the two when undertaking their analysis (Santa Maria et al., 2014).

1.4.2.8 Soft surgery in CI

Overall, it appears that rather than the approach itself, whether it be via the round window or via cochleostomy, the way in which the cochlea is opened, using a controlled and meticulous manner is the more relevant and vital factor in minimising trauma and preserving hearing. Aside from direct mechanical trauma, several other factors in CI are a potential source of injury and have the ability to compromise residual hearing. These include the displacement of blood

and bone particles into the perilymph during surgery, use of the drill giving rise to acoustic and vibratory trauma and the disruption of cochlear homeostasis and the endocochlear potential (Bas et al., 2012a). The concept of 'soft surgery' was first introduced in 1993 by Lehnhardt and has remained an important part of CI surgical methodology, especially with the increasing emphasis on hearing preservation (Lehnhardt 1993). The main aim of soft surgery is to avoid mechanical trauma to the cochlea and to minimise the initiation of factors that may promote adverse reactions such as the formation of fibrosis and neo-osteogenesis. The key factors, outlined in a review by Friedland et al. (2009) include the prevention of blood and bone dust entering the perilymph, as well as care in avoiding contact of the drill with the ossicular chain and cochlear endosteum. The use of hyaluronate, both as a protective agent and as a lubricant is also supported, as is the avoidance of suction of the perilymph and the use of systemic steroids (Friedland and Runge-Samuelson 2009; Laszig et al., 2002). Attention must also be paid to insertion depth and any resistance felt when introducing the electrode array as this may indicate that the tip is abutting the basilar membrane, lateral wall or osseous spiral lamina. Continued force could in turn lead to damage and potential misplacement of the electrode outside of the scala tympani (Carlson et al., 2012; Friedland and Runge-Samuelson 2009).

1.4.2.9 CI and therapeutics

Cochlear implants allow access to the inner ear and therefore the possibility of combining hearing rehabilitation with pharmacotherapy. Another area of key interest, therefore, is the use of drugs and therapeutics to reduce the adverse effects of inflammation and fibrosis and to also slow and potentially reverse the loss of neural components. Steroids have wide-ranging activity including anti-oxidative and inflammatory effects and have already been shown to be valuable in helping to preserve hearing in implantation-related trauma models by a number of groups (Eshraghi et al., 2007; James et al., 2008; Vivero et al., 2008). An apoptotic-inhibitor AM111 (D-JNK-1 inhibitor) has also been investigated in relation to implantation trauma by Eshraghi and Van de Water (2006) who demonstrated that treatment with D-JNKI-1 could

prevent the progression of hearing loss following electrode insertion trauma (Eshraghi and Van De Water 2006).

Trophic support for the spiral ganglion cells is provided by a variety of factors including brain-derived neurotrophic factor (BDNF) and neurotrophin 3 (NT-3), together with their receptors, tyrosine kinase B and tyrosine kinase C. Most hair cells have been found to express both neurotrophins, with the majority of neurons also expressing both receptors. Several studies investigating the role of the exogenous application of neurotrophins, BDNF or NT-3 in the deafened ear have found significant improvements spiral ganglion neuron survival (Altschuler et al., 1999; Nakaizumi et al., 2004; Staecker et al., 1998). In addition, the role of these factors in neuritogenesis also shows huge potential with in vivo studies demonstrating growth of peripheral neuronal fibres following aminoglycoside deafening and neurotrophin administration via the perilymph (Altschuler et al., 1999; Miller et al., 2007; Wise et al., 2005). Although regrowth has been disordered, more recent studies using viral vectors have shown directional growth patterns towards the basement membrane which will prove more useful in terms of CI where they will lie in closer apposition to the electrode array (Shibata et al., 2010; Wise et al., 2011). The combined effects of neurotrophic factors together with electrical stimulation have also been described with reductions in hearing thresholds and significantly greater spiral ganglion neuron rescue compared to the use of neurotrophins alone (Kanzaki et al., 2002; Shepherd et al., 2005).

Overall, the act of opening the cochlea and inserting a foreign body can provoke a biological response. Although this may be inevitable, the response can be modified through changes in surgical technique and through alterations in electrode design. It may also require further clarification into which of the intracochlear responses, provoked by implantation, has the most detrimental effect on residual hearing. This would subsequently help focus efforts towards other interventions in the form of therapeutics and allow the long-awaited gains in hearing preservation CI surgery to be made.

1.5 Role of animal models in CI

Aside from the assessment of human temporal bones, high resolution computed tomography (Aschendorff 2011; Kong et al., 2012; Tamir et al., 2012) and analysis of tissue on explanted electrode arrays (Clark et al., 2014; Fishpool et al., 2012) are the only other means of evaluating the effects of CI in humans. This inability to explore the biological effects of CI in patients has therefore led to the development of various animal models which play a key role in CI research to date. Animal models are the only means of assessing the effects of CI at a cellular and molecular level. Some of the first implants performed were in cats (Brennan and Clark 1985; Shepherd et al., 1983). Since then, several authors have taken advantage of this model. Chow et al. (1995) examined intracochlear ossification in relation to CI and found a significant correlation between the extent of new bone formation and an elevation in hearing thresholds (Chow et al., 1995). Kretzmer et al. (2004) used deaf white cats as a model of early-onset deafness to study their feasibility for investigating the neuronal aspects of CI (Kretzmer et al., 2004). More recently, Irving et al. (2014) devised a partial hearing model using kittens and adult cats to assess EAS (Irving et al., 2014b). Aside from cats, guinea pigs have been the other major animal model for CI. Early studies assessed electrical activity and morphological changes as a result of implantation (Duckert and Miller 1982; Duckert and Miller 1986; Hildesheimer et al., 1979; Spelman et al., 1980). More recently authors have continued to use guinea pigs as a means to assess delivery of therapeutics to the inner ear via pumps and gene therapy, quantify soft tissue responses, and assess nerve survival patterns in relation to CI (Addams-Williams et al., 2011; Atkinson et al., 2012; Nguyen et al., 2009; Pfingst et al., 2011). Other animal models for CI have included primates (Parkins 1989; Pfingst et al., 1979; Pfingst et al., 1995; Shepherd et al., 1995), sheep (Schnabl et al., 2012) and the chinchilla (Saunders et al., 1994). A key component in the selection of the previously mentioned animal models for CI has been the size and accessibility to the cochlea. In many cases, a full size human electrode array could also be used rather than the additional need to manufacture a bespoke array. Other factors such as well-established anaesthetic protocols and post-operative care will also have played a part in their selection.

In comparison to these models, the use of rodents such as rats, gerbils and mice is considered more challenging. This is due to the relatively small size of the cochlea as well as the presence of the stapedial artery running through the middle ear cavity, impeding access to the scala tympani for implantation. Another issue is the difficulty in developing a multichannel electrode array small enough for the rodent cochlea. Despite this, a number of authors have overcome such difficulties in both the rat (Hsu et al., 2001; Lu et al., 2005a; Nagase et al., 2000; Vischer et al., 1997) and the gerbil (Adunka et al., 2010; Ahmad et al., 2012; Campbell et al., 2010a; Campbell et al., 2010b; DeMason et al., 2012; Hessel et al., 1997).

1.5.1 Mice as a model for auditory research

The mouse is considered an invaluable model for investigating the genetic basis of human disease and is already widely used to explore a variety of conditions including cancer and diabetes. Advantages of mice over other animal models include their short life span, the fact that they can be handled in a controlled environment, their limited genetic heterogeneity and the ease with which they can be manipulated experimentally. In addition to this is the low cost in housing and maintaining mice, which can have significant economic benefits for researchers. Another key advantage is the availability of isogenic mice which allow more controlled studies within these groups and enable comparisons between groups. Next to the human, the mouse genome is the most well-characterised of all mammals. As such, over the last 50 years, mice have become an established model for auditory research and hold several advantages over other animal models.

The major similarities in anatomical structure of the auditory systems have resulted in mouse studies providing important insights into human ear function and ontogenesis. The histopathological evaluation of human auditory tissue can only be performed following death when numerous other factors can have an effect on investigative outcomes. Mice are therefore extremely useful for such assessment as analysis can be undertaken in a more controlled manner (Ahituv and Avraham 2002; Avraham 2003; Kikkawa et al., 2012). The human hearing range is between 20Hz to 20kHz whereas mouse hearing goes into the much

higher ultrasonic frequencies, with a range of between 1 and 100kHz (Reynolds et al., 2010). Although this means that the overlap is only around three octaves (2.5 – 20 kHz), evoked potentials on auditory testing in the mouse are very similar to those of humans. Use of auditory brainstem response (ABR) audiometry testing in the mouse is also minimally-invasive, low cost and simple to perform and provides a consistent means of assessing the peripheral auditory neural pathway (Scimemi et al., 2014).

Mice share a high degree of genetic homology with humans, with many of the auditory mouse genes displaying strong geno- and phenotypic similarities to their human counterparts (Kikkawa et al., 2012). The diverse range of naturally occurring and genetically-modified mouse strains which mimic human deafness have allowed significant progress in the field of hearing research to be made. Mutant strains exist through the presence of spontaneous mutations or via mutations induced using radiation or chemicals. In the case of the latter, examples include the use of N-ethyl-N-nitrosourea (ENU) to create novel models of hearing impairment such the *Junbo* mouse model of otitis media (Parkinson et al., 2006). Gene-targeted knockouts are a more recent method of producing mutant strains. A key example is the specific removal of Cx26. The embryonic lethality of Cx26 knockouts had previously limited in vivo attempts to investigate the role of Cx26 in NSHL. However, with targeted ablation, the authors were able to overcome such problems, providing insight into the importance of Cx26 in the development of the organ of Corti and cochlear function (Cohen-Salmon et al., 2002).

Inbred mouse strains have been used extensively to investigate age-related and noise-induced hearing loss. Mouse models have helped to identify around 20 ARHL (*ahl)* loci for which 4 of the underlying genes have been isolated. The proteins encoded by three of the genes *(Cdh23, Gipc3 and Fscn2)* are vital for hair cell stereocilia structure. In particular, cadherin 23 is an important component of tip links, filamentous links which act as gates to transduction channels at the tip of the stereocilia of immature hair bundles (Michel et al., 2005). Several inbred strains possess the *Cdh23*^{ahl} allele including the C57BL/6J mouse which is homozygous for this defect. This strain in particular shows progressive loss of hair cells together with other changes such as spiral ligament, stria vascularis and afferent neuron

degeneration (Ohlemiller 2006). Elevated hearing thresholds in these mice are seen as early as 3 months of age and correlate with the progressive loss of both OHCs and IHCs, from the basal to apical cochlea, in an age-related fashion. OHC loss in the basal region occurs first, followed by basal IHC loss between 3-7 months with subsequent SGC loss and neuronal degeneration (Hequembourg and Liberman 2001). In contrast to the early-onset HL seen in the C57BL/6J mouse, another commonly used strain, the CBA mouse, exhibits a much later pattern of progressive HL at around 22-25 months of age. Hearing loss in these mice is not linked to the *Cdh23*^{ahl} allele. Instead, the presence of an ahl-allele causes a gradual deterioration in the high-frequencies as they age, similar to humans (Park et al., 2010).

1.5.2 Mice as a model for CI

Despite their suitability for auditory research, there are disadvantages to the use of mice and some of these may represent possible reasons as to why its use as a model for CI has been precluded thus far. The small auditory bulla and cochlea of the mouse makes access difficult. The mouse cochlea is around a third of the size of the guinea pig, with an average size of 2.8mm x 3.5mm (Jero et al., 2001). Electrode implantation is therefore technically challenging and this in combination with the lack of availability of an implant of sufficiently small size has meant that there are very few published studies of CI in mice to date.

Authors have, however, accessed the murine cochlea for other reasons. Jero et al.(2001) first described the paramedial (ventral) approach to access the mouse cochlea in order to deliver a gene therapy vector (Jero et al., 2001). This approach has also been used by other research groups (Chen et al., 2006; Jero et al., 2001). Do et al. (2004) used a postauricular approach in the CBA/Ca mouse to investigate acute hydraulic trauma in the cochlea. The authors did this by means of an alteration in perilymph volume, generated by a bolus injection into the basal turn via the round window (Do et al., 2004). Other authors have also used the postaural approach to gain access to the auditory bulla to enable cochleostomy and cell injection (Bogaerts et al., 2008) as well as for the inoculation of adenovirus vectors for gene therapy (Kawamoto et al., 2001; Praetorius et al., 2003). More recently, Akil et al. (2012) adopted both

the ventral and postauricular techniques to perform gene therapy via a round window and cochleostomy approach (Akil et al., 2012).

Devising a reproducible and viable model of mouse CI is the next logical step and would enable the many positive aspects, which are already being exploited in other areas of auditory research, to be harnessed in CI studies. Developing a mouse model of CI would provide a means for further exploring the interface between the biological and technological aspects of CI. With growing interest in drug delivery and neural engineering to enhance the efficacy of CI, many are looking towards the use of improved animal models. The establishment of a mouse model will also be advantageous in this area as it will allow further exploration of the regulation of neurotrophins and the development of mechanisms for delivering therapies to the cochlea.

1.6 AIMS

The aims of this study are to:

1. Develop a reproducible and viable surgical technique for mouse CI.

2. To assess functional outcomes following mouse CI in the absence of electrical stimulation.

3. To assess the histopathological effects of mouse CI, in the absence of electrical stimulation.

CHAPTER 2: MATERIALS AND METHODS

2.1 MATERIALS

2.1.1 Drugs and nutritional support

The various drugs and nutritional support used are given below in Table 2.1.

Table 2.1 Drugs and nutritional support

Drug/Product	Trade name	Concentration	Supplier
Ketamine	Narketan®-10	10mg/ml	Vétoquinol UK Limited (Buckingham, UK)
Medetomidine	Domitor®	0.1mg/ml	Orion Corporation (Espoo, Finland)
Atipamazole	Antisedan®	5mg/ml	Orion Corporation (Espoo, Finland)
Buprenorphine	Vetergesic®	0.3mg/ml	Reckitt Benckiser Healthcare UK Ltd (Kingston upon Thames, UK)
Carbomer (Liquid tears)	Viscotears®	2mg/g	Novartis AG (Basel, Switzerland)
Nutrient fortified water gel	DietGel® Recovery	n/a	Clear H2O (Portland, Maine, USA)

2.1.2 Surgical equipment

The surgical equipment used is given below in Table 2.2.

Table 2.2 Surgical equipment

Equipment	Supplier
All surgical instruments including dissecting forceps, scissors, blades, small animal magnetic fixator retraction system and small vessel cauteriser kit.	Fine Science Tools (Interfocus Ltd, Linton, UK)
Specialised animal recovery chamber	Harvard Apparatus Ltd (Kent, UK)
Skeeter drill with 0.5mm burr	Medtronic Ltd (Hertfordshire, UK)
Surgical drapes, disposable gowns, surgical skin preparation fluid and masks	3M Healthcare (Bracknell, UK)
Sterile surgical gloves	Premier Healthcare & Hygiene Ltd (Tyne and Wear, UK)
Fluorocarbon thread (‘dummy’ implant, 0.185mm tip diameter)	Grand Max Soft-Plus, Kureha Corporation (Tokyo, Japan)
Electrode array (0.21mm tip diameter)	Cochlear™Ltd
5-0 monocryl suture	Ethicon (Livingston, Scotland, UK)
Histoacryl® tissue adhesive	TissueSeal LLC (Ann Arbor, MI, USA

2.1.3 Laboratory equipment

All reagents and materials used in tissue preparation and for immunofluorescence were purchased from Sigma-Aldrich (Dorset, UK) unless otherwise stated.

2.2 METHODS

2.2.1 Animal Surgery

2.2.1.1 Choice of mouse strain

C57BL/6J mice aged 3 and 6 months were used. This strain exhibits an early-onset hearing impairment which begins in young adulthood around 3-4 months of age. This pre-disposition is related to a defect in the Cdh23ahl allele of the cadherin 23 gene, a vital component of stereocilia of hair cells (Ohlemiller 2006). Hearing loss occurs spontaneously without the need for ototoxins or noise, typically starting with the high frequencies at the basal cochlear portion and progressing to involve the lower frequencies over a time period of 12-15 months. In the latter stages, hearing loss is profound with corresponding sensorineural changes observed on cochlear histopathology (Henry and Chole 1980; Mikaelian et al., 1974; Ohlemiller 2006; Willott 1990). As a result of this progressive high to low frequency hearing loss, C57BL/6J mice are an established model to study age-related hearing loss (Ohlemiller 2006; Prosen et al., 2003; Shnerson and Pujol 1981; Spongr et al., 1997; Willott 1990).

For the purposes of the current study, mice aged 3 months and 6 months were used. Three month old mice typically have near normal hearing thresholds or may start to show signs of hearing loss affecting higher frequencies only. At 6 months, this high frequency sensorineural hearing loss is established and may progress to include mid-frequencies. Use of the older mice is important as it allows assessment of implantation on residual hearing and enables investigation to see whether or not the act of implantation accelerates hearing loss by comparing results with the younger age group.

C57BL/6J mice were obtained from our own breeding colony and were housed in suitable conditions with free access to food and water. All work was performed in accordance with regulated, licensed procedures of the British Home Office Project Code (1276). Work was approved by the Animal Ethics Committee of UCL.

2.2.1.2 Pre-, intra- and postoperative procedures

As the main aim of the project was to develop a viable and reproducible mouse model of cochlear implantation, much of the detail regarding the choice of anaesthetic, operative planning and procedure are discussed in the subsequent results chapter. A brief outline of the pre-, intra- and postoperative care undertaken is discussed below. The choice of surgical technique was influenced by a desire to maximise the information yielded from experiments whilst minimising the number of animals operated upon and of the invasiveness of the surgery in line with Home Office regulations.

A designated operating facility was set up and surgery performed under sterile conditions. C57BL/6J mice were weighed and anaesthetised using intraperitoneal ketamine (Narketan®-10, Vétoquinol UK Limited, 0.01ml/g of 10mg/ml) and medetomidine (Domitor®, Orion Corporation, Finland, 0.005ml/g of 0.1mg/ml). Half dose of buprenorphine (Vetergesic®, Reckitt Benckiser Healthcare (UK) Limited, 0.1mg/kg of 0.03mg/ml) was also given at induction and anaesthesia confirmed by the absence of pedal reflexes. Body temperature was maintained at 37˚C using a heated mat and monitored using a rectal thermometer. Following induction of anaesthesia, fur in the left post-aural region was shaved to expose the skin. This area was subsequently prepared using topical chlorhexidine and the animal placed on a heated mat in a semi-prone position. Surgical drapes were used to maintain a sterile operating field. Care was taken to ensure that the depth of anaesthesia could be monitored and if required, supplemental anaesthetic was given for maintenance purposes. Eyes were coated with a lubricating eye gel to protect the corneas from abrasions.

Following a post-auricular incision, the round window was accessed and implantation performed. Two types of implant were used. One was an inert fluorocarbon thread ('dummy' implant; 0.185mm tip diameter, Grand Max Soft-Plus, Kureha Corporation, Japan) (n=21). The other was a specialised electrode array (n=16) comprising parylene coated platinum/iridium wire with 4 electrodes, measuring 0.21mm in diameter at the tip (supplied by Cochlear Ltd). In all instances, the contralateral right cochlea acted as a control. Intraoperatively, great care was taken to maintain body temperature and prevent hypothermia using a heated mat and adequate draping of the animal. Temperature monitoring was performed using a rectal thermometer.

In the immediate post-operative period, the mouse was placed within an animal recovery chamber (Harvard Apparatus Ltd, Kent, UK) to maintain body temperature at 37˚C. The remaining dose of buprenorphine was administered together with subcutaneous warmed saline according to body weight and the reversal drug atipamazole (Antisedan®, Orion Corporation, Finland, 0.002ml/g of 0.5mg/ml subcutaneously). Supplemental oxygen was also given to support recovery via an adapted face mask.

Once the mouse had regained normal activity it was transferred to a cage and housed singly, with free access to water, wet mash and DietGel® Recovery (Clear H2O, Portland, ME). Mice were monitored for any signs of pain or distress and further analgesia was administered as required. Weighing and general examination of the surgical site for signs of haematoma, infection and wound dehiscence were undertaken on a daily basis for the first week and weekly thereafter. The animal's general appearance and behaviour was also noted, as was the presence of any signs to suggest vestibular dysfunction including circling, head-bobbing, head-tilting and abnormal reaching responses. Mice were sacrificed and tissue harvested at 48 hours, 1 week, 4 weeks and 12 weeks after implantation.

2.2.2 Auditory brainstem response audiometry (ABR)

ABRs were recorded in all animals preoperatively and at appropriate time points following implantation. General anaesthesia was induced and maintained using intraperitoneal ketamine (0.01ml/g of 10mg/ml) and medetomidine (0.003ml/g of 0.1mg/ml). Body temperature was maintained at 37˚C using a heated mat and checked using a rectal thermometer. Examination of the external auditory canal under the microscope was undertaken to check for occluding wax. If present this was carefully removed with a wax hook. Needle electrodes were placed subdermally at the hind leg (ground), vertex (active) and lateral to the cheek (reference) of the ear being tested. Testing was carried out in a soundproof booth and acoustic stimuli were delivered via a directional speaker into the external auditory canal (EAC) of the tested ear (See section 2.2.2.1 for justification of set-up used). Click-evoked responses were first acquired followed by those to tone pip stimuli at frequencies of 8, 12, 24, 32 and 40 kHz. Clicks and tones were delivered at 10dB intervals using the Tucker Davis Technologies System III (Tucker-Davis Technologies, Alachua, Florida, USA). Calibration of the equipment was performed regularly by Dr Ruth Taylor.

Thresholds were determined by visual inspection to identify the lowest sound pressure level at which clear waveforms were apparent. In cases where there was no ABR waveform, at the highest stimulus level, a threshold of 90dB was noted. For those mice in which the implant was retained for 4 weeks or more, ABR's were also performed at 2 and 4 weeks and at further time points of 8 and 12 weeks postoperatively in mice kept for up to 12 weeks. Comparisons between the implanted and control ears were made across the various time points and statistical analysis was performed using a paired samples T-Test (IBM SPSS Statistics 21.0) with a value of $P<0.05$ used to define significance.

2.2.2.1 Justification of ABR technique

When performing the ABR testing for individual ears, a directional sound delivery method was used into the EAC of the tested ear. The opposite, untested ear was not routinely occluded (Figure 2.1A). In order to ascertain the effects of occlusion and whether it is necessary ABR

testing was undertaken in the same mouse with and without the use of occlusion. Occlusion of the ear canal was performed using an expandable foam ear plug which filled the canal. The test was performed in the absence of any occlusion, occlusion of the opposite (untested ear), occlusion of the test ear (in order to check the contribution, if any, of the non-tested ear) and with both ears occluded (Figure 2.1B-E). From the results it can be seen that occlusion contributed little to the overall ABR outcomes (Figure 2.1 and Figure 2.2). The results with and without occlusion of the non-test ear were identical suggesting that use of the occlusive foam plug did not make any difference. Where the test ear was occluded, small changes were noted in thresholds (≤10dB). Figure 2.3 shows the mean thresholds of 3 mice tested under occluded and non-occluded conditions. As shown, there was found to be very little difference between the two test conditions suggesting that occlusion would not have significantly altered outcomes of functional testing.

2.2.3 Cone beam computed tomography

Cone beam CT (CBCT) is an upcoming imaging modality which has several advantages over other imaging techniques, including higher resolution images, faster image acquisition and a reduction in metal artefact. There is growing interest in its use to assess CI patients pre- and post-operatively, in particular with regards to the latter to assess scalar electrode position (Saeed et al., 2013; Saeed et al., 2014). In view of this, it was deemed an appropriate method to assess electrode placement in the mouse post-CI.

Following implantation with the electrode array and post-sacrifice, CBCT was performed to assess electrode placement using a 3D Accuitomo F170 scanner (J. Morita Mfg. Corp, USA - access courtesy of Cavendish Imaging, London, UK). The mouse was positioned for optimal imaging of the auditory bulla with the implanted electrode array in place. Parameters used for scanning included a tube voltage of 97kV and a tube current of 5-7 mA. The total scanner rotation time was 17.5 seconds with a cylindrical acquisition volume of 6 x 6cm (diameter x height). A 3D volumetric dataset was obtained with an isometric voxel size of 250µm and reconstructed images were examined using OneVolumeViewer™ and Amira® software.

A

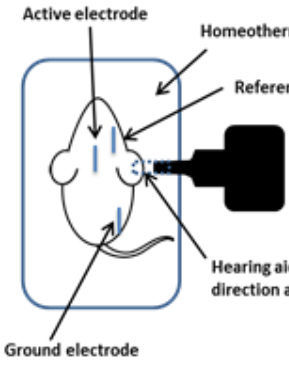

Standard ABR set-up – right ear being tested

B

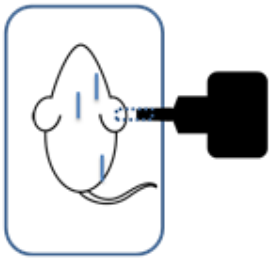

No occlusion

Stimulus	Right ear (dB)	Left ear (dB)
Click	10	10
8kHz	30	30
12kHz	20	20
24kHz	30	40
32kHz	60	60
40kHz	70	70

C

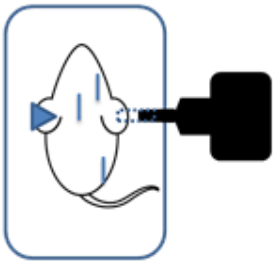

Opposite ear occluded

Stimulus	Right ear (dB)	Left ear (dB)
Click	10	10
8kHz	30	30
12kHz	20	20
24kHz	30	40
32kHz	60	60
40kHz	70	70

D

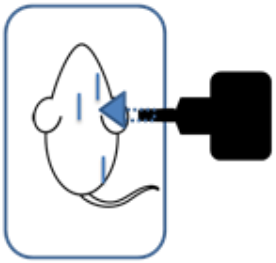

Test ear occluded

Stimulus	Right ear (dB)	Left ear (dB)
Click	20	20
8kHz	30	30
12kHz	30	30
24kHz	30	40
32kHz	60	70
40kHz	70	80

E

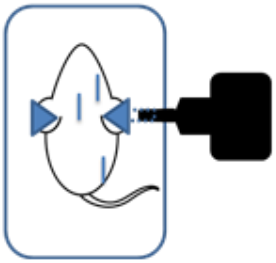

Both ears occluded

Stimulus	Right ear (dB)	Left ear (dB)
Click	20	20
8kHz	40	40
12kHz	20	20
24kHz	30	40
32kHz	60	70
40kHz	80	80

Figure 2.1 ABR set-up and occlusion experiment

Standard ABR set up (A) and results following occlusion experiment (B-E). NB: electrodes are shown on right side for example of right ear testing. Electrodes were moved accordingly to the opposite side for left sided testing.

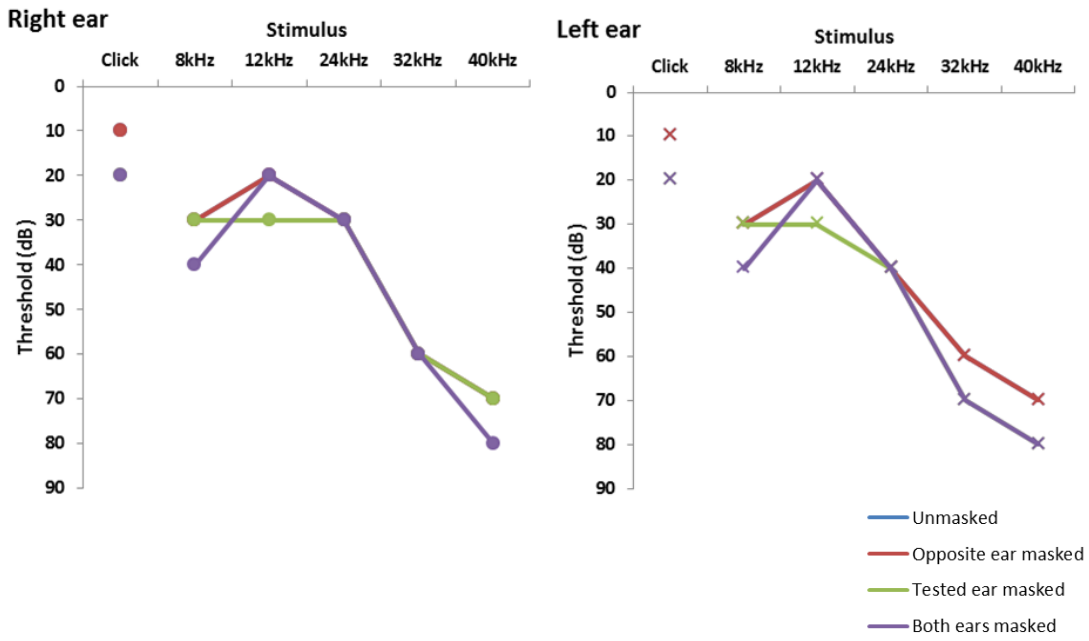

Figure 2.2 Results of occlusion experiment

Results from non-occluded and occluded ears revealed very similar thresholds on ABR testing.

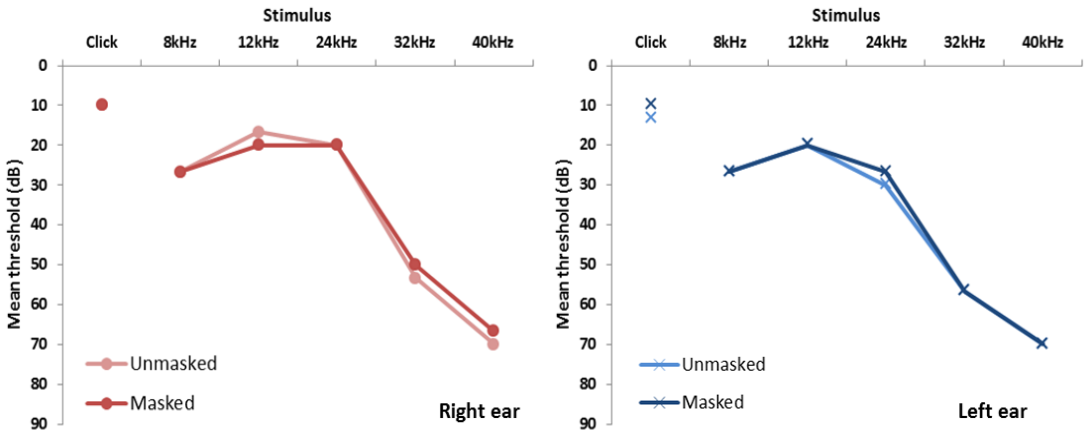

Figure 2.3 Mean ABR thresholds with and without occlusion

Mean thresholds in 3 mice who underwent ABR with and without occlusion.

2.2.4 Sacrifice and harvesting of cochleae

Mice were sacrificed following the final postoperative ABR either by cervical dislocation alone or by CO_2 inhalation followed by cervical dislocation in accordance with Schedule 1 of the United Kingdom Animals (Scientific Procedures) Act of 1986. Following decapitation, the overlying skin was cut and the bony skull exposed and opened along the sagittal suture line to access the brain tissue. Closed forceps were used to remove the brain tissue in a ventral to dorsal direction. Once the skull base was exposed, the auditory bullae were separated from the temporal bone and the cochleae exposed, taking care not to displace the implant.

2.2.5 Cochlear preparations

2.2.5.1 Tissue fixation

Once isolated, fixative was gently perfused into the cochlea via an opening made by removing a small section of bone at the apical tip of the cochlea. The implant was retained in position and the cochleae were then immersed in fixative at room temperature and left on a rotator for 2 hours. Fixative was either 4% paraformaldehyde in PBS for immunohistochemistry or 2.5% glutaraldehyde in 0.1M cacodylate buffer with 3mM $CaCl_2$ for examination by electron microscopy. Post fixation, cochleae were decalcified in 4.13% ethylenediamine tetra-acetic acid (EDTA) in phosphate buffered solution (PBS) or 0.1M cacodylate buffer respectively, for 48 hours at 4˚C. Following fixation, the implant was carefully removed unless otherwise stated.

2.2.5.2 Cryosections

Following decalcification, cochleae were rinsed in PBS and incubated in 30% sucrose in PBS at 4˚C overnight. They were then embedded in 1% low-temperature setting agarose gel in 18% sucrose in PBS with sodium azide (NaN_3). After pouring the gel into 35mm petri dishes, the cochleae were submerged and orientated and gel allowed to set at room temperature. Parafilm™ was used to seal the Petri dishes which were kept at 4˚C until required. Blocks of

agarose containing the cochleae were cut and mounted on cryostat supporting stubs with the aid of optimum cutting temperature (OCT) mounting medium (Tissue-Tek OCT Compound, Sakura, Finetek UK Ltd) before being rapidly frozen in liquid nitrogen. The mounted stubs were positioned within a Leica CM1900 cryostat for 30 minutes to allow the specimen to acclimatise to the temperature (-20˚C). Tissue was sectioned at 14µm and the sections mounted on poly-L-lysine-coated slides (VWR, UK). Slides were kept stored at -20˚C until they were required.

2.2.5.3 Toluidine blue staining

In preparation for examination, frozen sections were stained with toluidine blue (0.005%) and viewed by light microscopy.

2.2.5.4 Plastic embedded cochleae for light microscopy and transmission electron microscopy (TEM)

Cochleae implanted with the fluorocarbon thread were plastic embedded for further evaluation. The decalcified cochleae with the retained implant were immersed in 1% OsO_4 (osmium tetroxide) in 1 mM cacodylate buffer for 2 hours for further post-fixation. Dehydration was achieved in an ethanol series, en-bloc stained at the 70% ethanol stage using a saturated solution of uranyl acetate in 70% ethanol at 4˚C overnight. The dehydration process was then completed to 100% ethanol and the whole cochlea embedded in plastic resin. In order to assess the position and orientation of the implant within the cochlea, sections were cut approximately parallel to the modiolus at 0.5-1µm thick for light microscopy analysis and stained with toluidine blue. For the purposes of TEM, a series of thin sections (80nm) were cut. This preparation of cochleae was carried out by Mr Graham Nevill. TEM images were taken and collected using a Gatan camera by Professor Andy Forge.

2.2.5.5 Whole mounts

Following decalcification, cochleae were dissected as per the method used by Charles Liberman at Eaton Peabody Laboratories (Massachusetts Eye and Ear Hospital, Boston, MA, USA). Cochleae were bisected through the modiolus to yield two half turns. Each half was then cut into half turns to provide a series of arcs which were then trimmed. The modiolar nerve stump and spiral ligament of each half turn was removed, above and below the basilar membrane, together with the remnants of any bony cochlear capsule. Both the Reissner's and tectorial membranes were also removed. Whole mount sections were stored in PBS containing NaN_3 at 4˚C until required.

2.2.6 Immunofluorescence and confocal microscopy

Prior to the application of reagents, sections on slides were marked using a PAP pen (ImmEdge Hydrophobic Barrier Pen, Vector Laboratories, Peterborough, UK) to ensure that reagents remained localized. In the case of whole mounts, 72-well plates were used to retain the organ of Corti segments for immunolabelling. All processing was performed at room temperature in humidified chambers unless otherwise detailed. Frozen sections or whole mount segments were permeabilised by incubation in 0.5% Triton X-100 (Sigma) for 20 minutes (30 minutes for whole mounts) at room temperature then exposed to a blocking solution consisting of 10% goat serum in PBS for 2 hours at room temperature. After brief PBS washes the samples were incubated with the primary antibody (see Table 7a below) in 10% goat serum in PBS overnight at 4°C. In the case of negative controls, primary antibodies were omitted. After six 3 minute washes in PBS, the specimens were incubated with appropriate fluorescently conjugated secondary antibodies (see Table 7b below) for 2 hours at room temperature. Alexa Fluor® 633 phalloidin (Invitrogen, Paisley UK) was added at a dilution of 1:500 to the secondary antibody solution. After six 3 minute washes in PBS the slides were cover slipped using an antifade mountant containing 4',6- diamidino-2-phenylindole (DAPI) to label nuclei (Vectashield; Vector Laboratories, Peterborough, UK) and sealed with clear nail varnish.

Slides were imaged using a Zeiss LSM 510 confocal laser scanning microscope. Images were obtained using various objectives (20x (dry), 40x (oil), and 63x (water)) and documented as single, sequential or Z-series stacks (optical slice thickness of 1µm). Settings such as the pinhole and power of the lasers were kept consistent to allow comparative assessments to be made. The fluorochromes used for immunofluorescence included DAPI (excitation/emission 358/461nm), FITC (Fluorescein Isothiocyanate, ex/em 490/525nm), TRITC (Tetramethylrhodamine isothiocyanate, ex/em 544/572nm) and Alexa 633 (ex/em 632/647nm) and were excited by wavelengths of 405nm, 488nm, 543nm and 633nm laser lines respectively.

Table 2.3 Primary antibodies used for immuno-labelling

Antibody	Host/Type	Source	Dilution	Antibody Number	Labelling
Calretinin	Rabbit polyclonal	Thermo Scientific (Fisher, Loughborough, UK)	1:200	11521663	Inner hair cells, neurons, SGCs
CD45 (leucocyte common antigen)	Rat monoclonal	Chemicon (Millipore, Watford, UK)	1:200		Macrophages
F4/80	Rat monoclonal	Abcam (Cambridge, UK)	1:200	ab6640	Macrophages
Myosin VI	Rabbit polyclonal	Sigma-Aldrich	1:100 1:200	M5187	Inner and outer hair cells
Myosin VIIa	Mouse monoclonal	Hybridoma Bank, Univeristy of Iowa	1:200	N/A	Inner and outer hair cells
Parvalbumin	Mouse monoclonal	Sigma-Aldrich	1:50 1:100	P3088	Inner and outer hair cells

Table 2.4 Secondary antibodies and fluorescent-conjugated probes

Antibody/Probe	Host/Type	Source	Dilution	Antibody Number
Anti-rabbit FITC	Goat	Sigma-Aldrich	1:200	F6005
Anti-rabbit TRITC	Goat	Sigma-Aldrich	1:200	T6778
Anti-rat FITC	Goat	Sigma-Aldrich	1:200	F6258
Anti-mouse TRITC	Goat	Sigma-Aldrich	1:200	T5393
Anti-mouse Alexa Fluor 488	Goat	Invitrogen	1:200	A10667
Phalloidin Alexa Fluor 633	N/A	Invitrogen	1:500	A22284

2.2.7 Cell counts

Cochlear sections taken from mice at each of the four time points (48 hours, 1 week, 1 month and 3 months) for both types of implant (fluorocarbon rod and specialised electrode array) and immunostained with CD45 and calretinin were analysed. CD45 positively-labelled cells at lower basal, upper basal and apical turns of mid-modiolar sections were counted using ImageJ software (http://rsbweb.nih.gov/ij/). Only cells demonstrating characteristics typical of leucocytes such as being pleomorphic in shape with an irregularly shaped nucleus, were counted. Comparisons of mean counts based on location in the cochlea and across time points were made. Statistical analysis of data was performed using T-Test (IBM SPSS Statistics 21.0) with a value of $P<0.05$ used to define significance.

In the same sections, calretinin staining demonstrated SGCs within Rosenthal's canal. Projections of z-stacked images were taken and the density of SGCs calculated. This was done by defining the area of Rosenthal's canal in each analysed section using ImageJ software and counting only those cells with a visible nucleus. Comparisons were made using a T-Test (IBM SPSS Statistics 21.0) with a value of $P<0.05$ used to define significance.

Hair cell counts were performed on whole mount segments taken from implanted mice and immunolabelled with myosin VIIa. The total number of IHCs and OHCs in 100µm sections

were counted at basal, mid-basal, mid-apical and apical regions of the cochlea. The number of hair cells in implanted and control cochleae were ascertained and comparisons made using a T-Test (IBM SPSS Statistics 21.0) with a value of $P<0.05$ used to define significance.

CHAPTER 3: DEVELOPING A MOUSE MODEL OF COCHLEAR IMPLANTATION

3.1 Introduction

One of the main challenges facing CI researchers investigating biological effects of implantation is the lack of access to human auditory tissue during life. This has therefore led to the development of animal models which play a key role in research and, at present, are the only means of assessing effects of CI at a cellular and molecular level. The development of an appropriate animal model requires a number of factors to be taken into consideration. To provide an accurate reflection of human disease, similarities in physiology and anatomy are important, as are the animal's ability to correctly represent the biochemical and morphological characteristics of the disease in question. Other factors such as life-span, genetic background, availability, cost, housing, handling and reproductive capacity are also important (Smith and Baran 2013).

In view of the aforementioned characteristics, the mouse is considered to be a prime model for the investigation of human disease and over the last 50 years has become an established model for auditory research. Mice share a high degree of genetic homology with humans. There are also anatomical and physiological similarities between the mouse and human auditory systems, which to date have provided important insights into human ear function and ontogenesis (Ahituv and Avraham 2002; Avraham 2003).

Despite the similarities between the murine and human ear there are very few published studies of CI in mice. This is largely due to the technical difficulty of implantation and, until recently, CI technology has not been able to deliver an implant small enough. Overcoming these challenges to produce a viable and reproducible model of mouse CI would be hugely valuable and enable the many positive aspects, which are already being exploited in other areas of auditory research, to be utilised in CI studies.

3.2 Aims

The main aim of this thesis is to develop a viable and reproducible mouse model of CI. In order to achieve this, the following aims were set out and will be discussed in this chapter.

1. To develop an anaesthetic protocol to allow CI in mice.
2. To perform sham surgery in mice to assess the viability of the surgical and anaesthetic approaches.
3. To assess morbidity and mortality of the surgical and anaesthetic techniques.
4. To find a suitable ‘dummy’ implant.
5. To clarify correct positioning of the implant within the cochlea.
6. To perform CI using a ‘dummy’ implant.
7. To perform CI using the specialised electrode array.

3.3 Development of the surgical approach to CI in mice: Cadaveric dissection

In order to become familiar with the anatomy and to ascertain the best approach to the cochlea for implant insertion, cadaveric dissection on C57BL/6J mice was undertaken. Two approaches to the mouse cochlea have been described; postauricular (Akil et al., 2012; Bogaerts et al., 2008; Do et al., 2004; Kawamoto et al., 2001; Praetorius et al., 2003) and ventral (Akil et al., 2012; Chen et al., 2006; Jero et al., 2001). Both methods were trialled (postauricular n=3, ventral n=3) to assess ease of access together with other important factors such as invasiveness, risk of damage to surrounding structures and the potential for blood loss and postoperative pain. Both approaches allow access to the round window and this was chosen as the site for CI.

Regulations set out by the Home Office in reference to surgical procedures on protected animals, state that the design should allow maximum gain of information with the use of minimum animal numbers. The procedures themselves should also be refined to be as less invasive as possible (Home Office 2014). This was taken into consideration when deciding on the most suitable approach for CI.

3.3.1 Postauricular approach

Following removal of fur in the postauricular region using a battery operated shaver, the skin was exposed and a 1-1.5cm incision made. Dissection through the superficial fascial layers of the neck was performed to reveal the greater auricular nerve overlying the prominent sternocleidomastoid muscle. The nerve was either retracted or cut and the sternocleidomastoid muscle retracted in a superior and caudal direction. Further dissection of the deeper fascial layers revealed important structures such as the cartilaginous portion of the auditory canal and facial nerve (Figure 3.1). The facial nerve, lying in a more cranial and superficial position, served as a key anatomical landmark to the location of the auditory or tympanic bulla. A specialised small animal retractor system (Fine Science Tools, Interfocus Ltd, Linton, UK) was used to create a clear unobstructed view of the desired structures. Once

the bony bulla was identified, careful dissection of the overlying posterior belly of the digastric muscle was performed. Arising from the posterior half of the bony bulla, the muscle was carefully dissected and a small vessel cauteriser (Fine Science Tools, Interfocus Ltd, Linton, UK) used for haemostasis.

Once exposed, entry into the bulla was required to access the round window niche. An otologic skeeter drill (Medtronic Ltd, Hertfordshire, UK) with a 0.5mm diamond burr was trialled in the first instance. Although the size of the burr was compact, vibration at the tip within the comparatively confined working area meant that the drill felt unstable. It was also found that due to the smooth surface of the bulla, there was a high risk of the burr sliding off the bony target and inadvertently causing damage to the surrounding structures. A 25G needle was then trialled. The needle was rotated at one point under direct microscopic vision until the bony periosteum was breached and tympanic mucosa removed with forceps to gain entry to the middle ear cavity. Micro forceps were then used to enlarge the hole (bullotomy) until the round window was visualised. The stapedial artery was noted to run immediately beneath the round window niche over the cochlear promontory before advancing between the crura of the stapes at the oval window.

The mean time taken from starting surgery to reaching the round window niche was 7 minutes. Figure 3.1 illustrates key steps and anatomical landmarks of this technique.

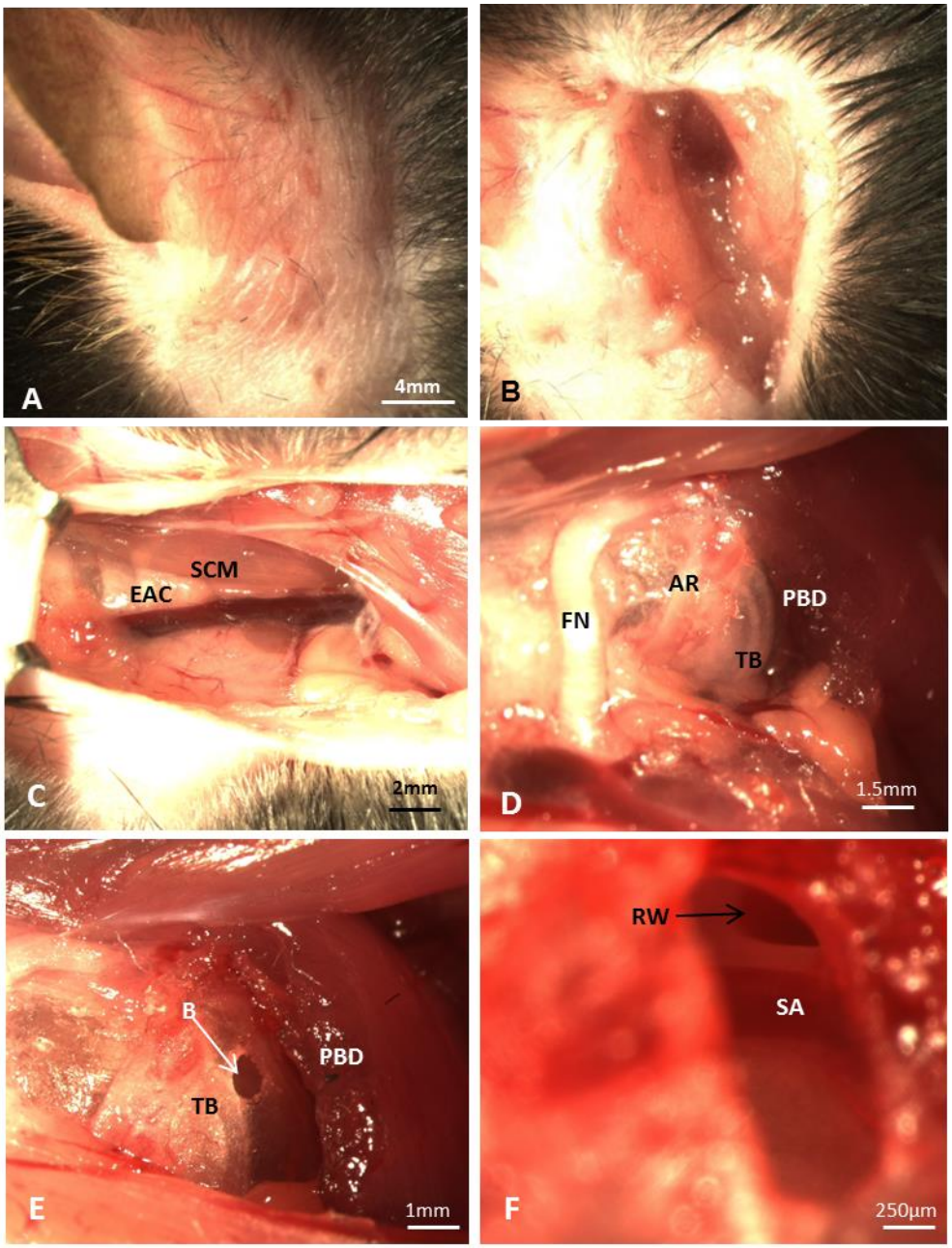

Figure 3.1 Postauricular approach to the round window in the mouse

A. Fur removed in left postauricular region

B. Postauricular incision

C. Cartilaginous portion of the external auditory canal (EAC) and the sternocleidomastoid muscle (SCM) are exposed

D. Tympanic bulla exposed partially (TB) following dissection of part of the posterior belly of digastric (PBD). Tympanic annular ring (AR) seen at transition between cartilaginous AC and bony TB. The facial nerve (FN) is a key anatomical landmark for the tympanic bulla.

E. Cut edge of PBD is seen allowing adequate exposure of the TB. A bullotomy (B) has been performed (opening in TB).

F. Bullotomy widened to expose round window (RW) niche. Stapedial artery (SA) seen running directly beneath RW

3.3.2 Ventral Approach

Described by Jero et al. (2001), this approach offers an alternative to the postauricular method. It has also been performed by authors in order to access the inner ear for intracochlear drug delivery and to perform viral-mediated gene therapy (Akil et al., 2012; Chen et al., 2006; Jero et al., 2001). Following a 2cm longitudinal ventral incision extending from just above the mandible down to the clavicle, dissection through the superficial tissues was performed to expose the submandibular gland in its lateral aspect. The superior edge of the pectoralis muscle and the inferior edge of the masseter muscle define the lower and upper borders of the dissection. Careful dissection and medial retraction of the submandibular gland was then performed to expose the sternocleidomastoid muscle, digastric muscle and the trachea. Dissection at the posterolateral aspect of the sternocleidomastoid muscle to identify the anterior facial vein was performed and this vessel subsequently retracted laterally to expose the auditory canal and tympanic annular ring. With such an extensive exposure, vital structures contained within the carotid sheath which runs along the posterolateral aspect of the trachea, including the vagal nerve and common carotid artery, are visible and vulnerable to damage if care is not taken.

The tympanic bulla is found beneath the inferior half of the digastric muscle and therefore, this muscle was carefully divided using a cauteriser. Once divided, the tympanic bulla lay exposed, a small opening was then made about 1.5mm from where the stapedial artery enters the bulla, in order to visualise the round window. Although Jero et al. (2001) recommended the use of a micro-drill, a needle was used for the reasons described previously. Forceps were then used to enlarge the opening so that better access to the round window could be gained.

The mean time taken from starting surgery to reaching the round window niche was 40 minutes.

3.3.3 Choice of approach

The postauricular approach was associated with a less extensive dissection and therefore less morbidity and reduced likelihood of postoperative pain. These factors, in combination with the fact that it had a far shorter operative time, meant that it was selected as the technique of choice. It also encounters fewer vital structures unlike the ventral approach in which structures such as the submandibular gland, trachea and carotid sheath are widely exposed. Any inadvertent damage to the latter two structures would almost certainly be fatal to the animal. The time taken to perform surgery is an important factor which needs to be taken into consideration, especially in terms of minimising anaesthetic time.

3.4 Anaesthesia and analgesia

Anaesthesia is defined as 'a state of controllable, reversible insensibility in which sensory perception and motor responses are both markedly depressed' (Flecknell 1993). Selection of the most suitable anaesthetic agent is dependent on a number of variables. The type and length of surgical procedure, together with the level of expertise of the person administering the anaesthetic and equipment which is available all need to be taken into account. According to the National Centre for the Replacement, Refinement and Reduction of Animals in Research the following points should be considered when choosing the best anaesthetic (National Institute on Deafness and Other Communication Disorders 2016):

1. *Depth and duration of anaesthesia required*
2. *Mode of administration – should not cause distress to the animal and be simple to administer.*
3. *Techniques used should have minimal side-effects and allow an uncomplicated recovery.*
4. *Minimal interference with the research at hand.*

Other points which should be taken into consideration are as follows: the level of analgesia provided by the anaesthetic and whether additional agents are required to provide pain-relief, the ease with which the depth of anaesthesia can be assessed, whether the regimen is species-appropriate as well as the reliability, reproducibility, reversibility and cost of the anaesthetic (Flecknell 1996).

3.4.1 Inhalational versus injectable anaesthesia

Both inhalational and injectable anaesthetics can be used in rodent surgery. Inhalational anaesthesia involves the use of agents such as isoflurane, sevoflurane and halothane. These volatile gases are delivered via specialised machines which generally consist of a vaporiser, carrier gas source (100% oxygen in the main), flow meter and pressure valves (Flecknell 1996). In comparison to injectable agents, inhalational anaesthesia has a more favourable safety profile as it is rapid acting, allows adjustment of dose according to anaesthetic depth, is associated with quicker recovery and has less of an impact on cardiovascular, renal and hepatic function (Gargiulo et al., 2012). In mice, dedicated anaesthetic chambers are used to induce anaesthesia and maintenance is provided via an open mask system as endotracheal intubation is difficult. This means waste anaesthetic gases may escape and be a potential hazard to the surgeon, although specialised scavenging systems can be used to reduce this risk. Another drawback to the open mask system is the fact that the animal cannot be manually ventilated should respiratory arrest occur. Additional disadvantages to the use of inhalational anaesthetics include their weak analgesic properties and the depressive effects on respiratory and myocardial function (Flecknell 1996; Gargiulo et al., 2012).

Injectable anaesthetics are commonly used to induce and maintain anaesthesia in rodents and can be administered via intravenous, intraperitoneal, intramuscular or subcutaneous routes. The intravenous route produces the most rapid and predictable anaesthetic using the smallest dose. However, difficulties with animal restraint and access to superficial veins often mean that this mode of administration is not used. Advantages of the other routes include the

fact that they are relatively simple and can be given by a lone operator. The rate of absorption of drugs given by these routes can, however, vary considerably as can the anaesthetic effects. Frequently used drugs include ketamine, pentobarbitone and tribromoethanol. They are often used in combination with other drugs such as xylazine and medetomidine to provide a balanced anaesthetic. This ensures that the therapeutic doses are within a suitable range, provoking an appropriate level of anaesthesia and muscle relaxation in the absence of significant respiratory depression. Once administered, the duration of the anaesthetic can vary but the animal can be monitored and top-up doses given as required. There is also less equipment associated with this method and less interference when performing surgery. Although the doses are prescribed in relation to the weight of the animal, there can be significant variations in the response of individual animals, not only between species and strains, but also amongst animals of the same strain of mice. One of the main disadvantages with this form of anaesthesia is the fact that adjustment of the dose is not possible according to the animal's response as they are given as a bolus at induction. With some of agents having a very narrow anaesthetic index this means that mortality secondary to anaesthesia can be high. Another problem with injectable anaesthetics especially via the intramuscular and intraperitoneal routes is the relatively larger doses which are required to produce the desired anaesthetic effect. These larger doses mean prolonged recovery times which in turn can leave animals vulnerable to respiratory failure and hypothermia in the postoperative period (Flecknell 1993; Flecknell 1996). However, the availability of reversal agents, means that these issues can be offset and their use is highly recommended by some (Hu et al., 1992).

In order to choose the optimal type of anaesthetic for mouse CI, guidance was sought from the Named Veterinary Surgeon (NVS) affiliated with the Institute and other groups in the lab experienced in mouse anaesthesia. There appeared to be clear advantages to the use of injectable anaesthetic for mouse CI: the ease of administration, availability, lack of interference with the surgical site, no requirement for complex equipment, low cost, availability of reversal agents and the fact that it can be performed by a lone operator. Despite the superior safety profile of inhalational anaesthesia, one of the major difficulties anticipated with its use was the

fact that the facemask used to deliver the anaesthetic gases would overlap with the site of surgery. Another disadvantage to the use of the face mask was that the mouse would require frequent re-positioning during the procedure. Thus there were strong concerns that the mask may be misplaced resulting in suboptimal anaesthesia and possible distress to the animals. Furthermore, at the time of developing the mouse model of CI, inhalational anaesthetics were not available within our unit. Although provision on the main University campus could have been sought, the logistical problems with regards to pre- and postoperative care of the animals and access for performing ABRs were deemed to be significant and as a result the use of inhalational anaesthetic use was not considered any further.

3.4.2 Choice of injectable anaesthesia

The established laboratory regime for performing ABRs, using a combination of intraperitoneal ketamine and medetomidine, was adapted. This protocol is a well-tested, reliable and reproducible method for inducing the level of anaesthesia required to perform an ABR. It has been used successfully in a number of strains of mice in our lab including the C57BL/6J mouse. Profiles of the drugs are given below.

Ketamine

Ketamine is classed as a dissociative anaesthetic agent which is thought to induce a cataleptic state of sedation without awareness of the surroundings. It can be administered by a variety of routes and causes immobility with variable analgesic properties. It gives rise to an increase in blood pressure and skeletal muscle tone and can also cause significant respiratory depression in small rodents such as mice. The latter is dose-dependent and as such large amounts are required to induce surgical anaesthesia in mice, ketamine is often combined with other agents such as medetomidine, xylazine or diazepam. Although laryngeal and pharyngeal reflexes are maintained, ketamine does increase the production of salivary secretions. With

chronic use, it has adverse effects on hepatic enzyme function which can subsequently reduce its efficacy (Flecknell 1996).

Medetomidine

Medetomidine is an α-2-adrenergic agonist and a potent sedative with variable analgesic properties. Like other α-2-adrenergic agonists such as xylazine, medetomidine also has other beneficial effects such as anxiolysis and muscle relaxation. In addition, its anaesthetic-sparing properties, when combined with other injectable agents such as ketamine, make it a frequent choice in small animal anaesthesia. Unlike xylazine, the side effect profile is more favourable as medetomidine is much more specific α-2-adrenergic agonist. Producing complete immobilization and deep sedation when used alone, its use can avoid the need for general anaesthesia. At high doses, undesirable effects on the cardiovascular system including, cardiac arrhythmias, hyper- or hypotension and a reduction in cardiac output can occur as well as respiratory depression. The reversal agent atipamezole can, however, be used to completely reverse the effects of medetomidine (Flecknell 1996; Sinclair 2003).

3.4.3 Analgesia

When performing operative procedures on animals, the administration of analgesia both pre-operatively (pre-emptive analgesia) and within the postoperative period is very important. Both ketamine and medetomidine have some analgesic properties, however the use of adjunctive analgesia is necessary to ensure adequate pain relief intra- and post-operatively. Not only does the presence of pain cause distress, it also slows recovery and can reduce the intake of food and water (Flecknell 1993).

Buprenorphine administered intraperitoneally was chosen following veterinary advice (Vetergesic®, Reckitt Benckiser Healthcare (UK) Limited, 0.1mg/kg of 0.03mg/ml). It is one of the most common analgesics used in mice, providing pain relief for up to 6 hours. In order to provide pre-emptive analgesia, half of the buprenorphine was given at induction of

anaesthesia and the remainder given in the immediate postoperative period. In the first 48 hour period, the mice were monitored closely and observations of animal behaviour in terms of their movement, posture, appearance, vocalizations, feeding and temperament was used to guide further pain relief administration (Flecknell 1996). Attenuation of the analgesic effects of drugs such as buprenorphine when using the reversal agent atipamezole has been a previous concern. However, a recent study confirmed that such a reduction in anti-nociceptive effects is unlikely, especially if analgesia is administered pre-emptively (Izer et al., 2014).

Non-steroidal anti-inflammatory drugs are another type of commonly used analgesic, however, they were not chosen for use due to their potential to dampen any inflammatory response which could occur as a result of CI – an important outcome measure in terms of assessing the effects of implantation.

3.4.4 Anaesthetic management and monitoring

In order to monitor adequate depth of anaesthesia, absence of the pedal reflexes as well as the clinical observation of the rate, pattern and depth of respiration was used. In the majority of rodents, impending respiratory failure is indicated by a decrease in the respiratory rate to <40% of the pre-anaesthetic rate. Although experience is required, when a single agent or combination of agents is used repeatedly in the same species, developing an awareness of the anaesthetic depth is relatively straightforward (Flecknell 1996).

When a mouse was deemed to be 'light' in terms of the depth of anaesthesia (rise in respiratory rate, slow return of pedal reflex), an additional dose of anaesthetic was administered for maintenance. Hypothermia was prevented following induction of anaesthesia using a heated mat and the body temperature monitored using a rectal thermometer. Postoperatively, the reversal drug atipamazole (Antisedan 0.002ml/g of 0.5mg/ml) was administered subcutaneously to counteract the effects of medetomidine and hasten recovery from the anaesthetic.

3.5 Sham surgery to assess viability of surgical and anaesthetic approaches

In order to put into practice the aforementioned anaesthetic and surgical techniques, sham surgery was undertaken in C57BL/6J mice (n=15) aged between 2-10 months. The main objective was to optimise and refine the surgical approach, with minimal complications and survival of the animal postoperatively for up to 4 weeks. Sham surgery involved all of the surgical steps described in the postauricular approach in order to access the cochlea but did not involve implantation.

3.5.1 Operative procedure

Surgery was undertaken on the left ear in every case with the contralateral right cochlea acting as the non-operated control. In the first 12 mice, following bullotomy, the round window membrane was visualised but not breached. A small amount of muscle harvested from the surrounding tissues was used to carefully occlude the bullotomy without filling the middle ear cleft, prior to closure. In the remaining mice (n=3), a fine straight needle (5 μm radius at tip) was used to pierce the round window membrane in its central portion. Muscle was then used to seal the site at the round window to prevent perilymph leakage into the middle ear. The bullotomy was also occluded as in previous cases. Wound closure was performed in two layers using an absorbable Monocryl™ suture (Ethicon Ltd, Livingston, Scotland, UK) and Histocryl® tissue glue (TissueSeal LLC, Ann Arbor, MI, USA) applied to the skin edges to ensure close apposition.

3.5.2 Evaluation of anaesthetic technique

In all but two cases, the anaesthetic was well-tolerated. Two of the 12 animals suffered a respiratory arrest that could not be reversed. These animals died. The total anaesthetic time varied between 30 and 45 minutes and the total sleep time between 60 and 90 minutes. Depth of anaesthesia was assessed using a variety of markers including muscular tone, loss of the

righting reflex, response to noxious stimuli, loss of limb withdrawal reflex and rate and depth of respiration (Flecknell 1993). In cases where the level of anaesthesia was deemed too light, a top-up of the ketamine/medetomidine mixture was administered at half the dose.

3.5.3 Evaluation of surgical technique: initial experience of 5 cases

The outcomes for the initial 5 cases of sham surgery are shown in a Figure 3.2. The time taken to perform the surgical procedure varied from 20-40 minutes. In the case of 3 of the mice (mice 2, 4 and 5), intraoperative bleeding occurred such that it resulted in death of the animal. The bleeding occurred at the time of dissection of the overlying muscle at the posterior-lateral aspect of the tympanic bulla and could not be arrested with the use of the small cauteriser or with manual compression. At the onset of bleeding it was difficult to isolate the relevant vessel and this factor in combination with the confined operating area precluded the use of hand-ties and/or sutures to occlude the ends of the vessel lumen for purposes of haemostasis. The relatively small circulating blood volume of the animal in relation to the human means that even the loss of 1-2mls of blood can be catastrophic.

In the case of mouse 3, the anaesthetic and surgical procedures were straight-forward and completed without any complications. In the initial postoperative period the animal had a smooth recovery, with no evidence of any complications. Twenty-four hours post-operatively, the animal was found to have some swelling in the left pre-auricular region extending forwards over the left cheek towards the mandible. The swelling appeared unrelated to the wound and surgical site. On day 3 post-operatively, the cheek swelling increased in size and appeared to be causing discomfort to the animal; advice from the NVS was sought and it was advised that the animal be sacrificed.

Following sacrifice, post-mortem examination of the area was performed to try and ascertain the underlying cause for the swelling. Dissection confirmed the swelling to be unrelated to the surgical site and wound. There was a large amount of oedema in the superficial fascial planes overlying the masseter muscle on the left as well as within the superficial layers of the muscle

itself. There was no evidence of haematoma or abscess formation. On reflection, the cause may have been due to trauma or misplacement of the subdermal electrode when performing ABR pre-operatively. This was taken into account and greater care observed in subsequent cases.

As a result of the loss of animals when performing these initial sham operations (mainly secondary to intraoperative blood loss) it was decided that a return to cadaveric dissection to further refine the operative technique was necessary.

Figure 3.2 Outcomes following initial sham surgery

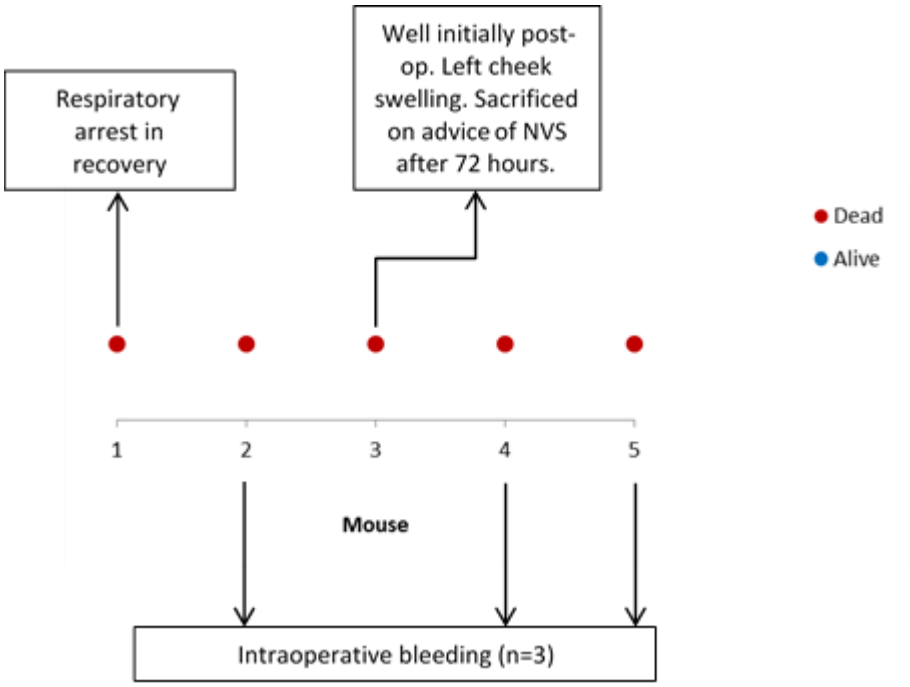

3.5.4 Cadaveric dissection: development of technique to avoid perioperative haemorrhage

Further cadaveric dissection was performed to help identify the cause of the major intraoperative bleeding which had led to the death of 3 of the 5 animals in the initial sham surgery group. Dissection down to the posterior belly of digastric was found to be straight-

forward and did not encounter any large vessels. It was during the dissection of the posterior belly of digastric from the posterior half of the tympanic bulla that bleeding was consistently encountered. A more extensive dissection of the area revealed the source of bleeding to be due to trauma to the stapedial artery as it entered the bulla at posterior medial aspect (Figure 3.3A). Following damage to the artery in this region, haemostasis was not possible due to the very limited access. This in combination with the small size of the artery and lack of visualisation once the profuse bleeding had commenced meant that the best means to deal with the bleeding was to prevent it in the first instance. As a result, the technique was adapted to ensure a much more limited dissection was performed in subsequent procedures.

The principle of surgery was to perform CI with as minimally invasive an approach as possible and on reviewing the technique further, other refinements were also made as follows.

1. Limited dissection of posterior belly of digastric – restricted to posterior-superior aspect of auditory bulla as this was the region for planned placement of the bullotomy.

2. Rotation of the animal away from the operating surgeon to visualise and gain access to the round window. By performing such a simple manoeuvre, it meant that a much more limited bullotomy was required, thereby minimising tissue trauma and reducing the amount of muscle tissue required to occlude the bullotomy when closing.

3. More specific and limited bullotomy (Figure 3.3B). By performing further cadaveric dissections it was noted that the thin and more transparent bone in the superior posterior aspect of the bulla was the most suitable place to gain entry to the middle ear cleft. As the bone was thin, less force was required to perform the bullotomy, which could be easily performed using a 25G needle. It was also located away from the facial nerve to avoid potential trauma and was also placed posterior enough to avoid any inadvertent damage to the ossicular chain.

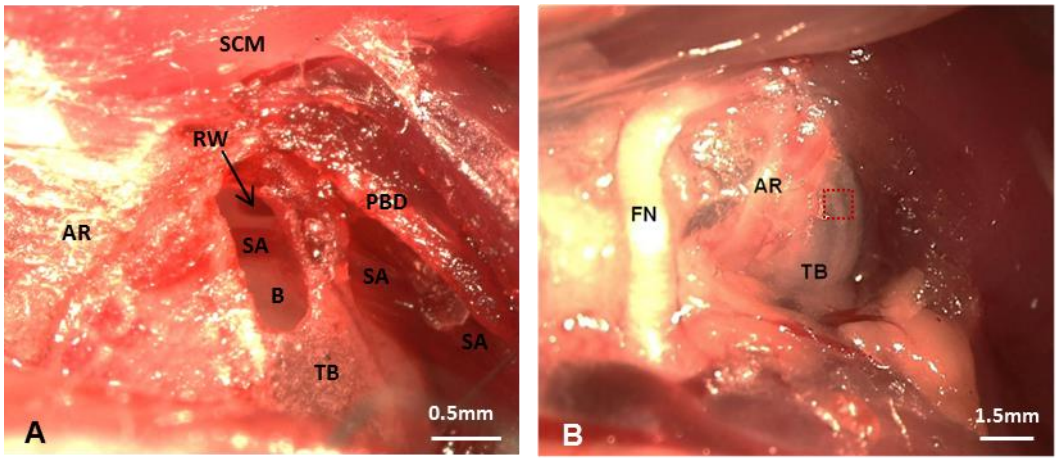

Figure 3.3 Cadaveric dissection

A. Extensive dissection of posterior belly of digastric muscle (PBD) from its insertion on the bony tympanic bulla (TB). The stapedial artery (SA) can be clearly seen beneath the dissected portion of the PBD entering the TB at its posterior-medial aspect and coursing beneath the round window (RW) within the tympanic cavity. The annular ring represents the junction between the TB and the cartilaginous part of the EAC.

B. Image showing exposed TB after dissection of the PBD. The red dotted box shows the ideal site for placing the bullotomy over the thinner bone.

3.5.5 Evaluation of surgical technique: further experience of 10 cases

Sham surgery was continued once the refinements to the surgical techniques had been made and tested under cadaveric conditions. The overall outcomes of the sham operations, including the remaining 10 mice that underwent surgery, are summarised in Figure 3.4. Of these animals 2 died. Mouse 10 died due to haemorrhage from damage to the stapedial artery within the bulla when performing bullotomy. Mouse 11 died of respiratory depression. The anaesthetic was poorly tolerated by the animal throughout the procedure as seen by the intermittently rapid and shallow depth of breathing. The depth of anaesthesia was regularly checked as it appeared that the animal may be 'light', however, the absence of pedal reflexes was noted and the decision not to give an incremental dose of anaesthetic taken. Oxygen was administered intraoperatively and in the immediate postoperative period together with atipamezole and normal saline whilst in recovery. Although the animal survived the procedure, it suffered a respiratory arrest and died shortly after the operation. The changes to the surgical technique appeared effective. The survival rate of surgery increased from 20% to 80%

between the initial 5 and subsequent 10 animals, with perioperative mortality due to haemorrhage decreasing from 60 to 10%.

Figure 3.4 Outcomes following sham surgery

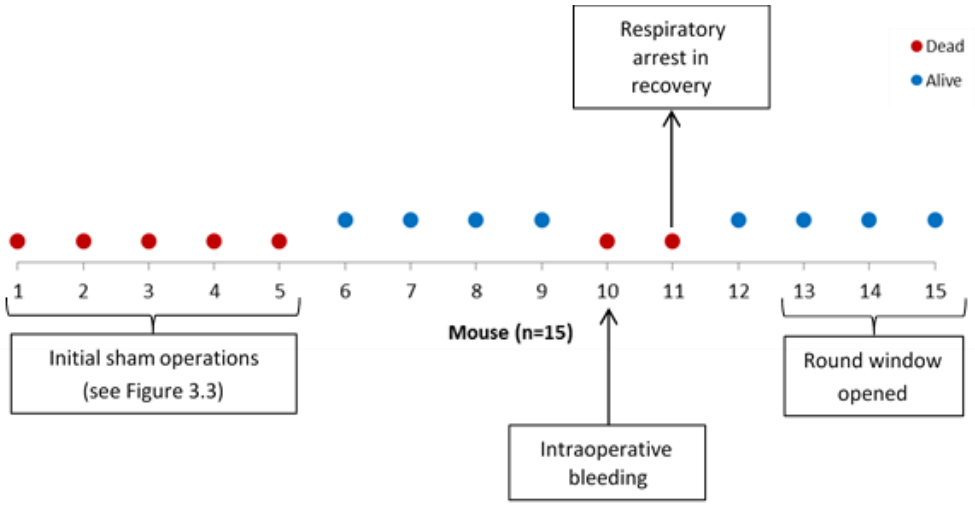

In animals 13, 14 and 15 the round window was opened with a fine needle. This was performed without any complications. A slow ooze of perilymph was noted but there were no cases in which there was a profuse rush of fluid. In order to minimise perilymph loss, a small patch of muscle was used to close the round window perforation as soon as possible.

Postoperatively, the eight surviving mice were kept for 4 weeks and monitored daily. The three mice in which the round window was opened showed no signs of vestibulopathy such as circling, head-bobbing, head-tilting and abnormal reaching responses. Weights were recorded daily for the first week and weekly thereafter (see Appendix 1). All mice maintained their pre-operative body weights within 10%, with some gaining weight by the end of the 28 days (Table 3.1).

Table 3.1 Percentage change in body weight of sham operated mice surviving to 28 days. A negative change indicates weight loss.

	% Change in body weight		
	Day 1	Day 7	Day 28
Mouse 6	-8.2	-9.1	-1.2
Mouse 7	-5.6	-4.6	4.2
Mouse 8	-4.9	-5.2	3.7
Mouse 9	-6	0.6	3.8
Mouse 12	-6.3	-4.7	2.7
Mouse 13	-1.3	0	-0.7
Mouse 14	-2.2	-4	-0.3
Mouse 15	-1.5	0	1.2
Mean % change in body weight	**-4.5**	**-3.375**	**1.675**

3.6 CI in mice: the implants

As implantable devices, cochlear implants are required to fulfil a number of essential requirements including biocompatibility, mechanical stability and long-term material integrity. The technological advances in terms of implant design have been significant since their introduction more than forty years ago. Initial designs drew on the experience of other established implantable devices such as pacemakers, to identify safety limits in terms of electrical stimulation, biocompatibility and electrode insulation (Zeng et al., 2008). The biological and chemical interaction that occurs between the implant and the surrounding tissue with which it comes into contact encompasses surface biocompatibility. As previously discussed, the introduction of a foreign material into the body will elicit an immune response, the extent of which is dependent on the material in question. A substrate that induces a minimal and stable fibrotic response and encapsulation is advantageous in this respect and a variety of materials have proved suitable for CI, including silicone, platinum, titanium and ceramics (Hassler et al., 2011; Stover and Lenarz 2009). At present, most modern cochlear implants consist of Teflon-coated platinum-iridium wires linking to platinum contacts encased in a

silicone carrier. The alloy of platinum and iridium forming the lead wires are wound in a helical or zig zag pattern to reduce the risk of breakage and improve flexibility (Zeng et al., 2008).

For the purposes of this study, implantation was performed using two types of implant. One was a dummy implant and the other a specialised electrode array comprising of parylene coated platinum/iridium wire with 4 electrodes, measuring 0.21mm in diameter at the tip (supplied by Cochlear Ltd). Both materials are biocompatible and known to be widely used in medical applications. The dummy implants were used in order to optimise the technique of mouse CI prior to use of the bespoke arrays and allowed assessment of the general biological response of the mouse cochlea to implanted foreign material. They also had the advantage that they could be sectioned in-situ, to confirm correct placement within the scala tympani.

3.6.1 Choosing a suitable dummy implant

A variety of materials were trialled in order to find a suitable dummy implant. Candidate implants needed to fulfil a number of criteria including: a diameter of suitable size to pass through the round window, biocompatibility and flexibility in order to follow the basal turn without causing trauma to the delicate intracochlear structures. Studies have shown that the average height and width of the round window niche in mice varies between 0.3 and 0.54mm respectively, with an average area of 0.13mm^2. With regards to the dimensions of the round window, the average height and width can vary between 0.19 and 0.31mm and an average area of 0.05mm^2 (Jero et al., 2001).

Following sacrifice, dissection to access the round window niche was performed and various materials trialled in order to identify a suitable dummy implant. Materials were secured at the round window with epoxy glue before further dissection and harvest of the cochleae. Following isolation, the cochleae were further dissected and examined under the light microscope. Fine metal threads including platinum and tungsten (diameters ranging from 0.1 – 0.5mm) were tested (Agar Scientific, UK). At wider diameters they were found to be too stiff and lack suitable flexibility to follow the curve of the basal cochlea turn (Figure 3.5A). Further dissection

demonstrated the wires abutting the lateral cochlea wall suggesting trauma and possible displacement of the wire from the scala tympani. The narrower wires were too fine and kinked on passage through the basal turn (Figure 3.5B). Polyimide tubing was also trialled (Product code 054, inner diameter 0.15mm MicroLumen, Florida, USA) both alone and in combination with the narrow diameter metal threads (0.1 – 0.125mm) which were passed through the lumen of the tubing. Polyimides are polymer thermoset plastics which are commonly used in the medical fields as catheters, stents and as flexible neural interface devices due to their chemical resistance, tensile strength, thermal stability and biocompatibility (Bellamkonda et al., 2012; Talbot and Hartley 2008). When used alone, the polyimide tubing was found to lack sufficient stiffness to allow passage along the basal turn (Figure 3.5B). The combination of using polyimide tubing with the narrower metal threads was appealing, however, in practice the same problem occurred.

Following consultation with one of the lead technicians within the UCL Biosciences Mechanical Workshop (Duncan Farquharson), a fluorocarbon thread was trialled. This is a thermoplastic fluoropolymer also known as polyvinylidene fluoride (PVDF). Polymers are known to have excellent properties for the purpose of implantation in that they are demonstrate long-term stability in unfavourable environments, have low material stiffness, provoke minimal tissue reactions and are good insulators of metallic conductors (Hassler et al., 2011). PVDF displays many of these strengths including flexibility, resistance to chemical corrosion and heat as well as biocompatibility making it a popular choice of material for a wide variety of applications within construction, aviation, defence and medical industries. The potential of PVDF monofilament as a vascular suture has been demonstrated both in-vitro and in-vivo (Laroche et al., 1995; Mary et al., 1998; Urban et al., 1994). More recently, it has also been used as the basis for surgical meshes with promising results (Klinge et al., 2002; Kohler et al., 2015). The fluorocarbon thread trialled had a tip diameter of 0.185mm and was found to pass easily, with minimal resistance and followed the contours of the basal turn of the cochlea (Figure 3.5C). It could also be sectioned in situ and was therefore chosen as they material of choice for the dummy implants.

Figure 3.5 Diagrammatic representation of materials trialled as 'dummy' implants.

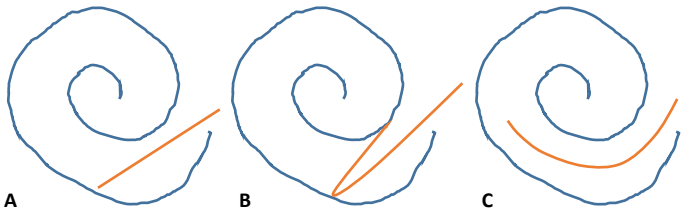

A. Platinum and tungsten threads were found to be too stiff and lacked flexibility required to follow the curve of the basal cochlea turn, abutting the lateral wall and therefore potentially causing trauma to delicate intracochlear structures. With increased pressure, the threads did flex but due to the memory of metal would remain kinked, causing more trauma with further advancement.

B. Polyimide (with and without metal thread) and finer platinum and tungsten threads lacked the stiffness required to follow the turn of the basal cochlea coil and kinked.

C. Fluorocarbon thread passed into basal cochlea turn with ease and minimal resistance.

3.6.2 Specialised electrode array

As stated, the specialised electrode array consisted of a parylene coated platinum/iridium wire with 4 electrodes, measuring 0.21mm in diameter at the tip (supplied by Cochlear Ltd, developed at the Bionics Institute, Melbourne, Australia) (Figure 3.6). The parylene electrode is an excellent model as it is essentially a much smaller version of the cochlear implants manufactured and used in humans, where electrodes are usually fabricated from platinum iridium alloy and partly encased within a silicone elastomer sheath, leaving the electrode contacts exposed. Parylene is a type of polymer based on paraxylene which is a medical grade coating also frequently used in conventional cochlear implant manufacture and other devices such as stents and pacemakers (Stover and Lenarz 2009; Zeng et al., 2008).

Figure 3.6. Mouse cochlear electrode array (all dimensions are in mm unless stated otherwise).

A. Electrode array consists of three platinum/iridium parylene insulated wires (Ø 25µm)

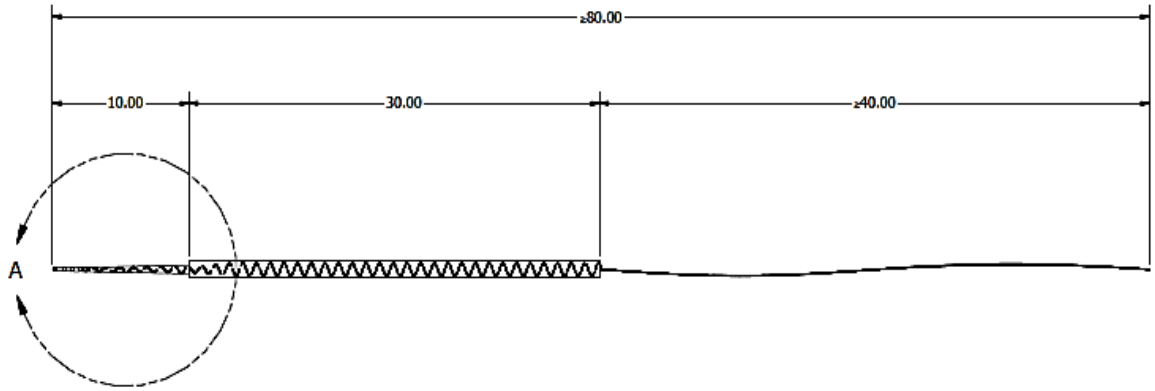

B. Detail A (scale 10:1) of intracochlear part of electrode array. Includes two active platinum ring electrode 4 (tip, Ø 0.21) and 2 (Ø 0.25) in combination with two structural rings 3 (Ø 0.23) and 1(Ø 0.27). The electrode tip has two welded connections for two of the wires to increase electrode stiffness.

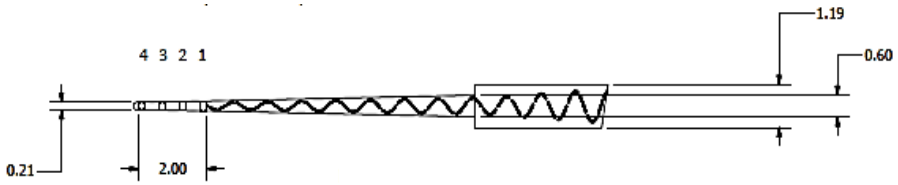

3.7 Clarifying the position of the implant within the mouse cochlea

Having established a working model of mouse CI, it was vital to ensure that the implants were correctly positioned within the scala tympani of the cochlea. This was established using two methods: CBCT and plastic embedded cochleae analysed using light microscopy. Initially CBCT was used to confirm placement of the electrode. Two mice implanted with electrode arrays, one for a period of 4 weeks and one for 12 weeks, underwent CBCT scanning following ABR testing and sacrifice. The images obtained of the implanted mice confirmed the presence of the electrode array within the cochlea (Figure 3.7 – 3.9). The array was inserted 1.5mm into the first part of the basal turn, with the first two electrodes being inserted fully. This finding was also complemented by sectioned cochleae with the fluorocarbon thread in-situ. Here, sections stained with toluidine blue (Figure 3.10) demonstrated the implant position to be within the scala tympani. Examination of the sections also showed tissue integrity was maintained

following implantation and there was no disruption of the basilar membrane, or inadvertent insertion of the implant into the scala media or scala vestibuli. Subsequently assessment of array position was confirmed with light microscopy following decalcification after sacrifice.

Figure 3.7 Three-dimensional reconstructed CBCT images of a 3 month old mouse implanted for 4 weeks with electrode array.

(**A)** and (**B)** show electrode array in position (as shown by white arrow) on left fronto-lateral and left lateral views respectively.

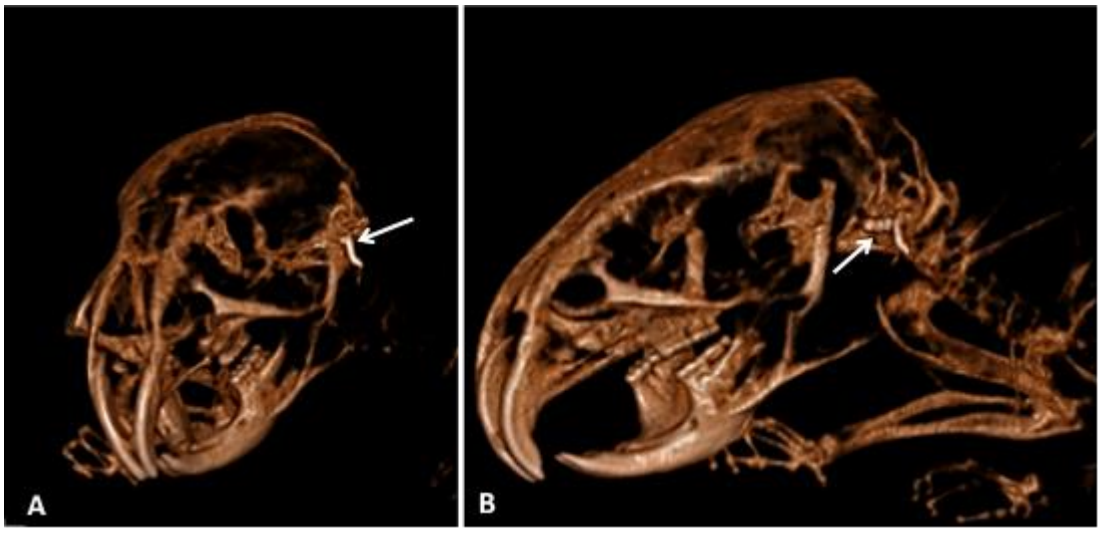

Figure 3.8 Axial CBCT images of a 3 month old mouse implanted for 12 weeks with electrode array (successive images passing from (A) ventral to (D) dorsal). Image on left is identical to the image on the right but has been left unlabelled.

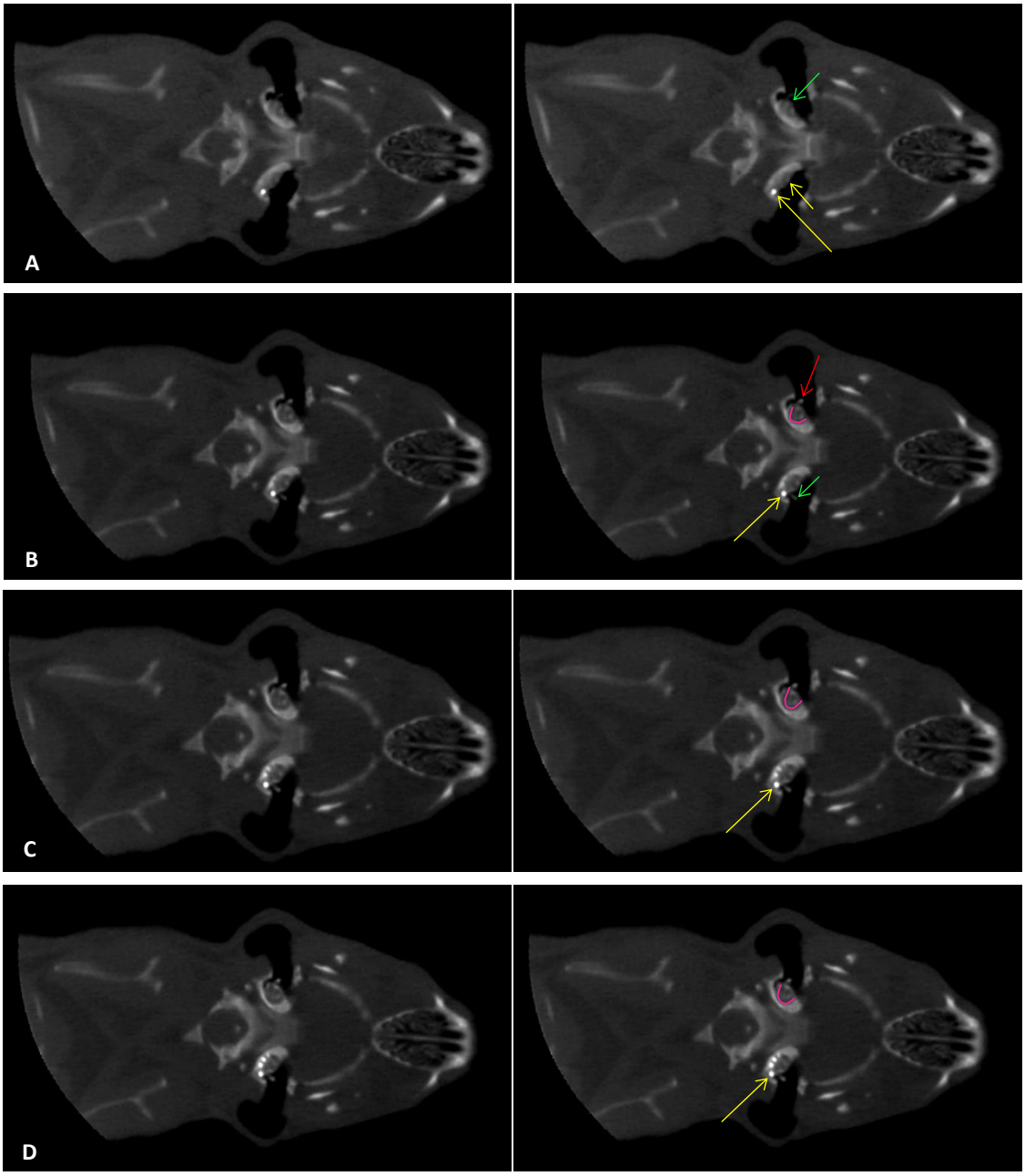

A. Green arrow – right (control/non-implanted) cochlea; small yellow arrow – left (implanted) cochlea; large yellow arrow – electrode array.

B. Red arrow – right stapes; pink line – follows basal turn of right cochlea; green arrow – left stapes; yellow arrow – electrode array entering basal turn at round window.

C. and **D.** Pink line – follows basal turn of right cochlea; yellow arrow shows electrode array within basal turn of cochlea.

Figure 3.9 Coronal CBCT images of a 3 month old mouse implanted for 12 weeks with electrode array (successive images passing from (A) posterior/caudal to (C) anterior/cranial). Image on left is identical to the image on the right but has been left unlabelled.

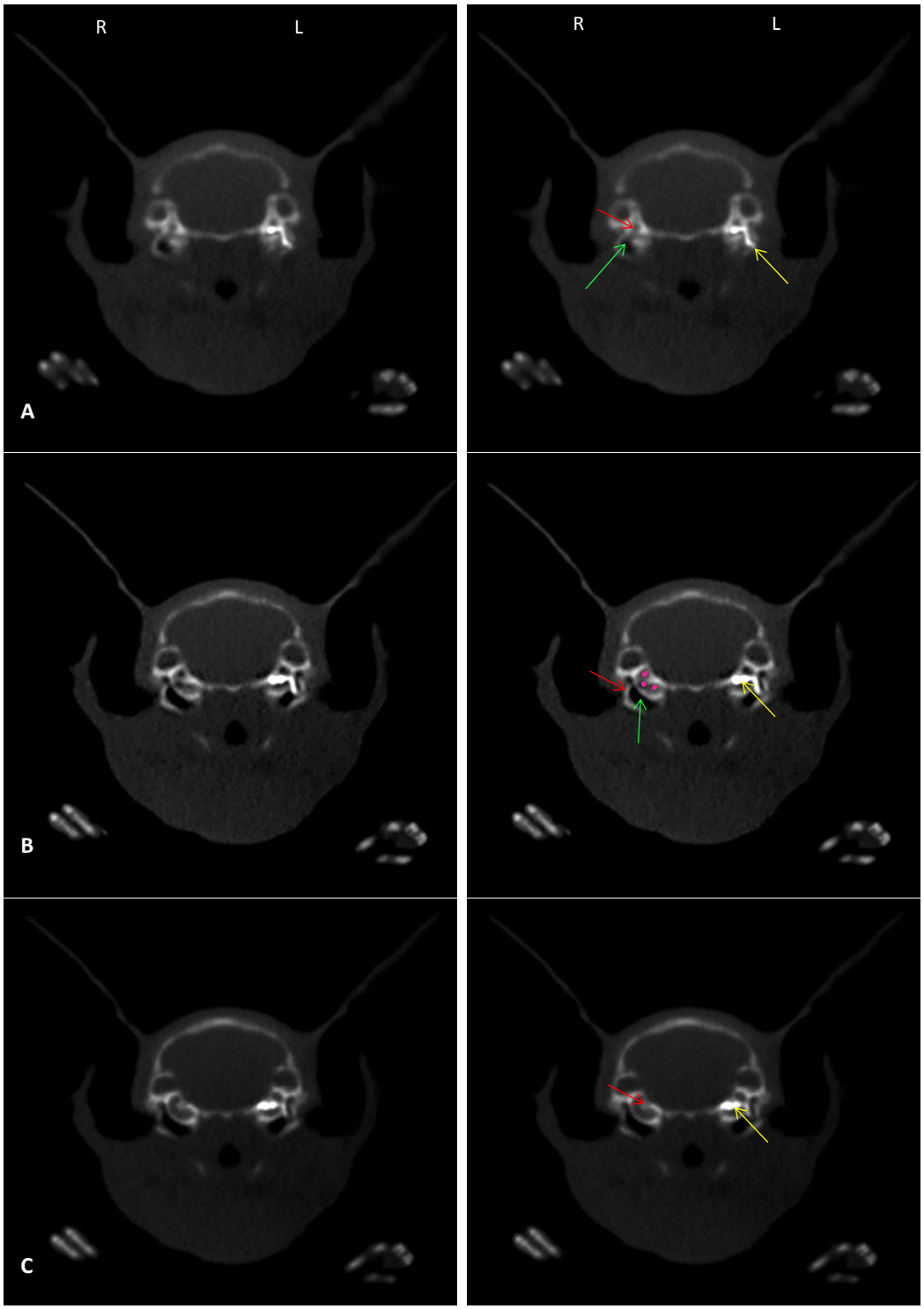

A. Red arrow – right (control/non-implanted) cochlea; yellow arrow – electrode array entering left cochlea via round window; green arrow – right middle ear cleft

B. Red arrow – bony tympanic bulla; pink dots – fluid-filled turns of right cochlea; green arrow – right middle ear cleft; yellow arrow – electrode within basal turn of left cochlea.

C. Red arrow – right modiolus; yellow arrow shows electrode array within basal turn of left cochlea.

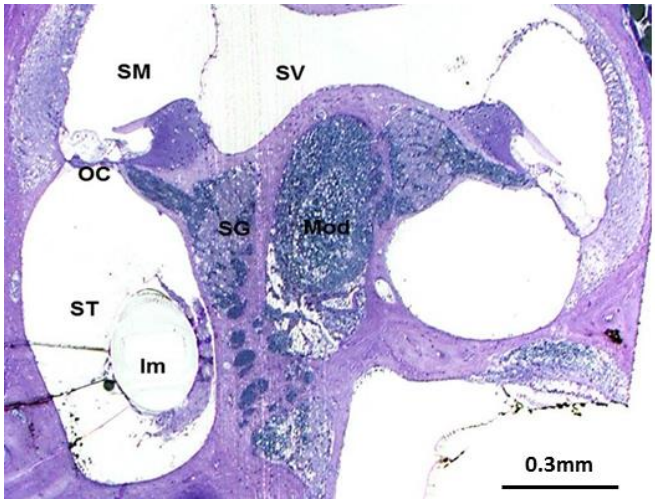

Figure 3.10 Plastic-embedded cochlear section with the fluorocarbon thread in-situ taken from 6 month old mouse implanted for 1 week.

Cochlea with fluorocarbon thread implant in-situ shows evidence of fibrotic-like tissue surrounding the implant (Im) within the scala tympani (ST). Labels as follows: scala media (SM), scala vestibuli (SV), organ of Corti (OC), spiral ganglion (SG), modiolus (Mod). (NB: bowing of Reissner's membrane is seen suggestive of endolymphatic hydrops, however, this change was secondary to tissue processing rather than a pathological change and was also seen in controls (not shown here).

Preparation of section by Mr Graham Nevill.

3.8 Cochlear implantation in the mouse

Having optimised the anaesthetic and surgical techniques, chosen suitable implants and established correct positioning and placement of the implants within the cochlea, CI in two groups of C57BL/6J mice was undertaken. Groups of mice aged 3 (n=18) and 6 (n=19) months were implanted. Figure 3.11 shows the numbers, ages and types of implants, together with the duration of implantation. Having optimised the procedure, survival rates improved dramatically. The mean ages within the 3 and 6 month groups were 101 days (p90 – p107) and 199 days (p176 – p221) respectively.

Within the implanted group of mice, the survival rates were 95% (35/37). In the case of the two deaths (mouse 18 and mouse 34) the first occurred as a result of anaesthetic complications and post-operative respiratory arrest. The second mouse survived 24 hours following implantation and was found dead, the cause of which was unknown. Despite this, 35 mice were implanted successfully and underwent functional testing at the specified time points and were sacrificed following the desired duration of implantation (Figure 3.12).

Figure 3.11 Details of mice used for the development of surgical technique and cochlear implantation.

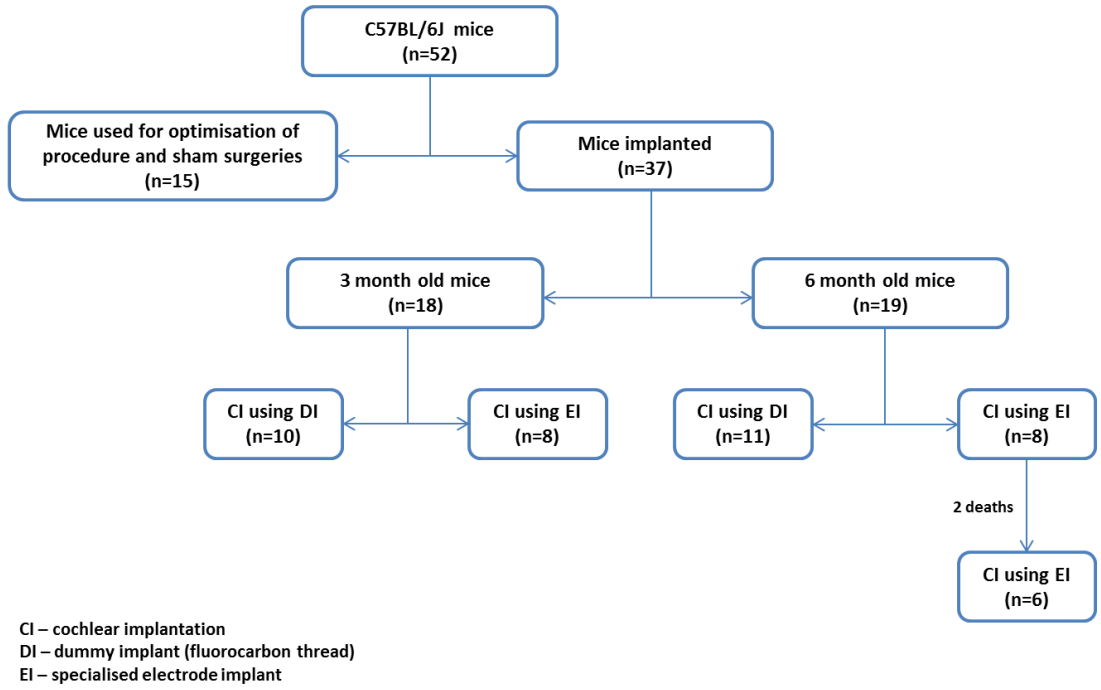

Figure 3.12 Outcomes for all mice and surgical learning curve. Upper part of figure shows the number of mice used and details for those which did not survive. This correlates with the lower part of the figure shows the corresponding mean survival rate and represents the surgical learning curve.

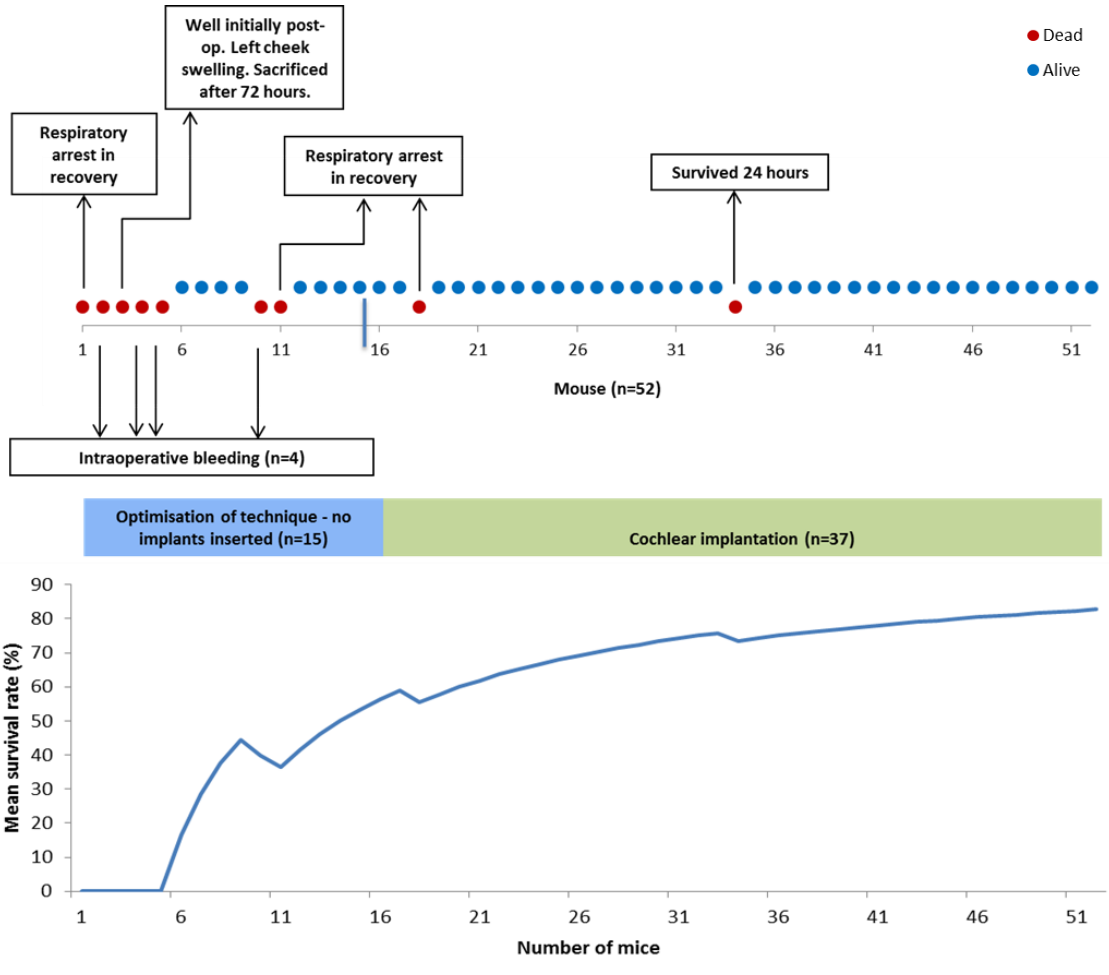

3.9 Discussion

The major anatomical and physiological similarities between the auditory systems of mice and humans, together with the diverse range of naturally occurring and genetically-modified mouse strains which mimic human deafness, have allowed significant progress in the field of hearing research to be made. The lack of access to human auditory tissue for histopathological examination during life has also meant that the use of mouse models has become vital for such assessment.

In this regard, despite the wealth of information provided by existing animal models in the area of CI research, producing a mouse model of CI remains highly desirable. However, various obstacles such as the technical difficulties involved in accessing the murine cochlea for implantation, the small size of the cochlea, the presence of the prominent stapedial artery within the middle ear cleft and the requirements for a suitably-sized implant have previously precluded this. Overcoming these challenges to produce a model of mouse CI is deemed hugely valuable and would enable their auditory research potential to be unlocked in CI studies.

Within this chapter, the development of a robust and reproducible method for mouse CI via the round window has been described. Although surgically challenging, the results demonstrate low rates of mortality and morbidity using the technique outlined. There are very few studies of mouse CI (Irving et al., 2013; Soken et al., 2013) and at the time of developing this model (October 2011), there were no published studies in the literature, making this model novel and a clear advancement in CI research.

3.9.1 Surgical approach

The post-auricular approach used to access the mouse cochlea is less invasive compared to the ventral approach previously described (Jero et al., 2001). It requires a much smaller skin incision and more limited dissection to access the auditory bulla. The current technique allows important structures such as the facial nerve to be clearly identified and damage avoided. The

time taken to perform surgery is short thereby minimising anaesthetic administration, which in mice is known to be associated with difficulties related to dosing and their relatively small body weight. The advantages of initiating access to the mouse cochlea via the post-auricular approach have also been noted by other authors (Bogaerts et al., 2008; Iguchi et al., 2004; Irving et al., 2013; Jero et al., 2001; Soken et al., 2013).

3.9.2 Stapedial artery

The stapedial artery, a branch of the internal carotid artery, is present within the middle ear of adult rodents. This is in contrast to humans, where the artery usually involutes during embryonic development and rarely remains into the postnatal period (Govaerts et al., 1993; Yamamoto et al., 2003). In mice it enters the auditory bulla at its posterior-medial aspect and courses along the medial wall of the tympanic cavity and then superiorly to pass between the crura of the stapes and into the middle cranial fossa (Albiin et al., 1983; Albiin et al., 1985; Govaerts et al., 1993). In the initial phase of developing this mouse model of CI, there were 3 deaths secondary to intra-operative bleeding from trauma to the stapedial artery. This occurred during removal of the muscle overlying the bulla and was due to excessive dissection, especially at the posterior aspect of the bulla. As a result, the technique was adapted to ensure that a more limited approach was undertaken in this region in subsequent procedures, with no further complications due to bleeding.

There is limited information available regarding the preservation of the stapedial artery in mice with regards to hearing outcomes. A recent analysis of cautery of the stapedial artery in C57BL/6J mice was undertaken (Irving et al., 2013). Cautery was performed using bipolar forceps (n=5) and functional testing in the form of click-evoked ABR was done pre-cautery and 4 weeks following cautery. The results revealed mean threshold shifts in the cauterised ears of 21dBHL ± 9.5 (p=0.102), with some animals (numbers not stated) exhibiting threshold shifts of up to 40dBHL. Findings also revealed evidence of heat trauma to the cochlea at the site of cauterisation which they suggest may have contributed to the increased thresholds on ABR testing. The authors found that cautery did not affect spiral ganglion neuron densities when

compared to the control ear. Another study in rats where the artery was cauterised did not demonstrate adverse effects on hearing outcomes or on cochlear spiral ganglion density, however, the number of animals used (n=5) may have been too small to draw clear conclusions (Lu et al., 2005b). Despite the elevated hearing thresholds and potential for trauma, Irving et al. (2013) still recommended cauterising the stapedial artery due to the potential for fatal haemorrhage (Irving et al., 2013). In our experience with the technique as described, cautery is unnecessary if adequate care and attention is applied when performing implantation and is supported by others (Praetorius et al., 2001; Soken et al., 2013; Yamamoto et al., 2003). Aside from potential adverse effects of ceasing blood flow in the stapedial artery on both hearing and survival of the animal, the potential thermal effects of cautery on the cochlea cannot be ignored, especially when the aim is to evaluate the effects of implantation in a residual hearing model.

3.9.3 Surgical learning curve

The surgical learning curve is a well-recognised concept which applies when acquiring a new surgical skill or technique. The curve is most commonly shown graphically with performance plotted against experience. Performance can be based on a number of variables which can be broadly divided into those relating to patient outcomes including cumulative survival rates morbidity and mortality, or measures related to the surgical process, for example, blood loss, and duration of operation. An improvement in performance is indicated by the gradient of the curves ascent up to a point before tailing off and flattening out as the technique is refined and an eventual plateau is reached (Hopper et al., 2007). There was a definite surgical learning curve with regards to the technique of mouse CI. Figure 3.12 clearly demonstrates this, plotting the number of cases against cumulative mean survival. To start with there was a steady and more gradual ascent rather than a steep curve which correlates with the complexity of the procedure. As the technique was refined a plateau appeared to have been reached as there was just one mortality within the last 34 animals (furthermore, this death was unexplained with the animal found dead 24 hours following uneventful surgery).

3.9.4 The implants

One of the main difficulties which has precluded use of the mouse as a model for CI in the past, has been the small size of the cochlea and the relative difficulties in finding an array of suitable dimensions. The fluorocarbon thread provided an appropriate alternative to the electrode array to assess the general response of the mouse cochlea to implanted material. It was possible to insert the fluorocarbon thread the length of the basal turn. As the tip diameter of the electrode array was slightly larger (0.2mm *vs.* 0.185mm), only partial insertion into the first part of the basal turn was possible before resistance was encountered. Deeper insertion of the electrode array may have been possible by removal of bone superiorly at the roof of the round window niche and may become necessary in the future should electrical stimulation of the implant be required.

3.10 Conclusions

In this chapter we have successfully established a viable and reproducible method for mouse CI. Although the mouse cochlea is small and the surgery challenging, with careful surgical technique, meticulous haemostasis and attentive perioperative care, mouse CI is possible.

CHAPTER 4: FUNCTIONAL OUTCOMES FOLLOWING COCHLEAR IMPLANTATION IN THE MOUSE

4.1 Introduction

Auditory brainstem response (ABR) audiometry is an objective test of brainstem function in response to auditory stimuli. Jewett (1970) first described the application of recording such auditory evoked potentials in humans generated as a result of activity in the cochlear nerve and brainstem (Jewett et al., 1970). Since then, the use of ABR has become the most common method of recording auditory evoked potentials with multiple applications including the site-identification of retrocochlear lesions, e.g. acoustic neuromas, and for the assessment of auditory thresholds in 'difficult to test' patients and laboratory animals (Boettcher 2002). In its most basic terms, auditory stimuli in the form of tone pips or clicks are relayed via an acoustic transducer to the ear in either a freefield manner or via headphones or inserts. The evoked potential that is generated is measured as a waveform at surface electrodes placed at the scalp vertex and ear. The amplitude of response signal is averaged and plotted against time. Following a moderate-level stimulus, waveforms will be seen around 1-7 ms later, each being attributed to activity at a specific point in the auditory pathway (Bhattacharyya and Meyers 2015).

ABR testing in mice is a well-established method which allows a reliable and reproducible appraisal of hearing function. Advantages of the technique include the fact that it is low-cost, minimally invasive and simple to perform (Parham et al., 2001). In both humans and mice, the evoked potentials that are generated at the brainstem reflect synaptic activity at specific points along the auditory neural pathway. In the presence of a normal response, this is typically represented by a series of four or five robust potential peaks, labelled I-V. Wave I represents an evoked potential from the auditory nerve and synapse with the cochlea itself, arising approximately 1 msec following stimulus initiation. Evoked potentials generated thereafter arise from the various auditory relay centres within the midbrain: the cochlear nuclei,

contralateral superior olivary complex, lateral leminsicus and contralateral inferior colliculus representing waves II to V respectively, with the fifth wave arising around 5 msec following the onset of the stimulus. In the mouse, as wave IV is the most consistent and stable component of the ABR recording, this is usually chosen as a marker to assess hearing thresholds (Boettcher 2002; Scimemi et al., 2014).

The range of frequencies over which normal mice can hear spans from 0.5 to 120 kHz, with 12 to 24 kHz being the most sensitive. For the purposes of testing in this study, a range around this optimum was used from 8 to 40 kHz, with 40 kHz representing the limit of testing on the equipment used. Clicks and tones were delivered at 10 dB intervals and thresholds were determined by visual inspection to identify the lowest sound pressure level at which clear waveforms were apparent (Figure 4.1). In cases where there was no ABR, at the highest stimulus level, a threshold of 90 dB was noted. A focus on auditory thresholds was used as a comparative marker to assess the effects of implantation and the presence of any hearing impairment rather than specific analyses of intensity-amplitude and intensity-waveform.

Comparisons between the implanted and control ears were made across the various time points for both the fluorocarbon implant and electrode array groups. Combined age-specific comparisons were also performed as one of the major concerns regarding functional response was the preservation of low frequency hearing following implantation and an assessment of whether implantation exacerbates progressive loss at these frequencies in the two age groups of mice used.

4.2 Aims

The main aims of the work presented in this chapter are to:

1. Assess the functional response to CI in the current mouse model
2. Assess the effect of age on functional outcomes following CI in the mouse: comparison of 3 and 6 month old mice.

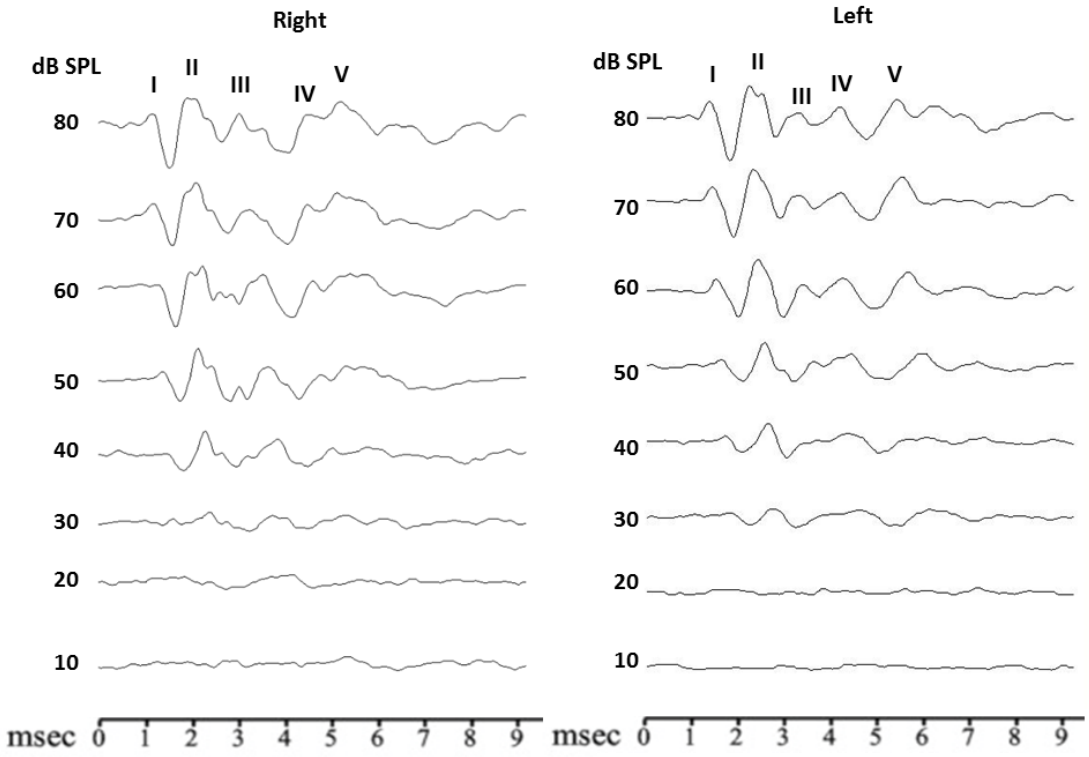

Figure 4.1 pre-operative click ABR recording from 6 month old C57BL/6J mouse. Stimuli are presented at decreasing 10 dB intervals. In this mouse, an auditory evoked potential is identifiable as low as 30 dB.

4.3 ABR outcomes following sham surgery

Although the primary objective of the sham surgeries was to create a stable and replicable anaesthetic and surgical technique rather than assess the functional response, click-evoked ABR testing was performed preoperatively in the initial 12 mice that underwent sham surgery (all steps of the surgical implantation approach were performed but without opening of the round window). Postoperative ABR testing was performed 4 weeks following surgery where possible. The results are shown in Table 4.1 and Figure 4.2. As the mortality rate was initially high when optimising the surgical approach, data was available for only 5 of the mice. For these mice, results from click-evoked responses showed shifts of up to 10 dB postoperatively.

Table 4.1 Click ABR responses for five surviving mice from sham operations

Mouse	Right Click (dB)		Left Click (dB)		Threshold shift R ear	Threshold shift L ear
	Pre-op	Post-op	Pre-op	Post-op		
6	20	20	20	30	0	10
7	50	50	50	60	0	10
8	20	30	20	30	10	10
9	20	20	20	30	0	10
12	30	20	20	20	0	0

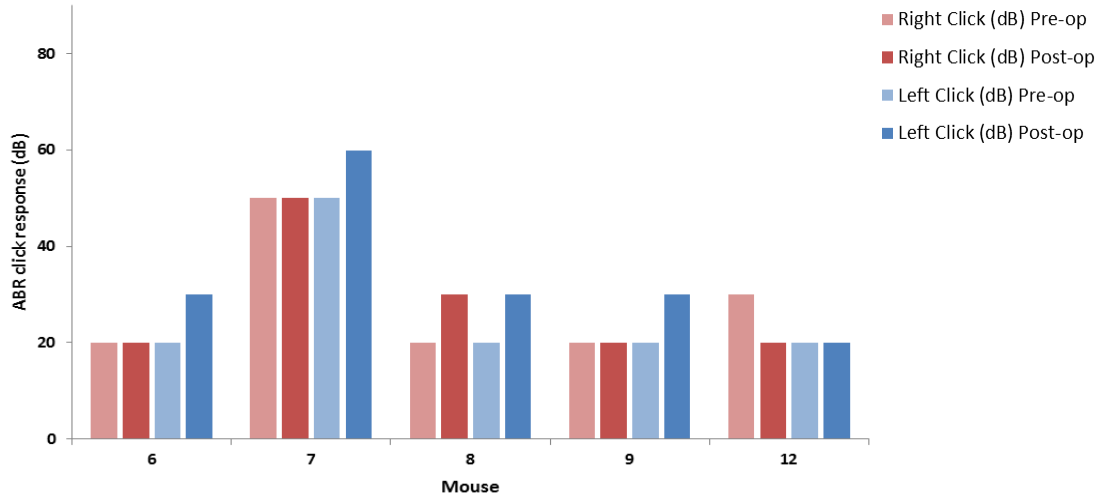

Figure 4.2 Pre- vs. post-operative ABR click responses in the five surviving mice. Post-operative increases of no more than 10dB were noted following surgery suggesting that process of accessing the round window does not cause significant disruption in hearing thresholds as assessed by click ABR.

In the final 3 mice in which the round window membrane was breached, both click and tone burst testing was performed, pre-operatively and then at 48 hours and one week following surgery. This allowed a baseline against which the results of CI could be assessed and acted as a true sham. Figure 4.3 shows the mean threshold shifts in the right control ear and the left sham operated ear at 48 hours and 1 week post-operatively. As with the previous sham ops where the round window was not breached, mean threshold changes in the operated ear were 10dB or less compared to preoperative levels. The results suggest that the operative technique

alone (in the absence of cochlear implantation) does not appear to have a significant effect on hearing thresholds.

Figure 4.3 Mean threshold shifts for three true shams at (A) 48 hours and (B) 1 week post-operatively. Error bars represent standard error of the mean (±2SEM).

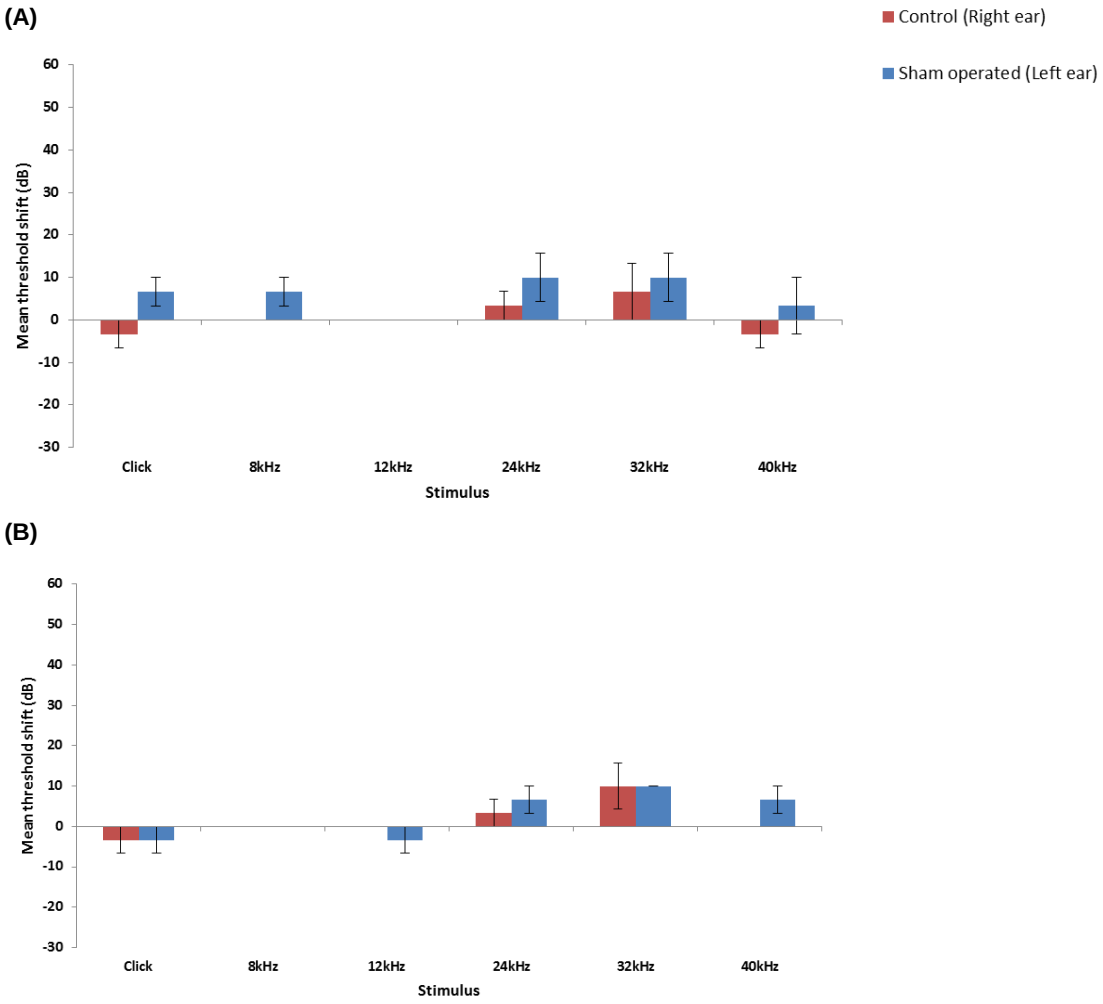

4.4 ABR outcomes in fluorocarbon implant group

The fluorocarbon group included 21 mice implanted for variable periods of time. Within the 3 month group (n=10), the average age at implantation was 99 days (range p90 – p122) compared to 196 days (range p156 – p221) in the 6 month old group (n=11) (Details of individual mice given in Appendix 2).

4.4.1 Animals implanted at three months of age

Greater threshold shifts in the implanted ear were seen compared to the non-implanted control ear (Figure 4.4). This was more apparent at the 48 hour, 4 week and 12 week mark following implantation, with 24 kHz and 32 kHz appearing to be most sensitive frequencies susceptible to change. At 48 hours, postoperative mean threshold shifts of around 20 dB were noted at 32 kHz and 40 kHz following implantation when compared to preoperative thresholds. This may have been due changes in the middle ear cleft and inner ear immediately following surgery. At one week postoperatively, these shifts were not as apparent with mean threshold shifts of no more than 10db at any of the frequencies tested. At 4 weeks following implantation, there were minimal changes in thresholds across the majority of frequencies when comparing pre- and postoperative thresholds following implantation apart from at 32 kHz. At this frequency, a mean threshold shift of around 20 dB was noted in the implanted ear compared to preoperative levels.

Of all of the time points assessed, the most marked increases in thresholds following implantation were seen at 12 weeks. In terms of the non-operated control ear, there were no notable alterations in hearing thresholds when comparing pre- and postoperative levels at the other time points tested, however, at 12 weeks, changes did become apparent, namely at 24 kHz and 32 kHz, likely due to age-related increases in hearing thresholds. In the implanted ear, mean threshold shifts at 24 kHz and 32 kHz were found to be 40 dB and 15 dB respectively, compared to 10 dB and 15 dB in the control ears, suggesting that the larger shifts in the implanted ear were due to a combination of implantation effects as well as age-related deteriorations in hearing thresholds.

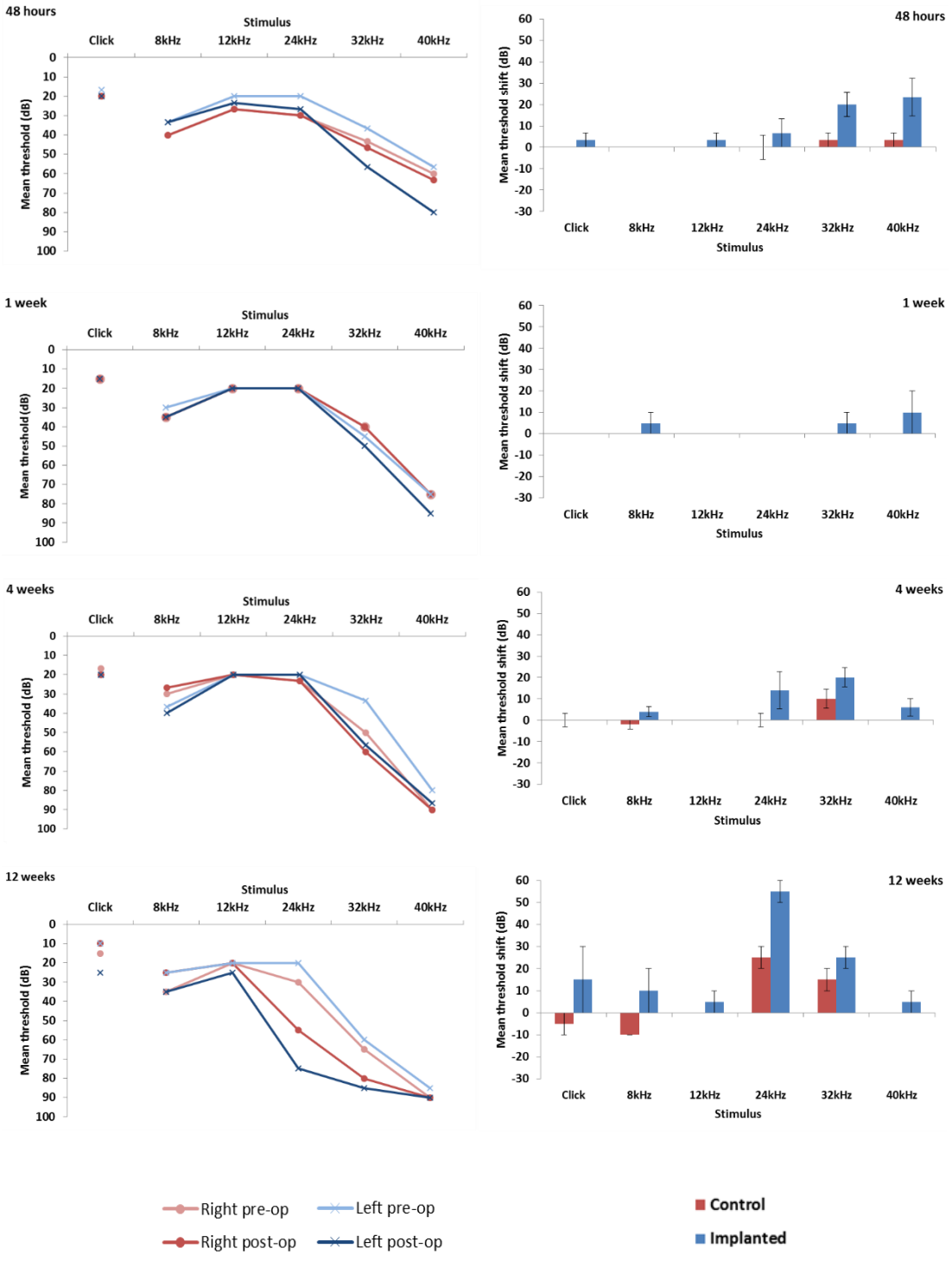

Figure 4.4 Comparison of thresholds recorded pre- and post-operatively in 3 month old mice implanted with the fluorocarbon thread for variable time periods. Numbers in each group: 48 hours (n=3), 1 week (n=2), 4 week (n=3) and 12 week (n=2). Error bars represent two standard error of the mean (±2SEM). In view of the small numbers in each group, statistical analysis was not performed.

4.4.2 Animals implanted at six months of age

Animals implanted at 6 months of age showed greater threshold shifts in the implanted ear compared to the control ear, mainly at 1 week and 12 weeks postoperatively (Figure 4.5). At 48 hours, comparatively smaller threshold shifts were observed in both the implanted and control ears as were at 4 weeks. At one week, a more marked mean threshold shift at 24 kHz was seen, compared to the control ear following implantation. This was also the case at 12 weeks post-implantation where notable threshold differences were present between the implanted ear pre- and postoperatively, especially on testing click responses and tone bursts at 8 kHz and 24 kHz (mean threshold shifts of 20 dB and 35 dB respectively). However, mean threshold shifts were also noted in the control ear again likely due to an age-related decline in hearing, suggesting that the changes in the implanted ear are likely to be due to a combination of implantation effects and age-related changes in hearing thresholds.

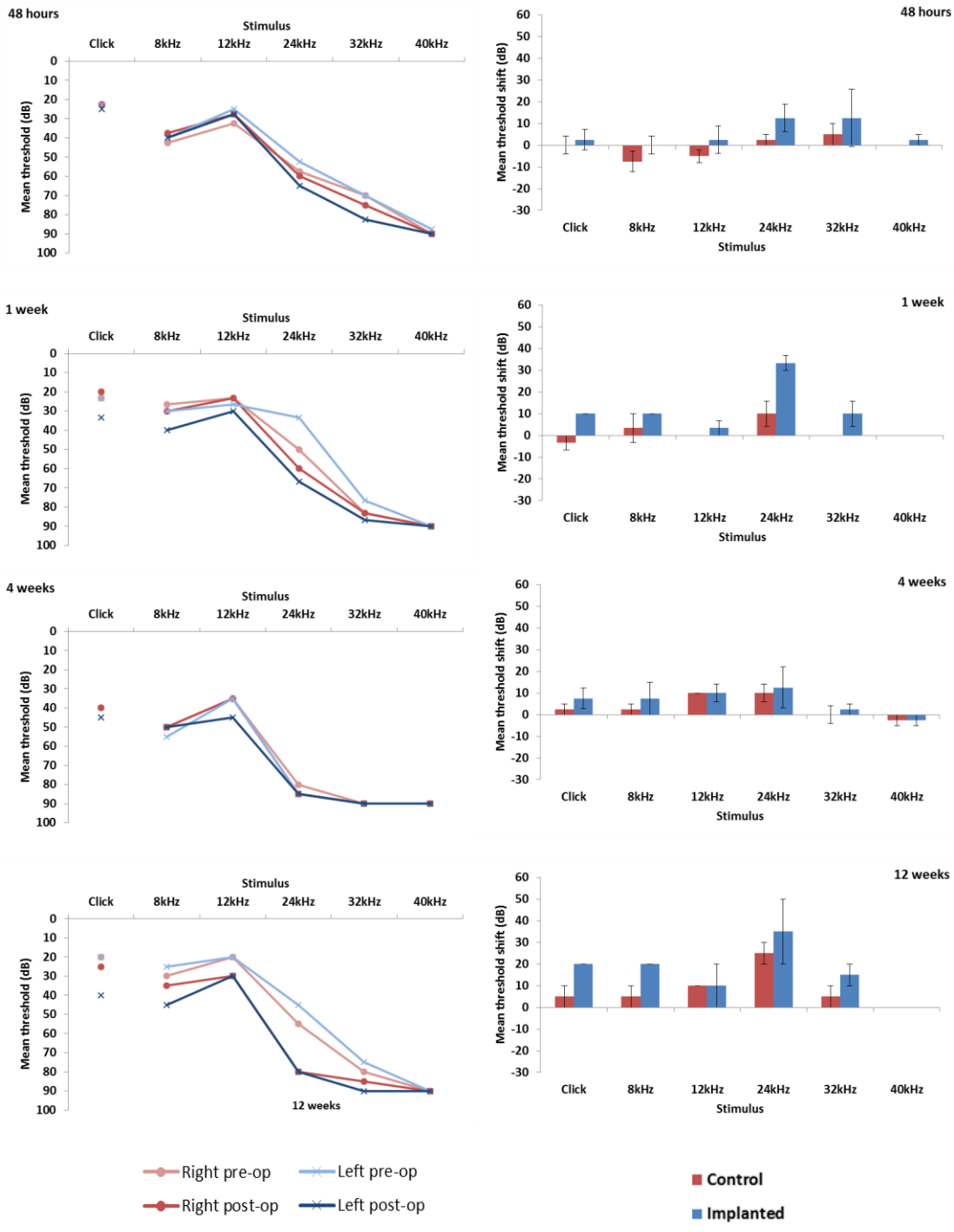

Figure 4.5 Comparison of thresholds recorded pre- and post-operatively in 6 month old mice implanted with the fluorocarbon thread for variable time periods. Numbers in each group: 48 hours (n=4), 1 week (n=3), 4 week (n=2) and 12 week (n=2). Error bars represent ±2SEM. In view of the small numbers in each group, statistical analysis was not performed. .

4.5 ABR outcomes in electrode implant group

The electrode array group included 14 mice implanted for variable periods of time. Within the 3 month group (n=8), the average age at implantation was 105 days (range p91 – p147) compared to 206 days (range p189 – 243) in the 6 month old group (n=6).

4.5.1 Animals implanted at three months of age

The changes seen following implantation in the 3 month electrode implant group were very similar to those seen in the 3 month fluorocarbon group. In general, there were greater threshold shifts in the implanted ear compared to the non-implanted control ear were seen (Figure 4.6). As with the 3 month fluorocarbon group, this was more apparent at the 48 hour, 4 week and 12 week mark following implantation. At 48 hours, only small threshold changes (≤10 dB) were seen in the implanted ear compared to preoperative levels. This was true for all frequencies tested except 32 kHz, where a more marked change was apparent in the implanted ear with a mean threshold shift of 27 dB. However, there was also an increase in the mean threshold seen in the non-implanted ear at this frequency (13 dB). At one week post-implantation, only minor differences between pre- and post-operative thresholds were seen.

At 4 weeks following implantation, the most notable changes in threshold were noted at 32 kHz in both the implanted and non-implanted ears (25 dB vs. 15 dB). At 12 weeks, only one animal was implanted and therefore a mean threshold was not possible. Again a large shift in the implanted ear was seen at 32 kHz post-operatively (50 dB), however, there were also marked deteriorations in hearing thresholds in the control ear seen mainly at 24 kHz and 32 kHz of 40 dB and 30 dB respectively. It is difficult and inaccurate to draw conclusions based on one animal, however, it is likely that the changes seen in the implanted ear were likely to be a combination of both age-related changes as well as the implantation process.

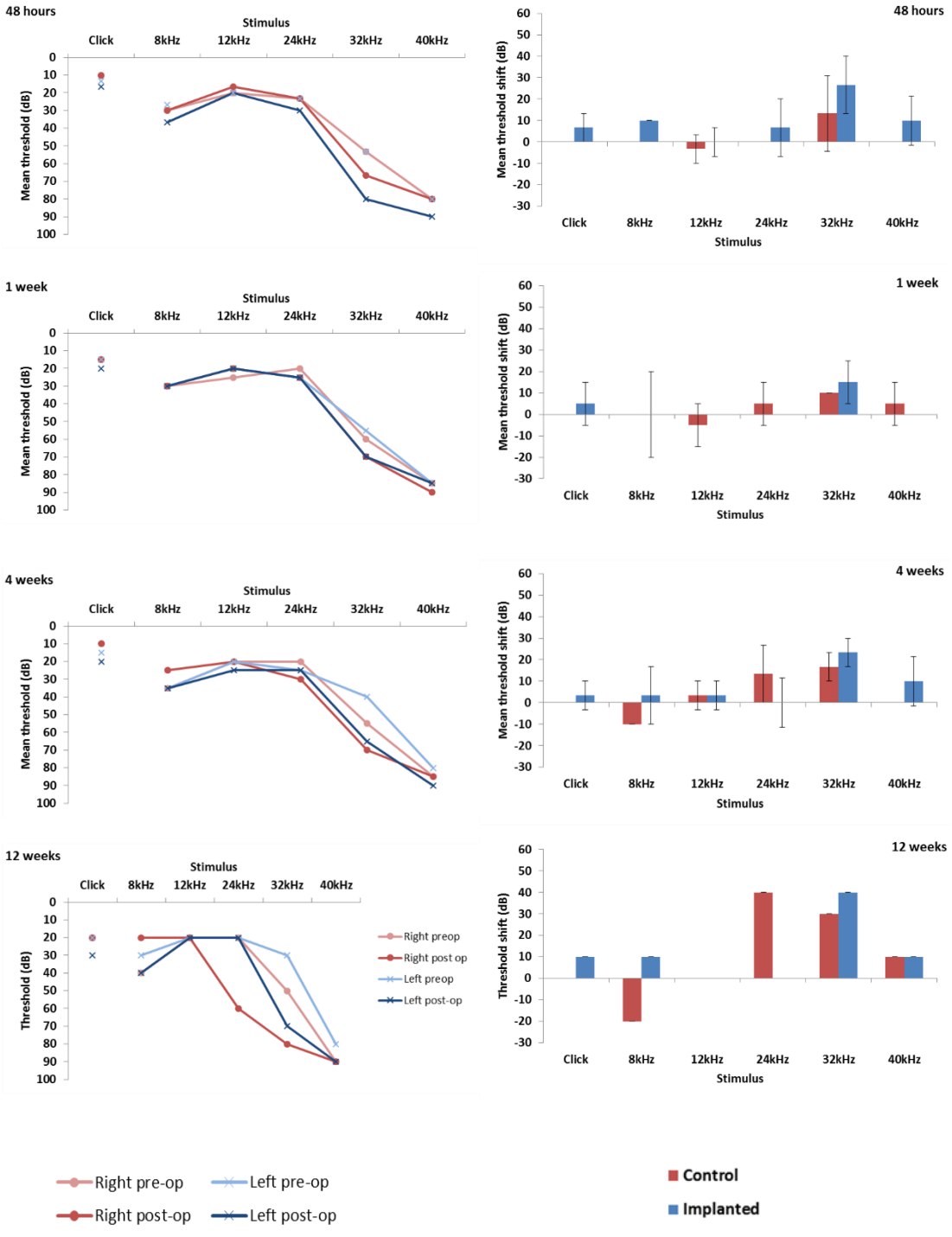

Figure 4.6 Comparison of thresholds recorded pre- and post-operatively in 3 month old mice implanted with the electrode array for variable time periods. Numbers in each group: 48 hours (n=3), 1 week (n=2), 4 week (n=2) and 12 week (n=1). Error bars represent ±2SEM. In view of the small numbers in each group, statistical analysis has not performed.

4.5.2 Animals implanted at six months of age

Despite the smaller numbers in this six month old electrode implantation group, a similar pattern to those changes seen in the fluorocarbon implant group was noted, with most marked threshold changes seen 1 and 12 weeks following implantation (Figure 4.7). At one week, an increase in threshold of 20 dB at 8 kHz was seen in the implanted ear compared to the control ear however, minimal alterations were seen at the other frequencies tested. At 12 weeks, increases in thresholds in both the implanted and control ear were seen compared to pre-operative levels. Within the control group, mean threshold shifts of between 0–15 dB (median 10 dB) were noted and were likely due to age-related deteriorations. A similar picture was seen in the implanted mice (mean threshold shifts; median 12.5 dB and range 0-20 dB); likely to be a combination of implantation as well as age-related changes.

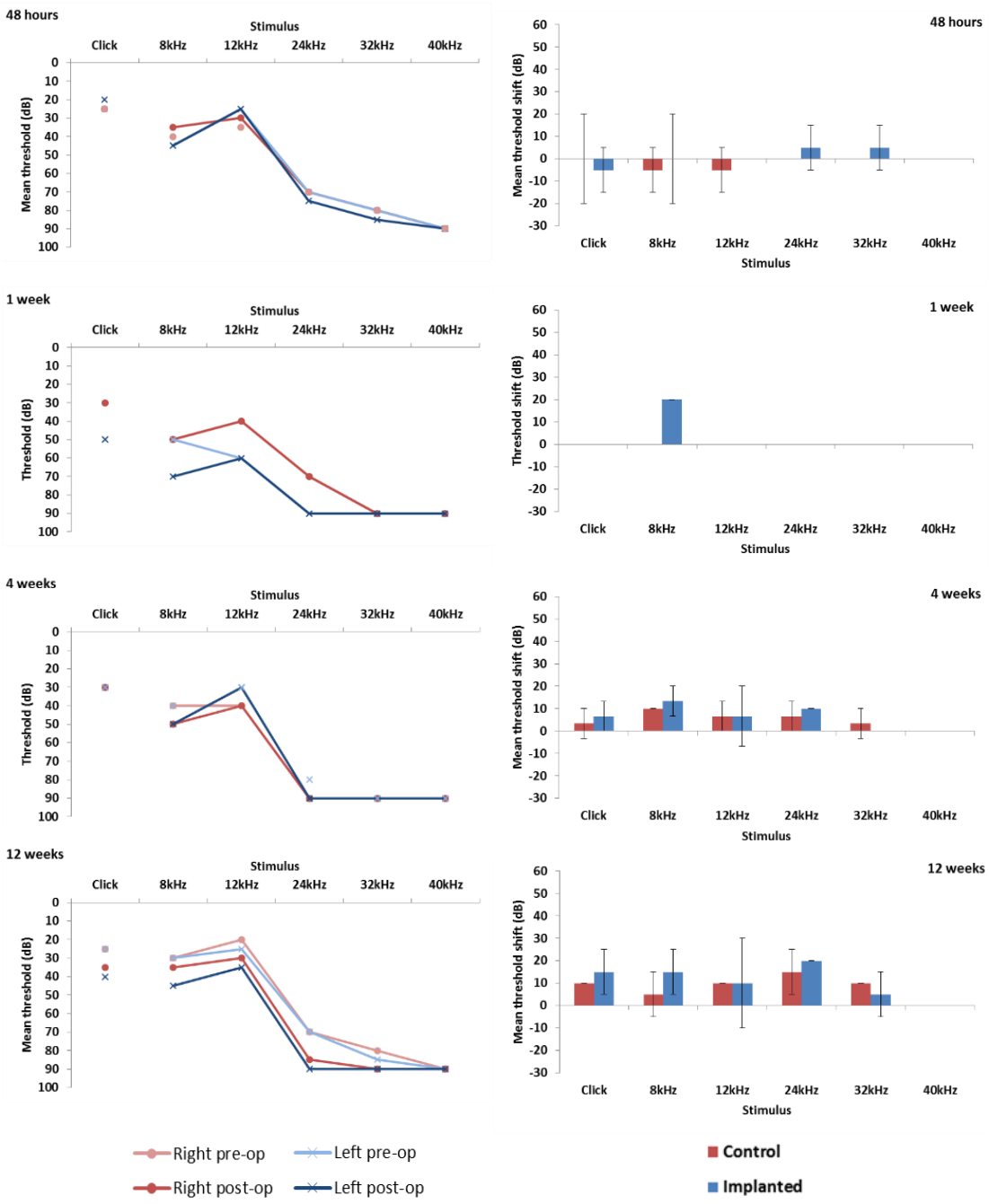

Figure 4.7 Comparison of thresholds recorded pre- and post-operatively in 6 month old mice implanted with the electrode array for variable time periods. Numbers in each group: 48 hours (n=2), 1 week (n=1), 4 week (n=1) and 12 week (n=2). In view of the small numbers in each group, statistical analysis was not performed. Error bars represent ±2SEM. (NB: At 4 weeks, although there was only one mouse implanted, ABR results were available at this time point for those mice implanted for up to 12 weeks and therefore a mean threshold for n=3 was performed.)

4.6 ABR outcomes following implantation: comparison of age-specific groups

The aforementioned ABR results based on the age and type of implant used, although interesting, limit the conclusions which can be drawn due to the small numbers in each individual group. One of the major concerns regarding the functional response was to investigate the preservation of low frequency hearing following implantation and assess whether implantation exacerbates progressive loss at these frequencies in the two age groups of mice used. What is clear from the results so far is that there were no cases of complete hearing loss following implantation in either the fluorocarbon thread or the electrode implant group. In order to examine whether ABR outcomes differed between the two age groups and to allow for more robust numbers in each study group, age-matched comparisons of the pre- and postoperative ABR data were performed. No significant difference was found between the fluorocarbon thread and the electrode implant group (paired T-Test, $p > 0.05$). Data for the two groups were therefore combined and have been presented as two sets according to age at implantation: 3 months and 6 months (Individual mouse data shown in Appendix 2).

When comparing the pre-operative baseline mean thresholds between the two age groups, the 6 month old mice were found to have significantly higher thresholds than the 3 month old mice across all stimulus frequencies except for 8 kHz ($P < 0.05$) (Figure 4.8A and B). This was to be expected due to the age related decline in hearing which occurs in this strain.

(A)

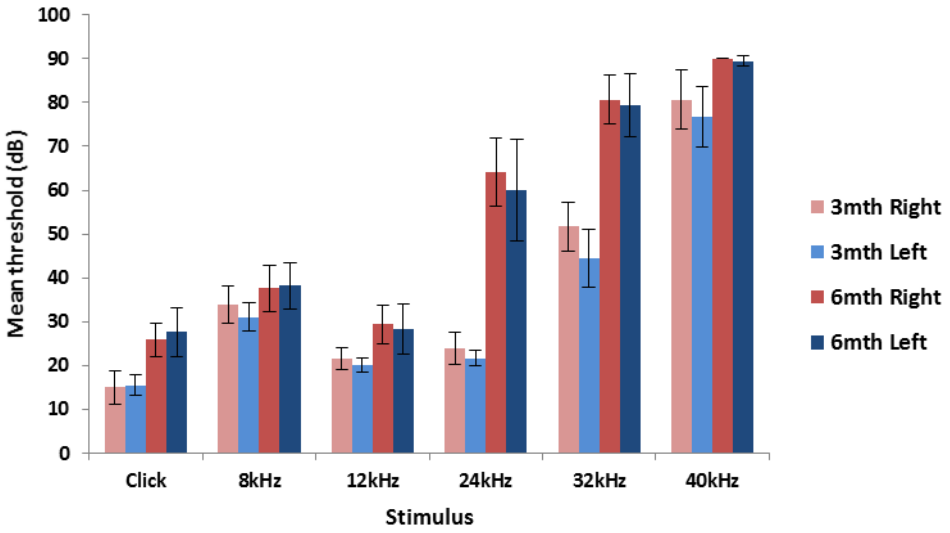

(B)

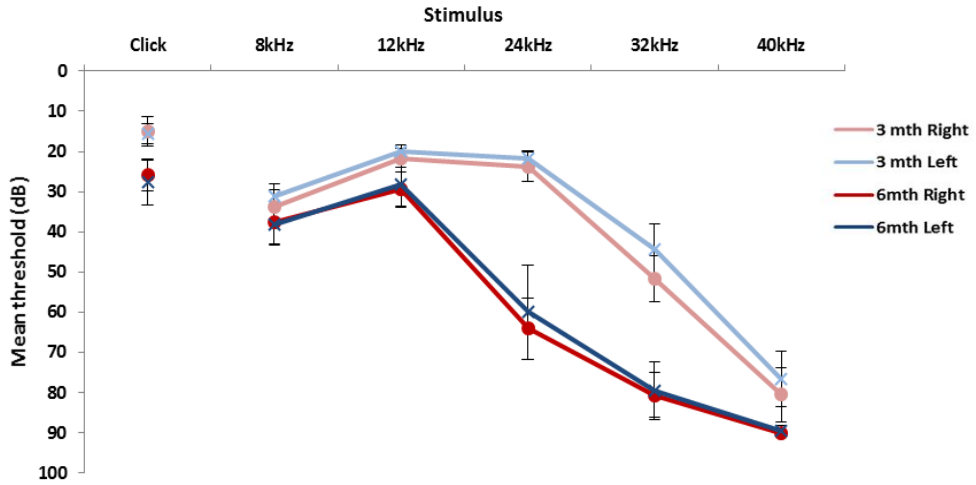

Figure 4.8A and B. Comparison of preoperative mean thresholds for 3 month and 6 month old mice. Mean thresholds were found to be significantly higher across all stimulus frequencies in the 6 month (6 mth) old mice compared to the 3 month (3 mth) old mice except for 8 kHz on statistical testing (*P < 0.05). Error bars represent standard error of the mean (±2SEM).

4.6.1 Comparison of mean threshold shifts: 3 month and 6 month groups

Figure 4.8 shows the mean threshold shifts for the 3 and 6 month old groups at the various time points following implantation. In general, greater mean threshold shifts were observed in the implanted ears compared to the control ears in both of these groups but were not always found to be statistically significant on testing.

In the case of animals implanted at 3 months of age, mean thresholds were found to be significantly greater in the implanted ear compared to the control ear at the following points post-implantation when compared to the control ear: at 48 hours following implantation at 32 kHz (P=0.007); at 8 kHz (P=0.048) and 40 kHz (P=0.049) at 2 weeks following implantation and also at one month post implantation at 8 kHz (P=0.041), 32 kHz (P=0.006) and 40 kHz (P=0.048) (Figure 4.9). Although these comparative losses are statistically significant, the actual functional deficit is unlikely to be, as there was no shift greater than 20 dB at any point. Furthermore, there was no significant difference at 8 kHz at 3 months, therefore suggesting preservation of hearing.

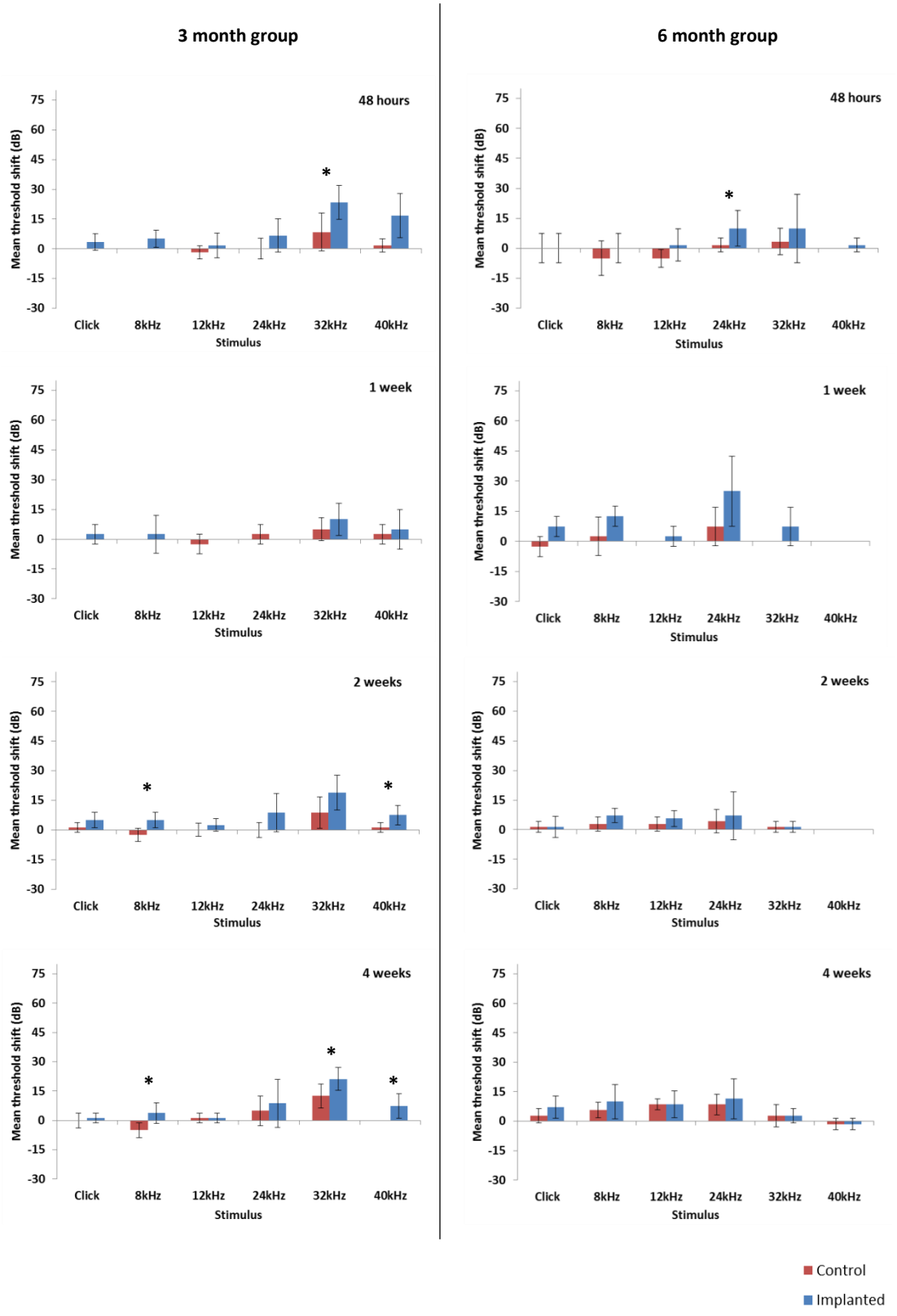
3 month group
6 month group
48 hours
1 week
2 weeks
4 weeks
Mean threshold shift (dB)
75
60
45
30
15
0
-15
-30
Click
8kHz
12kHz
24kHz
32kHz
40kHz
Stimulus
*
Control
Implanted

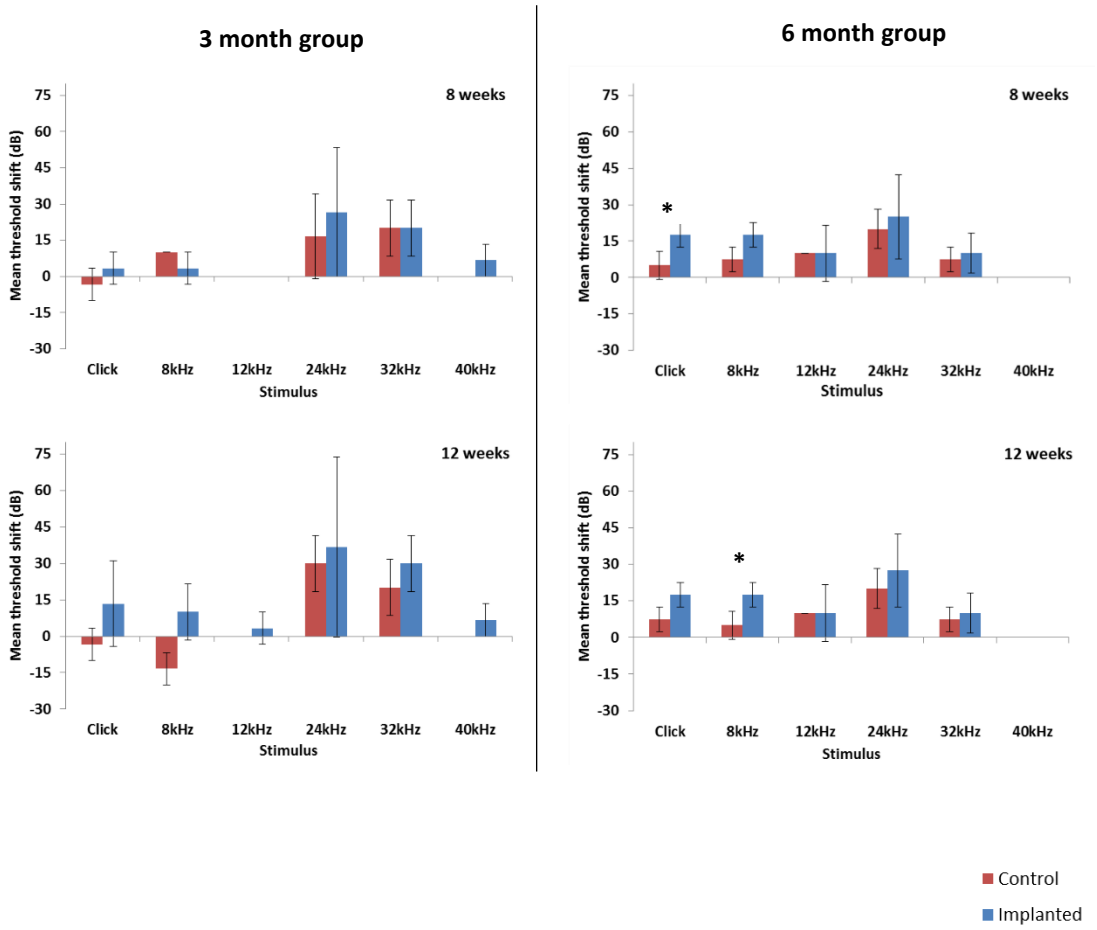

Figure 4.9 Mean threshold shifts post-implantation in (a) 3 month old mice and (b) 6 month old mice (*P < 0.05). Numbers of mice at each time point: 3 month group: 48 hours n=6; 1 week n=4; 2 weeks n=8; 4 weeks n=8; 8 weeks n=3; 12 weeks n=3. 6 month group: 48 hours n=6; 1 week n=4; 2 weeks n=7; 4 weeks n=7; 8 weeks n=4; 12 weeks n=4. Error bars represent ±2SEM.

Greater mean threshold shifts were seen at the higher frequencies of 24 kHz and 32 kHz in both the implanted and control ears at the later time points of 8 weeks and 12 months following implantation. This could be indicative of the naturally occurring progressive hearing loss which occurs with age in this strain.

In the case of animals implanted at 6 months of age, mean thresholds were found to be significantly greater in the implanted ear compared to the control ear at the following points post implantation: at 48 hours following implantation at 24 kHz (P=0.042); on click testing at 8 weeks and 8 kHz at 12 weeks. Again, as with the changes seen in the 3 month group, despite these changes being significant on statistical testing, the actual change was no more than 12.5

dB which may not lead to a significant deficit in functional terms. At the highest frequency tested, 40 kHz, there was no difference between the implanted and control ears, in line with the almost complete absence of detectable hearing at this frequency pre-operatively.

4.6.2 Comparison of mean threshold shifts in implanted ear only: 3 month vs. 6 month groups

Figure 4.10 shows a comparison between the mean threshold shifts in the implanted (left) ear only, for the 3 and the 6 month old mice. Since the age-related changes as well as CI have effects on the high frequencies, only lower frequencies have been compared. In general, greater mean threshold shifts were seen in the 6 month old mice compared to the 3 month old mice post-implantation. These changes were significant on statistical testing at 24 kHz at one week post-implantation (P=0.028) and at click and 8 kHz at 8 weeks following implantation (P=0.018). These findings suggest the presence of an age-dependent acceleration of low frequency hearing loss (i.e. greater threshold shifts) in the older mice following CI compared to the younger mice.

There were a few exceptions where the mean threshold shifts were found to be higher in the 3 month mice compared to the 6 month mice. These were at 24 kHz at 2 weeks following implantation (difference of 1.61 dB) and at 24 kHz at 8 and 12 weeks post-implantation (difference of 1.67 dB and 9.17 dB respectively). These changes were not found to be significant on statistical testing. As these changes occurred at 24 kHz, age-related changes may have started to have an impact on the older 6 month mice, especially at the later time points of 8 and 12 weeks post-implantation, resulting in higher pre-operative thresholds and relatively smaller changes on mean threshold shift as post-operative thresholds verged on or reached the limits of testing.

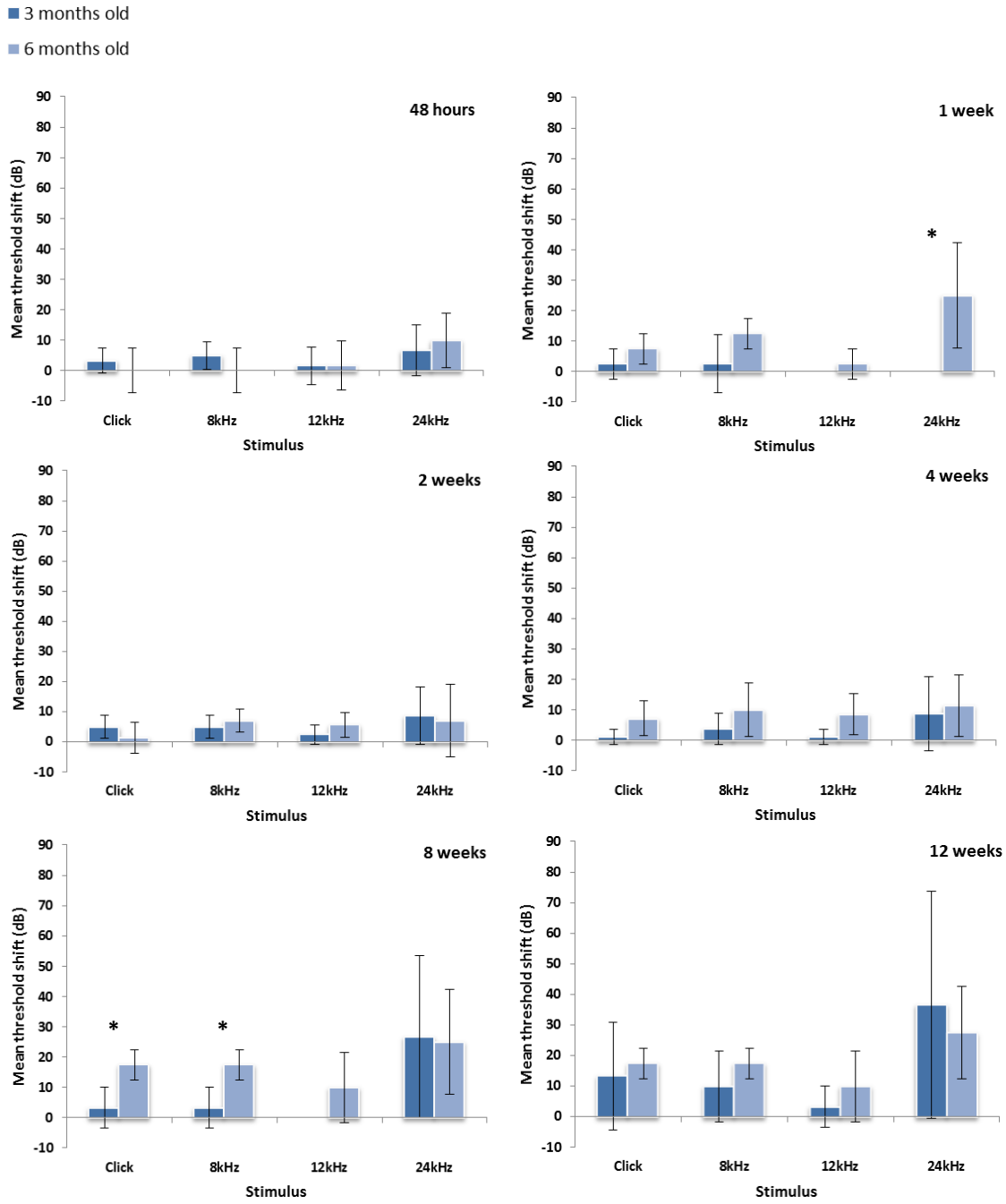

Figure 4.10 Mean threshold shifts for implanted (left) ear post-implantation in 3 and 6 month old mice (*P < 0.05). Error bars represent ±2SEM.

4.7 Discussion

4.7.1 Functional effects of mouse cochlear implantation

In terms of the functional response to implantation, although greater mean threshold shifts in the implanted ear were seen postoperatively, equating to some loss of hearing, there were no cases in which implantation caused a complete hearing loss across all frequencies for any of the animals tested. This is reassuring since it suggests that the process of implantation itself does not cause profound damage at a physiological level. The changes that were noted in terms of mean threshold shifts post-implantation ranged from 0 dB to 37 dB in the implanted ear compared to -5 dB to 30 dB in the control ear. The largest mean threshold shift of 37 dB was seen at 24 kHz in 3 month old mice implanted for 12 weeks. Within the same group, however, the mean threshold shift in the control ear (non-implanted ear) was also found to be 30 dB suggesting the likely effect of age-related changes in combination with implantation. Many of the ABR changes in the implanted ear were found to be statistically significant at certain frequencies and time points tested when compared to the control ear. However, as other types of auditory investigation, such as behavioural testing, were not performed in the current study, the actual functional deficit that the mice experienced as a result of this loss could not be ascertained.

An important aspect of hearing preservation in CI surgery is maintaining low-frequency residual hearing. Comparison of mean threshold shifts for both the 3 and 6 month groups showed that hearing was preserved at the lower frequencies over the various time points tested. This is a crucial feature which could allow use of this mouse model to investigate potential changes in relation to CI and residual hearing over longer time periods. Changes in hearing thresholds were more pronounced in the 6 month group, suggesting an age-dependent acceleration of low frequency hearing loss (i.e. greater threshold shifts) in the older mice following CI compared to the younger mice. This could be explained by the effects of ageing sensitising the inner ear and making it more susceptible to damage following implantation within this age group. The progressive hearing loss that occurs in the C57BL/6J

mouse with age is well known and associated with the gradual loss of hair cells together with other changes such as spiral ligament, stria vascularis and afferent neuronal degeneration (Ohlemiller 2006). Elevated hearing thresholds at the high frequencies are seen as early as 3 months of age and correlate with the progressive loss of both OHCs and IHCs, from the basal to apical cochlea, in an age-related fashion (Henry and Chole 1980; Hequembourg and Liberman 2001; Ison et al., 2007; Spongr et al., 1997). With regards to the lower frequencies, an age-related decline has also been noted in this strain, albeit, at a slower and sometimes more varied rate (Hequembourg and Liberman 2001; Li and Borg 1991a). Hequembourg and Liberman (2001) noted low-frequency losses in their study of C57BL/6J mice aged between 1.5 to 15 months. Histological analysis showed a selective loss of OHCs within the apical segment of the cochlea with advancing age together with SGC loss and fibrocyte degeneration within the spiral ligament, postulating that these neuronal alterations could account for the low-frequency hearing loss in part (Hequembourg and Liberman 2001).

At the time of performing this study, due to the novel nature of the work, there were no published studies available assessing physiological outcomes following mouse CI. However, during the course of the write up, a few studies have been published. Soken et al. (2013) performed CI via the round window in 15 C57BL/6J mice (aged 44 – 56 days) and performed auditory testing in the form of click ABR and distortion product otoacoustic emissions (DPOAEs) preoperatively and at 2 weeks following implantation. Their findings revealed significantly increased mean threshold shifts on click ABR testing in the implanted ear compared to the control ear (27.8 dB vs 0.6 dB) with threshold shifts in the implanted ear ranging from -3 to 60 dB compared to -9 to 9 dB in the control ear (Soken et al., 2013). These shifts seen within the implanted ear were greater than those seen in our study. Mean threshold shifts seen on click ABR in our 3 month old mice ranged from 1.25dB to 13.3dB in the implanted group compared to -3.3dB to 1.25dB in the control group over the various time points tested. Specifically, at 2 weeks post-implantation, the mean threshold shift in click ABR was 5 dB vs. 1.25 dB in the implanted ear vs. control ear respectively. In the 6 month mice, mean threshold shifts in click ABR ranged from 1.43 dB to 17.5 dB in the implanted ear

compared to -2.5 dB to 7.5 dB in the control ear. At the 2 week mark, the mean threshold shift was 1.43 dB in both the implanted and control ears.

The same group also went on to publish a second study in which sixty-five C57BL/6J mice underwent CI with various implant materials (two types of implant grade silicone (diameter 0.15mm) and an uncoated platinum wire (diameter 0.08mm)) (Kopelovich et al., 2015). As in the previous study, click-evoked ABR testing as well as DPOAEs were performed preoperatively and at time points between 2 and 22 weeks post-implantation. The age of the animals implanted was not specified. Fifty-four of the 65 mice survived to 22 weeks. Their results again revealed much greater increases in thresholds post-implantation compared to our study with mean threshold shifts as follows: silastic 1 = 49.8 dB; silastic 2 58.1 dB and platinum wire = 46.0d B. The majority of the shifts in threshold were seen within the first 2 weeks post-implantation followed by a slower decline in all groups thereafter. Similar results were found in mice which retained their DPOAEs post-implantation.

Despite the similarities with our study in terms of surgical technique, there may well have been slight differences in the approach to the round window and the insertion itself in the aforementioned studies. Soken et al. (2013) used a 0.127mm diameter platinum–iridium wire as their implant and inserted to depths of 1.5mm to 2mm (Soken et al., 2013), whereas silastic coated implants and a platinum wire of 0.15mm and 0.08mm respectively were used by Kopelovich et al. (2015) (Kopelovich et al., 2015). The use of a non-coated platinum–iridium wire may have led to a greater degree of trauma at an ultrastructural level, possibly breaching the basilar membrane and causing damage to the organ of Corti. However, the authors did not perform any histological analysis to assess this in the first study. Kopelovich et al. (2015) found that the larger silicone implants were associated with greater loss of hearing compared to the platinum wire, however, interestingly, they did not find any correlation between the type of implant used and the degree of damage to the organ of Corti (Kopelovich et al., 2015). Soken et al. (2013) (Soken et al., 2013) found that a number of animals had a loss of DPOAEs postoperatively (n=6) which resulted in higher threshold shifts compared to those animals who maintained recordable DPOAEs postoperatively. Although effusions within the middle ear

were only noted otoscopically in 2 of the animals following implantation, the authors speculated that the presence of residual effusion could have contributed to the increased loss of hearing in these cases.

Potential causes of mean threshold shifts seen following implantation in our study could be due to the alteration in perilymph volume, as a result of displacement of some of the fluid at the time of performing implantation, although this was minimised by sealing the round window with muscle tissue immediately after insertion had been performed. Another cause could be the presence of an inflammatory and fibrotic response. Further investigation continues in the subsequent chapter to try and correlate the functional findings and with histological findings to give a clearer idea of the underlying cause of hearing loss.

4.7.2 Appraisal of the ABR technique used to assess hearing outcomes following cochlear implantation

As a purely electrophysiological measure, ABR does not provide data in relation to the animal's capacity to discriminate sounds and is not a measure auditory sensitivity rather it is more accurately a measure of neural coordination. The alternative is behavioural testing which involves conditioning procedures or which utilise reflex responses which are unconditioned (Heffner and Heffner 2001). From a practical perspective and for the purposes of this study, the use of ABR testing can be justified as our main concern was to be able to determine the effects of implantation on hearing thresholds rather than assess the intricacies of auditory sensitivity. It was important to be able to test each ear separately in a controlled environment allowing consistency and repeatability so that comparisons could be made. Generating such circumstances might not be as easy to attain when undertaking behavioural testing.

Although the use of broadband stimuli in the form of click-evoked responses alone provides limited information, the use of tone burst testing has the advantage of being frequency-specific. Our study demonstrated clear advantages in this regard over the aforementioned studies (Kopelovich et al., 2015; Soken et al., 2013), as despite the technique being more time intensive, the data collected gives much more information regarding the physiological

response post-implantation. One advantage that these other studies (Kopelovich et al., 2015; Soken et al., 2013) had, however, was the measurement of DPOAEs.

Otoacoustic emissions (OAEs) are generated by vibrations of the OHCs in response to auditory stimulation, their transmission occurring in the form of an oscillatory wave which travels from the cochlea to the external auditory canal via the ossicles and tympanic membrane (Kemp 1978). DPOAEs use tonal stimulation, usually in the form of two stimulus tones applied to the cochlea, giving an assessment of cochlear function. As with other types of OAEs, the status of the middle ear and external canal is very important as even minimal conductive losses due to middle ear effusions and debris within the ear canal can affect the detection of DPOAEs (Kemp 2002). As such, some authors have recommended their use in in the evaluation of middle ear conditions, such as screening for otitis media with effusion in children (Yeo et al., 2002).

Measurements of DPOAEs in C57BL/6J mice have been used to assess age-related hearing loss in relation to OHC function (Parham 1997). The results suggested that high to low frequency progression of DPOAE thresholds occurs with age and is likely to reflect the changes that occur in OHC function with age. In this paper, mice with clinical evidence of middle ear infections or large amounts of cerumen build up within the ear canal were excluded in an attempt to remove the possible confounding effects of middle and external ear pathology on DPOAE outcomes. This was also the case in the previously mentioned studies (Kopelovich et al., 2015; Soken et al., 2013) where otoscopy was performed to assess the presence of middle ear effusion or haemotympanum. Soken et al. (2013) found that 2 animals had otomicroscopic evidence of middle ear effusion but went on to comment that there may have been more animals with residual effusions present which were not detected clinically but which could account for the greater threshold shifts post-implantation in those who had loss of DPOAEs on testing (Soken et al., 2013). Kopelovich et al. (2015) found one animal had clinical evidence of middle ear effusion but that no other cases were detected either on otomicroscopy or histology. In contrast to the previous study, although a number of animals lost DPOAEs following implantation and had greater thresholds on ABR, analysis of those who retained

DPOAEs post-operatively revealed a similar pattern of hearing loss, with the majority occurring within the first 2 weeks post-implantation. The authors went on to suggest that loss of hearing, including the loss of DPOAEs, could be accounted for by the extent of implantation trauma rather than the presence of middle ear effusion (Kopelovich et al., 2015).

In our study, although DPOAEs were not undertaken, otomicroscopic examination of the animals' ears was performed prior to every ABR test done. Any occluding wax was removed using a small wax hook. No cases of effusion were clinically apparent. As with DPOAEs, in order for ABR to be accurate and reliable, the middle ear and external auditory canal needs to be healthy and free from pathology such as effusion, haematoma or wax. It could be possible that some animals tested may have had residual effusions post-operatively that were not detected clinically, although, at the time of histological preparation and analysis, no cases of middle ear effusion were seen. As DPOAEs do not always provide definitive answers in terms of the presence or absence of middle ear effusion, a more appropriate measure could be the use of tympanometric testing which would allow a fast and simple measure of middle ear status (Zheng et al., 2007).

Another potential disadvantage to the use of ABR in non-human subjects is the lack of standardisation across laboratories which exist with regards to recording parameters, calibration, electrode siting and stimulation (Scimemi et al., 2014). Although this is valid point, in our laboratory, ABR testing is performed routinely and the method and equipment are all rigorously tested and calibrated. The technique in terms of the set-up, sound proofing, electrode placement and anaesthesia are well established, consistent and reproducible.

Further limitations to the technique include the fact that in cases where there was no ABR waveform at the highest stimulus level, a threshold of 90dB was used. This was due to the limits of testing being reached using the current equipment. As the threshold could have been 95dB or 100dB, the analysis of threshold shifts between ears was therefore difficult to interpret. Attempts to justify the method of ABR testing in terms of occlusion were previously discussed. However, a significant limitation of the technique used in the current study was the lack of contralateral masking of the non-test ear to avoid the presence of crossover stimulation

(Megerian et al., 1996). The most definitive method to ensure that the only response being assessed using the ABR technique was from the implanted ear, would have been to deafen the control ear. Although useful in terms of gaining functional information, this approach would have eliminated access to control cochleae for histological analysis and was therefore not considered an option.

4.8 Conclusion

The results presented in this chapter show the effects of CI on functional outcomes in the mice tested. One of the most positive and reassuring results was the fact CI did not lead to a complete or profound loss in any of the mice implanted, lending evidence towards it being a suitable and viable model to investigate CI in relation to residual hearing. The findings also form a baseline against which the results of future studies involving electrical stimulation can be compared.

Greater mean threshold shifts in the implanted ear were seen postoperatively, equating to some loss of hearing, the underlying cause of which requires further analysis. This will be investigated further in the following chapter where histological findings are examined for correlation with functional outcomes.

CHAPTER 5: MACROSCOPIC AND HISTOLOGIC OUTCOMES FOLLOWING COCHLEAR IMPLANTATION IN THE MOUSE

5.1 Introduction

Expanding candidacy for CI has become a key focus within CI research. As such, extending the use of cochlear implants to those with low-frequency residual hearing has become a major aim. The use of EAS is gaining popularity in providing some restoration of hearing through the use of combined electrical and acoustic stimulation to many of these patients. Despite the ongoing developments and improvements in EAS, patient outcomes have varied. Many patients have experienced an immediate or delayed loss of part or all of their residual hearing following implantation (Mowry et al., 2012; Santa Maria et al., 2013). The latter outcome is concerning, especially as maintaining residual hearing is fundamental for EAS. The underlying cause of this loss remains unclear and prompts questions regarding the biological effects of CI on cochlear structure and function. Various factors have been cited as potential reasons for the loss of residual hearing. These include surgical factors (choice of the electrode array, depth of insertion, trauma secondary to electrode insertion), the presence of an immune reaction in response to the implant and the combination of both electrical and acoustic stimulation on the remaining hair cell population (Irving et al., 2014a; Mowry et al., 2012).

In light of the above, further investigation into the effect of CI on the cochlea is crucial now more than ever. To date, the majority of histopathological information regarding the effects of CI in humans has come from cadaveric temporal bone studies (Cervera-Paz and Linthicum, Jr. 2005; Fayad et al., 2009; Kawano et al., 1998; Linthicum, Jr. et al., 1991; Marsh et al., 1992; Nadol, Jr. 1997; Nadol, Jr. et al., 2001; Somdas et al., 2007). Due to the relative inaccessibility of the implanted human cochlea during life, animal models are essential to providing an insight into the changes occurring at a cellular level following implantation. These have included CI in cats, guinea pigs, primates and the rat amongst others (Lu et al., 2005a; Pfingst et al., 1979; Shepherd et al., 1983; Spelman et al., 1980). More recently, since

developing the novel mouse model within this study (Mistry et al., 2014), other groups have also realised the benefits of implantation in the mouse (Bas et al., 2015; Irving et al., 2013; Kopelovich et al., 2015; Soken et al., 2013).

A key concept of the current mouse model is to allow the effects of CI to be investigated and to enable the exploration of the possible underlying mechanisms which could lead to residual hearing loss. The work presented in this chapter is an initial analysis of the macroscopic and histologic findings following CI (in the absence of electrical stimulation).

5.2 Aims

The main aims of the work presented in this chapter are to:

3. Assess effects of CI on mouse cochlea at a macroscopic level
4. Assess effects of CI on mouse cochlea at a microscopic level, including:
    a. Assessment of the presence of inflammation and fibrosis
    b. Preservation of SGC numbers
    c. Preservation of hair cells

5.3 Macroscopic findings following cochlear implantation in the mouse

Figure 5.1 shows images of postoperative dissection of the operative site following sacrifice at various time points. At 48 hours following implantation, the wound at the site of incision had started to heal and at 12 weeks was no longer visible with complete regrowth of the overlying fur. In animals sacrificed at 48 hours to 1 week following implantation, there was evidence of oedema in the tissues together with small haematomas (collections of blood) in the muscle on occasion, indicative of recent trauma from surgery. Minor fibrosis in the underlying muscle was present at 4 and 12 weeks post-implantation. Dissection of the auditory bulla revealed an overgrowth of tissue over the area of previous bullotomy and also showed signs suggestive of osteoneogenesis in some mice implanted for 4 and 12 weeks (Figure 5.2A). In all cases, the implants maintained their position through the round window (Figure 5.2B).

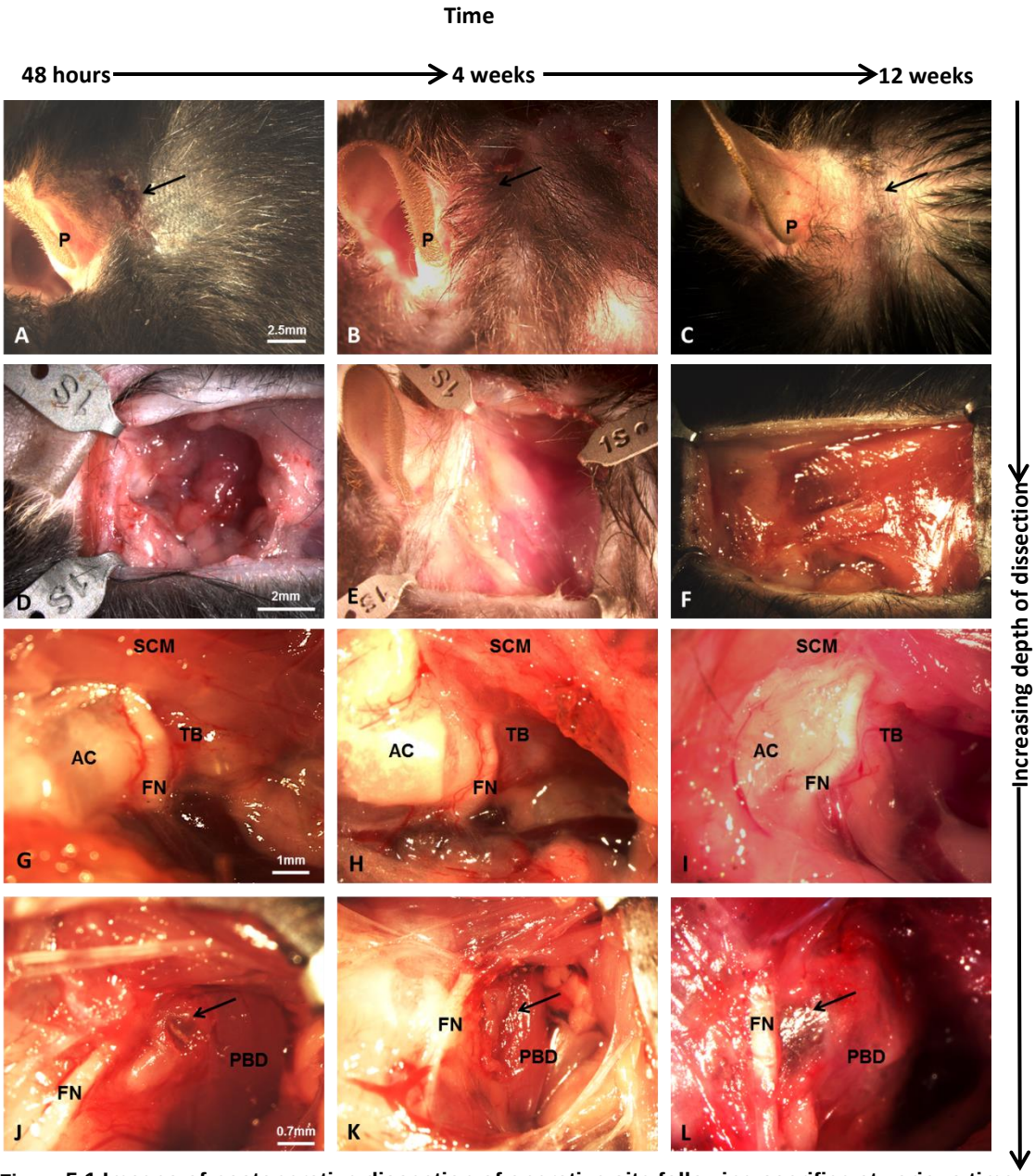

Figure 5.1 Images of postoperative dissection of operative site following sacrifice at various time points post-CI.

A - C: Postauricular wounds (indicated by black arrow), even as early as 48 hours to 1 week post-implantation, have healed well. P indicates mouse pinna.

D - F: Superficial dissection following opening of the post-auricular wound at 48 hours (d) reveals oedema in the superficial tissues and muscles. At 4 and 12 weeks this is less pronounced.

G - I: Dissection down towards the bulla (TB) reveals the facial nerve (FN), cartilaginous portion of the auditory canal (AC) and sternocleidomastoid muscle (SCM). Again at the earlier time points oedema in the tissue is more evident.

J - L: Further dissection over the bulla reveals a thin layer of tissue over the previous bullotomy site (indicated by black arrow) overlying the implant. Posterior belly of digastric muscle is noted. At later time points partial closure/complete closure of the bullotomy had taken place with new bone formation (osteoneogenesis) (see Figure 5.2).

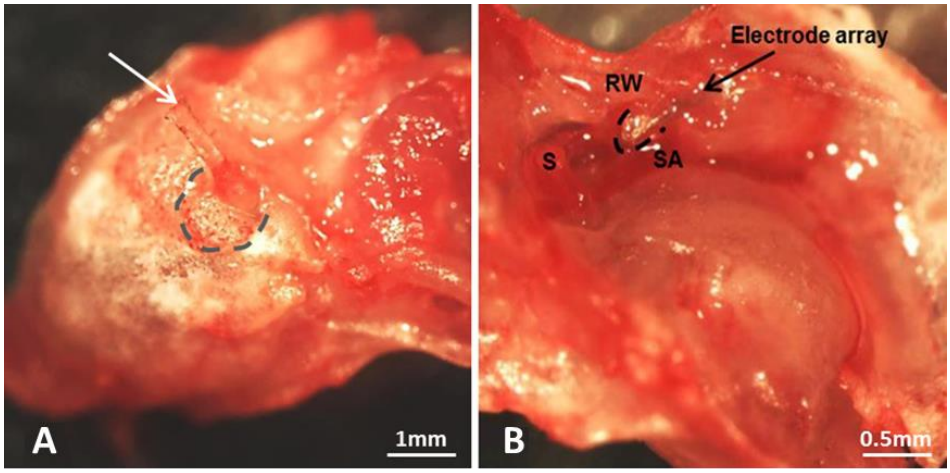

Figure 5.2 Postoperative responses in the auditory bulla. A) Auditory bulla of 3 month old mouse at 4 weeks post-implantation with fluorocarbon thread (indicated by the white arrow). New tissue suggestive of osteoneogenesis is evident at site of previous bullotomy (grey dashed line). B) Electrode array in place at round window (RW, outline marked). The stapedial artery (SA) is seen inferior to the RW and passing through the crura of the stapes (S).

5.4 Microscopic findings following cochlear implantation

5.4.1 Toluidine blue staining of cochlear cryosections and light microscopy

5.4.1.1 Sham mice

Figure 5.3 shows cochlear cryosections stained with toluidine blue taken from 3 month old mice that underwent sham surgery. In these cases, in the sham (left) operated ear, the round window was opened using a fine needle but no implant was inserted. The round window was subsequently sealed using a small amount of muscle tissue to prevent perilymph leak. In the section taken both at 48 hours and 1 week following the sham operation, small amounts of cellular debris can be seen within the scala tympani of the far lower basal turns (Figure 5.3B and C). However, subsequent sections (D and E) do not reveal such changes suggesting that this debris is confined only to the lower basal turns. The cellular debris may represent intrascalar blood or remnants from the muscle tissue used to seal the opening or could be an inflammatory reaction in response to the trauma of opening the round window membrane. The control sections do not demonstrate such changes within the scala tympani.

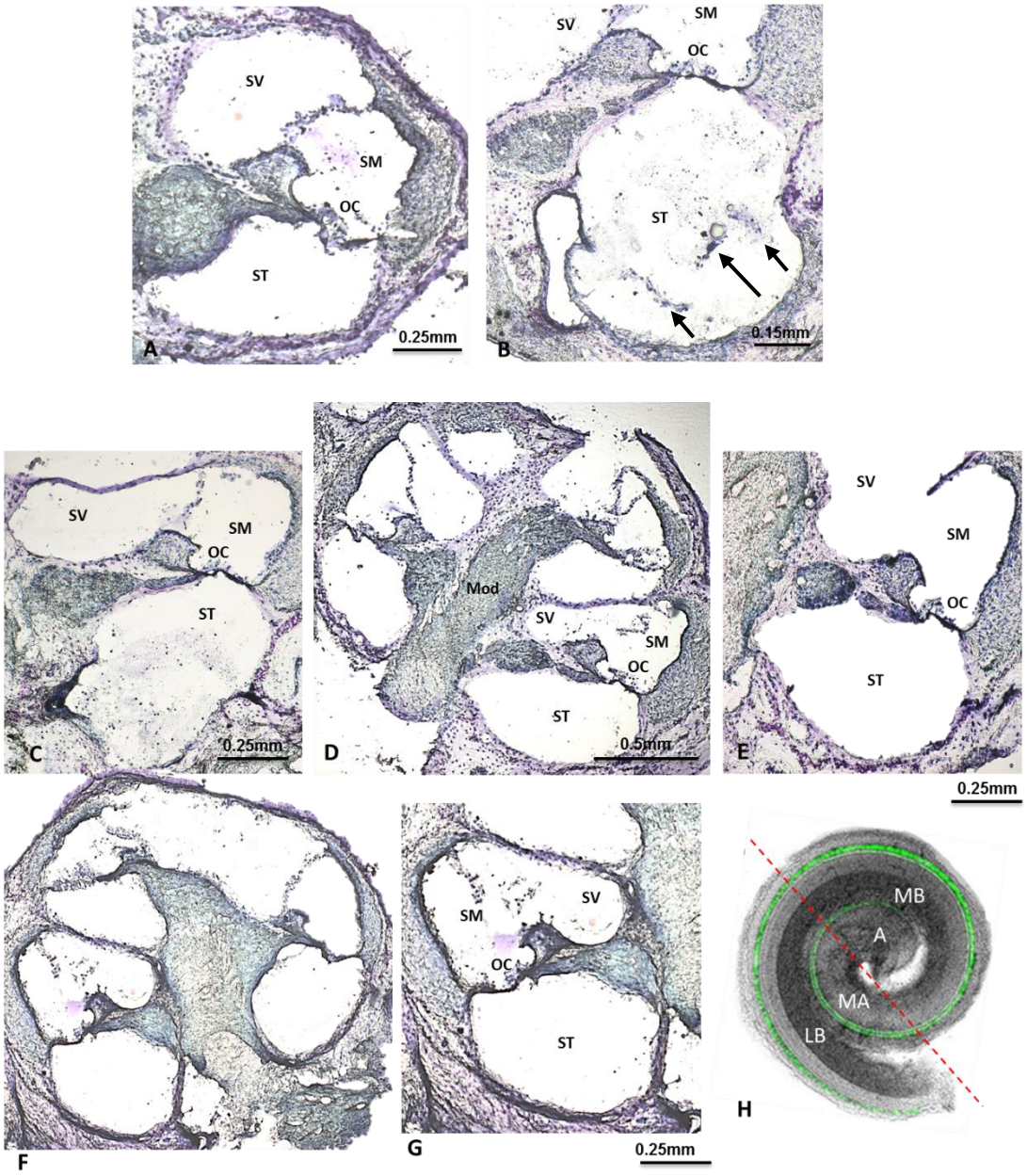

Figure 5.3 Cochlear cryosections taken from 3 month old mice that underwent sham surgery and were sacrificed at 48 hours and 1 week postoperatively. Sham surgery involved opening of the round window but no implantation. The round window was subsequently sealed with a small amount of muscle tissue. Sections have been stained with toluidine blue.

48 hours: Sections labelled A and B taken from right control, unoperated right ear and left sham operated ear respectively. There is evidence of cellular debris (black arrows) in the scala tympani (ST) of the left ear (B) compared to the control ear (A).

1 week: Sections C – E are taken from left operated ear, sections F and G are from the unoperated (right) ear. Similar to 48 hours, in the left lower basal turn (C) there is some evidence of cellular debris (black arrows) within the ST, however, on subsequent sections this is not as apparent (D and E) and appears to be limited to the far basal turn. In the control sections (F and G) the ST appears clear.

Image H included to indicate areas of cochlea from which sections were taken. Areas of cochlea defined as lower basal (LB), mid basal (MB), mid-apical (MA) and apical (A). Sections shown A – H taken from far lower basal turn (taken and adapted from Lee et al. 2006.

5.4.1.2 Implanted mice

An example of cochlear sections where implantation was performed is shown in Figure 5.4. These cochlear cryosections are taken from 3 month old and 6 month old mice implanted for 48 hours (Figure 5.4A and B) and 4 weeks (Figure 5.4C and D) respectively, with an electrode array. The implant was carefully removed following fixation, prior to sectioning and staining with toluidine blue. Sections from the left (implanted) cochlea (Figure 5.4A and B) from the mouse implanted for 48 hours revealed evidence of cellular tissue within the scala tympani. At higher magnification, this was found to be highly suggestive of erythrocytes. The presence of intrascalar blood is likely to be as a result of surgery on opening the round window membrane and following insertion of the implant. These findings were also seen in other animals at the earliest time point of 48 hours but less so at later time points, most likely due to absorption of intrascalar blood.

In sections taken from the mouse implanted for 4 weeks, evidence of cellular debris is again seen within the scala tympani of the implanted ear (Figure 5.4 D) but not in the unoperated (control) ear (Figure 5.4C). These findings were noted in sections taken from other implanted mice (with either the fluorocarbon implant or the electrode array) at all time points over which implantation occurred. The response appeared to be limited to the basal turn.

5.4.2 Light microscopy of plastic-embedded cochlear sections

Plastic-embedded cochlear sections were examined with the fluorocarbon thread in-situ and revealed encapsulation of the implant with fibrotic-like tissue within the scala tympani (Figure 5.5). The tissue appeared to have features of a dense fibrocollagenous capsule with scattered fibroblast-type cells and immune-type cells including macrophages. Other important structures including the organ of Corti, spiral ganglion cells and stria vascularis (Figure 5.5b) were also intact and not damaged as a result of CI. Both implant groups (fluorocarbon thread and electrode array) exhibited similar fibrotic-like tissue. This encapsulation was present as early

as 1 week post implantation, and persisted for all time points examined (up to 12 weeks), but remained confined to the basal turn of the cochlea.

Figure 5.4 Cochlear cryosections stained with toluidine blue from mice implanted with electrode array.

A and B Cochlear cryosections taken from a 3 month old mouse implanted with an electrode array for 48 hours. Sections from the implanted (left) ear are shown depicting the presence of cellular debris within the scala tympani (A), which at higher magnification (B) suggests the presence of erythrocytes

C and D: Cochlear cryosections taken from a 6 month old mouse implanted with an electrode array for 4 weeks. The sections are taken from comparable regions of the basal turn of the control and implanted ears respectively. (C) Section from right (control) cochlea shows absence of excess tissue in scala tympani. (D) Section from left (implanted) cochlea with evidence of reactive tissue within scala tympani. Loss of hair cells is notable at this age and corresponds to the high frequency loss seen in this strain.

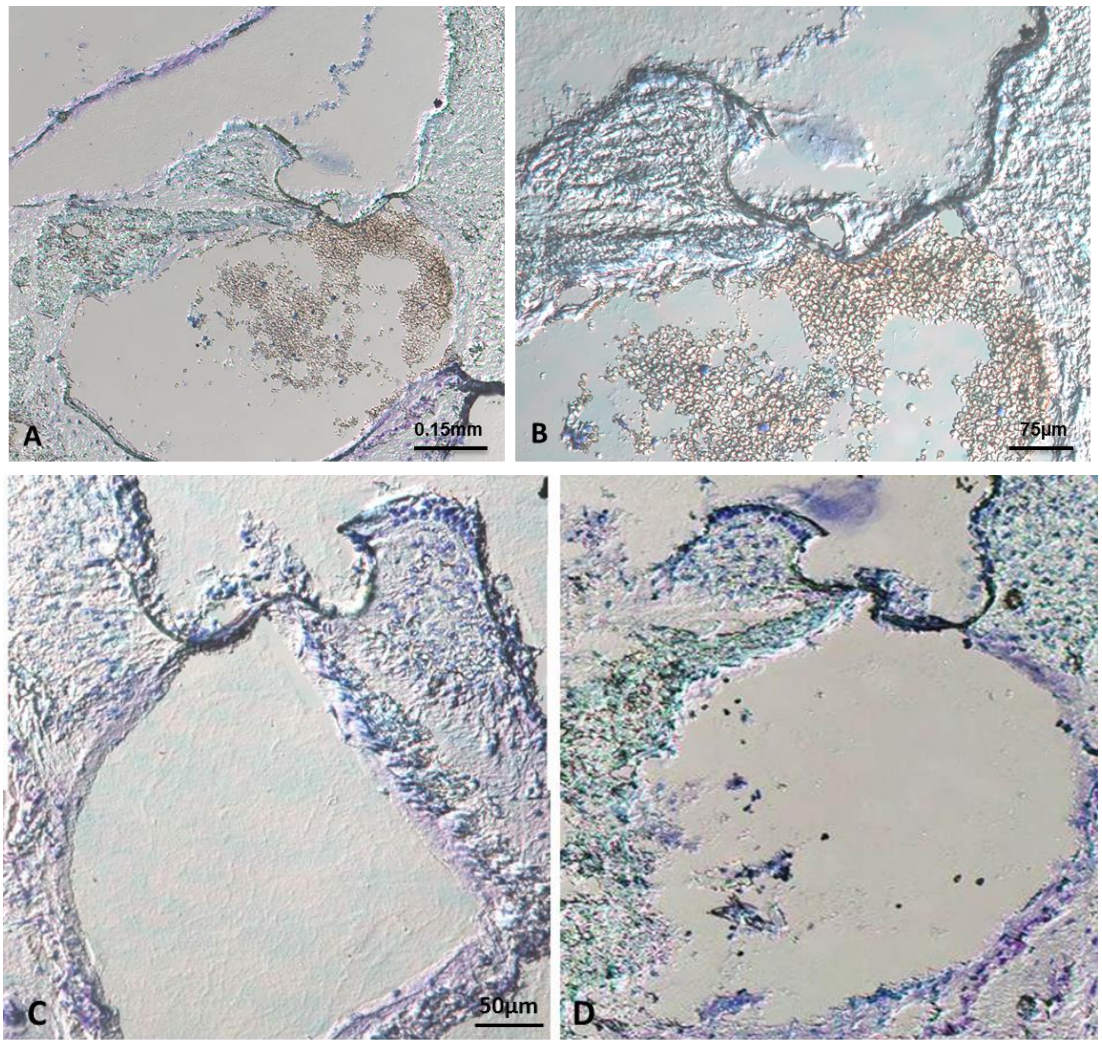

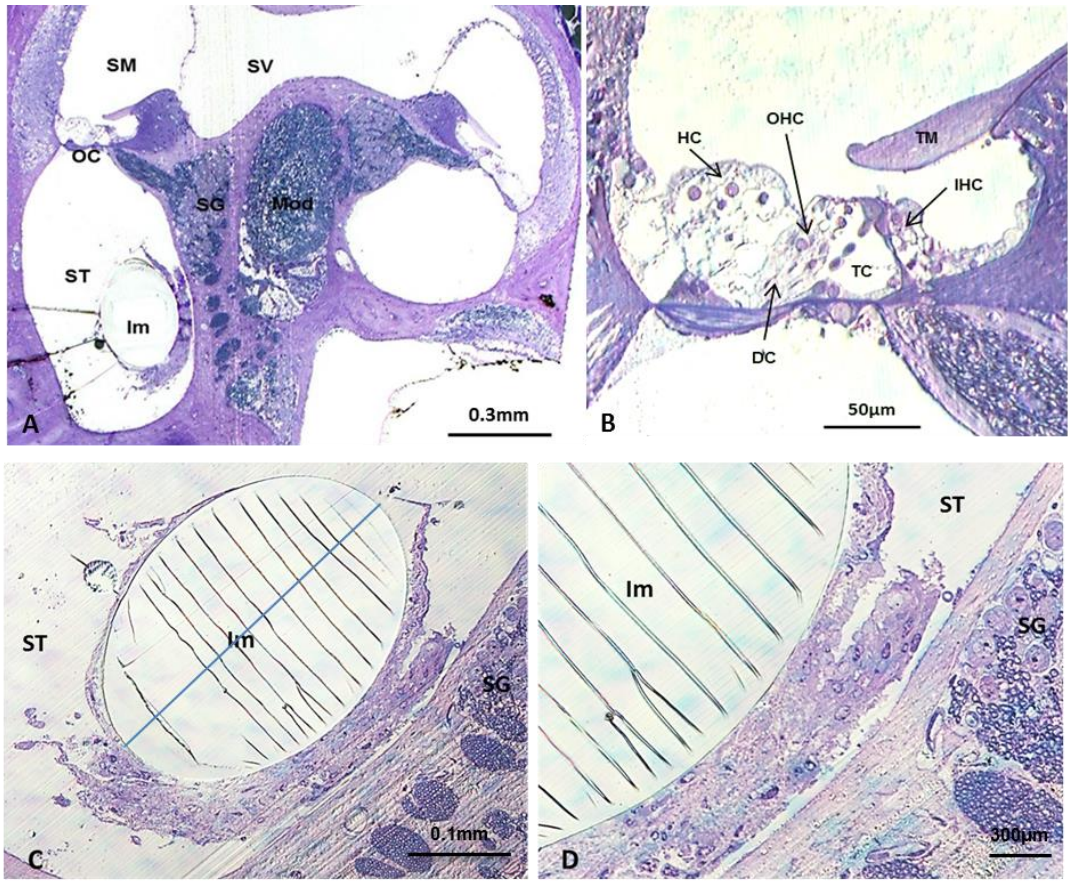

Figure 5.5 Plastic-embedded cochlear sections with the fluorocarbon thread in-situ taken from 6 month old mouse implanted for 1 week. (A) Cochlea with fluorocarbon thread implant in-situ shows evidence of fibrotic-like tissue surrounding the implant (Im) within the scala tympani (ST). Sections (C) and (D) show this fibrotic-like tissue at higher magnification. Scala media (SM), scala vestibuli (SV), organ of Corti (OC), spiral ganglion (SG), modiolus (Mod) are clearly seen. (B) Organ of Corti at higher magnification. Outer hair cells (OHC), inner hair cells (IHC), tectorial membrane (TM), tunnel of Corti (TC), Deiters' cells (DC) and Hensen's cells (HC) are labelled.

(NB: bowing of Reissner's membrane is seen in section A, suggestive of endolymphatic hydrops, however, this change was secondary to tissue processing rather than a pathological change and was also seen in controls (not shown here).

Sections prepared by Mr Graham Nevill.

5.4.3 Transmission electron microscopy (TEM)

Plastic embedded fluorocarbon-implanted cochleae were also analysed by TEM for further evaluation (Figure 5.6). The preparation and TEM scanning was undertaken by Mr Graham Nevill and Professor Andrew Forge respectively. Analysis of sections revealed further detail regarding the encapsulating tissue present around the electrode confirming the presence of fibroblast-type cells together with collagen fibrils and inflammatory cells. Sections also showed

evidence of organised tissue of epithelial origin suggesting the possibility of epithelial cells growing along the implant following round window insertion.

Figure 5.6 Plastic-embedded cochlear sections with the fluorocarbon thread in-situ taken from 6 month old mouse implanted for 1 week analysed by TEM.

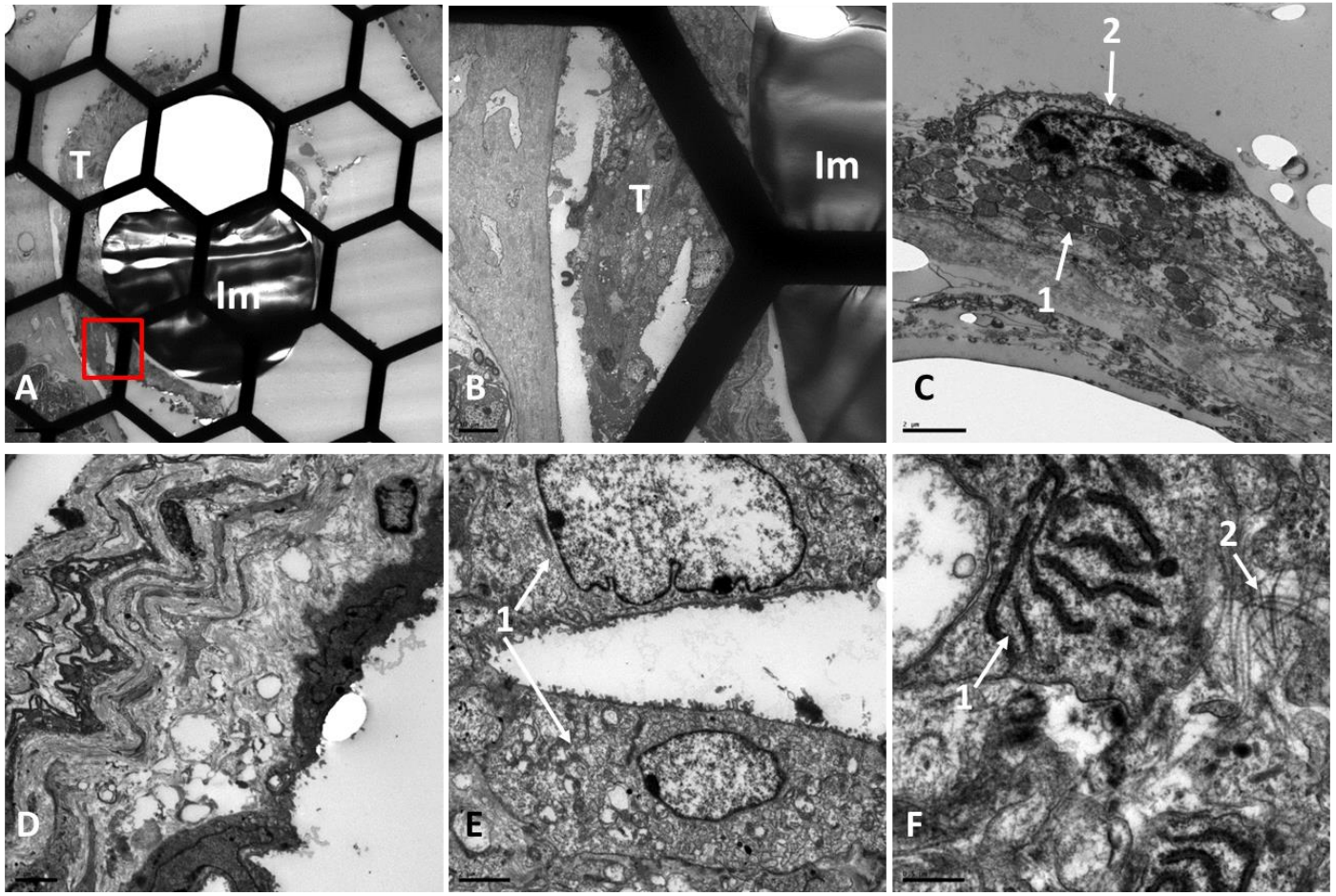

A. Low magnification image shows implant (Im) encapsulated by tissue (T). Hexagons represent grid bars to aid identification of location. Red square shows area which has been magnified in subsequent panels (Scale bar = 50µm).

B. Higher power image shows encapsulating tissue (T) in further detail around the implant (Im) (Scale bar = 10µm).

C. Numerous mitochondria (1) associated with mesothelial cell (2) (Scale bar = 2µm).

D. Laminated appearance of encapsulating tissue (Scale bar = 10µm).

E. Epithelial cells are present within the tissue (1) and may have originated from the round window membrane at the time of implantation (Scale bar = 2µm).

F. Rough endoplasmic reticulum (RER) (1) is noted together with numerous collagen fibrils (2) (Scale bar = 0.5µm)

5.5 Analysis of inflammatory response to cochlear implantation in the mouse

To assess the inflammatory response of the tissue to implantation, the technique of immunofluorescence was used. Two antibodies, CD45 and F480, were trialled in the initial phase to decide which would be the most appropriate and also to optimise conditions for their use in the detection of inflammatory-type cells. CD45 or common leucocyte antigen as it is otherwise known, is a tyrosine phosphatase integral membrane protein expressed on the cell surface of all haematopoietic cells with the exception of platelets and mature erythrocytes (Charbonneau et al., 1988). It is through its role in the regulation of protein-tyrosine kinases, which are key to signal transduction, and through the mediation of cell-to-cell interactions, that CD45 acts to promote B and T cell activation. CD45 is also involved in the migration of immune cells and plays a crucial role in integrin-mediated adhesion (Trowbridge and Thomas 1994).

In the murine cochlea, studies have utilised these qualities of CD45 to investigate the presence of an inflammatory response to insults including acoustic trauma. Hirose et al. (2005) performed immunohistochemistry for CD45 to study the effects of acoustic trauma on the cochleae of CBA/CaJ mice. Results revealed many CD45 positively-labelled cells, mainly within the spiral limbus and ligament of the cochlea following noise injury. Through further experiments the authors found that the majority of cells present were of monocyte/macrophage lineage with a few lymphocytes and natural killer cells present. It was suggested that the primary aim of these inflammatory cells was to aid in the reestablishment of the endocochlear potential through the clearance of debris and repair of the reticular lamina, which was ruptured with noise exposures of 116 dB or greater, rather than to promote repair of sensory epithelia damaged as a result of acoustic trauma (Hirose et al., 2005). Similarly, other studies have also used CD45 to investigate the cochlea's immune response and the role of inflammatory cells following acoustic injury (Miyao et al., 2008; Tan et al., 2008).

F4/80 is a monoclonal antibody which was first described as a marker for mouse monocytes and macrophages (Austyn and Gordon 1981). It forms part of the epidermal growth factor-seven transmembrane (EGF-TM7) family which represent a group of heptahelical

transmembrane receptors principally expressed by cells of the immune system. EGF-module-containing mucin-like hormone receptor (EMR) 1 (EMR1) is the human equivalent and has been found to show high levels of expression on monocyte and macrophage lines on reverse transcriptase polymerase chain reaction (RT-PCR) and is thought to share 68% homology with its mouse counterpart (Taylor et al., 2005). Expression during development and through adult life in a variety of infectious and inflammatory disease models, means that F4/80 has lent itself widely as a mouse macrophage antigen marker (Gordon et al., 2011). In the mouse auditory system, F4/80 has been used in a similar manner to CD45 to detect immune cell recruitment following acoustic trauma within the cochlea (Tornabene et al., 2006) and to characterise and investigate the inflammatory response of perivascular-resident macrophage-like melanocytes in the vestibular system (Zhang et al., 2013).

5.5.1 Optimisation of antibodies

For the purposes of the current study, the aim was to investigate the presence of inflammatory cells within cochlear sections taken from mice implanted with both the fluorocarbon implant and the electrode array. Both CD45 and F4/80 antibodies were trialled at concentrations of 1:100 and 1:200 in conjunction with other antibodies. Following optimisation, CD45 at 1:100 concentrations gave the best results and was used together with calretinin (1:100) to stain sections for CD45 and spiral ganglion cell counts respectively (Figure 5.7).

Figure 5.7A. Immunofluorescence using CD45 and MyoVIIa antibodies – control sections taken from 3 month old mouse for optimisation of antibodies

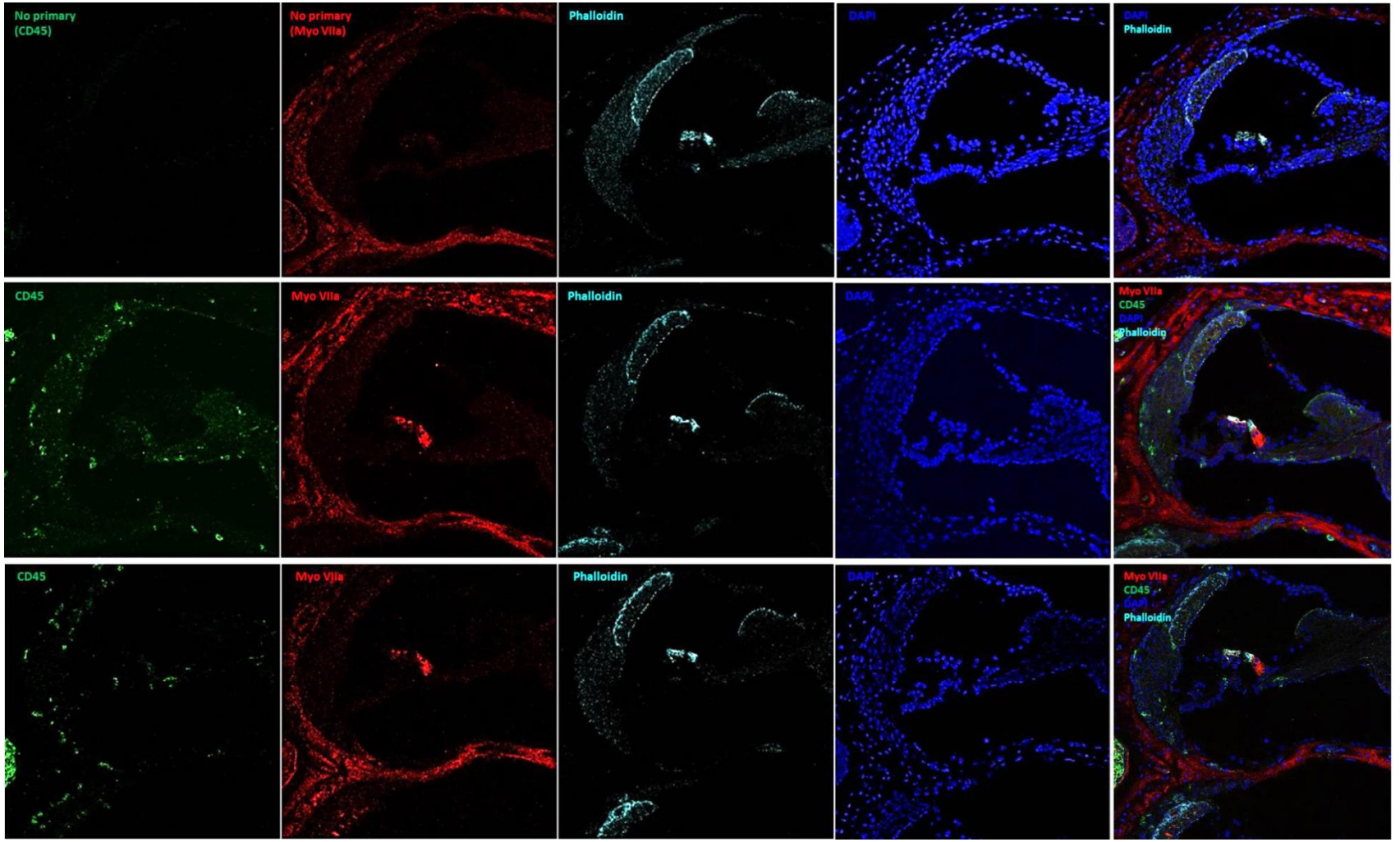

Figure 5.7B. Immunofluorescence using F4/80 and MyoVI antibodies – control sections taken from 3 mo nth old mouse for optimisation of antibodies

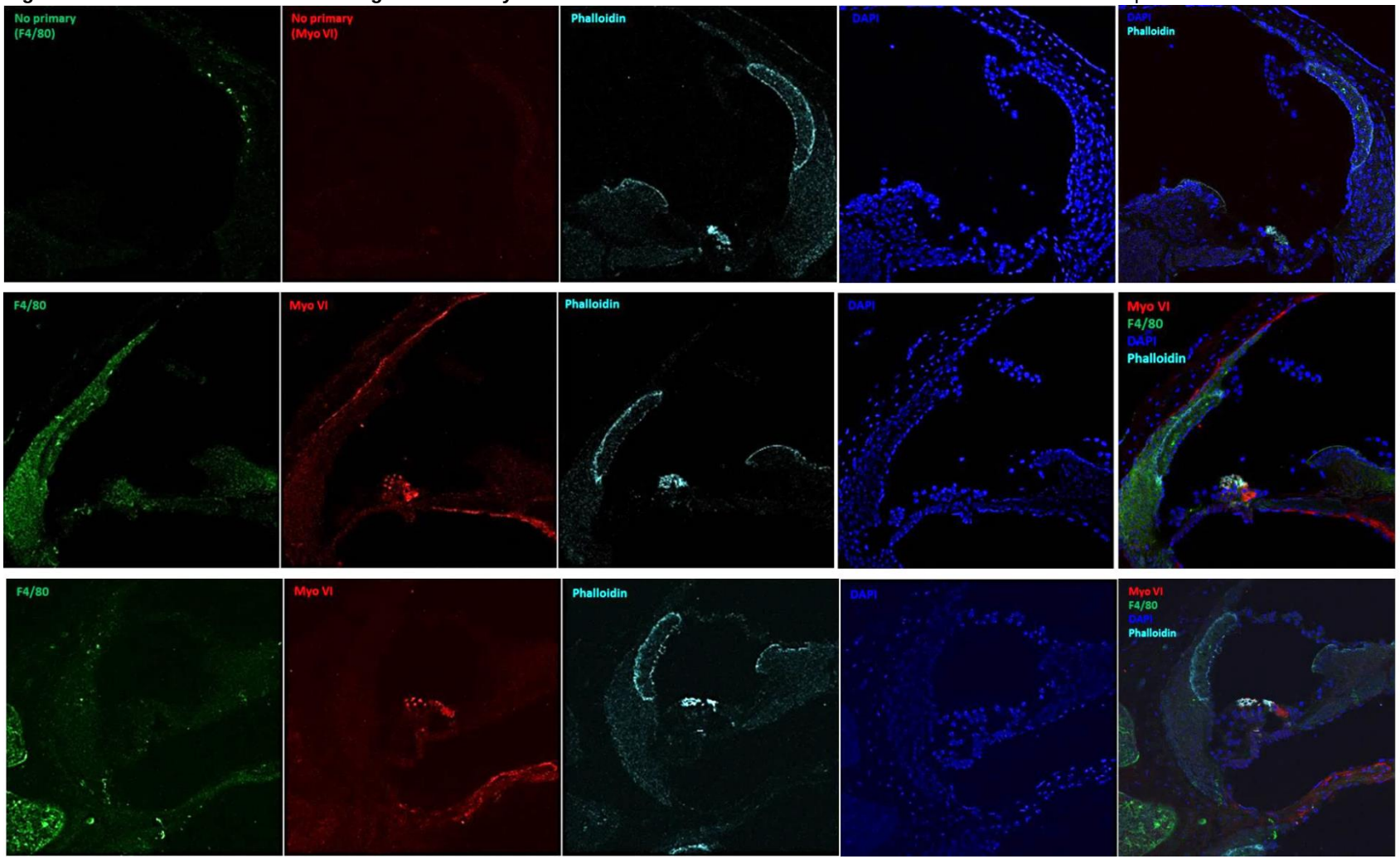

Figure 5.7C. Immunofluorescence using MyoVIIa and calretinin antibodies – control sections taken from 3 month old mouse for optimisation of antibodies

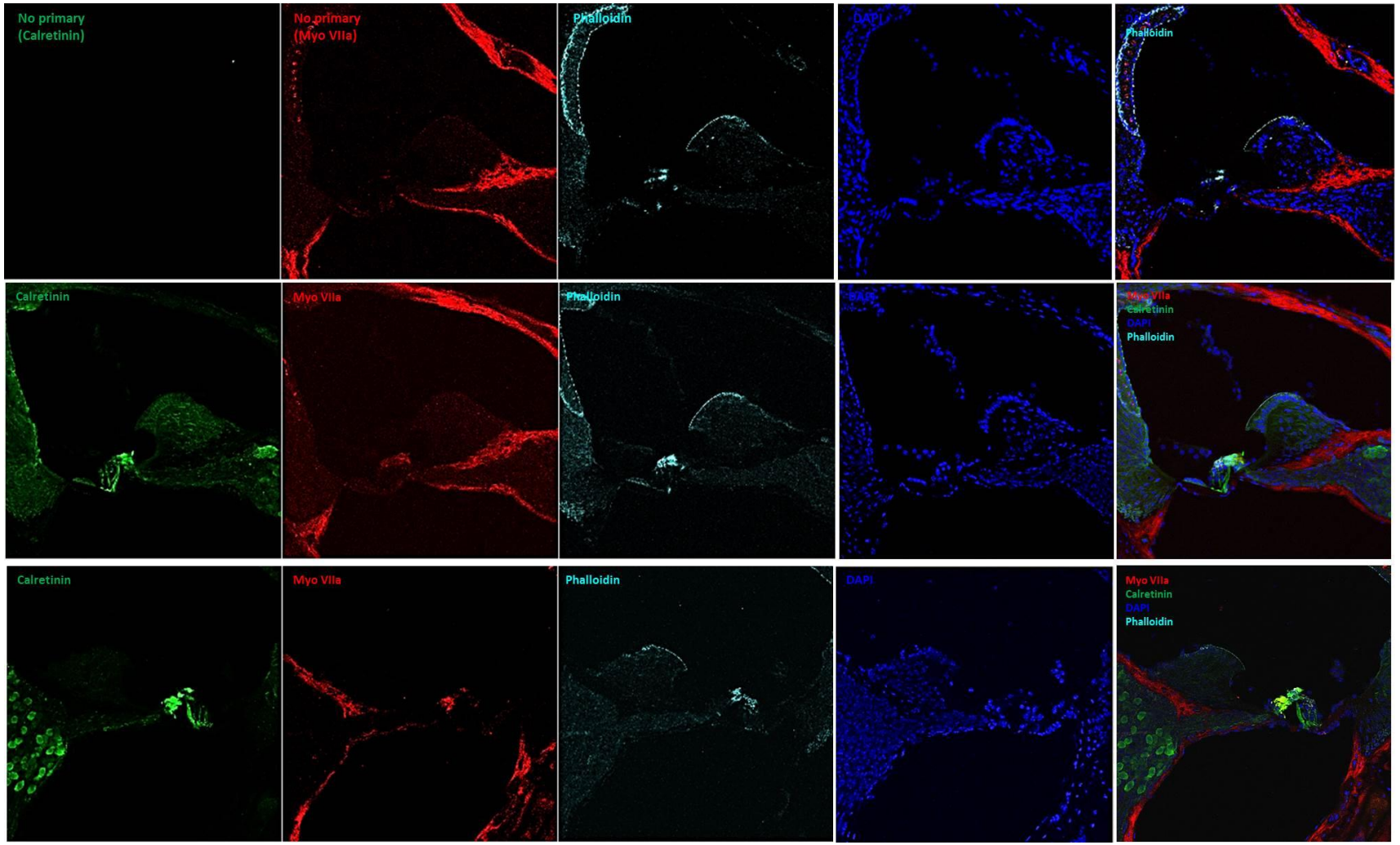

5.5.2 Analysis of inflammatory response

Counts of CD45-positively labelled cells were performed on sections taken from cochleae of mice implanted with both the fluorocarbon thread as well as the electrode array. Multiple sections from the implanted and control ears of 14 mice were analysed using immunofluorescence, the group having an average age of 186 days. Numbers in each group were as follows, fluorocarbon implants: 48 hours (n=3), 1,4,12 weeks (n=2); electrode array 48 hours (n=2), 1,4,12 weeks (n=1).

When comparing CD45-postively labelled cells from implanted and control cochleae, a clear difference was noted, with significantly greater numbers of positively-labelled cells within the implanted cochleae compared to the control cochleae at the majority of time points and regardless of the type of implant used (T-Test, $P<0.05$) (Table 5.1). Figure 5.8 shows the mean number of CD45-positively labelled cells for combined implants across the different time points for all three cochlear regions. When analysing the various cochlear turns of the implanted ear, significantly greater numbers of CD45-positively labelled cells were noted in the lower basal region compared to upper basal and apical regions (T-Test, $P<0.05$). As the implant is physically located in the lower basal turn of the cochlea, these results suggest a more pronounced inflammatory response confined to this region in response to implantation. The inflammatory response can also be seen to peak between 1 and 4 weeks in all three cochlear regions before decreasing to lower levels at 12 weeks. These findings are particularly important with regards to the potential location of delivery and timing of therapeutic agents to reduce inflammation.

Figures 5.9 to 5.12 show sections demonstrating the presence of CD45-positively labelled cells in control and implanted ears at various times post-implantation. At all four time points tested, for both implantation with fluorocarbon thread or electrode array, more CD45-positively labelled cells were noted in similar regions of the cochlea, namely, the basilar membrane, scala tympani, spiral ligament and within the region of the osseous spiral lamina. As well as the presence of CD45-positively labelled cells in sections from implanted cochleae, the presence of cellular debris and possible fibrosis was noted within the scala tympani. At 48

hours, the presence of cellular material within the scala tympani may have been due to the presence of residual blood secondary to haemorrhage at the time of surgery and as a result of sealing the round window with muscle tissue. This was also seen on toluidine blue staining of sections taken from implanted mice at this time point (Figure 5.4 A and B). At later time points of 1, 4, and 12 weeks this staining within the scala tympani is likely to be due to the presence of fibrotic tissue forming as demonstrated previously (Figure 5.5 and 5.6).

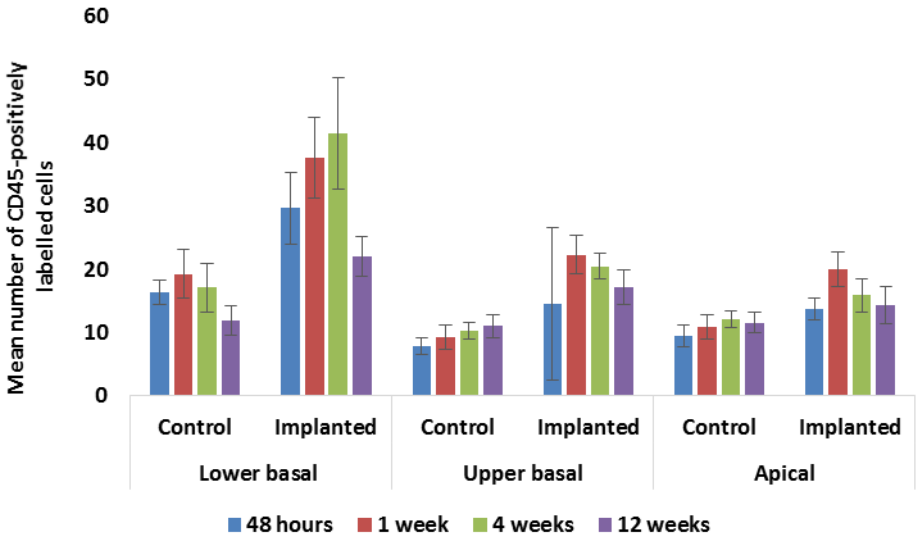

Figure 5.8 Comparison of the mean number of CD45-positively labelled cells for combined implants across the different time points for all three cochlear regions.

Significantly greater numbers of cells are present in the lower basal turn of the implanted ear compared to the other regions ($P<0.05$). This is also the case when the lower basal implanted ear is compared to the control ear ($P<0.05$). The inflammatory response can be seen to peak at between one and four weeks in all three cochlear regions before decreasing to lower levels at 12 weeks. (Numbers in each group: 48 hours, n=5; 1,4,12 weeks, n=3. Error bars represent ±2SEM.

Table 5.1 Mean numbers of CD45-postiviely labelled cells from implanted (left) and control (right) cochleae. Comparisons made based on the presence of CD45-positively labelled cells seen in each of the three cochlear regions: lower basal, upper basal and apical. T-test performed to compare implanted and control ears at each time point within each region (±2SEM shown in brackets next to mean in table). Numbers in each group: fluorocarbon implants n=3 48 hours, n=2 for 1,4,12 weeks; electrode array n=2 for 48 hours, n=1 for 1,4,12 week.

		Mean CD45 counts								
		Lower basal			Upper basal			Apical		
Implant type	Duration of implantation	Control	Implanted	P-value	Control	Implanted	P-value	Control	Implanted	P-value
Fluorocarbon implant	48 hours	19 (1.59)	37 (7)	<0.001	12 (2)	18 (2)	0.001	11 (2)	15 (2)	0.004
	1 week	14 (3)	35 (4)	<0.001	10 (2)	25 (2)	<0.001	10 (2)	23 (3)	<0.001
	4 weeks	13 (3)	37 (11)	<0.001	12 (1)	18 (2)	<0.001	13 (2)	18 (3)	0.006
	12 weeks	11 (2)	18 (4)	0.003	11 (2)	17 (3)	0.002	11 (2)	10 (3)	0.698

		Mean CD45 counts								
		Lower basal			Upper basal			Apical		
Implant type	Duration of implantation	Control	Implanted	P-value	Control	Implanted	P-value	Control	Implanted	P-value
Electrode array	48 hours	9 (1)	16 (3)	0.004	5 (1)	11 (2)	<0.001	6 (2)	10 (2)	0.02
	1 week	24 (5)	41 (15)	0.028	8 (4)	14 (7)	0.168	8 (2)	14 (2)	0.001
	4 weeks	25 (7)	51 (9)	0.001	7 (2)	24 (3)	<0.001	10 (2)	15 (4)	0.08
	12 weeks	14 (5)	26 (4)	0.003	12 (4)	17 (5)	0.083	14 (4)	20 (3)	0.019

		Mean CD45 counts								
		Lower basal			Upper basal			Apical		
Implant type	Duration of implantation	Control	Implanted	P-value	Control	Implanted	P-value	Control	Implanted	P-value
Combined implants	48 hours	16 (2)	30 (6)	<0.001	8 (1)	15 (12)	<0.001	10 (2)	14 (2)	0.001
	1 week	19 (4)	38 (6)	<0.001	9 (2)	22 (3)	<0.001	11 (2)	20 (3)	<0.001
	4 weeks	17 (4)	42 (9)	<0.001	10 (1)	21 (2)	<0.001	12 (1)	16 (3)	0.009
	12 weeks	12 (2)	22 (3)	<0.001	11 (2)	17 (3)	<0.001	12 (2)	14 (3)	0.186

Figure 5.9 Immunofluorescence of cochlear cryosections (basal turn) taken from mice implanted for 48 hours.

(A) Control (right) and (B) implanted (left) ear of mouse implanted with a fluorocarbon thread for 48 hours. CD45 staining reveals increased numbers of CD45-positively labelled cells in the implanted ear (white arrows) compared to the control ear, particularly in the regions of the basilar membrane (BM), scala tympani (ST), spiral lamina (SLa) and spiral limbus (SLi). There is also evidence of cellular debris within the ST (red arrow).

(C) and (D) Immunolabelling of cochlear cryosection from mouse implanted for 48 hours with electrode array. Increased numbers of CD45-positively labelled cells confirmed by their characteristic appearance at higher magnification (D).

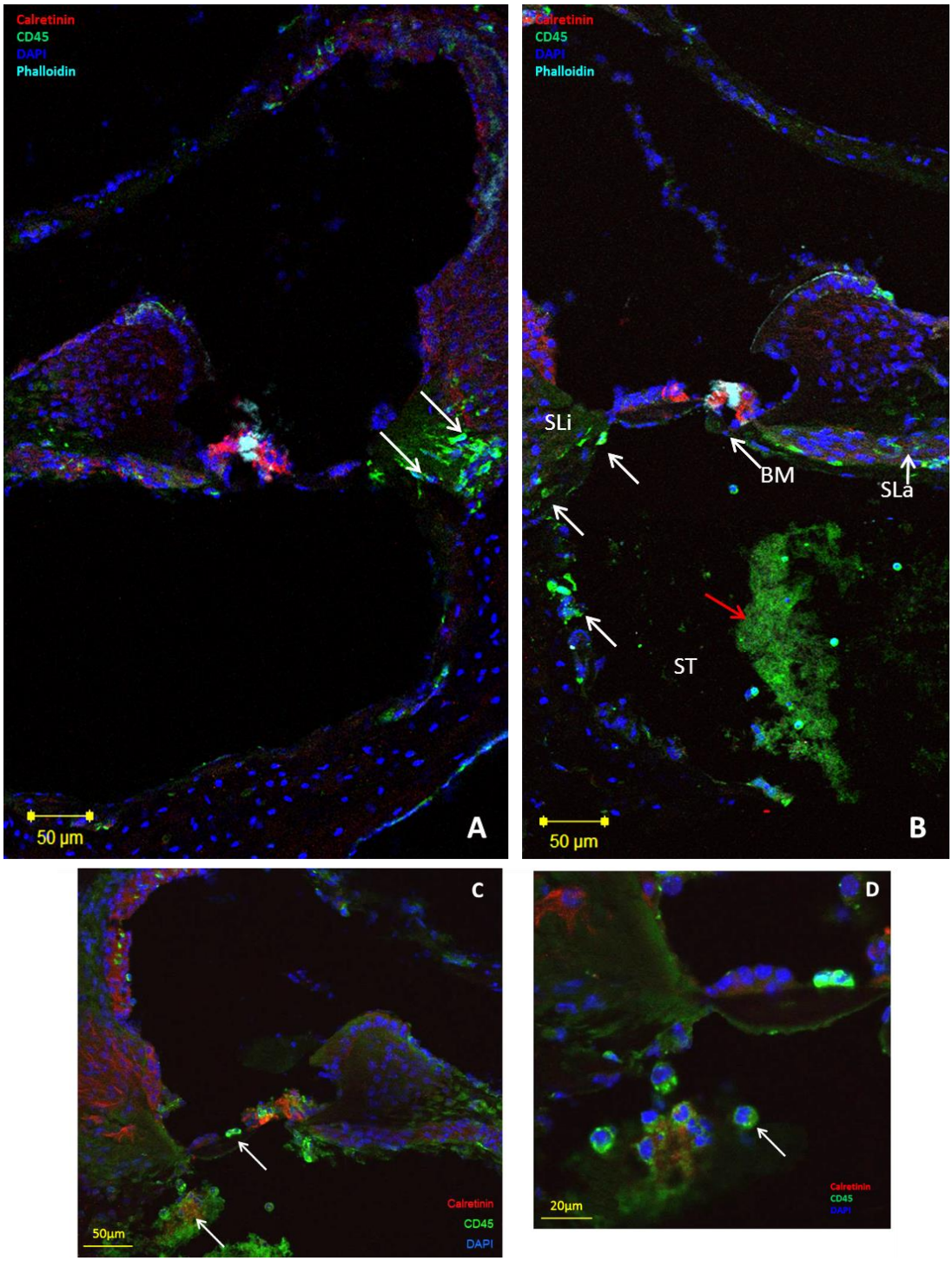

Figure 5.10 Immunofluorescence of cochlear cryosections (basal turn) taken from mouse implanted for 1 week with electrode array.

Sections reveal increased numbers of CD45-positively labelled cells in the (B) implanted ear (white arrows) compared to the (A) control ear particularly in the regions of the spiral lamina (SLa) and spiral limbus (SLi). There is also evidence of cellular debris within the scala tympani (ST) which may represent the presence of fibrosis (red arrow).

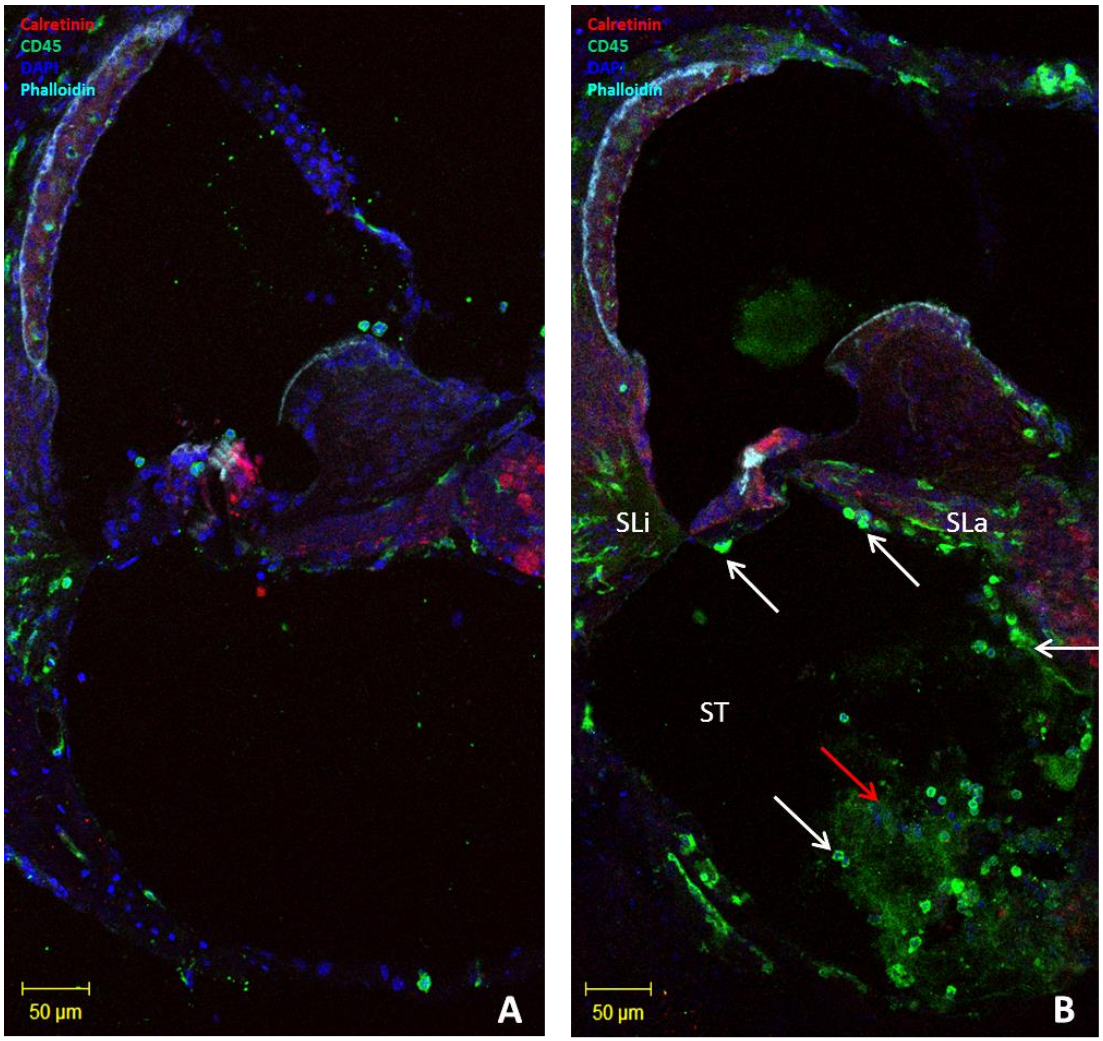

Figure 5.11 Immunofluorescence of cochlear cryosections (basal turn) taken from mouse implanted for 4 weeks with fluorocarbon thread.

Sections reveal increased numbers of CD45-positively labelled cells in the implanted ear (B) (white arrows) compared to the control ear (A) particularly in the region of the basilar membrane (BM) and scala tympani (ST). There is also evidence of cellular debris within the scala tympani (ST) (red arrow).

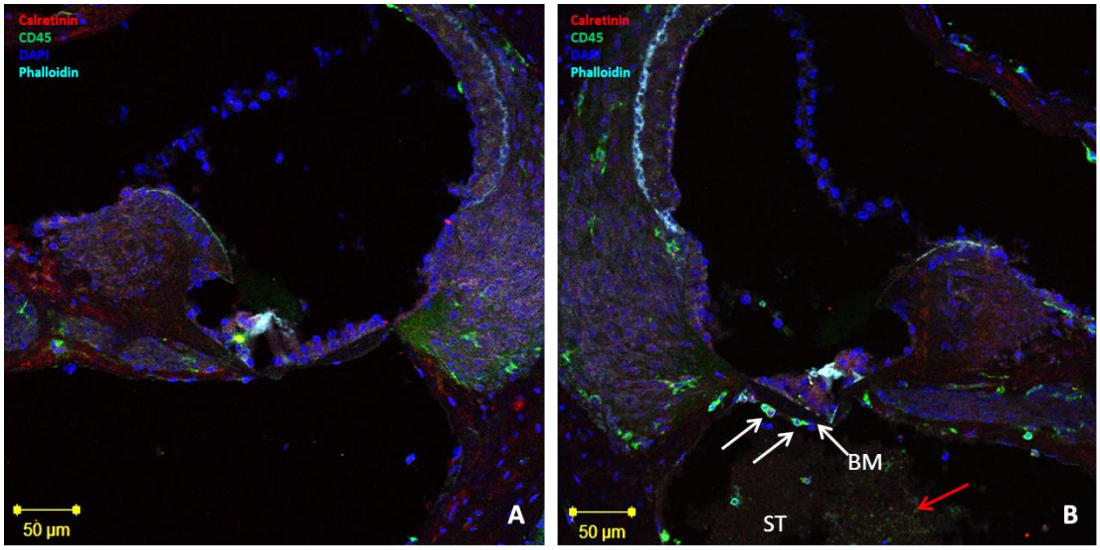

Figure 5.12 Immunofluorescence of cochlear cryosections (basal turn) taken from mouse implanted for 12 weeks with electrode array.

The presence of CD45-positively labelled cells in the implanted ear (B) compared to the control ear (A) is not so pronounced at this stage. In the implanted ear, evidence of deposition of possible fibrosis at the periphery of the ST is present (tissue surrounded by red-dashed line).

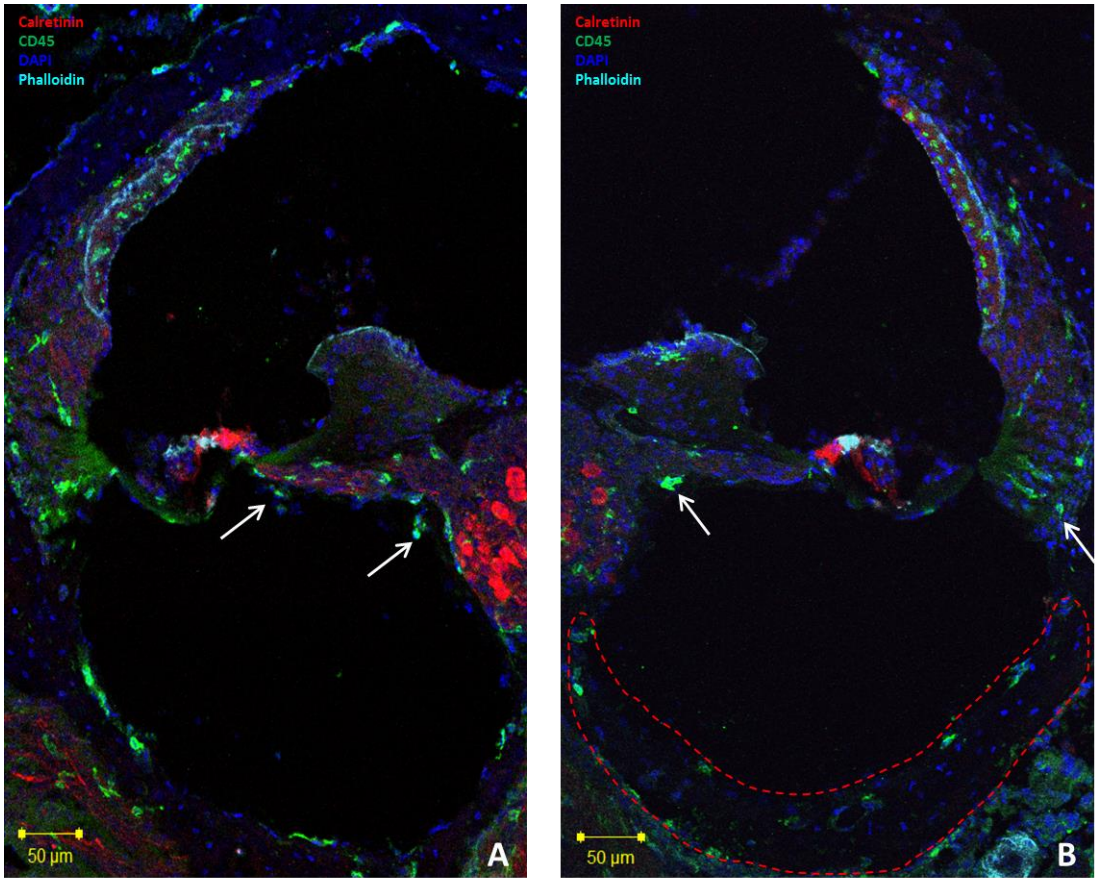

5.6 Quantitative analysis of spiral ganglion cells following cochlear implantation in the mouse

As electrical stimulation of spiral ganglion neurons by the electrode array is the main basis of hearing restoration in CI, preserving and maintaining the health of these cells and their connections is vital (Bas et al., 2015; Nadol, Jr. et al., 1989). In order to perform a quantitative analysis of SGCs following CI in the mouse, immunofluorescence was used. Anti-calretinin, based on the intracellular calcium-binding protein calretinin, was used as the primary antibody. As a member of the calmodulin family, calretinin plays a key role in calcium homeostasis and is a vital in component of many of the regulatory pathways requiring calcium within the central nervous system. It is also expressed by some groups of peripheral neurons and found within the olfactory bulb and auditory pathways (Arai et al., 1991; Dechesne et al., 1991; Rogers 1987).

In order to perform a quantitative analysis following CI in the mouse, counts of SGCs within the area of Rosenthal's canal were performed and expressed as a density. As numbers were small within each individual implant group, a combined analysis of all implants, fluorocarbon thread and electrode array, was performed in the 6 month old group.

The mean SGC densities for the implanted and control ears at each cochlear region and at the various time points following implantation are shown in Table 5.2 and Figure 5.13. Comparisons of implanted and control ears did not reveal statistically significant differences in SGC density for any of the cochlear regions at any time points tested (T-Test, $P>0.05$).

Changes in SGC density measured across the various time points for each cochlear region were assessed (Jonckheere–Terpstra test for repeated measures). In the lower basal region (Figure 5.14A) overall SGC density did not decline significantly in the control ear ($P=0.801$) and showed only a slight decline in the left ear by 12 weeks ($P=0.327$). When plotted as the difference between the two ears (Figure 5.14B), however, a downward slope is seen suggesting the progressive loss of SGCs in the implanted ear with time. In the case of the upper basal and apical regions, the converse was seen with a slight increase in SGC densities over time in both the implanted and control ears ($P>0.05$) (Figure 5.14C and E). This is also

case when the mean difference between the ears is plotted over time, where greater SGC densities are seen in the implanted ear (Figure 5.14D and F). These latter results did not prove significant on statistical testing.

Examples of images obtained following labelling for calretinin in spiral ganglion cell bodies of cochlear cryosections are shown in Figure 5.15.

	Mean SGC density (number/mm^2)					
	Right lower basal	**Left lower basal**	**Right upper basal**	**Left upper basal**	**Right Apical**	**Left Apical**
48 hours	1843 (204)	1718 (154)	1637 (136)	1569 (124)	1533 (98)	1554 (148)
	0.339		0.465		0.816	

	Mean SGC density (number/mm^2)					
	Right lower basal	**Left lower basal**	**Right upper basal**	**Left upper basal**	**Right Apical**	**Left Apical**
1 week	1530 (190)	1497 (212)	1529 (93)	1528 (194)	1884 (240)	1635 (141)
	0.817		0.997		0.132	

	Mean SGC density (number/mm^2)					
	Right lower basal	**Left lower basal**	**Right upper basal**	**Left upper basal**	**Right Apical**	**Left Apical**
4 weeks	1736 156)	1687 (121)	1574 (116)	1480 (241)	1937 (199)	2170 (226)
	0.638		0.459		0.128	

	Mean SGC density (number/mm^2)					
	Right lower basal	**Left lower basal**	**Right upper basal**	**Left upper basal**	**Right Apical**	**Left Apical**
12 weeks	1721 (320)	1529 (193)	1789 (193)	1908 (177)	1735 (314)	1927 (203)
	0.294		0.370		0.298	

Table 5.2 Mean SGC densities (±2SEM) are shown for the combined group of implants undertaken in the 6 month old mice (n=3 mice at each time point except 48 hours where n=4). T-Test was performed to assess for the presence of significant differences between the implanted and control ears. P values are shown in the table. There were no significant differences between SGC densities at the various regions at the four different time points (P>0.05).

Figure 5.13 Mean SGC densities for the three cochlear regions are shown over the various implantation time points tested. SGC densities were similar across the three regions and there were no significant differences noted when comparing implanted and control ears on statistical testing. Error bars represent two SEM (n=3 mice at each time point except 48 hours where n=4).

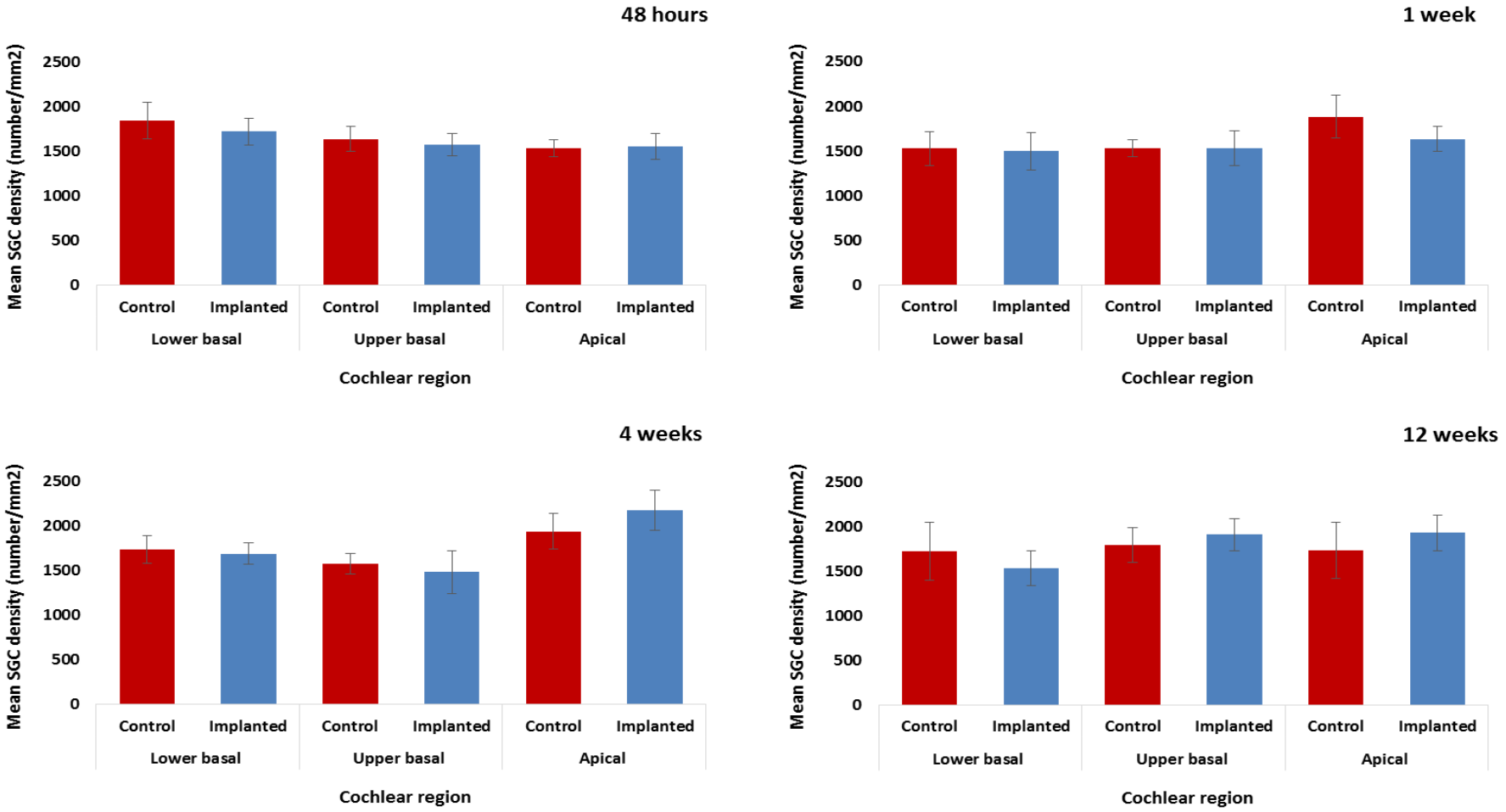

Figure 5.14 A - F Mean SGC densities and difference in mean SGC densities between implanted and control ear are shown over the various implantation time points tested. Graphs A, C, and E show the implanted (left) ear compared to the control (right) ear over the various time points. Graphs B, D and F show the difference between the implanted and control ears over the various time points. Trend lines have also been shown.

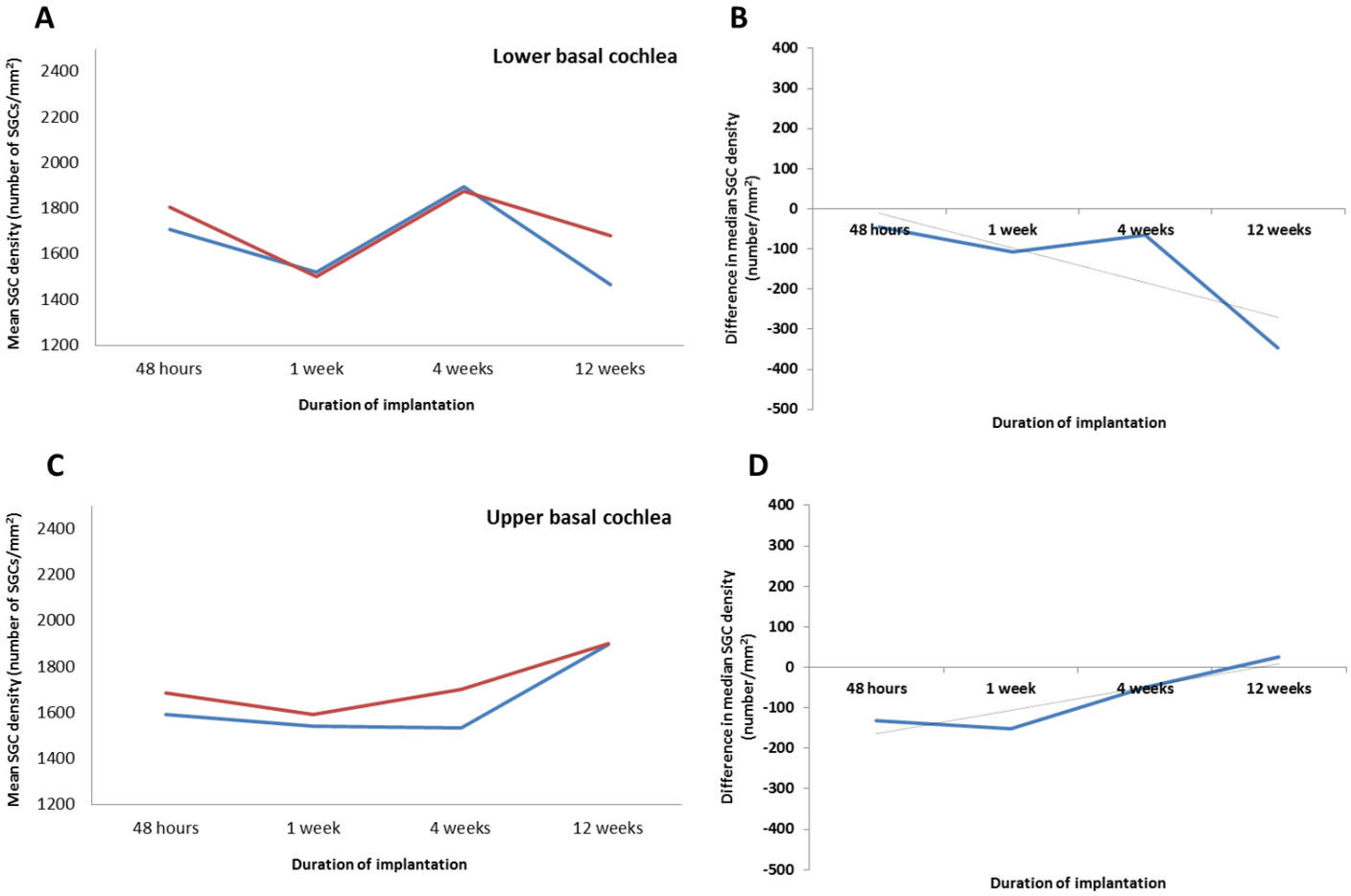

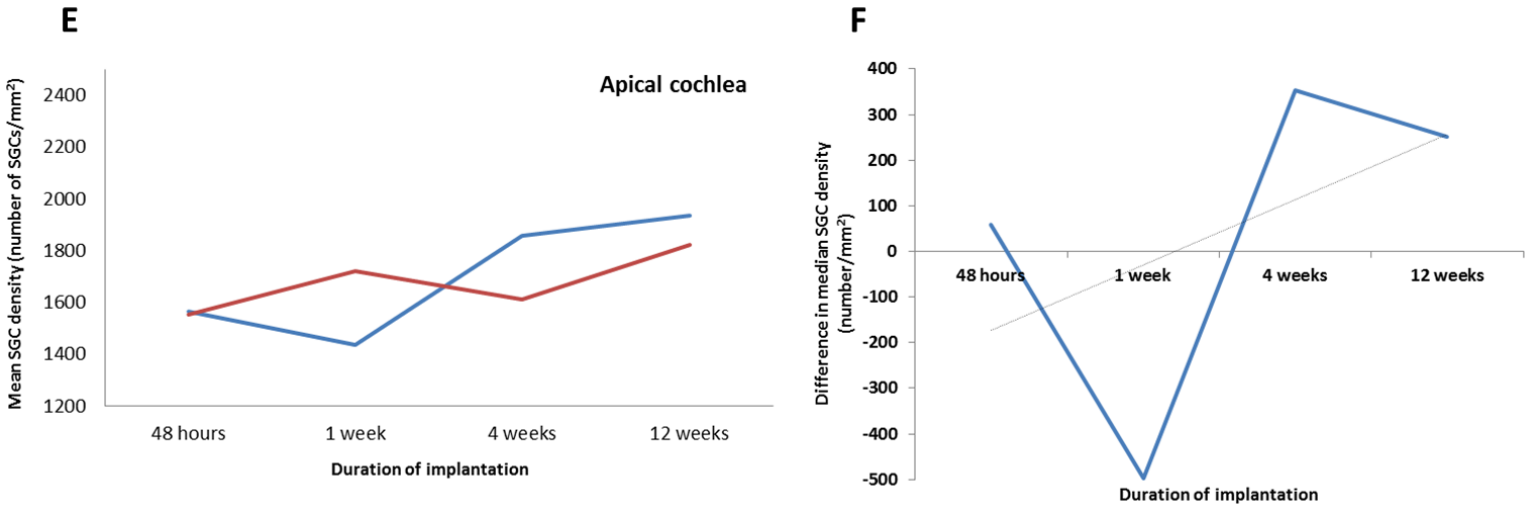
E
Apical cochlea
Mean SGC density (number of SGCs/mm²)
2400
2200
2000
1800
1600
1400
1200
48 hours
1 week
4 weeks
12 weeks
Duration of implantation
F
Difference in median SGC density (number/mm²)
400
300
200
100
0
-100
-200
-300
-400
-500
48 hours
1 week
4 weeks
12 weeks
Duration of implantation

Figure 5.15 Immunofluorescence labelling for calretinin in spiral ganglion cell bodies of cochlear cryosections (lower basal turn) at various time points following implantation in 6 month old mice. The images suggest a reduction in SGC numbers over time in both the control and implanted ears. However, the overall SGC density was not found to decline significantly in either the control ear or the implanted ear over time (P>0.05).

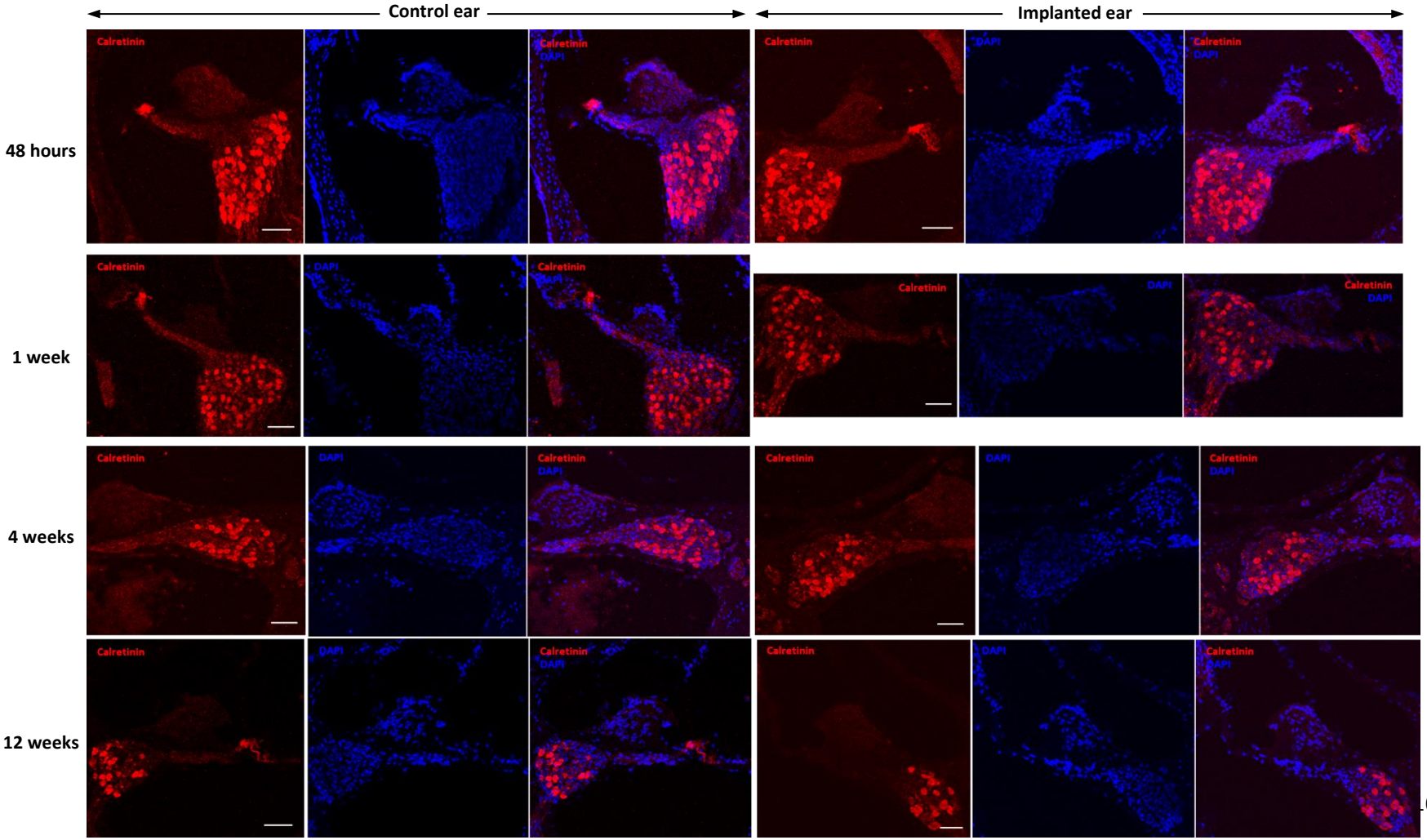

5.7 Quantitative analysis of hair cells following cochlear implantation in the mouse

A quantitative analysis of hair cells following CI in the mouse was performed using whole mounts of the organ of Corti taken from 3 month old mice. As numbers of mice in each group were small, a combined analysis of all implants, fluorocarbon thread and electrode array, was again performed. The mean age of the mice included in this analysis was 99.25 days. Mean hair cell counts for each of the cochlear regions analysed over the various time points are shown in table 5.3 and represented graphically in Figure 5.16.

a)	Mean inner hair cells/100µm							
	Implanted (Left) Ear				Control (Right) Ear			
	Basal	Mid-basal	Mid-apical	Apical	Basal	Mid-basal	Mid-apical	Apical
48 hours		11	11	12		10	12	12
1 week		11	11	12		11	12	13
4 weeks	11	11	12	12	16	12	13	11
12 weeks		12	11	13		11	11	11

b)	Mean outer hair cells/100µm							
	Implanted (Left) Ear				Control (Right) Ear			
	Basal	Mid-basal	Mid-apical	Apical	Basal	Mid-basal	Mid-apical	Apical
48 hours		35	38	37		22	36	38
1 week		39	38	38		35	38	37
4 weeks	18	37	37	44	41	35	38	38
12 weeks		39	39	35		35	36	36

(c)	Inner hair cells				Outer hair cells			
	Basal	Mid-basal	Mid-apical	Apical	Basal	Mid-basal	Mid-apical	Apical
48 hours	-	0.459	0.520	0.700	-	0.535	0.229	0.483
1 week	-	0.163	0.094	0.346	-	0.423	0.772	0.605
4 weeks	0.034	0.440	0.072	0.381	0.022	0.144	0.810	0.499
12 weeks	-	0.784	0.922	0.584	-	0.199	0.166	0.724

Table 5.3 Mean inner and outer hair cell counts for the four cochlear regions (a) inner hair cells and (b) outer hair cells - basal, mid-basal, mid-apical and apical areas assessed at each time point for implanted and control ears. (c) P-values are shown following statistical testing to compare implanted and control ears (Paired T-test, significance level: P<0.05). N=3 mice at each time point.

Comparisons of mean hair cell counts between the implanted and control ears did not show significant differences across the various cochlear regions over the four time points tested. There were, however, two exceptions to this, at 4 weeks where a significantly lower mean number of inner and outer hair cells were found in the basal region of the implanted ear compared to the control ear (P=0.03 and 0.02 respectively) (Figure 5.16 and 5.17). Unfortunately, reproducibility of this finding within the basal cochlea at the various other time points (48 hours, 1 week and 12 weeks) was not possible due to architectural damage to the whole mount sections, sustained during dissection and processing, which prevented counts from being performed accurately. Examples of whole mount segments are shown in Figure 5.17.

Figure 5.16 Mean hair cell counts post-implantation (*P < 0.05) n=3 mice at each time point. Error bars represent two standard error of the mean (±2SEM).

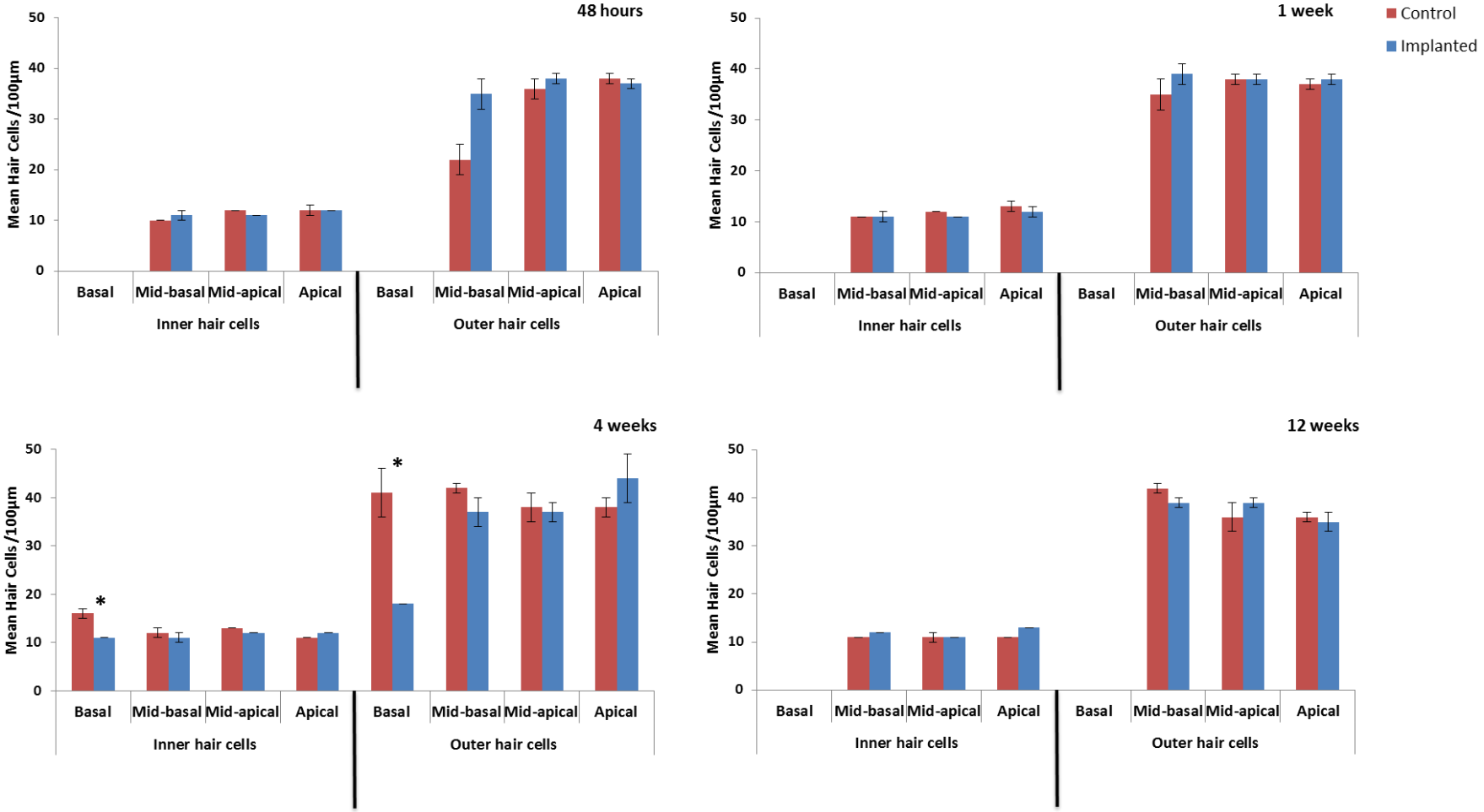

Figure 5.17 Organ of Corti whole mount segments taken from 3 month old mice. Immunoabelling of hair cells has been performed using Myosin VIIa (Myo VIIa). DAPI labelled nuclei. Example sections are shown for implanted and control ears at each time point **(A - D)**. Comparisons of mean hair cell counts between the implanted and control ears did not show significant differences across the various cochlear regions over the four time points tested **(A, B, D)**. However, an exception to this was at 4 weeks where a significantly lower mean number of inner and outer hair cells were found in the basal region of the implanted ear compared to the control ear ($P<0.05$). This is demonstrated in the sections below **(C)**.

(A) Comparison of mid-apical turn sections taken from mouse implanted for 48 hours. Upper sections (i) taken from right (control) ear, lower sections (ii) from left (implanted) ear.

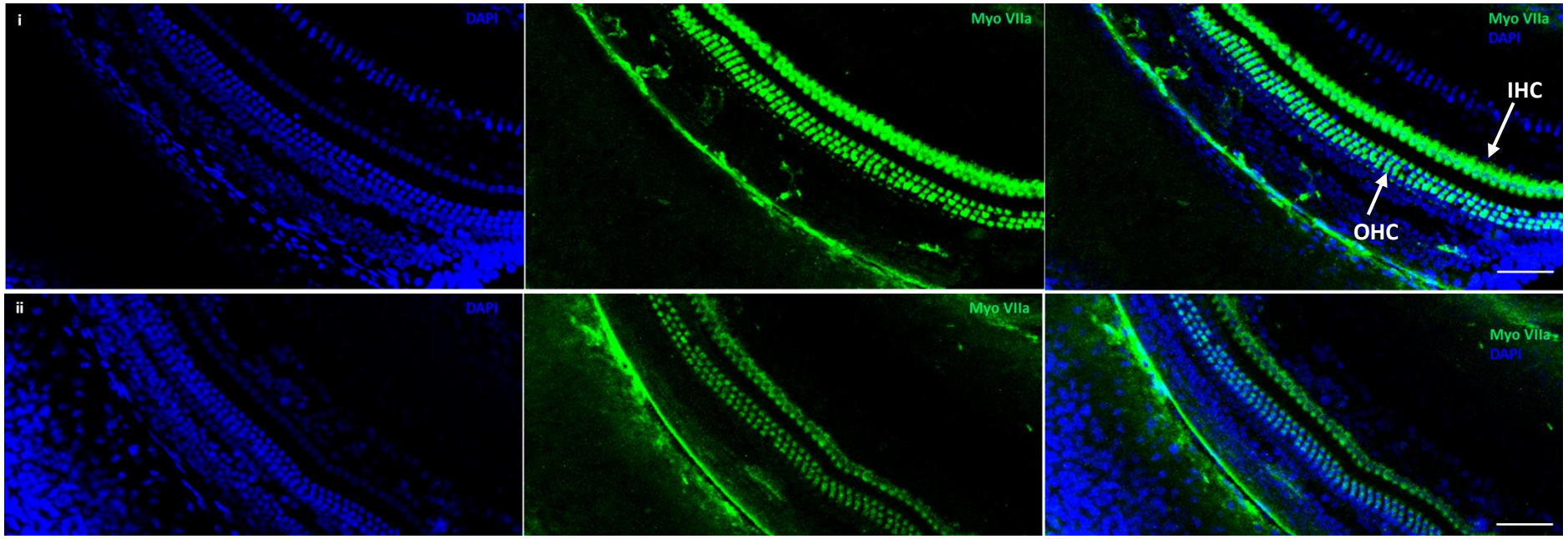

(B) Comparison of mid-basal turn sections taken from mouse implanted for 1 week. Upper sections (i) taken from right (control) ear, lower sections (ii) from left (implanted) ear.

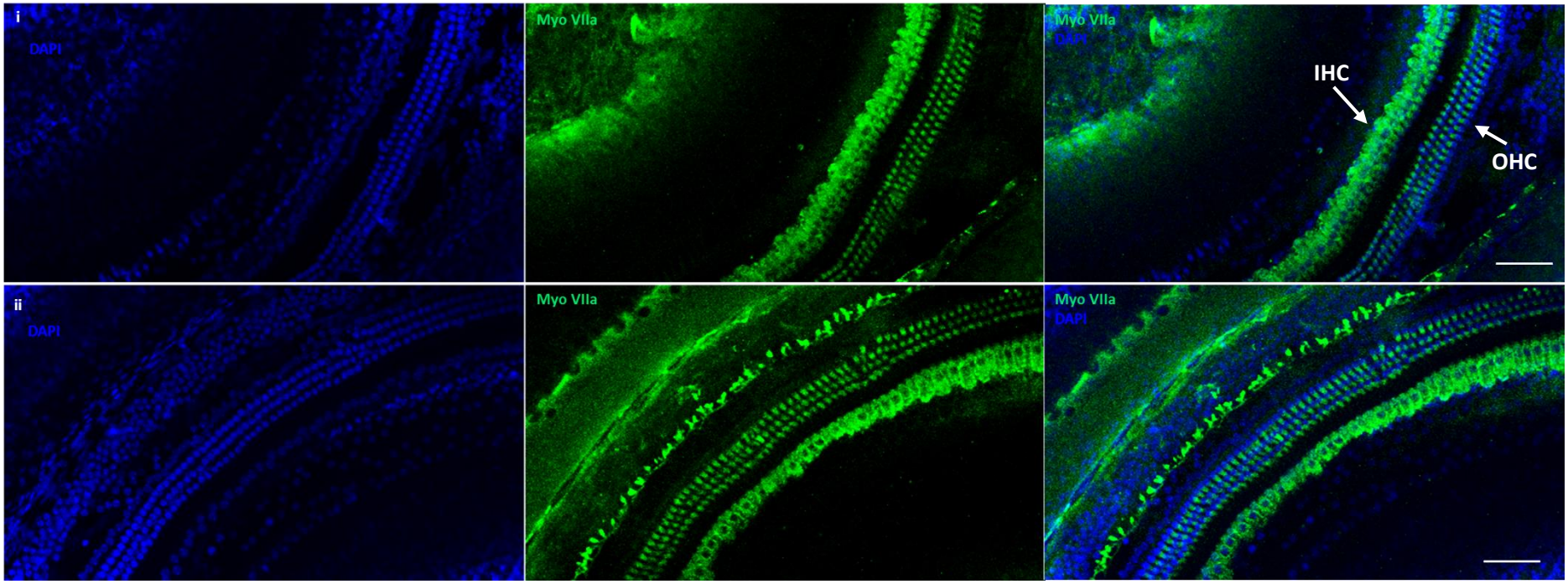

(C) Comparison of basal turn sections taken from mouse implanted for 4 weeks. Upper sections (i) taken from right (control) ear, lower sections (ii) from left (implanted) ear. A greater loss of inner and outer hair cells are observed in the implanted ear (ii) compared to the control ear (i).

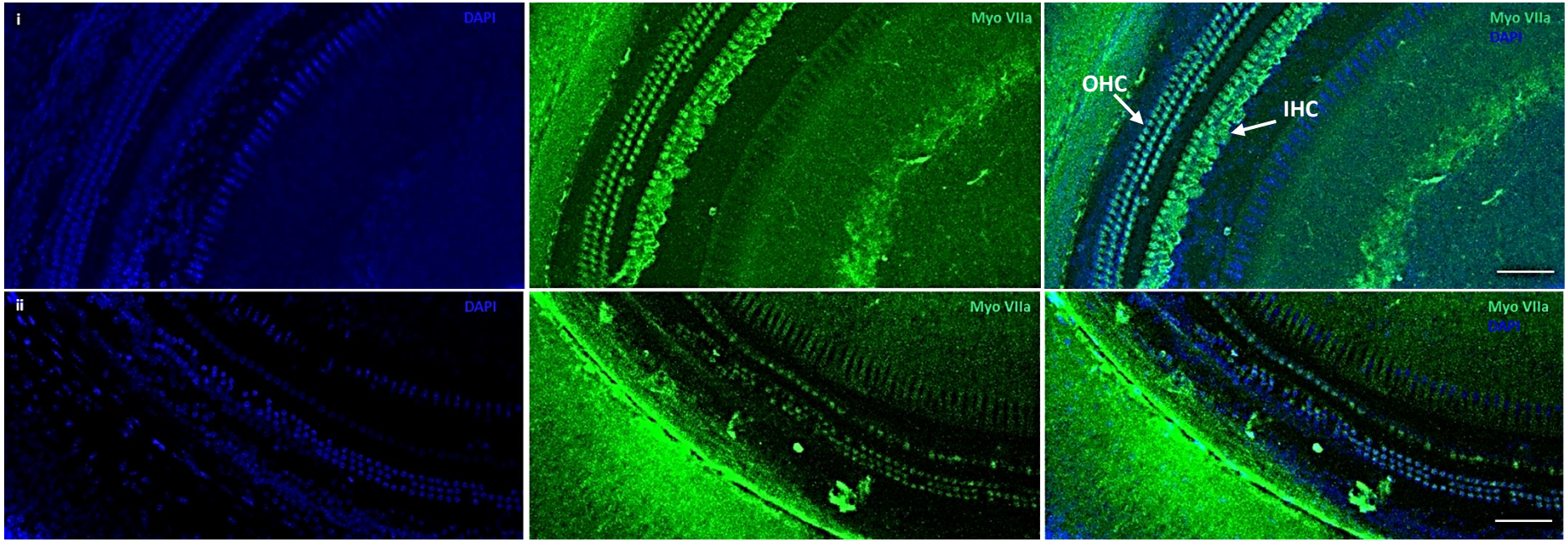

(D) Comparison of mid-apical turn sections taken from mouse implanted for 12 weeks. Upper sections (i) taken from right (control) ear, lower sections (ii) from left (implanted) ear.

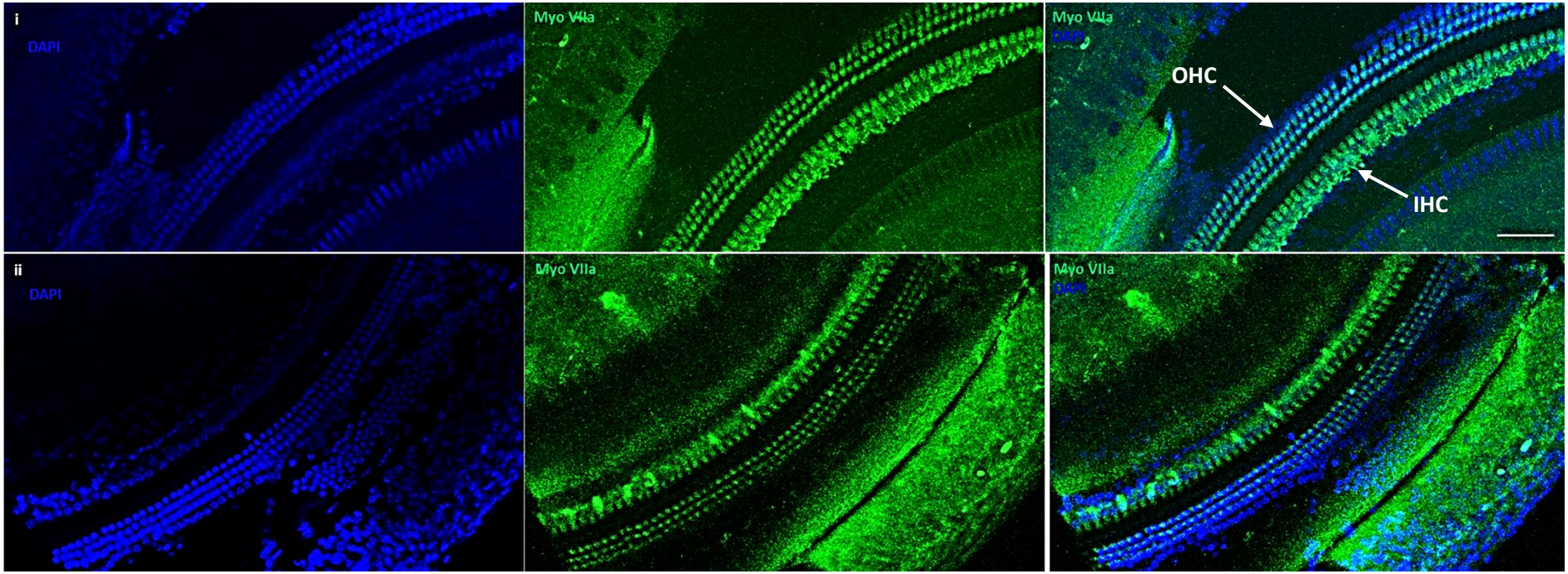

5.8 Discussion

5.8.1 Cochlear inflammation and fibrosis following cochlear implantation in the mouse

The main aim of the current chapter was to investigate the effect of CI in the mouse at a cellular level. The concept of cochlear damage following CI is well-recognised and can occur immediately at the site of insertion, along the electrodes trajectory and as a result of disruption to cochlear fluids. A more delayed response is thought to arise following activation of the host's response to CI and due to the loss of function of the delicate intracochlear structures (Li et al., 2007). As with other biomedically-active implantable devices, cochlear implants represent the presence of a foreign body within the cochlea which has the potential to provoke an acute inflammatory reaction. Progression then occurs to the chronic phase if the presence of the electrode is sustained, with the ultimate formation of a fibrous capsule around the implant (Bas et al., 2012a; Bas et al., 2012b; Bas et al., 2015; Richard et al., 2012). Such a response was confirmed within the current mouse model of CI. The initial inflammatory reaction was noted within 48 hours of implantation as demonstrated by the presence of significantly greater numbers of positively labelled CD45 cells within the scala tympani of implanted cochleae compared to the controls. This response predominated within the lower basal region of the implanted cochleae and was sustained up to 12 weeks following implantation. As further work to establish the type of leucocytes present within sections from implanted cochleae was not performed, it cannot be confirmed as to whether the inflammatory cellular infiltrate seen on CD45 labelling at 48 hours differed from the inflammatory infiltrate found at 12 weeks.

Following cochlear implantation, any associated trauma, for example to the lateral cochlear wall, is met with an immediate inflammatory response to repair the damaged site. Following injury localised capillary permeability and vasodilatation is induced due to the release of vasoactive amines such as histamine from mast cells. Leucocytes are recruited which migrate and adhere to sites of tissue damage. A variety of inflammatory mediators play a part in the tissue response, including chemokines, neuropeptides, proteolytic enzymes and cytokines. The persisting presence of the cochlear implant also promotes a foreign body reaction in the

form of chronic inflammation characterised by mononuclear cells such as macrophages, together with evidence of fibrosis and angiogenesis. The complex cascade of events which occur include the interplay between pro-inflammatory cytokines such as TNF-α and interleukin (IL) 1-β, chemokines and growth factors such as TGF–β1. At high levels, this latter precursor for fibrosis leads to the scar tissue encapsulating the implant (Bas et al., 2012a; Bas et al., 2012b; Bas et al., 2015). The events are summarised in Figure 5.18.

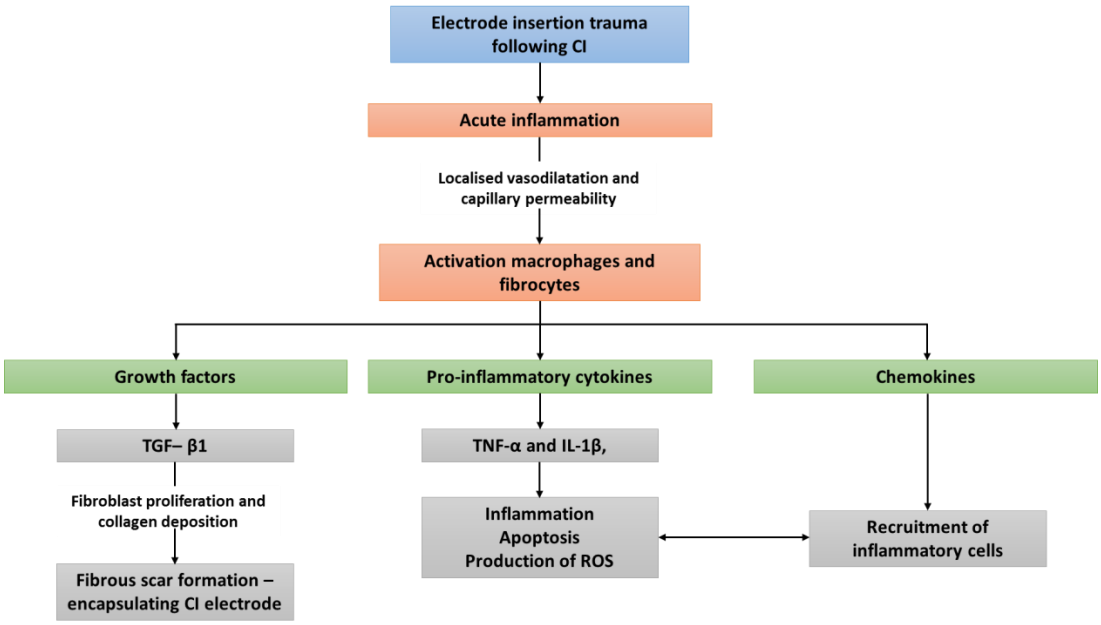

Figure 5.18 Sequence of events leading to inflammation and fibrosis within the cochlea following CI. An acute inflammatory reaction is initiated following trauma secondary to electrode insertion into the cochlea. The release of vasoactive amines such as histamine causes vasodilatation and promotes the migration and activation of leucocytes such as monocytes which mature into macrophages. Macrophages and fibrocytes release chemokines, which encourage inflammatory cell recruitment and release of cytokines and reactive oxygen species (ROS), and growth factors which promote wound healing and formation of a fibrous scar around the electrode (adapted from Bas et al. 2012).

The presence of fibrous tissue within the cochlea and surrounding the electrode array is an accepted consequence of CI (Friedland and Runge-Samuelson 2009). The current mouse model of CI was no exception to this as fibrotic-like tissue was found within the lower basal turn and encapsulating the implant as early as 1 week following CI. This tissue persisted in mice implanted for 12 weeks but remained confined to the lower basal turn in the vicinity of the implant. This finding correlates with data from recent mouse studies (Irving et al., 2014b;

Kopelovich et al., 2015) as well as human temporal bone studies (Cervera-Paz and Linthicum, Jr. 2005; Fayad et al., 2009; Li et al., 2007; Linthicum, Jr. et al., 1991; Marsh et al., 1992; Nadol, Jr. 1997; Nadol, Jr. et al., 2001; Somdas et al., 2007). Li et al. found a strong correlation between the volume of new tissue (fibrosis and neo-osteogenesis) within the cochlea with damage to the lateral cochlear wall sustained during insertion, emphasising the importance of soft surgical techniques to minimise trauma (Li et al., 2007). In the latter study, cochleostomy was performed to allow implant insertion. It was within the vicinity of the cochleostomy and extending into the lower basal turn that the greatest volume of fibrous and new bone tissue was found. These findings are not limited to the cochleostomy approach, however, as others have noted similar findings with round window insertions (Irving et al., 2013; Kopelovich et al., 2015; Ribari et al., 2000). This concurs with the findings of the current study where fibrotic-like tissue was evident within the basal turn following a round window approach.

In clinical practice, fibrous encapsulation of the implant is thought to significantly reduce electrical signal transmission between the device and target neurones, thus reducing the utility of the device by increasing power consumption, and increasing the spread of the electrical field generated by electrode stimulation (Clark et al., 1995b; Fayad et al., 2009). Fibrosis results in a reduction in the efficacy of signal coding, increases the implant size, reduces battery life and in many patients necessitates replacement of the device. In terms of performance, Kawano et al. (1998) studied various psychophysical percepts thought to play an important role in speech recognition and correlated them with histological findings in temporal bones of CI recipients. Results revealed reductions in dynamic range and increases in auditory thresholds for individual electrodes with greater amounts of fibrous tissue and new bone formation (Kawano et al., 1998). With regards to residual hearing, Choi and Oghalai (2005) developed a passive cochlea model and used computer simulation to predict the effects of fibrosis on residual hearing. Their findings suggested that fibrous tissue formation at the basal cochlea could alter basilar membrane velocity at the apex, thereby having a detrimental effect on residual hearing and impairing performance post-CI (Choi and Oghalai 2005). A recent study of human temporal bone pathology was performed from a patient previously implanted with a hybrid electrode who suffered delayed hearing loss post-CI. Histopathological

analysis revealed new bone formation and loose fibrous tissue filling the scala tympani of the basal cochlea turn. The authors suggested that the presence of such tissue could have contributed to the hearing loss observed due to reduced compliance at the round window and increased damping in the scala tympani (Quesnel et al., 2016). Conversely, Li et al. did not find a significant correlation between word recognition scores post-implantation and the total volume of new tissue deposition in the cochlea (Li et al., 2007). This was also seen in a guinea pig model of residual hearing where post-surgical hearing loss was not correlated with the area of fibrosis within the cochlea (Tanaka et al., 2014). Similarly, Kopelovich et al. (2015) did not find significant correlations between a greater degree of hearing loss and the presence of fibrotic tissue within the scala tympani in a mouse model of CI (Kopelovich et al., 2015)

5.8.2 Effect of cochlear implantation on spiral ganglion cells

With respect to hearing preservation CI surgery, successful outcomes are dependent not only on the maintenance of residual hair cells, but also on the viability of SGCs and their neurons. Two main factors require discussion in relation to the current mouse model: the effect of ageing on SGC populations as well as the potential effects of implantation.

5.8.2.1 Age and spiral ganglion cells

Age-related loss of hair cells and SGCs is well documented in the C57BL/6J mouse (Henry and Chole 1980; Li and Borg 1991b; Mikaelian 1979). As previously discussed, high-frequency hearing losses in these mice can occur from around 3 months of age, progressing to include lower frequencies and produce a severe to profound loss by 12 to 18 months (Hequembourg and Liberman 2001). At a histological level, this correlates with a loss of OHCs initially followed by loss of IHCs and SGCs (Mikaelian 1979). The survival of SGCs and their neurons is dependent upon pre- and post-synaptic trophic support from hair cells and central axons respectively. In the mouse, loss of the former leads to SGC death in a retrograde manner, starting distally at the dendritic processes and extending proximally to involve the cell body

(Hequembourg and Liberman 2001; Roehm and Hansen 2005; White et al., 2000). This is similar to the findings in human studies (Felder et al., 1997; Nadol, Jr. 1990; Otte et al., 1978; Suzuka and Schuknecht 1988). Primary degeneration can also occur in the absence of hair cell and central axonal loss within the apical cochlea, where neuronal losses can occur despite a steady increase in IHC numbers from midcochlear to apical regions (Hequembourg and Liberman 2001). Such losses have also been found to correlate with degenerative changes in pillar cells and Reissner's membrane, suggesting the interplay of various mechanisms including loss of trophic support and ion dysregulation (Ohlemiller and Gagnon 2004). The idea of primary SGC degeneration has also been shown in other mammals also where the involvement of independent cellular mechanisms such as the presence of reactive oxygen species have been proposed (Perez and Bao 2011).

In the present study, inclusion of a non-implanted control ear allowed an assessment of potential age-related change in SGC density over time. As six month old mice were used, an element of age-related change was already apparent from the outset, with evidence of missing SGCs and a reduction in volume of some of the cell bodies within Rosenthal's canal (Figure 5.10). Interestingly, however, median SGC density was not found to change significantly with time in this group (Table 5.2). It would have been reasonable to expect SGC numbers to decline, especially 12 weeks following initial implantation, however, this was not observed. This may have been due to the fact that the numbers of animals within each group were too small to demonstrate such a change. As SGC death occurs in a retrograde manner, degeneration of the peripheral dendritic processes may already have been present despite retention of the cell body.

5.8.2.2 Effect of cochlear implantation on spiral ganglion cells

As well as direct mechanical injury, the fact that CI leads to provocation of a robust inflammatory process can be damaging to SGCs as well as residual hair cells. Bas et al. found evidence of leucocyte recruitment and release of pro-inflammatory cytokines within the area of the spiral ganglia in the early stages following CI. The subsequent reparative phase also

showed persisting neuro-inflammation of the spiral ganglion neurons, both of which could have detrimental effects on the viability of SGCs (Bas et al., 2015). Kawano et al. found a negative correlation between SGC survival and the level of new bone and fibrous tissue (Kawano et al., 1998). In contrast to this, Li et al. (2007) found no correlation between the total number of SGCs and new tissue formation (Li et al., 2007).

In the current study, no significant reduction in SGC density was noted as a result of implantation. A decline in SGC density was seen in the lower basal turn of implanted cochleae compared to controls but this was not significant on statistical testing. This is supported by Kopelvich et al. (2015) who also found no significant difference in SGC body density or peripheral axon density when comparing implanted and non-implanted controls in a murine model of CI. The latter study similarly represented CI in the absence of any acoustic or electrical inputs (Kopelovich et al., 2015). In other animal models of CI, similar findings were noted, as spiral ganglion neuron density was not found to differ significantly between implanted and non-implanted cochleae (Addams-Williams et al., 2011; Kang et al., 2010; Lu et al., 2005a; Tanaka et al., 2014). Human temporal bone studies have also shown that implantation does not impact negatively upon the numbers of SGCs (Fayad et al., 2009; Linthicum, Jr. et al., 1991; Marsh et al., 1992; Nadol, Jr. 1997; Nadol, Jr. et al., 2001; Quesnel et al., 2016). The role of electrical stimulation on SGC numbers, as well as the relationship between SGC numbers and outcomes following CI, remain contentious issues and are discussed further in the following chapter.

5.8.3 Effect of cochlear implantation on hair cells

The survival of residual hair cells is important for a positive outcome following hearing preservation CI surgery and emphasises the importance of performing an atraumatic implant insertion to prevent or minimise damage and loss of these cells (Bas et al., 2012a; Coco et al., 2007; Mowry et al., 2012). There are a variety of potential traumatic stimuli which can promote loss of hair cells including direct trauma from the electrode array, vibrational and acoustic trauma secondary to use of a drill during surgery, the presence of intrascalar blood and bone

dust, trauma to the stria vascularis and spiral ligament, disruption of the basilar membrane leading to loss of the endocochlear potential, foreign body response to the electrode array and bacterial infection (Bas et al., 2012a). All of the aforementioned insults have the ability to initiate oxidative stress and an inflammatory response leading to the release of cytokines, enzymes and growth factors which lead to apoptosis of hair cells (Bas et al., 2012a; Bas et al., 2012b; Bas et al., 2015).

In the current study, three month old C57BL/6J mice were used to analyse the potential effects of implantation on hair cell counts. At this age, high frequency SNHL was already present as reflected by the greater mean thresholds seen at the higher frequencies of 32 kHz and 40 kHz on preoperative ABR testing (Figure 4.7a and b). As low frequency hearing was maintained in these mice, it functioned well as a residual hearing model. Comparisons of mean hair cell counts between the implanted and control ears did not show significant differences across the mid-basal, mid-apical and apical regions over the four time points tested. However, at 4 weeks a significantly lower mean number of inner and outer hair cells were found in the basal region of the implanted ear compared to the control ear. The latter result may have occurred as a result of implantation trauma due to the inflammatory and fibrotic changes which predominated within this region of the cochlea. These findings also correlate with functional outcomes as ABR testing revealed mean thresholds to be significantly greater in the implanted ear compared to the control ear at this time point at the higher frequencies of 32 kHz and 40 kHz, corresponding to changes in the basal turn. Apical hair cell counts did not appear to be affected by implantation in the cohort of mice analysed. In terms of functional outcomes, this was also reflected by the fact that low-frequency hearing was preserved (Figure 4.8).

Other studies have also examined the effect of implantation on hair cells. Bas et al. (2012) used novel organ of Corti explants from rats to demonstrate the detrimental effects of implantation on hair cells, specifically identifying the role of the activated caspase-3 pathway leading to apoptosis (Bas et al., 2012b). Hair cell loss following implantation trauma has also been seen in vivo in other animal models (Eshraghi et al., 2005; Vivero et al., 2008). Conversely, Kopelvich et al. (2015) did not find a significant difference in terms of organ of

Corti damage (including loss of hair cells) between control and implanted cochleae of mice (Kopelovich et al., 2015). This was also the case in the guinea pig, where hair cell loss following implantation was not observed (Kang et al., 2010; Tanaka et al., 2014). Human temporal bone studies have also shown preservation of inner and outer hair cells apical to the electrode array suggesting that factors other than hair cell loss may be contributing to the loss of residual hearing seen in some patients (Linthicum, Jr. et al., 1991; Quesnel et al., 2016).

5.8.4 Limitations and further work

There are a number of limitations related to the work performed in this chapter which requires discussion. One of the main drawbacks was related to the sample sizes used in the analysis of inflammation, SGC counts and hair cell counts. Although the findings were interesting and in line with those of other studies, as numbers were small, the data needs to be interpreted with this in mind. It would also have been useful to include both age groups of mice (3 month and 6 month old) in the analysis of SGC and hair cell counts as this would have enabled the presence of any age-related changes to also be discussed.

As mentioned, further analysis of the inflammatory response to identify the various subtypes of leucocytes present would have been beneficial in establishing the phase of the response over the various durations of implantation. Use of cell-specific antibodies would therefore be valuable in future studies. Confirmation and quantification of fibrous tissue developing in the mouse cochlea post-CI would have also be useful and allow correlation with functional outcomes.

When analysis of the plastic embedded fluorocarbon-implanted cochleae was undertaken by TEM, as well as presenting the fibrotic-like tissue in more detail, sections also showed evidence of tissue of epithelial origin. This suggested the possibility of epithelial remnants from the round window being pushed into the scala tympani on insertion of the implant or possibly migrating along the implant. Although the fibrotic reaction most likely results from the surgical trauma, initiation of inflammation and subsequent reparative response, there may also be

other factors at play such as the remnants from the round window membrane and the muscle tissue used in sealing the incision. The current mouse model could be used to investigate this area further, for example, through the use of fluorescently labelled cell-trackers to ascertain the origin of cells contributing to the scar tissue present post-CI.

5.9 Conclusion

With increasing interest in widening candidacy for CI to patients with low frequency residual hearing, knowledge of the potential effects of implantation, including the role of inflammation and fibrosis, on residual hearing is of paramount importance to avoid loss of remaining hair cells and neurons. In the current study, preservation of hair cells and spiral ganglion cells following CI in the mouse, correlates with functional findings and reinforces the suitability of the mouse as a model for the investigation of residual hearing in CI. As electrical stimulation was not used in the current model, the findings represent a baseline against which future studies incorporating electrical stimulation can be compared. This is important not only in terms of investigating hearing loss but also as a means to evaluate potential therapeutic interventions to preserve it and improve patient outcomes following CI.

CHAPTER 6: GENERAL DISCUSSION

Since their introduction cochlear implants have revolutionised the treatment of profound hearing loss and have now provided hearing rehabilitation to more than 300,000 individuals worldwide (National Institute on Deafness and Other Communication Disorders 2016). Alongside technological innovations, device improvements and the relaxation of eligibility criteria, candidacy for CI has also changed, with more and more individuals gaining benefit from implantation (Irving et al., 2014a). One of the main areas of change has been the extension of cochlear implants to patients with residual hearing loss through the use of combined electrical and acoustic stimulation. Despite many patients being implanted in this group, mixed outcomes have raised concerns regarding their potential benefits, as some patients have lost all or part of their residual hearing. The underlying cause of this loss has not been fully elucidated (Mowry et al., 2012; Santa Maria et al., 2013). With this in mind, deciphering the effects of CI on cochlear structure and function has become paramount, especially if these implants are to be offered more widely.

Animal models have formed a key aspect of CI research mainly due to the fact that CI in the human cochlea cannot be studied during life. Mice are an important model for auditory research, partly due to the wide range of naturally-occurring and genetically-modified strains which mimic human deafness, as well the their similarities to humans in terms of anatomy and physiology. As such, being able to harness these and many of the other advantageous features of mice as a model for CI research is highly sought after.

6.1 Development of a mouse model of CI

This thesis describes a body of research whose primary aim was to develop a mouse model of CI. Chapter 3 describes the successful development of this model. There was evidence of a clear learning curve with an initial high rate of mortality. As a result of refining the surgical

technique, however, mortality fell and survival rates reached 95%. The main driver for improved mortality was an increased understanding of murine anatomy together with the initial decision to use a post auricular approach to access the middle ear. Benefits of this approach included a less extensive dissection than is associated with the ventral approach, with reduced potential for morbidity and mortality. However, the principle modification to surgical technique was the avoidance of iatrogenic injury to the stapedial artery. This vessel arises from the internal carotid artery and runs within the deeper aspect of the posterior belly of digastric muscle to enter the bulla at its posterior-medial aspect. It is necessary to partly divide this muscle to obtain access to the auditory bulla. Careful and minimal dissection in this area resulted in a reduced incidence of injury to the stapedial artery and when combined with a more limited bullotomy meant that a targeted approach to the round window could be used. These are the key steps in the evolution of this postauricular approach to CI in the mouse.

At the time of developing this model (October 2011), there were no published studies of CI in the mouse, making this model novel and a clear advancement in CI research. Since developing this model, however, there have been a few studies of mouse CI published (Bas et al., 2015; Irving et al., 2013; Kopelovich et al., 2015; Soken et al., 2013). Although all of these studies also utilised a postauricular approach in order to access the mouse cochlea, other aspects of the surgical procedure and investigation varied. As part of their study Irving et al. (2013) assessed the effects of acute and chronic implantation in young C57BL/6J (aged 8-10 weeks) who had been deafened using neomycin. The group advocated cauterisation of the stapedial artery as part of their approach to access the round window. This was despite the recognised potential for thermal injury to the cochlea and also after they had demonstrated the fact that cautery of the artery can lead to elevated hearing thresholds on ABR. They suggested that the risk of fatal haemorrhage from the artery outweighed these consequences (Irving et al., 2013). In the present study there were no cases of mortality due to haemorrhage from the stapedial artery following implantation. It is an unnecessary step which is not required if adequate care is taken and is supported by others (Bas et al., 2015; Kopelovich et al., 2015; Soken et al., 2013).

Both Irving et al. (2013) and Soken et al. (2013) accessed the tympanic bulla using a drill with a diamond burr (Irving et al., 2013; Soken et al., 2013). Although this method was trialled initially, it was found that the potential for collateral damage was high and that the bony wall was thin enough to be breached with a hypodermic needle and could be increased in size with ease using micro-forceps. This also allowed a more targeted bullotomy to be performed. Soken et al. (2013) and Kopelovich et al. (2015) performed closure of the tympanic bulla using muscle tissue as in the current study (Kopelovich et al., 2015; Soken et al., 2013). However, a polycarboxylate cement (Irving et al., 2013) and tissue glue (Bas et al., 2015) were used by others.

Survival rates in the current study (95%) were favourable or similar compared to other studies that have reported overall survival rates of 83% (Kopelovich et al., 2015; Soken et al., 2013). The study by Irving et al did not report overall survival so it is unclear from this group what the procedural mortality was (Irving et al., 2013).

A successful surgical technique needs to be reproducible in the hands of other researchers, ideally regardless of whether they have a clinical or surgical background. Within our research group the method as described has been used by a post-doctoral research fellow with training in basic science. She experienced a learning curve with high early mortality as in the current study but towards the latter part of the experiments survival exceeded 90%. We are not aware that the technique has been adopted by other research groups yet and thus remains to be externally validated.

6.2 Functional and histological outcomes following CI in the mouse

6.2.1 Strain of mouse

The choice of C57BL/6J mice allowed investigation into the functional and histological consequences following CI in a naturally occurring partial or residual hearing model. As a validated model for age-related hearing loss, this strain offers the advantage of not requiring the exogenous application of ototoxic agents or noise exposure to induce hearing loss (Soken et al., 2013). This strain was also used successfully by others as a model for CI (Kopelovich et al., 2015; Soken et al., 2013).

An alternative strain to assess the baseline effects of cochlear implantation would have been the CBA mouse. This strain, which carries an ahl-resistant allele, also develops an age-dependent high frequency SNHL as a result of the loss of basal IHCs, but does so more gradually and at an older age (22-25 months) (Park et al., 2010). The genetically determined effects of ageing on the C57BL/6J mouse cochlea can be rapid and profound from as young as 3 months and therefore, defining the effects of implantation alone on cochlear pathology may have been more straight-forward in the CBA strain.

6.2.2 Functional outcomes following CI in the mouse

An important observation of this work is that the very process of CI (in the absence of electrical stimulation) is associated with some deterioration in hearing as assessed by ABR testing. However, the mean threshold shift in the implanted ear was no greater than 20 dB and 12.5 dB in the 3 month and 6 month old mice respectively. As behavioural testing in the mice post-implantation was not performed to assess the impact of this level of hearing loss in one ear, it can only be postulated that such a deficit would not be significantly detrimental in functional terms. Increased mean threshold shifts in the implanted ear compared to the control ear were also seen in other mouse studies and were found to be of greater magnitude compared to the current study (Kopelovich et al., 2015; Soken et al., 2013). This may reflect variations in surgical technique and differences in the types of electrode used.

Importantly, no animal demonstrated complete hearing loss postoperatively and up to 12 weeks following CI in the current study. Furthermore, results revealed that hearing in the low frequencies was maintained in both the 3 and 6 month old age groups over the four time points tested. This is an essential feature which could allow use of this mouse model to investigate potential effects of CI on residual hearing over longer time periods. The benefit of using the 3 and 6 month old groups of mice also meant that the effect of age on functional outcomes could be assessed, an important factor in the C57BL/6J strain. Results revealed greater mean threshold shifts in the older mice suggesting an age-dependent acceleration of low frequency hearing loss following CI. This finding could be attributed to the age-related sensitisation of the cochlea causing increased susceptibility to implantation-induced damage.

6.2.3 Histological outcomes following CI in the mouse

Histological sections of plastic-mounted implanted cochleae, in conjunction with CBCT of implanted mice, demonstrated that the implants were sited correctly within the scala tympani. This data validates the mouse model of CI as it is clearly essential that any surgical technique delivers the implant to the correct anatomical location.

The loss of hearing in the implanted ear following CI may in part relate to the observed presence of inflammatory cells and fibrotic-like tissue encapsulating the implant confirmed on immunofluorescence, light microscopy and TEM. These findings are in line with other studies where normal hearing (James et al., 2008; O'Leary et al., 2013) and residual or partial hearing models have been used to investigate the effects of CI (Choi and Oghalai 2005; Irving et al., 2014b; Kopelovich et al., 2015; Quesnel et al., 2016). The mechanism by which these factors give rise to or are associated with the existence of residual hearing loss remains to be clarified. Several theories regarding the effect of implantation-induced inflammation, fibrosis and osteoneogenesis have been proposed (Bas et al., 2012a; Bas et al., 2012b; Bas et al., 2015; Eshraghi et al., 2006; Li et al., 2007).

Other authors have also assessed the cochlea's response to implantation and its potential to promote loss of residual hearing. Reiss et al. (2015) investigated hearing loss following CI and EAS in a residual hearing guinea pig model. Elevated thresholds were found to be associated with stria vascularis capillary changes and reduced presynaptic ribbon and postsynaptic receptor counts. The authors speculated that the cause of residual hearing loss may be linked to lateral wall blood flow changes rather loss of hair cells following surgical trauma. They also proposed that delayed loss of hearing could be as a result of stimulation excitotoxicity or inflammation inducing loss of hair cell ribbons and post-synaptic receptors (Reiss et al., 2015).

Comparisons of insertion technique, comparing round window insertion with cochleostomy and their potential influence on residual hearing have also been performed. A recent systematic review did not find one technique to be superior over the other in terms of the degree of hearing preservation (Havenith et al., 2013). Hod et al. (2016) investigated the round window approach and cochleostomy in normal hearing rats and also found both techniques to have a similar risk of hearing loss. The majority of hearing loss was experienced at the stage of opening the membranous labyrinth, regardless of the approach and was reflected as a sensorineural hearing loss due to alterations in inner ear mechanics (Hod et al., 2016). Conversely, Rowe et al. (2016) studied delayed low frequency hearing loss in a guinea pig model, comparing round window with cochleostomy insertion. Delayed low frequency hearing loss was noted with round window insertions but not with cochleostomy. The authors speculated that this loss was unrelated to injury within the scala tympani or the extent of tissue reaction post-implantation, but rather related to the muscle graft used to seal the round window post-insertion. They suggested that this could be due to round window fibrosis causing changes in cochlear mechanics (Rowe et al., 2016). This latter point may also be applicable to the current model as a potential contribution to the elevated hearing thresholds noted.

Despite the numerous studies, it is still difficult to determine which of the various pathological responses are directly responsible for, or associated with, the loss of residual hearing following CI. Implantation may also act to accelerate the underlying cause of hearing loss rather than be a direct cause of it (Irving et al., 2014a). In this regard, the current mouse model will help

investigate this area further in an attempt to clarify factors which could be potentially modified to produce better outcomes for patients.

6.3 Limitations of study

There are several limitations with regards to the work described in the current study. The number of animals used was in line with Home Office regulations which state that the study design should allow maximum gain of information with the use of minimum animal numbers, for this reason there was judicious use of animals for experiments. Thus, the perioperative death of animals early in the study period reduced the subsequent availability of tissue for histological analysis. However, since the main aim of the study was to develop a working model of CI in mice, this observation was related to the development of the surgical and anaesthetic aspects.

Due to limitations of time related to the two year research program, there were a finite number of experiments that could be performed. With more time, it would have been more informative to verify the histological findings noted with regards to inflammation, SGC and hair cell counts in both age groups of mice rather than just one group as was performed. Comparing findings between the 3 and 6 month age groups would have helped validate the findings and allow for any age-related changes to be analysed.

Although both click and tone burst ABR testing were performed, the addition of tympanometry or DPOAEs would have added further information with regards to assessing the potential effect of middle ear effusions on functional outcomes following CI. The use of automated threshold detection when performing ABR testing would also remove the potential for the observer effect on results, as ABRs were analysed unblinded by the author.

With regards to the histological analysis, aside from the main limitation of having small numbers of mice in each group when performing analyses, several further avenues warrant

investigation to build upon the current findings. These include the use of cell-specific markers to identify inflammatory cells, quantification of fibrotic-like tissue and correlation with functional outcomes and use of cell-trackers to identify the origin of cells within the tissue encapsulating the electrode. Investigation of the effect of electrical stimulation in this mouse model on all of the above would also be extremely valuable (see below).

6.4 Experimental work performed

The vast majority of the experimental work was performed by the author unless otherwise stated. Work performed included the following: all animal work including cadaveric dissection, development of surgical techniques, administration of anaesthesia and other drugs, surgery to perform CI, recovery of animals and ABR testing. Laboratory work included sacrifice of animals, harvest of cochleae and cochlear preparation for histological analysis (tissue fixation, cryosectioning, toluidine blue staining of cryosections and whole mount preparation). Light microscopy of toluidine blue stained cryosections, immunofluorescence preparation and image acquisition using the confocal microscope was also performed by the author.

Preparation of plastic-embedded cochleae for light microscopy and TEM was performed by Mr Graham Nevill. TEM images were acquired by Professor Andrew Forge.

6.5 Future directions of study using the mouse model of CI

6.5.1 Use of other mouse strains to investigate the effects of CI

Although not formally assessed in the current study, this surgical model of CI could be used in other strains of mice, including the various naturally occurring and genetically modified strains which mimic various types of human deafness. These mice have contributed extensively to the identification of causative genes underlying human hereditary deafness as well as providing insight into disease-susceptibility genes, for example, in presbyacusis (Ahituv and Avraham 2000). As such, these models could also form an important role in CI research. In

the case of hereditary hearing loss, including those cases secondary to mutations in Cx26, the most common cause of non-syndromic hereditary hearing loss, cochlear implants form a major treatment option for hearing rehabilitation. Outcomes in these patients can vary and this is an area which still requires investigation (Varga et al., 2014; Vivero et al., 2010). A variety of reasons have been cited including age at implantation, social environment, inner ear malformations, duration of deafness and the presence of additional disabilities (Black et al., 2011; Varga et al., 2014). Some authors have suggested, however, that the underlying aetiology is one of the most important factors predicting outcomes in terms of auditory performance (Varga et al., 2014; Vivero et al., 2010). In this regard, the use of mouse models of hearing loss will allow the objective assessment of the effects of CI and further analyse how implantation can be optimised and translated to improve patient outcomes.

6.5.2 Use of mouse model of CI to assess the effect of electrical stimulation

The current study has assessed the effects of CI in the mouse in the absence of electrical stimulation. The next logical step would be to investigate the effect of electrical stimulation on both functional and histological outcomes in this model to allow a more realistic perspective to be gained, analogous to the setting experienced by CI patients. In essence the present work forms a baseline investigation against which future studies involving electrical stimulation can be compared.

From the few mouse CI studies that have been published to date, only one has involved the use of electrical stimulation. Irving et al. (2013) used an electrode array with a fully implantable stimulator to investigate the effects of acute and chronic electrical stimulation in young C57BL/6J mice deafened using neomycin. The team were able to successfully record electrically-evoked auditory brainstem responses (EABR) and magnetically-induced, electrically-evoked auditory brainstem responses (mEABR) in the mice following acute and chronic implantation respectively. Chronic stimulation over a 1 month period revealed stable mEABRs and no evidence of altered spiral ganglion neuron density when compared to the unstimulated controls, although these findings need to be interpreted in the context of the small

numbers of animals used (n=3) (Irving et al., 2013). As SGCs are the target for stimulation in CI, their survival is critical to producing a positive outcome following implantation. That said, however, several human temporal bone studies have shown a lack of correlation between numbers of SGCs and CI performance (Fayad and Linthicum, Jr. 2006; Irving et al., 2013; Khan et al., 2005; Nadol, Jr. et al., 2001). The effect of electrical stimulation on SGCs has remained a contentious issue in cochlear implant research. Some studies have suggested that SGC density can be increased with electrical stimulation (Hartshorn et al., 1991; Leake et al., 1991; Leake et al., 1999; Mitchell et al., 1997). Conversely, as per the findings from the aforementioned mouse study (Irving et al., 2013), many others have reported that chronic electrical stimulation has no effect on spiral ganglion neuron survival (Araki et al., 1998; Araki et al., 2000; Chen et al., 2010; Coco et al., 2007; Landry et al., 2011; Shepherd et al., 1994; Shepherd et al., 2005; Wise et al., 2011).

With regards to the effect of electrical stimulation on the survival of hair cells and maintenance of residual hearing, Coco et al. (2007) found that chronic stimulation did not affect residual hair cell function apical to the electrode array in a partial hearing feline model (Coco et al., 2007). These findings correlate with other studies in normal hearing animals which have demonstrated hair cell survival apical to the electrode array following atraumatic CI (Shepherd et al., 1983; Xu et al., 1997). Within their partial hearing model, the authors also noted evidence of fibrous tissue in the basal turn of implanted cochleae but did not find a significant difference in the extent of fibrous tissue between stimulated and non-stimulated cochleae (Coco et al., 2007). This was also the case in the mouse model where comparable amounts of fibrous tissue and new bone filled the scala tympani of both stimulated and unstimulated animals following CI (Irving et al., 2013).

Aside from the effects of chronic electrical stimulation alone on the cochlea following CI, one of the main areas of interest in relation to EAS is the interaction between electrical and acoustic stimuli. Ensuring optimal interactions between the two in spatial and temporal terms means that patients will be able to gain maximal benefit. There is the risk, however, that the quality of the incoming signal can deteriorate due to one stimulus masking the other (Irving et al., 2014a).

Use of the current mouse model will therefore prove invaluable in terms of investigating and further refining EAS strategies. It will also play a vital part in assessing the effects of electrical stimulation on residual hearing and allow a detailed histological assessment to be made.

6.5.3 Potential role of mouse model of CI in therapeutics

The role of therapeutics in CI is an expanding field. In the case of EAS, the development of agents to preserve residual hair cells and SGC function is gaining momentum alongside refinements in surgical technique and device advances. Localised drug delivery is the modality of choice in most cases as it allows targeted administration without the associated adverse outcomes that may arise from systemic delivery. Methods include infusion to the cochlear fluids at the time of implant insertion, drug-eluting electrode arrays, cell-based therapies and specific carriers which allow diffusion of agents across the round window membrane (Irving et al., 2014a).

A variety of therapeutic agents have been used to date including neurotrophic factors (BDNF and NT-3) to provide trophic support to SGCs (Altschuler et al., 1999; Kanzaki et al., 2002; Nakaizumi et al., 2004; Shepherd et al., 2005; Staecker et al., 1998). Corticosteroids (Bird et al., 2007; Bird et al., 2011; Chang et al., 2009; Eshraghi et al., 2007; James et al., 2008; Vivero et al., 2008) and anti-oxidants (Yamasoba et al. 1998; Eastwood et al. 2010; Kawamoto et al. 2004) have been used to ameliorate the adverse effects of inflammation and fibrosis and antiapoptotic agents to prevent hair cell degeneration (Eshraghi et al., 2006; Matsui et al., 2002). In addition, neurotrophins have demonstrated huge potential in the role of neuritogenesis (Altschuler et al., 1999; Miller et al., 2007; Staecker et al., 1996; Wise et al., 2005) and with the continual development of gene therapy, the application of these factors to the inner ear over the longer term is looking more promising (Atkinson et al., 2012; Shibata et al., 2010; Wise et al., 2011; Yagi et al., 2000).

In order for these therapeutic interventions to be translated to patients to improve CI outcomes, further work to determine the most suitable agent or combination of agents, delivery method,

duration and doses of treatment is required (Irving et al., 2014a). Animal models are essential for this type of investigation and the present mouse model of CI represents an excellent candidate for such purposes.

6.6 Conclusion

The work presented in this thesis describes the successful development of a viable and reproducible model of mouse CI. This model has many advantages over previously described animal models used in CI research. It provides numerous possibilities for exploring the interface between the biological and technological aspects of CI, as well as playing a vital potential role in the development of therapeutic interventions. Ultimately, it is hoped that the result of such investigations will one day translate to improved outcomes for patients undergoing CI.

REFERENCES

Action on Hearing Loss (2012). Hearing Matters.

Addams-Williams, J., Munaweera, L., Coleman, B., Shepherd, R., Backhouse, S. (2011). Cochlear implant electrode insertion: in defence of cochleostomy and factors against the round window membrane approach. *Cochlear. Implants. Int.* **12 Suppl 2**, S36-S39.

Adunka, O., Unkelbach, M.H., Mack, M., Hambek, M., Gstoettner, W., Kiefer, J. (2004). Cochlear implantation via the round window membrane minimizes trauma to cochlear structures: a histologically controlled insertion study. *Acta Otolaryngol.* **124**, 807-812.

Adunka, O.F., Mlot, S., Suberman, T.A., Campbell, A.P., Surowitz, J., Buchman, C.A., Fitzpatrick, D.C. (2010). Intracochlear recordings of electrophysiological parameters indicating cochlear damage. *Otol. Neurotol.* **31**, 1233-1241.

Ahituv, N., Avraham, K.B. (2000). Auditory and vestibular mouse mutants: models for human deafness. *J Basic Clin. Physiol Pharmacol.* **11**, 181-191.

Ahituv, N., Avraham, K.B. (2002). Mouse models for human deafness: current tools for new fashions. *Trends Mol. Med.* **8**, 447-451.

Ahmad, F.I., Choudhury, B., De Mason, C.E., Adunka, O.F., Finley, C.C., Fitzpatrick, D.C. (2012). Detection of intracochlear damage during cochlear implant electrode insertion using extracochlear measurements in the gerbil. *Laryngoscope* **122**, 636-644.

Akil, O., Seal, R.P., Burke, K., Wang, C., Alemi, A., During, M., Edwards, R.H., Lustig, L.R. (2012). Restoration of hearing in the VGLUT3 knockout mouse using virally mediated gene therapy. *Neuron* **75**, 283-293.

Albiin, N., Hellstrom, S., Salen, B., Stenfors, L.E. (1983). The stapedial artery in the rat. A microscopical study under normal conditions and in otitis media with effusion. *Acta Anat (Basel)* **115**, 134-140.

Albiin, N., Hellstrom, S., Salen, B., Stenfors, L.E., Wirell, S. (1985). The vascular supply of the rat tympanic membrane. *Anat Rec.* **212**, 17-22.

Alexander, A.J., Bartel, L., Friesen, L., Shipp, D., Chen, J. (2011). From fragments to the whole: a comparison between cochlear implant users and normal-hearing listeners in music perception and enjoyment. *J Otolaryngol. Head Neck Surg.* **40**, 1-7.

Alice, B., Silvia, M., Laura, G., Patrizia, T., Roberto, B. (2013). Cochlear implantation in the elderly: surgical and hearing outcomes. *BMC. Surg.* **13 Suppl 2**, S1

Altschuler, R.A., Cho, Y., Ylikoski, J., Pirvola, U., Magal, E., Miller, J.M. (1999). Rescue and regrowth of sensory nerves following deafferentation by neurotrophic factors. *Ann. N. Y. Acad. Sci.* **884**, 305-311.

Arai, R., Winsky, L., Arai, M., Jacobowitz, D.M. (1991). Immunohistochemical localization of calretinin in the rat hindbrain. *J. Comp Neurol.* **310**, 21-44.

Araki, S., Kawano, A., Seldon, H.L., Shepherd, R.K., Funasaka, S., Clark, G.M. (2000). Effects of intracochlear factors on spiral ganglion cells and auditory brain stem response after long-term electrical stimulation in deafened kittens. *Otolaryngol. Head Neck Surg.* **122**, 425-433.

Araki, S., Kawano, A., Seldon, L., Shepherd, R.K., Funasaka, S., Clark, G.M. (1998). Effects of chronic electrical stimulation on spiral ganglion neuron survival and size in deafened kittens. *Laryngoscope* **108**, 687-695.

Aschendorff, A. (2011). Imaging in cochlear implant patients. *GMS. Curr. Top. Otorhinolaryngol. Head Neck Surg.* **10**, Doc07

Ashmore, J.F., Kolston, P.J. (1994). Hair cell based amplification in the cochlea. *Curr. Opin. Neurobiol.* **4**, 503-508.

Atkinson, P.J., Wise, A.K., Flynn, B.O., Nayagam, B.A., Hume, C.R., O'Leary, S.J., Shepherd, R.K., Richardson, R.T. (2012). Neurotrophin gene therapy for sustained neural preservation after deafness. *PLoS. One.* **7**, e52338

Austyn, J.M., Gordon, S. (1981). F4/80, a monoclonal antibody directed specifically against the mouse macrophage. *Eur. J. Immunol.* **11**, 805-815.

Avraham, K.B. (2003). Mouse models for deafness: lessons for the human inner ear and hearing loss. *Ear Hear.* **24**, 332-341.

Balkany, T.J., Connell, S.S., Hodges, A.V., Payne, S.L., Telischi, F.F., Eshraghi, A.A., Angeli, S.I., Germani, R., Messiah, S., Arheart, K.L. (2006). Conservation of residual acoustic hearing after cochlear implantation. *Otol. Neurotol.* **27**, 1083-1088.

Bas, E., Dinh, C.T., Garnham, C., Polak, M., Van De Water, T.R. (2012a). Conservation of hearing and protection of hair cells in cochlear implant patients' with residual hearing. *Anat. Rec. (Hoboken.)* **295**, 1909-1927.

Bas, E., Goncalves, S., Adams, M., Dinh, C.T., Bas, J.M., Van De Water, T.R., Eshraghi, A.A. (2015). Spiral ganglion cells and macrophages initiate neuro-inflammation and scarring following cochlear implantation. *Front Cell Neurosci.* **9**, 303

Bas, E., Gupta, C., Van De Water, T.R. (2012b). A novel organ of corti explant model for the study of cochlear implantation trauma. *Anat. Rec. (Hoboken.)* **295**, 1944-1956.

Bellamkonda, R.V., Pai, S.B., Renaud, P. (2012). Materials for neural interfaces. *MRS Bulletin* **37**, 557-561.

Bhattacharyya, N., Meyers, A.D. (2015). http://emedicine.medscape.com/article/836277-overview.

Biedron, S., Westhofen, M., Ilgner, J. (2009). On the number of turns in human cochleae. *Otol. Neurotol.* **30**, 414-417.

Bird, P.A., Begg, E.J., Zhang, M., Keast, A.T., Murray, D.P., Balkany, T.J. (2007). Intratympanic versus intravenous delivery of methylprednisolone to cochlear perilymph. *Otol. Neurotol.* **28**, 1124-1130.

Bird, P.A., Murray, D.P., Zhang, M., Begg, E.J. (2011). Intratympanic versus intravenous delivery of dexamethasone and dexamethasone sodium phosphate to cochlear perilymph. *Otol. Neurotol.* **32**, 933-936.

Bitner-Glindzicz, M. (2008). Genetics of Non-Syndromic Deafness. In: Graham, J.M., Scadding, G.K., Bull, P.D. ed. *Pediatric ENT*. Springer, 327

Black, J., Hickson, L., Black, B., Perry, C. (2011). Prognostic indicators in paediatric cochlear implant surgery: a systematic literature review. *Cochlear. Implants. Int.* **12**, 67-93.

Boettcher, F.A. (2002). Presbyacusis and the auditory brainstem response. *J. Speech Lang Hear. Res.* **45**, 1249-1261.

Bogaerts, S., Douglas, S., Corlette, T., Pau, H., Saunders, D., McKay, S., Oleskevich, S. (2008). Microsurgical access for cell injection into the mammalian cochlea. *J. Neurosci. Methods* **168**, 156-163.

Boggess, W.J., Baker, J.E., Balkany, T.J. (1989). Loss of residual hearing after cochlear implantation. *Laryngoscope* **99**, 1002-1005.

Bond, M., Mealing, S., Anderson, R., Elston, J., Weiner, G., Taylor, R.S., Hoyle, M., Liu, Z., Price, A., Stein, K. (2009). The effectiveness and cost-effectiveness of cochlear implants for severe to profound deafness in children and adults: a systematic review and economic model. *Health Technol. Assess.* **13**, 1-330.

Brennan, W.J., Clark, G.M. (1985). An animal model of acute otitis media and the histopathological assessment of a cochlear implant in the cat. *J. Laryngol. Otol.* **99**, 851-856.

Briggs, R.J., Tykocinski, M., Xu, J., Risi, F., Svehla, M., Cowan, R., Stover, T., Erfurt, P., Lenarz, T. (2006). Comparison of round window and cochleostomy approaches with a prototype hearing preservation electrode. *Audiol. Neurootol.* **11 Suppl 1**, 42-48.

British Society of Audiology (1988). Descriptors for pure tone audiograms. *British Journal of Audiology* **22**, 123

Cable, J., Steel, K.P. (1991). Identification of two types of melanocyte within the stria vascularis of the mouse inner ear. *Pigment Cell Res.* **4**, 87-101.

Campbell, A.P., Suberman, T.A., Buchman, C.A., Fitzpatrick, D.C., Adunka, O.F. (2010a). Correlation of early auditory potentials and intracochlear electrode insertion properties: an animal model featuring near real-time monitoring. *Otol. Neurotol.* **31**, 1391-1398.

Campbell, A.P., Suberman, T.A., Buchman, C.A., Fitzpatrick, D.C., Adunka, O.F. (2010b). Flexible cochlear microendoscopy in the gerbil. *Laryngoscope* **120**, 1619-1624.

Carlson, M.L., Breen, J.T., Gifford, R.H., Driscoll, C.L., Neff, B.A., Beatty, C.W., Peterson, A.M., Olund, A.P. (2010). Cochlear implantation in the octogenarian and nonagenarian. *Otol. Neurotol.* **31**, 1343-1349.

Carlson, M.L., Driscoll, C.L., Gifford, R.H., McMenomey, S.O. (2012). Cochlear implantation: current and future device options. *Otolaryngol. Clin. North Am.* **45**, 221-248.

Cervera-Paz, F.J., Linthicum, F.H., Jr. (2005). Cochlear wall erosion after cochlear implantation. *Ann. Otol. Rhinol. Laryngol.* **114**, 543-546.

Chang, A., Eastwood, H., Sly, D., James, D., Richardson, R., O'Leary, S. (2009). Factors influencing the efficacy of round window dexamethasone protection of residual hearing post-cochlear implant surgery. *Hear. Res.* **255**, 67-72.

Charbonneau, H., Tonks, N.K., Walsh, K.A., Fischer, E.H. (1988). The leukocyte common antigen (CD45): a putative receptor-linked protein tyrosine phosphatase. *Proc. Natl. Acad. Sci. U. S. A* **85**, 7182-7186.

Chen, I., Limb, C.J., Ryugo, D.K. (2010). The effect of cochlear-implant-mediated electrical stimulation on spiral ganglion cells in congenitally deaf white cats. *J Assoc. Res. Otolaryngol.* **11**, 587-603.

Chen, Z., Mikulec, A.A., McKenna, M.J., Sewell, W.F., Kujawa, S.G. (2006). A method for intracochlear drug delivery in the mouse. *J. Neurosci. Methods* **150**, 67-73.

Chisolm, T.H., Willott, J.F., Lister, J.J. (2003). The aging auditory system: anatomic and physiologic changes and implications for rehabilitation. *Int. J. Audiol.* **42 Suppl 2**, 2S3-10.

Choi, C.H., Oghalai, J.S. (2005). Predicting the effect of post-implant cochlear fibrosis on residual hearing. *Hear. Res.* **205**, 193-200.

Chow, J.K., Seldon, H.L., Clark, G.M. (1995). Experimental animal model of intracochlear ossification in relation to cochlear implantation. *Ann. Otol. Rhinol. Laryngol. Suppl* **166**, 42-45.

Ciuman, R.R. (2009). Stria vascularis and vestibular dark cells: characterisation of main structures responsible for inner-ear homeostasis, and their pathophysiological relations. *J. Laryngol. Otol.* **123**, 151-162.

Clark, G.M., Clark, J., Cardamone, T., Clarke, M., Nielsen, P., Jones, R., Arhatari, B., Birbilis, N., Curtain, R., Xu, J. et al. (2014). Biomedical studies on temporal bones of the first multi-channel cochlear implant patient at the University of Melbourne. *Cochlear. Implants. Int.* **15 Suppl 2**, S1-15.

Clark, G.M., McAnally, K.I., Black, R.C., Shepherd, R.K. (1995a). Electrical stimulation of residual hearing in the implanted cochlea. *Ann. Otol. Rhinol. Laryngol. Suppl* **166**, 111-113.

Clark, G.M., Shute, S.A., Shepherd, R.K., Carter, T.D. (1995b). Cochlear implantation: osteoneogenesis, electrode-tissue impedance, and residual hearing. *Ann. Otol. Rhinol. Laryngol. Suppl* **166**, 40-42.

Coco, A., Epp, S.B., Fallon, J.B., Xu, J., Millard, R.E., Shepherd, R.K. (2007). Does cochlear implantation and electrical stimulation affect residual hair cells and spiral ganglion neurons? *Hear. Res.* **225**, 60-70.

Coelho, D.H., Yeh, J., Kim, J.T., Lalwani, A.K. (2009). Cochlear implantation is associated with minimal anesthetic risk in the elderly. *Laryngoscope* **119**, 355-358.

Cohen-Salmon, M., Ott, T., Michel, V., Hardelin, J.P., Perfettini, I., Eybalin, M., Wu, T., Marcus, D.C., Wangemann, P., Willecke, K. et al. (2002). Targeted ablation of connexin26 in the inner ear epithelial gap junction network causes hearing impairment and cell death. *Curr. Biol.* **12**, 1106-1111.

Cosetti, M.K., Waltzman, S.B. (2011). Cochlear implants: current status and future potential. *Expert. Rev. Med. Devices* **8**, 389-401.

Dechesne, C.J., Winsky, L., Kim, H.N., Goping, G., Vu, T.D., Wenthold, R.J., Jacobowitz, D.M. (1991). Identification and ultrastructural localization of a calretinin-like calcium-binding protein (protein 10) in the guinea pig and rat inner ear. *Brain Res.* **560**, 139-148.

DeMason, C., Choudhury, B., Ahmad, F., Fitzpatrick, D.C., Wang, J., Buchman, C.A., Adunka, O.F. (2012). Electrophysiological properties of cochlear implantation in the gerbil using a flexible array. *Ear Hear.* **33**, 534-542.

Do, K., Baker, K., Praetorius, M., Staecker, H. (2004). A mouse model of implantation trauma. *International Congress Series* **1273**, 167-170.

Dorman, M.F., Loizou, P.C., Fitzke, J., Tu, Z. (1998). The recognition of sentences in noise by normal-hearing listeners using simulations of cochlear-implant signal processors with 6-20 channels. *J. Acoust. Soc. Am.* **104**, 3583-3585.

Dror, A.A., Avraham, K.B. (2009). Hearing loss: mechanisms revealed by genetics and cell biology. *Annu. Rev. Genet.* **43**, 411-437.

Duckert, L.G., Miller, J.M. (1982). Acute morphological changes in guinea pig cochlea following electrical stimulation. A preliminary scanning electron microscope study. *Ann. Otol. Rhinol. Laryngol.* **91**, 33-40.

Duckert, L.G., Miller, J.M. (1986). Mechanisms of electrically induced damage after cochlear implantation. *Ann. Otol. Rhinol. Laryngol.* **95**, 185-189.

Duman, D., Tekin, M. (2012). Autosomal recessive nonsyndromic deafness genes: a review. *Front Biosci. (Landmark. Ed)* **17**, 2213-2236.

Eshraghi, A.A., Adil, E., He, J., Graves, R., Balkany, T.J., Van De Water, T.R. (2007). Local dexamethasone therapy conserves hearing in an animal model of electrode insertion trauma-induced hearing loss. *Otol. Neurotol.* **28**, 842-849.

Eshraghi, A.A., He, J., Mou, C.H., Polak, M., Zine, A., Bonny, C., Balkany, T.J., Van De Water, T.R. (2006). D-JNKI-1 treatment prevents the progression of hearing loss in a model of cochlear implantation trauma. *Otol. Neurotol.* **27**, 504-511.

Eshraghi, A.A., Polak, M., He, J., Telischi, F.F., Balkany, T.J., Van De Water, T.R. (2005). Pattern of hearing loss in a rat model of cochlear implantation trauma. *Otol. Neurotol.* **26**, 442-447.

Eshraghi, A.A., Rodriguez, M., Balkany, T.J., Telischi, F.F., Angeli, S., Hodges, A.V., Adil, E. (2009). Cochlear implant surgery in patients more than seventy-nine years old. *Laryngoscope* **119**, 1180-1183.

Eshraghi, A.A., Van De Water, T.R. (2006). Cochlear implantation trauma and noise-induced hearing loss: Apoptosis and therapeutic strategies. *Anat. Rec. A Discov. Mol. Cell Evol. Biol.* **288**, 473-481.

Fayad, J.N., Linthicum, F.H., Jr. (2006). Multichannel cochlear implants: relation of histopathology to performance. *Laryngoscope* **116**, 1310-1320.

Fayad, J.N., Makarem, A.O., Linthicum, F.H., Jr. (2009). Histopathologic assessment of fibrosis and new bone formation in implanted human temporal bones using 3D reconstruction. *Otolaryngol. Head Neck Surg.* **141**, 247-252.

Felder, E., Kanonier, G., Scholtz, A., Rask-Andersen, H., Schrott-Fischer, A. (1997). Quantitative evaluation of cochlear neurons and computer-aided three-dimensional reconstruction of spiral ganglion cells in humans with a peripheral loss of nerve fibres. *Hear. Res.* **105**, 183-190.

Fettiplace, R., Hackney, C.M. (2006). The sensory and motor roles of auditory hair cells. *Nat. Rev. Neurosci.* **7**, 19-29.

Fischel-Ghodsian, N. (2005). Genetic factors in aminoglycoside toxicity. *Pharmacogenomics.* **6**, 27-36.

Fishpool, S.J., Osborne, J.E., Looker, N. (2012). Staphylococcus aureus biofilm formation on an explanted cochlear implant demonstrated using an ultrasonication technique. *Cochlear. Implants. Int.* **13**, 181-183.

Flecknell, P.A. (1993). Anaesthesia of animals for biomedical research. *Br. J. Anaesth.* **71**, 885-894.

Flecknell, P.A. (1996). Anaesthesia. *In: Laboratory Animal Anaesthesia: A practical introduction for research workers and technicians* **2nd ed**, Academic Press Ltd, 14-73.

Forge, A., Jagger, D.J., Kelly, J.J., Taylor, R.R. (2013). Connexin30-mediated intercellular communication plays an essential role in epithelial repair in the cochlea. *J Cell Sci.* **126**, 1703-1712.

Forge, A., Wright, T. (2002). The molecular architecture of the inner ear. *Br. Med. Bull.* **63**, 5-24.

Fraysse, B., Macias, A.R., Sterkers, O., Burdo, S., Ramsden, R., Deguine, O., Klenzner, T., Lenarz, T., Rodriguez, M.M., Von, W.E. et al. (2006). Residual hearing conservation and electroacoustic stimulation with the nucleus 24 contour advance cochlear implant. *Otol. Neurotol.* **27**, 624-633.

Friedland, D.R., Runge-Samuelson, C. (2009). Soft cochlear implantation: rationale for the surgical approach. *Trends Amplif.* **13**, 124-138.

Friesen, L.M., Shannon, R.V., Baskent, D., Wang, X. (2001). Speech recognition in noise as a function of the number of spectral channels: comparison of acoustic hearing and cochlear implants. *J. Acoust. Soc. Am.* **110**, 1150-1163.

Fu, Q.J., Shannon, R.V., Wang, X. (1998). Effects of noise and spectral resolution on vowel and consonant recognition: acoustic and electric hearing. *J Acoust. Soc. Am* **104**, 3586-3596.

Furness, D.N., Hackney, C.M. (2008). Form and ultrastructure of the cochlea and its central connections. In: Gleeson,M., Browning,G.G., Burton,M.J., Clarke,R., Hibbert,J., Jones,N.S., Lund,V.J., Luxon,L.M., Watkinson,J.C., ed. **7th ed**, *Scott-Brown's Otorhinolaryngology, Head and Neck Surgery.* Edward Arnold Ltd, 3126-3146.

Gantz, B.J., Hansen, M.R., Turner, C.W., Oleson, J.J., Reiss, L.A., Parkinson, A.J. (2009). Hybrid 10 clinical trial: preliminary results. *Audiol. Neurootol.* **14 Suppl 1**, 32-38.

Gantz, B.J., Turner, C. (2004). Combining acoustic and electrical speech processing: Iowa/Nucleus hybrid implant. *Acta Otolaryngol.* **124**, 344-347.

Gantz, B.J., Turner, C., Gfeller, K.E., Lowder, M.W. (2005). Preservation of hearing in cochlear implant surgery: advantages of combined electrical and acoustical speech processing. *Laryngoscope* **115**, 796-802.

Gantz, B.J., Turner, C.W. (2003). Combining acoustic and electrical hearing. *Laryngoscope* **113**, 1726-1730.

Gargiulo, S., Greco, A., Gramanzini, M., Esposito, S., Affuso, A., Brunetti, A., Vesce, G. (2012). Mice anesthesia, analgesia, and care, Part I: anesthetic considerations in preclinical research. *ILAR. J.* **53**, E55-E69.

Gates, G.A., Mills, J.H. (2005). Presbycusis. *Lancet* **366**, 1111-1120.

Gfeller, K., Knutson, J.F., Woodworth, G., Witt, S., DeBus, B. (1998). Timbral recognition and appraisal by adult cochlear implant users and normal-hearing adults. *J Am Acad. Audiol.* **9**, 1-19.

Gfeller, K.E., Olszewski, C., Turner, C., Gantz, B., Oleson, J. (2006). Music perception with cochlear implants and residual hearing. *Audiol. Neurootol.* **11 Suppl 1**, 12-15.

Gibbin, K.P. (2008). Management of the Deaf Child. In: Graham, J.M., Scadding, G.K., Bull, P.D. ed. *Pediatric ENT*. Springer, 327

Glowatzki, E., Fuchs, P.A. (2002). Transmitter release at the hair cell ribbon synapse. *Nat. Neurosci.* **5**, 147-154.

Gordon, S., Hamann, J., Lin, H.H., Stacey, M. (2011). F4/80 and the related adhesion-GPCRs. *Eur. J. Immunol.* **41**, 2472-2476.

Govaerts, P.J., Marquet, T.F., Cremers, W.R., Offeciers, F.E. (1993). Persistent stapedial artery: does it prevent successful surgery? *Ann. Otol. Rhinol. Laryngol.* **102**, 724-728.

Gstoettner, W., Plenk, H., Jr., Franz, P., Hamzavi, J., Baumgartner, W., Czerny, C., Ehrenberger, K. (1997). Cochlear implant deep electrode insertion: extent of insertional trauma. *Acta Otolaryngol.* **117**, 274-277.

Han, D., Zhou, N., Li, Y., Chen, X., Zhao, X., Xu, L. (2007). Tone production of Mandarin Chinese speaking children with cochlear implants. *Int. J Pediatr. Otorhinolaryngol.* **71**, 875-880.

Hardy M (1938). The length of the organ of Corti in man. *Am J Anat* **63**, 291-311.

Hartshorn, D.O., Miller, J.M., Altschuler, R.A. (1991). Protective effect of electrical stimulation in the deafened guinea pig cochlea. *Otolaryngol. Head Neck Surg.* **104**, 311-319.

Hassler, C., Boretius, T., Stieglitz, T. (2011). Polymers for Neural Implants. *Polymer Physics* **49**, 18-33.

Havenith, S., Lammers, M.J., Tange, R.A., Trabalzini, F., della, V.A., van der Heijden, G.J., Grolman, W. (2013). Hearing preservation surgery: cochleostomy or round window approach? A systematic review. *Otol. Neurotol.* **34**, 667-674.

Heffner, H.E., Heffner, R.S. (2001). Behavioural assessment of hearing in mice. In: Willott, J.F. *Handbook of Mouse Auditory Research: From Behavior to Molecular Biology*. CRC Press LLC, 19-30.

Henry, K.R., Chole, R.A. (1980). Genotypic differences in behavioral, physiological and anatomical expressions of age-related hearing loss in the laboratory mouse. *Audiology* **19**, 369-383.

Hequembourg, S., Liberman, M.C. (2001). Spiral ligament pathology: a major aspect of age-related cochlear degeneration in C57BL/6 mice. *J. Assoc. Res. Otolaryngol.* **2**, 118-129.

Hereditary Hearing Loss Homepage (2013). Hereditary Hearing Loss Homepage. http://hereditaryhearingloss.org/main

Hessel, H., Ernst, L.S., Walger, M., von, W.H., Dybek, A., Schmidt, U. (1997). Meriones unguiculatus (Gerbil) as an animal model for the ontogenetic cochlear implant research. *Am. J. Otol.* **18**, S21

Hildesheimer, M., Rubinstein, C.M., Creter, D., Rubinstein, M. (1979). Long-term electrode implantation for recording cochlear electrical activity in guinea pigs. *Acta Otolaryngol.* **88**, 37-40.

Hinojosa, R., Marion, M. (1983). Histopathology of profound sensorineural deafness. *Ann. N. Y. Acad. Sci.* **405**, 459-484.

Hirose, K., Discolo, C.M., Keasler, J.R., Ransohoff, R. (2005). Mononuclear phagocytes migrate into the murine cochlea after acoustic trauma. *J. Comp Neurol.* **489**, 180-194.

Hod, R., Attias, J., Raveh, E., Nageris, B.I. (2016). Cochlear implantation via round window or cochleostomy: Effect on hearing in an animal model. *Laryngoscope* **126**, E375-E378.

Hodges, A.V., Schloffman, J., Balkany, T. (1997). Conservation of residual hearing with cochlear implantation. *Am J Otol.* **18**, 179-183.

Home Office (2014). Guidance on the Operation of the Animals (Scientific Procedures) Act 1986.

Hopper, A.N., Jamison, M.H., Lewis, W.G. (2007). Learning curves in surgical practice. *Postgrad. Med. J* **83**, 777-779.

Hsu, W.C., Campos-Torres, A., Portier, F., Lecain, E., Van Den Abbeele, T., De, W.C., Tran Ba, H.P. (2001). Cochlear electrical stimulation: influence of age of implantation on Fos immunocytochemical reactions in inferior colliculi and dorsal cochlear nuclei of the rat. *J. Comp Neurol.* **438**, 226-238.

Hu, C., Flecknell, P.A., Liles, J.H. (1992). Fentanyl and medetomidine anaesthesia in the rat and its reversal using atipamazole and either nalbuphine or butorphanol. *Lab Anim* **26**, 15-22.

Iguchi, F., Nakagawa, T., Tateya, I., Endo, T., Kim, T.S., Dong, Y., Kita, T., Kojima, K., Naito, Y., Omori, K. et al. (2004). Surgical techniques for cell transplantation into the mouse cochlea. *Acta Otolaryngol. Suppl* 43-47.

Irving, S., Gillespie, L., Richardson, R., Rowe, D., Fallon, J.B., Wise, A.K. (2014a). Electroacoustic stimulation: now and into the future. *Biomed. Res. Int.* **2014**, 350504

Irving, S., Trotter, M.I., Fallon, J.B., Millard, R.E., Shepherd, R.K., Wise, A.K. (2013). Cochlear implantation for chronic electrical stimulation in the mouse. *Hear. Res.* **306**, 37-45.

Irving, S., Wise, A.K., Millard, R.E., Shepherd, R.K., Fallon, J.B. (2014b). A partial hearing animal model for chronic electro-acoustic stimulation. *J. Neural Eng* **11**, 046008

Ison, J.R., Allen, P.D., O'Neill, W.E. (2007). Age-related hearing loss in C57BL/6J mice has both frequency-specific and non-frequency-specific components that produce a hyperacusis-like exaggeration of the acoustic startle reflex. *J. Assoc. Res. Otolaryngol.* **8**, 539-550.

Izer, J.M., Whitcomb, T.L., Wilson, R.P. (2014). Atipamezole Reverses Ketamine-Dexmedetomidine Anesthesia without Altering the Antinociceptive Effects of Butorphanol and Buprenorphine in Female C57BL/6J Mice. *J. Am. Assoc. Lab Anim Sci.* **53**, 675-683.

Jagger, D.J., Forge, A. (2006). Compartmentalized and signal-selective gap junctional coupling in the hearing cochlea. *J Neurosci.* **26**, 1260-1268.

Jagger, D.J., Housely, G.D. (2003). Membrane properties of type II spiral ganglion neurones identified in a neonatal rat cochlear slice. *J Physiol* **552**, 525-533.

James, C., Albegger, K., Battmer, R., Burdo, S., Deggouj, N., Deguine, O., Dillier, N., Gersdorff, M., Laszig, R., Lenarz, T. et al. (2005). Preservation of residual hearing with cochlear implantation: how and why. *Acta Otolaryngol.* **125**, 481-491.

James, C.J., Fraysse, B., Deguine, O., Lenarz, T., Mawman, D., Ramos, A., Ramsden, R., Sterkers, O. (2006). Combined electroacoustic stimulation in conventional candidates for cochlear implantation. *Audiol. Neurootol.* **11 Suppl 1**, 57-62.

James, D.P., Eastwood, H., Richardson, R.T., O'Leary, S.J. (2008). Effects of round window dexamethasone on residual hearing in a Guinea pig model of cochlear implantation. *Audiol. Neurootol.* **13**, 86-96.

Jero, J., Tseng, C.J., Mhatre, A.N., Lalwani, A.K. (2001). A surgical approach appropriate for targeted cochlear gene therapy in the mouse. *Hear. Res.* **151**, 106-114.

Jewett, D.L., Romano, M.N., Williston, J.S. (1970). Human auditory evoked potentials: possible brain stem components detected on the scalp. *Science* **167**, 1517-1518.

Kang, S.Y., Colesa, D.J., Swiderski, D.L., Su, G.L., Raphael, Y., Pfingst, B.E. (2010). Effects of hearing preservation on psychophysical responses to cochlear implant stimulation. *J. Assoc. Res. Otolaryngol.* **11**, 245-265.

Kanzaki, S., Stover, T., Kawamoto, K., Prieskorn, D.M., Altschuler, R.A., Miller, J.M., Raphael, Y. (2002). Glial cell line-derived neurotrophic factor and chronic electrical stimulation prevent VIII cranial nerve degeneration following denervation. *J Comp Neurol.* **454**, 350-360.

Kawamoto, K., Oh, S.H., Kanzaki, S., Brown, N., Raphael, Y. (2001). The functional and structural outcome of inner ear gene transfer via the vestibular and cochlear fluids in mice. *Mol. Ther.* **4**, 575-585.

Kawano, A., Seldon, H.L., Clark, G.M., Ramsden, R.T., Raine, C.H. (1998). Intracochlear factors contributing to psychophysical percepts following cochlear implantation. *Acta Otolaryngol.* **118**, 313-326.

Kemp, D.T. (1978). Stimulated acoustic emissions from within the human auditory system. *J. Acoust. Soc. Am.* **64**, 1386-1391.

Kemp, D.T. (2002). Otoacoustic emissions, their origin in cochlear function, and use. *Br. Med. Bull.* **63**, 223-241.

Khan, A.M., Handzel, O., Burgess, B.J., Damian, D., Eddington, D.K., Nadol, J.B., Jr. (2005). Is word recognition correlated with the number of surviving spiral ganglion cells and electrode insertion depth in human subjects with cochlear implants? *Laryngoscope* **115**, 672-677.

Kiefer, J., Gstoettner, W., Baumgartner, W., Pok, S.M., Tillein, J., Ye, Q., von, I.C. (2004). Conservation of low-frequency hearing in cochlear implantation. *Acta Otolaryngol.* **124**, 272-280.

Kikkawa, Y., Seki, Y., Okumura, K., Ohshiba, Y., Miyasaka, Y., Suzuki, S., Ozaki, M., Matsuoka, K., Noguchi, Y., Yonekawa, H. (2012). Advantages of a mouse model for human hearing impairment. *Exp. Anim* **61**, 85-98.

Kikuchi, T., Adams, J.C., Miyabe, Y., So, E., Kobayashi, T. (2000a). Potassium ion recycling pathway via gap junction systems in the mammalian cochlea and its interruption in hereditary nonsyndromic deafness. *Med. Electron Microsc.* **33**, 51-56.

Kikuchi, T., Kimura, R.S., Paul, D.L., Takasaka, T., Adams, J.C. (2000b). Gap junction systems in the mammalian cochlea. *Brain Res. Brain Res. Rev.* **32**, 163-166.

Klinge, U., Klosterhalfen, B., Ottinger, A.P., Junge, K., Schumpelick, V. (2002). PVDF as a new polymer for the construction of surgical meshes. *Biomaterials* **23**, 3487-3493.

Kochhar, A., Hildebrand, M.S., Smith, R.J. (2007). Clinical aspects of hereditary hearing loss. *Genet. Med.* **9**, 393-408.

Kohler, G., Pallwein-Prettner, L., Koch, O.O., Luketina, R.R., Lechner, M., Emmanuel, K. (2015). Magnetic resonance-visible meshes for laparoscopic ventral hernia repair. *JSLS.* **19**,

Kong, W.J., Cheng, H.M., Ma, H., Wang, Y.J., Han, P. (2012). Evaluation of the implanted cochlear implant electrode by CT scanning with three-dimensional reconstruction. *Acta Otolaryngol.* **132**, 116-122.

Kong, Y.Y., Cruz, R., Jones, J.A., Zeng, F.G. (2004). Music perception with temporal cues in acoustic and electric hearing. *Ear Hear.* **25**, 173-185.

Konings, A., Van, L.L., Wiktorek-Smagur, A., Rajkowska, E., Pawelczyk, M., Carlsson, P.I., Bondeson, M.L., Dudarewicz, A., Vandevelde, A., Fransen, E. et al. (2009). Candidate gene association study for noise-induced hearing loss in two independent noise-exposed populations. *Ann. Hum. Genet.* **73**, 215-224.

Kopelovich, J.C., Robinson, B.K., Soken, H., Verhoeven, K.J., Kirk, J.R., Goodman, S.S., Hansen, M.R. (2015). Acoustic Hearing After Murine Cochlear Implantation: Effects of Trauma and Implant Type. *Ann. Otol. Rhinol. Laryngol.* **124**, 931-939.

Kretzmer, E.A., Meltzer, N.E., Haenggeli, C.A., Ryugo, D.K. (2004). An animal model for cochlear implants. *Arch. Otolaryngol. Head Neck Surg.* **130**, 499-508.

Krstic, R.V. (1991). Human Microscopic Anatomy: An Atlas for Students of Medicine and Biology. **1st ed**,

Landry, T.G., Wise, A.K., Fallon, J.B., Shepherd, R.K. (2011). Spiral ganglion neuron survival and function in the deafened cochlea following chronic neurotrophic treatment. *Hear. Res.* **282**, 303-313.

Laroche, G., Marois, Y., Schwarz, E., Guidoin, R., King, M.W., Paris, E., Douville, Y. (1995). Polyvinylidene fluoride monofilament sutures: can they be used safely for long-term anastomoses in the thoracic aorta? *Artif. Organs* **19**, 1190-1199.

Laszig, R., Ridder, G.J., Fradis, M. (2002). Intracochlear insertion of electrodes using hyaluronic acid in cochlear implant surgery. *J Laryngol. Otol.* **116**, 371-372.

Leake, P.A., Hradek, G.T., Rebscher, S.J., Snyder, R.L. (1991). Chronic intracochlear electrical stimulation induces selective survival of spiral ganglion neurons in neonatally deafened cats. *Hear. Res.* **54**, 251-271.

Leake, P.A., Hradek, G.T., Snyder, R.L. (1999). Chronic electrical stimulation by a cochlear implant promotes survival of spiral ganglion neurons after neonatal deafness. *J Comp Neurol.* **412**, 543-562.

Lehnhardt, E. (1993). [Intracochlear placement of cochlear implant electrodes in soft surgery technique]. *HNO* **41**, 356-359.

Lenarz, T., Pau, H.W., Paasche, G. (2013). Cochlear implants. *Curr. Pharm. Biotechnol.* **14**, 112-123.

Lenarz, T., Stover, T., Buechner, A., Lesinski-Schiedat, A., Patrick, J., Pesch, J. (2009). Hearing conservation surgery using the Hybrid-L electrode. Results from the first clinical trial at the Medical University of Hannover. *Audiol. Neurootol.* **14 Suppl 1**, 22-31.

Lenarz, T., Stover, T., Buechner, A., Paasche, G., Briggs, R., Risi, F., Pesch, J., Battmer, R.D. (2006). Temporal bone results and hearing preservation with a new straight electrode. *Audiol. Neurootol.* **11 Suppl 1**, 34-41.

Li, H.S., Borg, E. (1991a). Age-related loss of auditory sensitivity in two mouse genotypes. *Acta Otolaryngol.* **111**, 827-834.

Li, H.S., Borg, E. (1991b). Age-related loss of auditory sensitivity in two mouse genotypes. *Acta Otolaryngol.* **111**, 827-834.

Li, P.M., Somdas, M.A., Eddington, D.K., Nadol, J.B., Jr. (2007). Analysis of intracochlear new bone and fibrous tissue formation in human subjects with cochlear implants. *Ann. Otol. Rhinol. Laryngol.* **116**, 731-738.

Linthicum, F.H., Jr., Fayad, J., Otto, S.R., Galey, F.R., House, W.F. (1991). Cochlear implant histopathology. *Am. J. Otol.* **12**, 245-311.

Lorens, A., Polak, M., Piotrowska, A., Skarzynski, H. (2008). Outcomes of treatment of partial deafness with cochlear implantation: a DUET study. *Laryngoscope* **118**, 288-294.

Lu, W., Xu, J., Shepherd, R.K. (2005a). Cochlear implantation in rats: a new surgical approach. *Hear. Res.* **205**, 115-122.

Lu, W., Xu, J., Shepherd, R.K. (2005b). Cochlear implantation in rats: a new surgical approach. *Hear. Res.* **205**, 115-122.

Lundin, K., Nasvall, A., Kobler, S., Linde, G., Rask-Andersen, H. (2013). Cochlear implantation in the elderly. *Cochlear. Implants. Int.* **14**, 92-97.

Mangus, B., Rivas, A., Tsai, B.S., Haynes, D.S., Roland, J.T., Jr. (2012). Surgical techniques in cochlear implants. *Otolaryngol. Clin. North Am.* **45**, 69-80.

Mann, Z.F., Kelley, M.W. (2011). Development of tonotopy in the auditory periphery. *Hear. Res.* **276**, 2-15.

Marsh, M.A., Jenkins, H.A., Coker, N.J. (1992). Histopathology of the temporal bone following multichannel cochlear implantation. *Arch. Otolaryngol. Head Neck Surg.* **118**, 1257-1265.

Mary, C., Marois, Y., King, M.W., Laroche, G., Douville, Y., Martin, L., Guidoin, R. (1998). Comparison of the in vivo behavior of polyvinylidene fluoride and polypropylene sutures used in vascular surgery. *ASAIO J.* **44**, 199-206.

Matsui, J.I., Ogilvie, J.M., Warchol, M.E. (2002). Inhibition of caspases prevents ototoxic and ongoing hair cell death. *J Neurosci.* **22**, 1218-1227.

Megerian, C.A., Burkard, R.F., Ravicz, M.E. (1996). A method for determining interaural attenuation in animal models of assymetric hearing loss. *Audiol Neurootol*. **1**, 214-219.

Michel, V., Goodyear, R.J., Weil, D., Marcotti, W., Perfettini, I., Wolfrum, U., Kros, C.J., Richardson, G.P., Petit, C. (2005). Cadherin 23 is a component of the transient lateral links in the developing hair bundles of cochlear sensory cells. *Dev. Biol.* **280**, 281-294.

Migirov, L., Taitelbaum-Swead, R., Drendel, M., Hildesheimer, M., Kronenberg, J. (2010). Cochlear implantation in elderly patients: surgical and audiological outcome. *Gerontology* **56**, 123-128.

Mikaelian, D.O. (1979). Development and degeneration of hearing in the C57/b16 mouse: relation of electrophysiologic responses from the round window and cochlear nucleus to cochlear anatomy and behavioral responses. *Laryngoscope* **89**, 1-15.

Mikaelian, D.O., Warfield, D., Norris, O. (1974). Genetic progressive hearing loss in the C57-b16 mouse. Relation of behavioral responses to chochlear anatomy. *Acta Otolaryngol.* **77**, 327-334.

Miller, J.M., Le Prell, C.G., Prieskorn, D.M., Wys, N.L., Altschuler, R.A. (2007). Delayed neurotrophin treatment following deafness rescues spiral ganglion cells from death and promotes regrowth of auditory nerve peripheral processes: effects of brain-derived neurotrophic factor and fibroblast growth factor. *J. Neurosci. Res.* **85**, 1959-1969.

Mistry, N., Nolan, L.S., Saeed, S.R., Forge, A., Taylor, R.R. (2014). Cochlear implantation in the mouse via the round window: effects of array insertion. *Hear. Res.* **312**, 81-90.

Mitchell, A., Miller, J.M., Finger, P.A., Heller, J.W., Raphael, Y., Altschuler, R.A. (1997). Effects of chronic high-rate electrical stimulation on the cochlea and eighth nerve in the deafened guinea pig. *Hear. Res.* **105**, 30-43.

Miyao, M., Firestein, G.S., Keithley, E.M. (2008). Acoustic trauma augments the cochlear immune response to antigen. *Laryngoscope* **118**, 1801-1808.

Morzaria, S., Westerberg, B.D., Kozak, F.K. (2004). Systematic review of the etiology of bilateral sensorineural hearing loss in children. *Int. J. Pediatr. Otorhinolaryngol.* **68**, 1193-1198.

Mowry, S.E., Woodson, E., Gantz, B.J. (2012). New frontiers in cochlear implantation: acoustic plus electric hearing, hearing preservation, and more. *Otolaryngol. Clin. North Am.* **45**, 187-203.

Nadol, J.B., Jr. (1990). Degeneration of cochlear neurons as seen in the spiral ganglion of man. *Hear. Res.* **49**, 141-154.

Nadol, J.B., Jr. (1997). Patterns of neural degeneration in the human cochlea and auditory nerve: implications for cochlear implantation. *Otolaryngol. Head Neck Surg.* **117**, 220-228.

Nadol, J.B., Jr., Ketten, D.R., Burgess, B.J. (1994). Otopathology in a case of multichannel cochlear implantation. *Laryngoscope* **104**, 299-303.

Nadol, J.B., Jr., Shiao, J.Y., Burgess, B.J., Ketten, D.R., Eddington, D.K., Gantz, B.J., Kos, I., Montandon, P., Coker, N.J., Roland, J.T., Jr. et al. (2001). Histopathology of cochlear implants in humans. *Ann. Otol. Rhinol. Laryngol.* **110**, 883-891.

Nadol, J.B., Jr., Young, Y.S., Glynn, R.J. (1989). Survival of spiral ganglion cells in profound sensorineural hearing loss: implications for cochlear implantation. *Ann. Otol. Rhinol. Laryngol.* **98**, 411-416.

Nagase, S., Miller, J.M., Dupont, J., Lim, H.H., Sato, K., Altschuler, R.A. (2000). Changes in cochlear electrical stimulation induced Fos expression in the rat inferior colliculus following deafness. *Hear. Res.* **147**, 242-250.

Nakaizumi, T., Kawamoto, K., Minoda, R., Raphael, Y. (2004). Adenovirus-mediated expression of brain-derived neurotrophic factor protects spiral ganglion neurons from ototoxic damage. *Audiol. Neurootol.* **9**, 135-143.

National Institute on Deafness and Other Communication Disorders (2016). Cochlear Implants. https://www.nidcd.nih.gov/health/cochlear-implants

Nguyen, Y., Couloigner, V., Rudic, M., Nguyen, Y., Couloigner, V., Rudic, M., Grayeli, A.B., Ferrary, E., Sterkers, O. (2009). An animal model of cochlear implantation with an intracochlear fluid delivery system. *Acta Otolaryngol.* **129**, 1153-1159.

Noble, W., Tyler, R.S., Dunn, C.C., Bhullar, N. (2009). Younger- and older-age adults with unilateral and bilateral cochlear implants: speech and spatial hearing self-ratings and performance. *Otol. Neurotol.* **30**, 921-929.

O'Leary, S.J., Monksfield, P., Kel, G., Connolly, T., Souter, M.A., Chang, A., Marovic, P., O'Leary, J.S., Richardson, R., Eastwood, H. (2013). Relations between cochlear histopathology and hearing loss in experimental cochlear implantation. *Hear. Res.* **298**, 27-35.

O'Leary, S.J., Richardson, R.R., McDermott, H.J. (2009). Principles of design and biological approaches for improving the selectivity of cochlear implant electrodes. *J. Neural Eng* **6**, 055002

Ohlemiller, K.K. (2006). Contributions of mouse models to understanding of age- and noise-related hearing loss. *Brain Res.* **1091**, 89-102.

Ohlemiller, K.K. (2009). Mechanisms and genes in human strial presbycusis from animal models. *Brain Res.* **1277**, 70-83.

Ohlemiller, K.K., Gagnon, P.M. (2004). Apical-to-basal gradients in age-related cochlear degeneration and their relationship to "primary" loss of cochlear neurons. *J. Comp Neurol.* **479**, 103-116.

Otte, J., Schunknecht, H.F., Kerr, A.G. (1978). Ganglion cell populations in normal and pathological human cochleae. Implications for cochlear implantation. *Laryngoscope* **88**, 1231-1246.

Parham, K. (1997). Distortion product otoacoustic emissions in the C57BL/6J mouse model of age-related hearing loss. *Hear. Res.* **112**, 216-234.

Parham, K., Sun, X.M., Kim, D.O. (2001). Noninvasive assessment of auditory function in mice: Auditory brainstem response and distortion product otoacoustic emissions. 37-58.

Park, S.N., Back, S.A., Park, K.H., Kim, D.K., Park, S.Y., Oh, J.H., Park, Y.S., Yeo, S.W. (2010). Comparison of cochlear morphology and apoptosis in mouse models of presbycusis. *Clin. Exp. Otorhinolaryngol.* **3**, 126-135.

Parkins, C.W. (1989). Temporal response patterns of auditory nerve fibers to electrical stimulation in deafened squirrel monkeys. *Hear. Res.* **41**, 137-168.

Parkinson, N., Hardisty-Hughes, R.E., Tateossian, H., Tsai, H.T., Brooker, D., Morse, S., Lalane, Z., MacKenzie, F., Fray, M., Glenister, P. et al. (2006). Mutation at the Evi1 locus in Junbo mice causes susceptibility to otitis media. *PLoS. Genet.* **2**, e149

Pau, H.W., Just, T., Bornitz, M., Lasurashvilli, N., Zahnert, T. (2007). Noise exposure of the inner ear during drilling a cochleostomy for cochlear implantation. *Laryngoscope* **117**, 535-540.

Perez, P., Bao, J. (2011). Why do hair cells and spiral ganglion neurons in the cochlea die during aging? *Aging Dis.* **2**, 231-241.

Pfingst, B.E., Bowling, S.A., Colesa, D.J., Garadat, S.N., Raphael, Y., Shibata, S.B., Strahl, S.B., Su, G.L., Zhou, N. (2011). Cochlear infrastructure for electrical hearing. *Hear. Res.* **281**, 65-73.

Pfingst, B.E., Donaldson, J.A., Miller, J.M., Spelman, F.A. (1979). Psychophysical evaluation of cochlear prostheses in a monkey model. *Ann. Otol. Rhinol. Laryngol.* **88**, 613-625.

Pfingst, B.E., Morris, D.J., Miller, A.L. (1995). Effects of electrode configuration on threshold functions for electrical stimulation of the cochlea. *Hear. Res.* **85**, 76-84.

Praetorius, M., Baker, K., Weich, C.M., Plinkert, P.K., Staecker, H. (2003). Hearing preservation after inner ear gene therapy: the effect of vector and surgical approach. *ORL J. Otorhinolaryngol. Relat Spec.* **65**, 211-214.

Praetorius, M., Limberger, A., Muller, M., Lehner, R., Schick, B., Zenner, H.P., Plinkert, P., Knipper, M. (2001). A novel microperfusion system for the long-term local supply of drugs to the inner ear: implantation and function in the rat model. *Audiol. Neurootol.* **6**, 250-258.

Prosen, C.A., Dore, D.J., May, B.J. (2003). The functional age of hearing loss in a mouse model of presbycusis. I. Behavioral assessments. *Hear. Res.* **183**, 44-56.

Quesnel, A.M., Nakajima, H.H., Rosowski, J.J., Hansen, M.R., Gantz, B.J., Nadol, J.B., Jr. (2016). Delayed loss of hearing after hearing preservation cochlear implantation: Human temporal bone pathology and implications for etiology. *Hear. Res.* **333**, 225-234.

Rafferty, A., Tapper, L., Strachan, D., Raine, C. (2013). Cochlear implantation in older patients: outcomes and comparisons. *Rev. Laryngol. Otol. Rhinol. (Bord.)* **134**, 119-124.

Raphael, Y., Altschuler, R.A. (2003). Structure and innervation of the cochlea. *Brain Res. Bull.* **60**, 397-422.

Rask-Andersen, H., Liu, W., Erixon, E., Kinnefors, A., Pfaller, K., Schrott-Fischer, A., Glueckert, R. (2012). Human cochlea: anatomical characteristics and their relevance for cochlear implantation. *Anat Rec. (Hoboken.)* **295**, 1791-1811.

Reiss, L.A., Stark, G., Nguyen-Huynh, A.T., Spear, K.A., Zhang, H., Tanaka, C., Li, H. (2015). Morphological correlates of hearing loss after cochlear implantation and electro-acoustic stimulation in a hearing-impaired Guinea pig model. *Hear. Res.* **327**, 163-174.

Reynolds, R.P., Kinard, W.L., Degraff, J.J., Leverage, N., Norton, J.N. (2010). Noise in a laboratory animal facility from the human and mouse perspectives. *J. Am. Assoc. Lab Anim Sci.* **49**, 592-597.

Ribari, O., Repassy, G., Kustel, M. (2000). Reoperations after cochlear implantation. *Acta Otolaryngol.* **120**, 160-163.

Richard, C., Fayad, J.N., Doherty, J., Linthicum, F.H., Jr. (2012). Round window versus cochleostomy technique in cochlear implantation: histologic findings. *Otol. Neurotol.* **33**, 1181-1187.

Robles, L., Ruggero, M.A. (2001). Mechanics of the mammalian cochlea. *Physiol Rev.* **81**, 1305-1352.

Roehm, P.C., Hansen, M.R. (2005). Strategies to preserve or regenerate spiral ganglion neurons. *Curr. Opin. Otolaryngol. Head Neck Surg.* **13**, 294-300.

Rogers, J.H. (1987). Calretinin: a gene for a novel calcium-binding protein expressed principally in neurons. *J. Cell Biol.* **105**, 1343-1353.

Roland, P.S., Wright, C.G., Isaacson, B. (2007). Cochlear implant electrode insertion: the round window revisited. *Laryngoscope* **117**, 1397-1402.

Rowe, D., Chambers, S., Hampson, A., Eastwood, H., Campbell, L., O'Leary, S. (2016). Delayed low frequency hearing loss caused by cochlear implantation interventions via the round window but not cochleostomy. *Hear. Res.* **333**, 49-57.

Saeed, S.R., Selvadurai, D., Beale, T., Biggs, N., Murray, B., Gibson, P., Risi, F., Boyd, P. (2014). The use of cone-beam computed tomography to determine cochlear implant electrode position in human temporal bones. *Otol. Neurotol.* **35**, 1338-1344.

Saeed, S.R., Selvadurai, D., Beale, T., Murray, B., Boyd, P., Biggs, N., Gibson, P., Risi, F. (2013). The use of cone beam imaging to determine cochlear implant electrode position in human temporal bones. *Cochlear. Implants. Int.* **14 Suppl 4**, S14-S15.

Saenz, M., Langers, D.R. (2014). Tonotopic mapping of human auditory cortex. *Hear. Res.* **307**, 42-52.

Santa Maria, P.L., Domville-Lewis, C., Sucher, C.M., Chester-Browne, R., Atlas, M.D. (2013). Hearing preservation surgery for cochlear implantation--hearing and quality of life after 2 years. *Otol. Neurotol.* **34**, 526-531.

Santa Maria, P.L., Gluth, M.B., Yuan, Y., Atlas, M.D., Blevins, N.H. (2014). Hearing preservation surgery for cochlear implantation: a meta-analysis. *Otol. Neurotol.* **35**, e256-e269.

Santos-Sacchi, J., Dallos, P. (1983). Intercellular communication in the supporting cells of the organ of Corti. *Hear. Res.* **9**, 317-326.

Saunders, J.E., Molter, D.W., McElveen, J.T., Jr. (1994). Cochlear implant-related osteoneogenesis in an animal model: fluorescent labeling. *Am. J. Otol.* **15**, 606-610.

Schafer, E.C., Thibodeau, L.M. (2004). Speech recognition abilities of adults using cochlear implants with FM systems. *J Am Acad. Audiol.* **15**, 678-691.

Schnabl, J., Glueckert, R., Feuchtner, G., Recheis, W., Potrusil, T., Kuhn, V., Wolf-Magele, A., Riechelmann, H., Sprinzl, G.M. (2012). Sheep as a large animal model for middle and inner ear implantable hearing devices: a feasibility study in cadavers. *Otol. Neurotol.* **33**, 481-489.

Schuknecht, H.F. (1955). Presbycusis. *Laryngoscope* **65**, 402-419.

Schuknecht, H.F. (1964). Further observations on the pathology of presbyacusis. *Arch. Otolaryngol.* **80**, 369-382.

Scimemi, P., Santarelli, R., Selmo, A., Mammano, F. (2014). Auditory brainstem responses to clicks and tone bursts in C57 BL/6J mice. *Acta Otorhinolaryngol. Ital.* **34**, 264-271.

Seyyedi, M., Nadol, J.B., Jr. (2014). Intracochlear inflammatory response to cochlear implant electrodes in humans. *Otol. Neurotol.* **35**, 1545-1551.

Shepherd, R.K., Clark, G.M., Black, R.C. (1983). Chronic electrical stimulation of the auditory nerve in cats. Physiological and histopathological results. *Acta Otolaryngol. Suppl* **399**, 19-31.

Shepherd, R.K., Clark, G.M., Pyman, B.C., Webb, R.L. (1985). Banded intracochlear electrode array: evaluation of insertion trauma in human temporal bones. *Ann. Otol. Rhinol. Laryngol.* **94**, 55-59.

Shepherd, R.K., Clark, G.M., Xu, S.A., Pyman, B.C. (1995). Cochlear pathology following reimplantation of a multichannel scala tympani electrode array in the macaque. *Am. J. Otol.* **16**, 186-199.

Shepherd, R.K., Coco, A., Epp, S.B., Crook, J.M. (2005). Chronic depolarization enhances the trophic effects of brain-derived neurotrophic factor in rescuing auditory neurons following a sensorineural hearing loss. *J Comp Neurol.* **486**, 145-158.

Shepherd, R.K., Javel, E. (1997). Electrical stimulation of the auditory nerve. I. Correlation of physiological responses with cochlear status. *Hear. Res.* **108**, 112-144.

Shepherd, R.K., Matsushima, J., Martin, R.L., Clark, G.M. (1994). Cochlear pathology following chronic electrical stimulation of the auditory nerve: II. Deafened kittens. *Hear. Res.* **81**, 150-166.

Shibata, S.B., Budenz, C.L., Bowling, S.A., Pfingst, B.E., Raphael, Y. (2011). Nerve maintenance and regeneration in the damaged cochlea. *Hear. Res.* **281**, 56-64.

Shibata, S.B., Cortez, S.R., Beyer, L.A., Wiler, J.A., Di, P.A., Pfingst, B.E., Raphael, Y. (2010). Transgenic BDNF induces nerve fiber regrowth into the auditory epithelium in deaf cochleae. *Exp. Neurol.* **223**, 464-472.

Shiomi, Y., Naito, Y., Honjo, I., Fujiki, N., Kaneko, K., Takahashi, H., Yamashita, M., Kawano, M. (1999). Cochlear implant in patients with residual hearing. *Auris Nasus Larynx* **26**, 369-374.

Shnerson, A., Pujol, R. (1981). Age-related changes in the C57BL/6J mouse cochlea. I. Physiological findings. *Brain Res.* **254**, 65-75.

Sinclair, M.D. (2003). A review of the physiological effects of alpha2-agonists related to the clinical use of medetomidine in small animal practice. *Can. Vet. J.* **44**, 885-897.

Skarzynski, H., Lorens, A. (2010). Electric acoustic stimulation in children. *Adv. Otorhinolaryngol.* **67**, 135-143.

Skarzynski, H., Lorens, A., D'Haese, P., Walkowiak, A., Piotrowska, A., Sliwa, L., Anderson, I. (2002). Preservation of residual hearing in children and post-lingually deafened adults after cochlear implantation: an initial study. *ORL J Otorhinolaryngol. Relat Spec.* **64**, 247-253.

Smith, J., Baran, S. (2013). Selecting an Appropriate Rodent Model for Research. http://www.alnmag.com/articles/2013/03/selecting-appropriate-rodent-model-research

Snyder, R.L., Middlebrooks, J.C., Bonham, B.H. (2008). Cochlear implant electrode configuration effects on activation threshold and tonotopic selectivity. *Hear. Res.* **235**, 23-38.

Soken, H., Robinson, B.K., Goodman, S.S., Abbas, P.J., Hansen, M.R., Kopelovich, J.C. (2013). Mouse cochleostomy: a minimally invasive dorsal approach for modeling cochlear implantation. *Laryngoscope* **123**, E109-E115.

Somdas, M.A., Li, P.M., Whiten, D.M., Eddington, D.K., Nadol, J.B., Jr. (2007). Quantitative evaluation of new bone and fibrous tissue in the cochlea following cochlear implantation in the human. *Audiol. Neurootol.* **12**, 277-284.

Spelman, F.A., Clopton, B.M., Pfingst, B.E., Miller, J.M. (1980). Design of the cochlear prosthesis: effects of the flow of current in the implanted ear. *Ann. Otol. Rhinol. Laryngol. Suppl* **89**, 8-10.

Spicer, S.S., Schulte, B.A. (1996). The fine structure of spiral ligament cells relates to ion return to the stria and varies with place-frequency. *Hear. Res.* **100**, 80-100.

Spongr, V.P., Flood, D.G., Frisina, R.D., Salvi, R.J. (1997). Quantitative measures of hair cell loss in CBA and C57BL/6 mice throughout their life spans. *J. Acoust. Soc. Am.* **101**, 3546-3553.

Sprinzl, G.M., Riechelmann, H. (2010). Current trends in treating hearing loss in elderly people: a review of the technology and treatment options - a mini-review. *Gerontology* **56**, 351-358.

Staecker, H., Gabaizadeh, R., Federoff, H., Van De Water, T.R. (1998). Brain-derived neurotrophic factor gene therapy prevents spiral ganglion degeneration after hair cell loss. *Otolaryngol. Head Neck Surg.* **119**, 7-13.

Staecker, H., Galinovic-Schwartz, V., Liu, W., Lefebvre, P., Kopke, R., Malgrange, B., Moonen, G., Van De Water, T.R. (1996). The role of the neurotrophins in maturation and maintenance of postnatal auditory innervation. *Am J Otol.* **17**, 486-492.

Steel, K.P., Barkway, C., Bock, G.R. (1987). Strial dysfunction in mice with cochleo-saccular abnormalities. *Hear. Res.* **27**, 11-26.

Stover, T., Lenarz, T. (2009). Biomaterials in cochlear implants. *GMS. Curr. Top. Otorhinolaryngol. Head Neck Surg.* **8**, Doc10

Suzuka, Y., Schuknecht, H.F. (1988). Retrograde cochlear neuronal degeneration in human subjects. *Acta Otolaryngol. Suppl* **450**, 1-20.

Talbot, K.N., Hartley, D.E. (2008). Combined electro-acoustic stimulation: a beneficial union? *Clin. Otolaryngol.* **33**, 536-545.

Tamir, S., Ferrary, E., Borel, S., Sterkers, O., Bozorg, G.A. (2012). Hearing preservation after cochlear implantation using deeply inserted flex atraumatic electrode arrays. *Audiol. Neurootol.* **17**, 331-337.

Tan, B.T., Lee, M.M., Ruan, R. (2008). Bone-marrow-derived cells that home to acoustic deafened cochlea preserved their hematopoietic identity. *J. Comp Neurol.* **509**, 167-179.

Tanaka, C., Nguyen-Huynh, A., Loera, K., Stark, G., Reiss, L. (2014). Factors associated with hearing loss in a normal-hearing guinea pig model of Hybrid cochlear implants. *Hear. Res.* **316**, 82-93.

Taylor, P.R., Martinez-Pomares, L., Stacey, M., Lin, H.H., Brown, G.D., Gordon, S. (2005). Macrophage receptors and immune recognition. *Annu. Rev. Immunol.* **23**, 901-944.

Taylor, R.R., Jagger, D.J., Forge, A. (2012). Defining the cellular environment in the organ of Corti following extensive hair cell loss: a basis for future sensory cell replacement in the Cochlea. *PLoS. One.* **7**, e30577

Todt, I., Basta, D., Ernst, A. (2008). Does the surgical approach in cochlear implantation influence the occurrence of postoperative vertigo? *Otolaryngol. Head Neck Surg.* **138**, 8-12.

Tornabene, S.V., Sato, K., Pham, L., Billings, P., Keithley, E.M. (2006). Immune cell recruitment following acoustic trauma. *Hear. Res.* **222**, 115-124.

Trowbridge, I.S., Thomas, M.L. (1994). CD45: an emerging role as a protein tyrosine phosphatase required for lymphocyte activation and development. *Annu. Rev. Immunol.* **12**, 85-116.

Trussell, L.O. (2002). Transmission at the hair cell synapse. *Nat. Neurosci.* **5**, 85-86.

U.S.National Library of Medicine (2006). Genetics Home Reference. http://ghr.nlm.nih.gov/condition/nonsyndromic-deafness

Urban, E., King, M.W., Guidoin, R., Laroche, G., Marois, Y., Martin, L., Cardou, A., Douville, Y. (1994). Why make monofilament sutures out of polyvinylidene fluoride? *ASAIO J.* **40**, 145-156.

Varga, L., Masindova, I., Huckova, M., Kabatova, Z., Gasperikova, D., Klimes, I., Profant, M. (2014). Prevalence of DFNB1 mutations among cochlear implant users in Slovakia and its clinical implications. *Eur. Arch. Otorhinolaryngol.* **271**, 1401-1407.

Vischer, M., Haenggeli, A., Zhang, J., Pelizzone, M., Hausler, R., Rouiller, E.M. (1997). Effect of high-frequency electrical stimulation of the auditory nerve in an animal model of cochlear implants. *Am. J. Otol.* **18**, S27-S29.

Vivero, R.J., Fan, K., Angeli, S., Balkany, T.J., Liu, X.Z. (2010). Cochlear implantation in common forms of genetic deafness. *Int. J. Pediatr. Otorhinolaryngol.* **74**, 1107-1112.

Vivero, R.J., Joseph, D.E., Angeli, S., He, J., Chen, S., Eshraghi, A.A., Balkany, T.J., Van De Water, T.R. (2008). Dexamethasone base conserves hearing from electrode trauma-induced hearing loss. *Laryngoscope* **118**, 2028-2035.

von Bekesy, G. (1956). Current status of theories of hearing. *Science* **123**, 779-783.

von Ilberg, C.A., Baumann, U., Kiefer, J., Tillein, J., Adunka, O.F. (2011). Electric-acoustic stimulation of the auditory system: a review of the first decade. *Audiol. Neurootol.* **16 Suppl 2**, 1-30.

Weisz, C., Glowatzki, E., Fuchs, P. (2009). The postsynaptic function of type II cochlear afferents. *Nature* **461**, 1126-1129.

Welling, D.B., Hinojosa, R., Gantz, B.J., Lee, J.T. (1993). Insertional trauma of multichannel cochlear implants. *Laryngoscope* **103**, 995-1001.

White, J.A., Burgess, B.J., Hall, R.D., Nadol, J.B. (2000). Pattern of degeneration of the spiral ganglion cell and its processes in the C57BL/6J mouse. *Hear. Res.* **141**, 12-18.

Willott, J.F. (1990). Central physiological correlates of ageing and presbycusis in mice. *Acta Otolaryngol. Suppl* **476**, 153-155.

Wilson, B.S., Dorman, M.F. (2008a). Cochlear implants: a remarkable past and a brilliant future. *Hear. Res.* **242**, 3-21.

Wilson, B.S., Dorman, M.F. (2008b). Cochlear implants: current designs and future possibilities. *J. Rehabil. Res. Dev.* **45**, 695-730.

Wilson, B.S., Dorman, M.F. (2009). The design of cochlear implants. **2nd**, 137-146.

Wise, A.K., Richardson, R., Hardman, J., Clark, G., O'Leary, S. (2005). Resprouting and survival of guinea pig cochlear neurons in response to the administration of the neurotrophins brain-derived neurotrophic factor and neurotrophin-3. *J. Comp Neurol.* **487**, 147-165.

Wise, A.K., Tu, T., Atkinson, P.J., Flynn, B.O., Sgro, B.E., Hume, C., O'Leary, S.J., Shepherd, R.K., Richardson, R.T. (2011). The effect of deafness duration on neurotrophin gene therapy for spiral ganglion neuron protection. *Hear. Res.* **278**, 69-76.

Wolfe, J., Schafer, E.C., Heldner, B., Mulder, H., Ward, E., Vincent, B. (2009). Evaluation of speech recognition in noise with cochlear implants and dynamic FM. *J Am Acad. Audiol.* **20**, 409-421.

World Health Organization (2012). Deafness and hearing impairment. **Fact Sheet No. 300 (updated Feb 2013)**, http://www.who.int/mediacentre/factsheets/fs300/en/index.html

World Health Organization (2013). Grades of hearing impairment. http://www.who.int/pbd/deafness/hearing_impairment_grades/en/index.html

Wright, A. (1983). Scanning electron microscopy of the human organ of Corti. *J R. Soc. Med.* **76**, 269-278.

Wright, T., Valentine, P. (2008). The anatomy and embryology of the external and middle ear. **7th**, 3105-3125.

Xu, J., Nicholson, B.J. (2013). The role of connexins in ear and skin physiology - functional insights from disease-associated mutations. *Biochim. Biophys. Acta* **1828**, 167-178.

Xu, J., Shepherd, R.K., Millard, R.E., Clark, G.M. (1997). Chronic electrical stimulation of the auditory nerve at high stimulus rates: a physiological and histopathological study. *Hear. Res.* **105**, 1-29.

Xu, L., Li, Y., Hao, J., Chen, X., Xue, S.A., Han, D. (2004). Tone production in Mandarin-speaking children with cochlear implants: a preliminary study. *Acta Otolaryngol.* **124**, 363-367.

Xu, L., Pfingst, B.E. (2003). Relative importance of temporal envelope and fine structure in lexical-tone perception. *J. Acoust. Soc. Am.* **114**, 3024-3027.

Yagi, M., Kanzaki, S., Kawamoto, K., Shin, B., Shah, P.P., Magal, E., Sheng, J., Raphael, Y. (2000). Spiral ganglion neurons are protected from degeneration by GDNF gene therapy. *J Assoc. Res. Otolaryngol.* **1**, 315-325.

Yamamoto, H., Tominaga, M., Sone, M., Nakashima, T. (2003). Contribution of stapedial artery to blood flow in the cochlea and its surrounding bone. *Hear. Res.* **186**, 69-74.

Yamasoba, T., Lin, F.R., Someya, S., Kashio, A., Sakamoto, T., Kondo, K. (2013). Current concepts in age-related hearing loss: epidemiology and mechanistic pathways. *Hear. Res.* **303**, 30-38.

Yeo, S.W., Park, S.N., Park, Y.S., Suh, B.D. (2002). Effect of middle-ear effusion on otoacoustic emissions. *J. Laryngol. Otol.* **116**, 794-799.

Zeng, F.G., Rebscher, S., Harrison, W., Sun, X., Feng, H. (2008). Cochlear implants: system design, integration, and evaluation. *IEEE Rev. Biomed. Eng* **1**, 115-142.

Zhang, F., Zhang, J., Neng, L., Shi, X. (2013). Characterization and inflammatory response of perivascular-resident macrophage-like melanocytes in the vestibular system. *J. Assoc. Res. Otolaryngol.* **14**, 635-643.

Zheng, J., Shen, W., He, D.Z., Long, K.B., Madison, L.D., Dallos, P. (2000). Prestin is the motor protein of cochlear outer hair cells. *Nature* **405**, 149-155.

Zheng, Q.Y., Tong, Y.C., Alagramam, K.N., Yu, H. (2007). Tympanometry assessment of 61 inbred strains of mice. *Hear. Res.* **231**, 23-31.

APPENDIX 1 Weight chart for sham operated mice

Sham operated mice - weight chart

Mouse	Time point	Weight	Mouse	Time point	Weight
6	Pre-operative	48.5	9	Pre-operative	31.3
	Day 1 post-op	44.5		Day 1 post-op	29.4
	Day 2 post-op	44		Day 2 post-op	30.1
	Day 3 post-op	43.2		Day 3 post-op	30.6
	Day 4 post-op	44.7		Day 4 post-op	31.4
	Day 5 post-op	44.6		Day 5 post-op	31.7
	Day 6 post-op	44.5		Day 6 post-op	31.9
	Day 7 post-op	44.1		Day 7 post-op	31.5
	Day 14 post-op	45.6		Day 14 post-op	33.3
	Day 21 post-op	45.9		Day 21 post-op	32.8
	Day 28 post-op	47.9		Day 28 post-op	32.5
7	Pre-operative	40.9	12	Pre-operative	36.4
	Day 1 post-op	38.6		Day 1 post-op	34.1
	Day 2 post-op	37.8		Day 2 post-op	34.5
	Day 3 post-op	38.1		Day 3 post-op	34.5
	Day 4 post-op	39.2		Day 4 post-op	35.9
	Day 5 post-op	39		Day 5 post-op	33.9
	Day 6 post-op	39		Day 6 post-op	35.3
	Day 7 post-op	39		Day 7 post-op	34.7
	Day 14 post-op	42.3		Day 14 post-op	35.1
	Day 21 post-op	43.4		Day 21 post-op	35.5
	Day 28 post-op	42.6		Day 28 post-op	37.4
8	Pre-operative	40.5	13	Pre-operative	42.3
	Day 1 post-op	38.5		Day 1 post-op	41
	Day 2 post-op	38.5		Day 2 post-op	40.4
	Day 3 post-op	38.1		Day 3 post-op	40.6
	Day 4 post-op	38.7		Day 4 post-op	41.4
	Day 5 post-op	38.4		Day 5 post-op	40.3
	Day 6 post-op	38.3		Day 6 post-op	40.7
	Day 7 post-op	38.4		Day 7 post-op	42.3
	Day 14 post-op	40.6		Day 14 post-op	42.5
	Day 21 post-op	42		Day 21 post-op	42.1
	Day 28 post-op	42		Day 28 post-op	42

Mouse	Time point	Weight
14	Pre-operative	37.9
	Day 1 post-op	35.7
	Day 2 post-op	35
	Day 3 post-op	34.1
	Day 4 post-op	34.3
	Day 5 post-op	36.5
	Day 6 post-op	36.4
	Day 7 post-op	36.4
	Day 14 post-op	36.8
	Day 21 post-op	38
	Day 28 post-op	37.8
15	Pre-operative	37.3
	Day 1 post-op	37.9
	Day 2 post-op	35.4
	Day 3 post-op	35.6
	Day 4 post-op	36.4
	Day 5 post-op	35.3
	Day 6 post-op	35.7
	Day 7 post-op	37.3
	Day 14 post-op	37.5
	Day 21 post-op	37.1
	Day 28 post-op	36.9

	mouse 6	mouse 7	mouse 8	mouse 9	mouse 12	mouse 13	mouse 14	mouse 15
Pre-op wt	48.5	40.9	40.5	31.3	36.4	42.3	37.9	37.3
Wt day 1	44.5	38.6	38.5	29.4	34.1	41	35.7	37.9
wt change	4	2.3	2	1.9	2.3	1.3	2.2	-0.55
% change	8.2	5.6	4.9	6.1	6.3	3.1	5.8	-1.5

	mouse 6	mouse 7	mouse 8	mouse 9	mouse 12	mouse 13	mouse 14	mouse 15
Pre-op wt	48.5	40.9	40.5	31.3	36.4	42.3	37.9	37.3
Wt day 7	44.1	39	38.4	31.5	34.7	42.3	36.4	37.3
wt change	4.4	1.9	2.1	-0.2	1.7	0	1.5	0
% change	9.1	4.6	5.2	-0.6	4.7	0	4.0	0

	mouse 6	mouse 7	mouse 8	mouse 9	mouse 12	mouse 13	mouse 14	mouse 15
Pre-op wt	48.5	40.9	40.5	31.3	36.4	42.3	37.9	37.3
Wt day 28	47.9	42.6	42	32.5	37.4	42	37.8	36.9
wt change	0.6	-1.7	-1.5	-1.2	-1	0.3	0.1	0.45
% change	1.2	-4.2	-3.7	-3.8	-2.7	0.7	0.2	1.2

Wt = weight

APPENDIX 2 Mouse details

Details of mice implanted in study

Details of all mice implanted mice in (a) 3 month and (b) 6 month age group

(a)

Number	Gender	Age (Days)	Group	Implant time	Implant type
1	M	97	3 month	48 hours	Fluorocarbon
2	M	97	3 month	48 hours	Fluorocarbon
3	M	122	3 month	48 hours	Fluorocarbon
4	M	98	3 month	48 hours	Electrode array
5	M	98	3 month	48 hours	Electrode array
6	M	99	3 month	48 hours	Electrode array
7	M	96	3 month	1 week	Fluorocarbon
8	M	92	3 month	1 week	Fluorocarbon
9	F	147	3 month	1 week	Electrode array
10	M	92	3 month	1 week	Electrode array
11	M	90	3 month	4 weeks	Fluorocarbon
12	M	96	3 month	4 weeks	Fluorocarbon
13	M	93	3 month	4 weeks	Fluorocarbon
14	M	109	3 month	4 weeks	Electrode array
15	M	109	3 month	4 weeks	Electrode array
16	M	97	3 month	12 weeks	Fluorocarbon
17	M	107	3 month	12 weeks	Fluorocarbon
18	M	91	3 month	12 weeks	Electrode array

(b)

	Gender	Age (Days)	Group	Implant time	Implant type
1	F	189	6 month	48 hours	Electrode array
2	F	194	6 month	48 hours	Electrode array
3	F	201	6 month	48 hours	Fluorocarbon
4	F	184	6 month	48 hours	Fluorocarbon
5	F	184	6 month	48 hours	Fluorocarbon
6	M	199	6 month	48 hours	Fluorocarbon
7	M	212	6 month	1 week	Electrode array
8	M	213	6 month	1 week	Fluorocarbon
9	F	194	6 month	1 week	Fluorocarbon
10	F	194	6 month	1 week	Fluorocarbon
11	M	243	6 month	4 weeks	Electrode array
12	M	207	6 month	4 weeks	Fluorocarbon
13	M	221	6 month	4 weeks	Fluorocarbon
14	M	198	6 month	12 weeks	Electrode array
15	M	199	6 month	12 weeks	Electrode array
16	F	156	6 month	12 weeks	Fluorocarbon
17	M	199	6 month	12 weeks	Fluorocarbon

APPENDIX 3 Presentations and publications

Publications

Mistry, N., Nolan, L.S., Saeed, S.R., Forge, A., Taylor, R.R. (2014). Cochlear implantation in the mouse via the round window: effects of array insertion. Hear. Res. 312, 81-90.

Published abstracts

Mistry N, Taylor R, Forge A and Saeed SR. Cochlear implantation in the mouse: a novel animal model. ORS Spring Meeting Royal College of Surgeons of England. Clin Otol. 2013; 38(4):361.

Mistry N, Forge A, Saeed S, Taylor R. Developing a mouse model for cochlear implantation. Assoc. Res. Otolaryngol. 2013 Abs.:135.

Oral presentations

Developing a mouse model of cochlear implantation. Joint Spring Meeting of the Midland Institute of Otology with JLO/RSM Visiting Professors Roadshow, Ardencote Manor Hotel, Warwickshire, May 2015.

Developing a mouse model of cochlear implantation. Novel interventions for the human cochlea: emerging research and therapies meeting. Meeting organised by RSM Otology section, British Society of Otology and Action on Hearing Loss, RSM, London, February 2015.

Cochlear implantation in mice: functional and histological outcomes. 13th International Conference on Cochlear Implants and Other Implantable Auditory Technologies, Munich, June 2014.

Development of a mouse model of cochlear implantation. RCS Freemasons research presentation, Northampton, September 2013.

Development of a mouse model of cochlear implantation. RCS Freemasons research presentation, Southend-on-Sea, July 2013.

Cochlear implantation in the mouse: a novel animal model. Otorhinolaryngological Research Society (ORS) Spring Meeting, March 2013.

Development of a mouse model of cochlear implantation. ORL Club, Harley Street Clinic Board Room, 79 Harley Street, November 2012.

Poster presentations

Mistry N, Nolan L, Forge A, Taylor R, Saeed S. Cochlear implantation in mice: functional and histological outcomes. 13th International Conference on Cochlear Implants and Other Implantable Auditory Technologies, Munich, June 2014.

Mistry N, Nolan L, Forge A, Saeed S, Taylor R. Functional and histological outcomes following cochlear implantation in the mouse. 50th Inner Ear Biology Workshop, Madrid, Spain, September 2013.

Mistry N, Forge A, Saeed S, Taylor R. Developing a mouse model for cochlear implantation. Association for Research in Otolaryngology 36th MidWinter Meeting, Baltimore, USA, February 2013.

Mistry N, Taylor R, Forge A, Saeed SR. Developing a mouse model for cochlear implantation. 14th British Academic Conference in Otolaryngology (BACO), July 2012.